EVALUATION OF THE BEST MANAGEMENT PRACTICES TO CONTROL AGRICULTURAL DIFFUSE POLLUTION IN LAKE MOGAN WATERSHED WITH SWAT MODEL

A THESIS SUBMITTED TO
THE GRADUATE SCHOOL OF NATURAL AND APPLIED SCIENCES
OF
MIDDLE EAST TECHNICAL UNIVERSITY

BY

ZEYNEP ÖZCAN

IN PARTIAL FULFILLMENT OF THE REQUIREMENTS
FOR
THE DEGREE OF MASTER OF SCIENCE
IN
ENVIRONMENTAL ENGINEERING

JUNE 2016

Approval of the thesis:

EVALUATION OF THE BEST MANAGEMENT PRACTICES TO CONTROL AGRICULTURAL DIFFUSE POLLUTION IN LAKE MOGAN WATERSHED WITH SWAT MODEL

submitted by **ZEYNEP ÖZCAN** in partial fulfillment of the requirements for the degree of **Master of Science in Environmental Engineering Department, Middle East Technical University** by,

Prof. Dr. Gülbin Dural Ünver _____
Dean, Graduate School of **Natural and Applied Sciences**

Prof. Dr. Kahraman Ünlü _____
Head of Department, **Environmental Engineering**

Assoc. Prof. Dr. Emre Alp _____
Supervisor, **Environmental Engineering Dept., METU**

Assoc. Prof. Dr. Elçin Kentel _____
Co-Supervisor, **Civil Engineering Dept., METU**

Examining Committee Members:

Prof. Dr. Ülkü Yetiş _____
Environmental Engineering Dept., METU

Assoc. Prof. Dr. Emre Alp _____
Environmental Engineering Dept., METU

Assoc. Prof. Dr. Elçin Kentel _____
Civil Engineering Dept., METU

Assoc. Prof. Dr. Orhan Gündüz _____
Environmental Engineering Dept., Dokuz Eylül University

Assist. Prof. Dr. Derya Dursun Balcı
Environmental Engineering Dept., METU _____

Date: June 29, 2016

I hereby declare that all information in this document has been obtained and presented in accordance with academic rules and ethical conduct. I also declare that, as required by these rules and conduct, I have fully cited and referenced all material and results that are not original to this work.

Name, Last name: Zeynep Özcan

Signature:

ABSTRACT

EVALUATION OF THE BEST MANAGEMENT PRACTICES TO CONTROL AGRICULTURAL DIFFUSE POLLUTION IN LAKE MOGAN WATERSHED WITH SWAT MODEL

Özcan, Zeynep
M.Sc., Department of Environmental Engineering
Supervisor : Assoc. Prof. Dr. Emre Alp
Co-Supervisor: Assoc. Prof. Dr. Elçin Kentel

June 2016, 178 pages

Lake Mogan which is located in Gölbaşı County, Ankara, Turkey is one of the most important wetlands of Turkey and it was declared as Special Environmental Protection Region in 1990. Total area of semi-arid Lake Mogan watershed is 970 km^2 and dry farming is practiced approximately in 40% of the basin. Therefore, agricultural diffuse source pollution is a serious concern in the watershed. In the context of this thesis, the effects of implementation of different agricultural best management practices on sediment, total nitrogen and total phosphorus loads were evaluated by using Soil and Water Assessment Tool (SWAT). Meteorological data, digital elevation model (DEM), land use/land cover (LULC) map, soil properties and the information on agricultural practices are required to build SWAT model. The model was calibrated with SWAT-CUP for streamflow, sediment, nitrogen and phosphorus by using monthly data (2007 – 2010) from Yavrucak monitoring station. The model validation was carried out in Sukesen monitoring station for the same time period with calibration. With the calibrated and validated model, 11 different agricultural best management practice (BMP) scenarios were developed. The most efficient scenario in terms of pollutant load reduction was the one in which 30% reduction in fertilizer, no tillage and terracing were combined. This study aimed to help decision-makers to decide on the most efficient BMPs and thus to develop sustainable watershed management plans in Lake Mogan watershed and in watersheds showing similar characteristics with Lake Mogan.

Keywords: Diffuse pollution, SWAT, Lake Mogan, Best Management Practices

ÖZ

MOGAN GÖLÜ HAVZASINDA TARIMSAL YAYILI KİRLİLİĞİN KONTROLÜ İÇİN EN İYİ YÖNTEM UYGULAMALARININ SWAT MODELİ İLE DEĞERLENDİRİLMESİ

Özcan, Zeynep
Yüksek Lisans, Çevre Mühendisliği Bölümü
Tez Yöneticisi : Doç. Dr. Emre Alp
Ortak Tez Yöneticisi: Doç. Dr. Elçin Kentel

Haziran 2016, 178 sayfa

Ankara ilinin Gölbaşı ilçesinde yer alan Mogan Gölü, Türkiye'nin en önemli sulak alanlarından bir tanesidir ve 1990 yılında Özel Çevre Koruma Bölgesi olarak ilan edilmiştir. Yarı kurak Mogan Gölü havzası toplam alanı 970 km^2'dir ve havzanın yaklaşık %40'ında kuru tarım gerçekleştirilmektedir. Bu sebeple, tarımsal yayılı kirlilik havzada ciddi bir sorundur. Bu tez kapsamında, farklı tarımsal en iyi yönetim uygulamalarının sediman, toplam azot ve toplam fosfor yükleri üzerindeki etkisi Soil and Water Assessment Tool (SWAT) modeli kullanılarak değerlendirilmiştir. SWAT modelini oluşturmak için meteorolojik veriler, sayısal yükseklik modeli (SYM), arazi kullanımı/arazi örtüsü haritası, toprak özellikleri ve tarımsal uygulamalar hakkında bilgiye ihtiyaç duyulmaktadır. Model, Yavrucak izleme istasyonundan elde edilen aylık veriler (2007 – 2010) ile SWAT-CUP kullanılarak debi, azot ve fosfor için kalibre edilmiştir. Model doğrulaması, Sukesen izleme istasyonunda kalibrasyon ile aynı zaman periyodunda gerçekleştirilmiştir. Kalibre edilmiş ve doğrulanmış model kullanılarak 11 farklı tarımsal iyi yönetim uygulaması senaryosu geliştirilmiştir. Kirletici yüklerinin azaltılması açısından en etkili senaryo %30 gübre azaltımı, toprak işlemesiz tarım ve teraslama uygulamalarının kombine edildiği senaryo olmuştur. Bu çalışma karar vericilerin Mogan ve Mogan'a benzer özellikler gösteren diğer havzalarda en verimli iyi yönetim uygulamalarını belirlemesinde ve sürdürülebilir havza yönetimi planları geliştirmesinde yardımcı olmayı amaçlamıştır.

Anahtar Kelimeler: Yayılı kirlilik, SWAT, Mogan Gölü, İyi Yönetim Uygulamaları

To my family

ACKNOWLEDGEMENTS

I would like to thank a number people for their support and guidance during the completion of this thesis. First of all, I would like to express my most sincere gratitude to my advisor Assoc. Prof. Dr. Emre Alp for his patient guidance, motivating comments and feedbacks, and encouragement throughout my graduate study. I will always be grateful for his endless support. I would also like to thank my co-advisor Assoc. Prof. Dr. Elçin Kentel for her valuable comments, suggestions and insight on this thesis.

I also want to extend my thanks to my dissertation committee members, Prof. Dr. Ülkü Yetiş, Assoc. Prof. Dr. Orhan Gündüz and Assist. Prof. Dr. Derya Dursun Balcı for their invaluable feedbacks and suggestions.

I would like to thank Assoc. Prof. Dr. Oğuz Başkan, Aynur Hatipoğlu, METU Limnology Laboratory and Gölbaşı Directorate of Food, Agriculture and Livestock for their help during the data acquisition stage of the project.

I wholeheartedly thank my lifelong friends Sıla Sezgin, Meltem Şahin, Büşra Tufan and Ezgi Topcu for supporting and motivating me. I deeply appreciate their belief in me. I really appreciate constant help and moral support provided by my friends and colleagues Hale Demirtepe and Elif Sena Uzunpınar through my thesis study. Special thanks to Özge Yücel and Sevil Avşaroğlu who always motivate me during my graduate study. I would also like to thank Ruken Dilara Zaf who always makes me cheer up.

I owe my deepest gratitude to my family who have always believed in me and encouraged me throughout my life. None of this would have been possible without their love and patience.

Finally, I gratefully acknowledge the financial support provided by the Scientific and Technological Research Council of Turkey (TÜBİTAK) through the project entitled ‘Evaluation of Agricultural Diffuse Pollution and its Control Alternatives with SWAT model in Lake Mogan Watershed’ with project number 111Y284.

TABLE OF CONTENTS

LIST OF TABLES

TABLES

LIST OF FIGURES

FIGURES

CHAPTER 1

INTRODUCTION

Development of sustainable strategies for the management and efficient use of water resources require that all the pressures on water resources such as point and nonpoint sources, urbanization, climate change etc. are assessed in an integrated manner. Contrary to point source pollution arising from industrial and sewage treatment plants, nonpoint source (NPS) or diffuse pollution originates from several dispersed and poorly defined sources (EPA, 2012). Therefore, unlike point source pollution, monitoring of diffuse source pollution at the source of origin is difficult or even impossible. Consequently, it is not possible to measure diffuse discharges in terms of effluent standards (Novotny, 2003). Diffuse source pollutants can adversely affect water quality in watersheds. The use of fertilizers and pesticides in agriculture, pollutants from roads and paved areas, and contaminants from construction sites and silviculture can be given as the typical examples of diffuse pollution. The fact that diffuse pollution has intermittent characteristics and thus hard to identify makes its management a challenge for decision makers.

Water Framework Directive (WFD)(2000/60/EC) aiming to protect water bodies in terms of both quality and quantity requires all surface and ground waters within the defined river basin districts to reach good water status until 2015 or 2027. As an EU candidate country, Turkey has already initiated the harmonization process with the European Union legislation and important steps have been taken especially for the prevention of pollution. As a result of this effort, integrated approaches were put in action to aid decision makers in developing sustainable integrated river basin management plans. One of the most important initiation was the preparation of watershed protection action plans for 25 basins in Turkey in coordination with Turkish Ministry of Forestry and Water Affairs. These management plans aim to protect water resources, provide optimum utilization, prevent pollution and improve water quality of contaminated water sources. During the preparation of these management plans intensive monitoring studies were carried out and agricultural diffuse pollution was

identified as the most serious problem threatening the quality of water bodies in the majority of the watersheds. In Turkey, assessment of diffuse pollution and evaluation of the effectiveness of pollution control strategies/policies through modeling studies have become a necessity for the decision makers. Therefore, the number of modeling studies carried out as a part of integrated watershed management plans supported by municipalities, ministries, universities and national funding agencies have drastically increased in Turkey.

The term Best Management Practice (BMP) is defined as a practice or combination of practices which is proved to be the most efficient way of preventing and reducing NPS pollution (Novotny, 2003). "Best" implies improving the water quality without giving harm to production (Walter et al., 1979). Evaluating the effectiveness of a specific BMP by field trials or by collecting monitoring data is both costly and time consuming. The amount of pollutant loads and removal rates are highly variable in every runoff event. The monitoring data should be collected repeatedly in order to obtain reliable results about the performance of a BMP. Especially for large watersheds with varying land use classes and soil characteristics, intensive monitoring studies should be carried out to correctly assess the effects of a particular BMP. However, such studies are not always possible at the watershed level. In this context, watershed models stand out as useful tools since they provide a relatively less expensive and time saving solution.

Modeling tools taking into account different land use and management options are of great importance for decision makers since they allow the evaluation or comparison of the methods developed to meet ecological standards (Chaplot et al., 2004; Kersebaum et al., 2003; Krause et al., 2008). Among these modeling tools, commonly used ones can be listed as follows: HSPF (Bicknell et al., 2005), AGNPS (Young et al., 1989), Soil and Water Assessment Tool (SWAT) (Arnold et al., 1998; Gassman et al., 2007; Neitsch et al., 2002) and SWIM (Krysanova et al., 1998). Water quality simulation models can assist in understanding the hydrological cycle and processes, simulating the hydrological and water-quality effects of land-use and management practices, and identifying alternative management strategies to improve water quality and ecosystem functions in watersheds (Qiu and Wang, 2013).

SWAT (Soil and Water Assessment Tool) is one of the watershed models that is commonly used all over the world for various purposes such as predicting the impacts of management practices on water bodies and calculating the pollutant loads. It is a conceptual and continuous time model that operates on a daily time step (Arnold et al., 1998; Neitsch et al., 2002). SWAT model has been applied in hundreds of watersheds so far with the purpose of simulating different agricultural conservation practices around the world, e.g., Santhi et al. (2006), Lee et al. (2010) and Liu and Lu (2014). It has also been applied in semi-arid watersheds, e.g., Chahinian et al. (2011), Niraula et al. (2012) and Shrestha et al. (2016). According to Borah and Bera (2003), SWAT is a promising continuous model in predominantly agricultural watersheds and useful for investigating impacts of agricultural practices. Due to its common usage and usefulness for assessment of agricultural practices, SWAT model was chosen for modelling purposes in this study.

In this study, SWAT model was applied in Lake Mogan watershed, a semi-arid watershed located in Ankara, Turkey, to evaluate the impacts of several BMPs on sediment, phosphorus, and nitrogen loads. Being an ecologically important area, Lake Mogan and its wetland ecosystem are under threat due to serious pollution. Uncontrolled urbanization, point and nonpoint pollution sources, and ineffective sewerage systems are some of the causes of the pollution. Extensive agriculture carried out in the watershed is one of the major reasons of the water quality deterioration in Lake Mogan watershed (Karakoç, 2003). Thus, it is important to control the agricultural diffuse pollution to prevent this deterioration. With this purpose, SWAT model was built, calibrated and validated by using extensive data sets including in-stream water quality and flowrate measurements, meteorological data, land use-land cover map developed using remote sensing algorithms, information about agricultural activities and soil data. With the calibrated and validated SWAT model, 11 different BMP scenarios were developed, and the efficiencies of these scenarios were compared in terms of reducing the amount of transported sediment and nutrient loads. Taking into account the model performance statistics and uncertainty in the model outputs, it is concluded that this study will help decision-makers to select efficient BMPs and to develop sustainable watershed management plans in Lake Mogan watershed and in watersheds showing similar characteristics with Lake Mogan.

CHAPTER 2

LITERATURE REVIEW AND THEORETICAL BACKGROUND: DIFFUSE POLLUTION AND SWAT MODEL

2.1. Diffuse Pollution and Its Sources

Water pollution is defined as "the man-made or man-induced alteration of chemical, physical, biological, and radiological integrity of water." by the Clean Water Act, Section 502-19 (U.S. Congress, 1987). In Turkish Water Pollution Control Regulation, water pollution is described as "… the alteration in the chemical, physical biological, and radiological condition of a water resource, and either directly or indirectly, discharge of material and energy wastes, which creates distortions in the biological resources, human health, fisheries, water quality, and water use for other purposes.

The sources of water pollution associated with human activities are divided into two broad categories as diffuse or nonpoint source (NPS) pollution and point source pollution. Point sources of pollution are defined as the identifiable discrete discharges, and they are easy to measure (Novotny, 2003). They are also known as "end of pipe" sources of pollution (Hranova, 2006). Point source pollution is mainly generated from sewered municipal and industrial wastewater sources (Novotny, 2003). Municipal wastewater has a quite stable characteristics which makes it easy to examine in terms of characteristic quality parameters. The characteristics of industrial wastewater, on the other hand, is very liable to vary. It depends on the production process. Thus, it is important to understand the production process in order to manage industrial wastewater as a source of pollution (Hranova, 2006). In contrast to point source pollution, diffuse or nonpoint source pollution originates from many diffuse sources (USEPA, 2012b). It enters water bodies in a diffuse manner at intermittent intervals (Novotny, 2003). Diffuse source pollution is closely related to rainfall runoff. Pollutants like sediments, nutrients, pesticides, and pathogens are transported across the land surface as the runoff moves before it reaches to receiving bodies such as lakes, streams, and ground waters (Ritter and Shirmohammadi, 2001; USEPA, 2012b). Diffuse pollution is a function of the characteristics of the area of interest.

Meteorological factors, topographical features, soil types, and land management activities have impacts on diffuse pollution (Ritter and Shirmohammadi, 2001). Therefore, the extent of diffuse pollution from one place to another, and from year to year varies significantly. Unlike point source pollution, monitoring of diffuse source pollution at the source of origin is difficult or even impossible. Consequently, it is not possible to measure diffuse discharges in terms of effluent standards (Novotny, 2003).

The types of diffuse source pollutants deposited into a receiving body change according to the human activities in the watershed. The major categories of these activities can be listed as agriculture, construction, urban runoff, mining, and silviculture. The types of pollutants associated with these categories are given in Table 1 which is adapted from Weiner and Matthews (2003).

Table 1. Major Diffuse Source Pollution Categories[a]

Category	Suspended solids	Dissolved solids	High BOD	Nutrients	Toxic metals	Pesticides	Pathogens	Synthetic organics /hydrocarbons[b]
Agriculture	***	***	***	***	*	***	***	n
Construction	***	n	*	**	n	n	n	n
Urban Runoff[c]	***	**	**	***	***	***	***	***
Mining[d]	**	**	n	n	***	n	n	n
Silviculture	***	n	*	**	n	**	n	n

[a]*** = potentially high pollutant source; ** = moderate source; * = low source; n = negligible source.
[b]Includes industrial solvents and reagents, detergents, oil and grease, petroleum hydrocarbons, and other organics not normally found in surface runoff
[c]Includes residential and urban runoff from buildings, roads, impervious surfaces, and landscaped areas.
[d]Primarily abandoned mine sites; active mine sites are usually regulated as point sources.

The main constituents of agricultural or rural runoff are composed of solids both in the suspended and dissolved forms, biodegradable organic matter, nutrients due to fertilizer applications, pesticides, and pathogens. Suspended solids and sedimentbound nutrients like phosphorus are the major compounds found in runoff originated from construction and silviculture sites (Weiner and Matthews, 2003). In pollution arising from urban areas which is the consequence of imperviousness, population, and traffic density, it is possible to observe each kind of pollutant shown in Table 1. As compared to agricultural runoff, urban runoff has higher volume and quantity.

Agricultural diffuse pollution, which is actually the main subject of this thesis study, is associated with agricultural activities such as tillage operations, fertilizer and

pesticide applications, and animal operations. Excessive application of fertilizers would result in soil enrichments with nutrients if the application rates exceed the assimilative capacity of the crops. It may even pollute the groundwater resources when the polluted runoff infiltrated through the soil (Hranova, 2006). Another major case representing one of the serious diffuse pollution problem related to agricultural activities is the irrigation return flow. Irrigation return flow is defined as the excess irrigation flow, and it has higher salt concentrations compared to original water used for irrigation (Hranova, 2006). Inadequate drainage in agriculture ends up with the salinization of soil and irrigation return flows (Novotny, 2003). This is usually the case in arid regions having high evaporation rates. In addition, when the irrigation return flow is reused by the downstream users, there occurs a repeated cycle of salinization (Hranova, 2006).

The pollutant loads resulting from agricultural activities depend on several factors. Novotny (2003) listed these factors as types of land use, types of crops or animals, crop rotation, soils on which crop is grown, climatic conditions, farming technology, irrigation and drainage, and proximity of polluting agricultural operations to watercourses.

According to United States Environmental Protection Agency (USEPA, 2012a) agricultural diffuse pollution was reported as "the leading source of water quality impacts on surveyed rivers and lakes, the second largest source of impairments to wetlands, and a major contributor to contamination of surveyed estuaries and ground water" in the 2000 National Water Quality Inventory. Therefore, it is really important to identify and control diffuse pollution sources together with point sources in terms of protecting and improving the quality of water resources. The importance of the control measures is greater especially for countries like Turkey where agricultural and livestock operations are widespread.

2.2. Agricultural Best Management Practices

Best management practices (BMPs) are defined as the soil and water conservation practices including social and cultural actions which have been recognized as the effective and practical ways for the environmental protection (Sharpley et al., 2006). BMPs are commonly designed with the purpose of ensuring the efficient use of agricultural chemicals; enhancing soil cover; reducing the velocity of surface runoff,

and improving the management of livestock waste (Cestti et al., 2003). Troeh et al. (2004) stated that soil and water conservation methods are usually classified into two as vegetative and mechanical practices. Vegetative practices ensure denser vegetative cover for a longer period. Crop rotation, efficient use of fertilizers, and narrow row spacing can be given as examples of vegetative practices. These practices provide both improved product yield and erosion control. Mechanical practices are different from the vegetative ones in a way that they permit growing of plants which provide less soil protection but reducing the erosion at the same time. Contour tillage, no tillage, and terrace systems are some of the mechanical BMPs. Novotny (2003), on the other hand, categorized BMPs under three categories as structural, vegetative, and management. The author also added that the effectiveness of each BMP changes according to the pollutant specie in concern. Moreover, it was stated that the pollutants and the forms of them while they are transported should be noted to select the proper BMPs for the pollution removal. In the report prepared by Minnesota Department of Agriculture (Miller et al., 2012), the removal efficiencies of agricultural BMPs were discussed based mainly on the monitored research data but some modelling studies especially strong and practical ones were also taken into account. According to this report the BMPs are classified as avoiding, controlling, and trapping BMPs. Avoiding BMPs aim at preventing the entry of pollutants into the environment while the controlling ones are used to control the risk of pollution if avoiding is not possible. Trapping BMPs are specified as the last step in order for catching the pollutants close to its source. In Table 2, list of BMPs according to categories is provided as adapted from Miller et al., (2012).

Within the scope of thesis study nutrient management, conservative tillage methods, contour farming, and terracing were considered. Nutrient management involves practices aiming to reduce the availability of excess nutrients by controlling the timing, application rate, and location selection for fertilizer application. Conservation tillage is defined as “any tillage or planting system in which at least 30% of the soil surface is covered by plant residue after planting to reduce erosion…” (Schertz, 1988). Troeh et al. (2004) stated that to select the appropriate implementation conservation tillage has to be flexible.

Table 2. Type of Best Management Practices

Type of BMPs		
Avoiding	**Controlling**	**Trapping**
Conservation Cover	Alternative Tile Intakes	Filter Strips and Field Borders
Conservation Crop Rotation	Contour strip-cropping	Sediment Basin
Contour Farming	Controlled Drainage	Grade Stabilization at Side Inlets
Cover Crops	Culvert Sizing/ Road Retention/Culvert Downsizing	Water and Sediment Control Basin
Grade Stabilization	Grassed Waterways	Constructed (Treatment) Wetlands
Livestock Exclusion/ Fencing	Irrigation Management	Wetland Restoration
Nutrient Management	Waste Storage Facility	Woodchip Bioreactor (Denitrification Beds)
Pest Management	Conservation Tillage	
Tile System Design	Riparian and Channel Vegetation	
	Rotational Grazing	
	Terrace	
	Two Stage Ditch	
	Feedlot/Wastewater Filter Strip and Clean Runoff Water Diversion	

In other words, while in some cases it would be necessary to leave all residue in the surface, it may be sometimes required to integrate part of the residue. In fact, deciding on the proper implementation necessitates the knowledge on the amount of residues required to control erosion, the quantity of residue available, and the fraction of residue integrated with each tillage operation. Novotny (2003) defined a terrace as "an earthen embankment, channel, or a combination ridge and channel constructed across the slope to intercept runoff." In humid regions, the terraces are functioning as the

structures improving the quality of water by reducing the rill erosion, avoiding the formation of gullies, and permitting the settling of sediment from the surface runoff. Terracing provides holding of surface runoff and, therefore the amount of water available for crops is enhanced in dry areas (Schwab et al., 1993). Contouring or the contour farming is plowing and the crops are planted so that field contours across the slope. Contouring is used for both erosion control in humid regions and for increasing soil moisture by decreasing runoff losses in sub-humid regions (Novotny, 2003; Troeh et al., 2004).

2.3. Watershed Modeling

The improvements and developments in economics and living standards has increased the dependency on water resources dramatically. Better living standards has resulted in more urbanization and industrialization, increased energy use, and more irrigation due to intensive agricultural activities. All of these advances has put more pressure on water resources. Reliable water supply to growing population, and control of water pollution stand as challenging tasks for the water resources managers, engineers, researchers, and especially for decision makers. These difficulties require that all of the individual processes and systems in a natural environment, and the interactions between them are examined in an integrated manner. Better understanding in physical, chemical, and biological processes influencing the quality of water bodies, and improvements in data monitoring, collection and analysis allows enhanced examination of watershed-scale processes. Therefore, watershed modeling which is the mathematical representations of components of the hydrologic cycle (Daniel et al., 2011), is an important tool to comprehend surface waters and groundwater resources, and to find out the interactions between the water bodies. In areas such as water quality and management of water resources, watershed models are very useful tools especially for decision making.

Watershed models can be examined under several groups according to the modelling approaches used in the model development (Daniel et al., 2011). The models can be empirical, conceptual, or physically based depending on the algorithms used. Empirical models use the statistical relationships between the input parameters and watershed characteristics (Singh and Frevert, 2006). Physically based models, on the other hand, use physically based equations which are derived based on the hydrologic

and water quality processes occurring in the watershed (Daniel et al., 2011). In addition, the watershed models can be categorized as either stochastic, or deterministic based on how input parameters are specified. Moreover, depending on the ability to represent spatial variability in watershed characteristics they are categorized into two as lumped and distributed models (Singh and Frevert, 2006). In fact, the model outputs are significantly depended on the methods used to develop the watershed model (Parajuli and Ouyang, 2013). In order to select the most suitable model for the watershed modeling studies, it is important to consider data availability, the capability of model to simulate design variables, accuracy, and temporal and spatial scales (Singh and Frevert, 2006).

The application areas of watershed models are numerous. In the process of dealing with various environmental and water resources problems, watershed models play an important role. They are used to evaluate the effects of human activities performed within the watershed on water quality and quantity of the receiving water bodies (Singh and Frevert, 2002). Furthermore, estimation of the pollutant loads transported to water bodies, and assessment of the effectiveness of abatement strategies like BMPs are carried out with the help of watershed models (Singh and Frevert, 2006). Especially for the evaluation of different BMPs on a watershed-scale, watershed models stand out as a useful tool since they provide an inexpensive and time saving way.

The first model which was built with the purpose of simulating the whole hydrologic cycle within a watershed is the Stanford Watershed Model – SWM. SWM was developed in 1966 by Crawford and Linsley (Crawford and Linsley, 1966). Since then, numerous mathematical models have been developed, and there has occurred a significant increase in the number of physically based models (Singh and Frevert, 2002). Some of the most common and widely used watershed models based on a literature review (Arheimer and Olsson, 2003; Borah and Bera, 2003; Oogathoo, 2006; Parajuli and Ouyang, 2013; Shen et al., 2011; Singh and Frevert, 2002; Xie et al., 2015) can be listed as follows: Agricultural Nonpoint Source Pollution (AGNPS)/ Annualized Agricultural Nonpoint Source (AnnAGNPS), Areal Nonpoint Source Watershed Environment Response Simulation (ANSWERS/ANSWERS-2000), Hydrological Simulation Program – FORTRAN (HSPF), the European Hydrological

System model or MIKE SHE, Storm Water Management Model (SWMM), and Soil and Water Assessment Tool (SWAT).

Among the watershed scale models AGNPS, AnnAGNPS, HSPF, and SWAT were identified as models for the assessment of agricultural BMPs (Xie et al., 2015). Since the evaluation of the agricultural BMPs is the main subject of this thesis, further information on these models are provided in Table 3. Among the given watershed models in Table 3, AnnAGNPS, HSPF, and SWAT are able to perform continuous simulations. Therefore, they are handy for examining the long-term impacts of hydrological modifications and watershed management practices. Moreover, Borah and Bera (2003) stated that these three models are able to simulate all major components (hydrology, sediment, and chemical) applicable to watershed-scale catchments. While HSPF is more favorable in watersheds with mixed agricultural and urban land uses, SWAT is favorable when the watershed is dominated with agricultural lands. Gassman et al. (2007) expressed that SWAT enables more effective watershed management and the development of better-informed policy decisions since it allows integration of various environmental processes. Moreover, Xie et al. (2015) specified that SWAT is more advantageous compared to other watershed models regarding the assessment ability. For instance, land use change (LUC) module of SWAT allows modification of fractional coverage of land use types in each hydrologic response units (HRUs). In addition, it is possible to adjust the amount, timing, and period of agricultural activities for BMPs addressing source loading reduction.

In their study, Glavan and Pintar (2012) identified SWAT as an easily available on-line model. Furthermore, they mentioned that there are numerous tools, interfaces and support software for SWAT owing to over 20 years work on model development. The simulation of agricultural environmental measures and best management practices was specified as the crucial power of SWAT model. Yang (1997) stated that SWAT is a very powerful tool for the evaluation of agricultural management practices on water quality problems thanks to its distributed-parameter and continuous-time simulation, and flexible watershed configuration. Randall (2012) selected SWAT model for his study to assess water quality benefits of agricultural conservation practices due to its ability to represent watershed properties spatially throughout the watershed.

Table 3. Brief information about the watershed models regarding BMPs assessment (adapted from Xie et al., (2015)).

Models	Temporal Resolution	Spatial Representation	Overland Flow Routing	Overland Sediment Routing	Channel Processes	Developer
AGNPS	Storm-event; One storm duration as a time step.	Cells of equal size with channels included.	SCS-CN[a] method for infiltration, and flow peak using a similar method with SWAT.	USLE[b] for soil erosion and sediment routing through cells with *n*, USLE factors to be concerned with.	Included in overland cells.	USDA[c]
AnnAGNPS	Continuous; daily or sub-daily time steps	Cells with homogeneous soil and land use.	SCS-CN method for infiltration and TR-55[d] method for peak flow.	RUSLE[e] to generate soil erosion daily or user-defined runoff event.	Channel degradation and sediment deposition with Modified Einstein equation and Bagnold equation.	USDA
HSPF	Continuous; variable constant steps (from 1 min up to 1 day).	Pervious and impervious land areas, stream; hydrologic response units.	Philip's equation for infiltration.	Rainfall splash and wash off of detached sediment calculated by an experimental non-liner equation.	Non-cohesive and cohesive sediment transport.	USGS[f] and USEPA[g]
SWAT	Continuous; Daily or sub-daily time steps.	Sub-basins or further hydrologic response units defined by soil and land use/land cover.	SCS-CN method for infiltration and peak flow rate by modified Rational form	MUSLE[h] represented by runoff volume, peak flow rate, and USLE factors.	Channel degradation and sediment deposition process including channel-specific factors.	USDA

[a] Soil Conservation Service Number; [b] Universal Soil Loss Equation; [c] United States Department of Agriculture; [d] Technical Release – 55; [e] Revised Universal Soil Loss Equation; [f] United States Geological Survey; [g] United States Environmental Protection Agency; [h] Modified Universal Soil Loss Equation

Jayakrishnan et al. (2005) stated that SWAT is a tool possessing a good potential for both time and cost-effective watershed studies and decision-making. Gassman et al. (2014) reported that as of the 2014 International SWAT Conference, 1700 SWAT-relevant studies were included in the SWAT Literature Database for Peer-Reviewed Journal Articles. These articles can be easily accessed from the homepage of SWAT model (USDA-ARS and Texas A&M, 2015). Due to its ability to simulate land management processes in large agricultural watersheds, to perform continuous simulations, to integrate a number of environmental processes and to provide better assessment ability in terms of agricultural best management practices, SWAT model

was chosen with the purpose evaluating several best management practices in Lake Mogan watershed. Having a comprehensive, easily accessed and rich documentation, and wide application in all over the world can also be listed among the reasons for selecting SWAT in this study. In the following sub-sections, more detailed information on SWAT model was provided.

2.3.1. Soil and Water Assessment Tool (SWAT)

SWAT Model was developed by United States of Agriculture - Agricultural Research Service (USDA-ARS) together with Texas A&M AgriLife Research with the purpose of predicting the impact of management practices on water, sediment and agricultural chemical yields in large ungauged basins (Arnold et al., 1998; Neitsch et al., 2002; USDA-ARS and Texas A&M, 2015). It is a conceptual, continuous time model that operates on a daily time step. The model has been used in many studies to estimate the impacts of climate change, to calculate pollutant loads and to evaluate the best management practices all over the world (Arabi et al., 2008; Chaplot et al., 2004; Dechmi et al., 2013; Dechmi et al. 2012; Kersebaum et al., 2003; Lam et al., 2011; Lee et al., 2010; Sood et al., 2013; Zhai et al. , 2014).

In order to carry out simulations SWAT divides a watershed into a number of sub-basins. These sub-basins are then subdivided into units having unique soil and land use properties. The name given to these units is hydrologic response units (HRUs) (Neitsch et al., 2002). HRUs are represented as a percentage of the sub-watershed area (Arnold et al., 2012a). In SWAT a sub-basin consists of at least one HRU, a tributary channel and a main channel so called reach. The HRUs in one sub-basin do not interact with each other. In other words, the loadings, e.g., sediment and nutrient loadings, from each HRU are calculated individually. Then, total loadings from the sub-basin are calculated by summing up the loadings from each HRU (Neitsch et al., 2002). The sub-basin components of SWAT are divided into 8 main modules. These modules are as follows: hydrology, weather, sedimentation, soil temperature, plant growth, nutrients, pesticides, and land management (Santhi et al., 2001).

HRUs are the smallest unit where the hydrological processes are calculated in SWAT. Since every mechanism simulated by SWAT depends on water balance, it is crucial to make sure that the hydrological cycle or the hydrological processes in the watershed are simulated correctly. This is important because the truthful representation of the

movement of sediment, nutrients, and pesticides depends on a well simulated hydrological cycle (Neitsch et al., 2009). The schematic representation of the hydrological cycle is provided in Figure 1. The primary hydrological processes simulated by SWAT are canopy interception of precipitation, evapotranspiration, infiltration, surface runoff, subsurface flow, base flow, soil moisture redistribution and percolation to deep aquifer (Tuppad et al., 2010). The hydrological processes can be categorized into two phases as land phase and channel/floodplain phase. In land phase sediment, nutrient and pesticide loads carried by runoff are calculated for each HRU. Then, the area-weighted loads are determined at sub-basin level. In channel/floodplain phase, the model routes the upland loadings from each sub-basin through the channel/stream network (Neitsch et al., 2009; Tuppad et al., 2010).

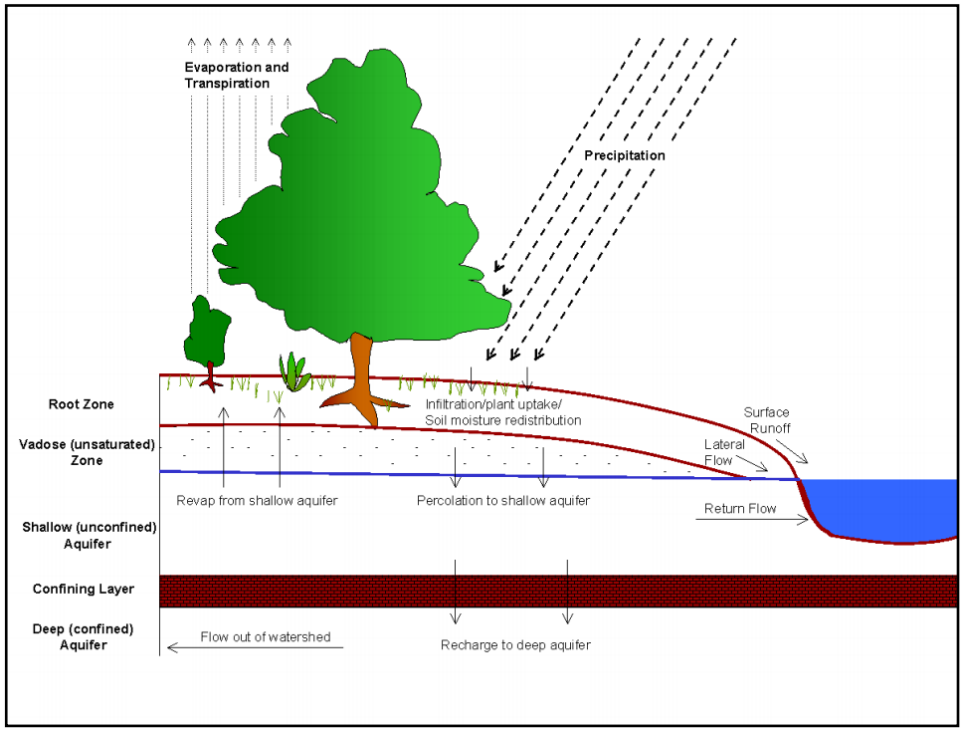

Figure 1. Schematic representation of the hydrologic cycle (adapted from Neitsch et al., 2009)

SWAT considers the following water balance equation in order to simulate hydrological cycle:

$$SW_t = SW_0 + \sum_{i=1}^{t} (R_{day} - Q_{surf} - E_a - w_{seep} - Q_{gw}) \qquad (1)$$

where SW_t is the final soil water content (mm H_2O), SW_0 is the initial soil water content on day i (mm H_2O), t is the time (days), R_{day} is the amount of precipitation on day i (mm H_2O), Q_{surf} is the amount of surface runoff on day i (mm H_2O), E_a is the amount of evapotranspiration on day i (mm H_2O), w_{seep} is the amount of water entering the vadose zone from the soil profile on day i (mm H_2O), and Q_{gw} is the amount of return flow on day i (mm H_2O) (Neitsch et al., 2009).

The required meteorological variables to simulate the hydrological processes are precipitation, maximum and minimum air temperature, solar radiation, wind speed and relative humidity (Arnold et al., 1998). Indeed, the required variables changes depending on the evapotranspiration method selected during the model simulations (Tuppad et al., 2010). For each sub-basin runoff is estimated separately by taking into account the differences in evapotranspiration for different crops, soils etc. Then, the total runoff for the basin is calculated by routing the runoff from individual sub-basins (Arnold et al., 1998). To estimate the surface runoff, SCS curve number method (Soil Conservation Service Engineering Division, 1972) or Green & Ampt infiltration method (Green and Ampt, 1911) can be used (Tuppad et al., 2010).

Evapotranspiration is a term comprising all of the processes by which liquid or solid phase water at or near earth surface transforms to atmospheric water vapor. Potential evapotranspiration, on the other hand, is defined as 'the rate at which evapotranspiration would occur from a large area completely and uniformly covered with growing vegetation which has access to an unlimited supply of soil water' (Neitsch et al., 2009). There are three options available within the model to predict the potential evapotranspiration; Hargreaves (Society & Agricultural, 1985), Priestley-Taylor (Priestley and Taylor, 1972), and Penman-Monteith (Monteith and Moss, 1977). Penman-Monteith method's data requirement is the greatest among the three options. To be able to use the Penman-Monteith method, solar radiation, air temperature, wind speed and relative humidity are required. In the absence of relative humidity, wind speed, and solar radiation data, Hargreaves or Priestley-Taylor method can be preferred (Arnold et al., 1998).

Modified Universal Soil Loss Equation (MUSLE) (Williams, 1975) is used to predict erosion and sediment yield in each sub-basin (Neitsch et al., 2009; Santhi et al., 2001). Sediment yield at the outlet of the watershed is affected by the two major processes

namely sediment deposition and degradation. Furthermore, sediment loadings from upland areas and transport capacity of the channel network determine which process takes place (Arabi et al., 2006). For the channel sediment routing, a modification of Bagnold's sediment transport equation (Bagnold, 1977) is utilized (Santhi et al., 2001).

The nitrogen (N) and phosphorus (P) processes are modeled by SWAT through transformation of nitrogen and phosphorus between organic and inorganic pools in the nutrient cycle (Tuppad et al., 2010). Forms and transformations of nitrogen simulated by SWAT is shown in Figure 2. Nitrogen is supplemented to the soil through fertilizer application, manure or residue application, bacteriological fixation, and rain. The removal mechanisms are plant uptake, soil erosion, leaching, volatilization, and denitrification (Lam et al., 2011; Zhai et al., 2014). Nitrogen consumed by plants is predicted by supply and demand approach (Williams et al., 1984). The amount of nitrogen demanded daily by the plant depends on plant biomass and biomass N concentration. The demand is supplied with the available nitrogen in the soil. If the amount of nitrogen required by the plant goes beyond the available nitrogen within the soil root depth, then nutrient stress occurs (Santhi et al., 2001). Estimation of the amount of NO_3-N in surface runoff, lateral flow, and percolation is carried out by multiplying the water volume with the average concentration (Neitsch et al., 2009; Santhi et al., 2001). Transport of Organic-N is predicted with a loading function developed by McElroy et al., (1976) and modified by Williams and Hann, (1978).

Similar to nitrogen, SWAT is able to simulate the movement and transformation of several forms of phosphorus. These forms and transformations of phosphorus is indicated in Figure 3. Phosphorus utilized by plants is estimated by the supply and demand approach as in the case of nitrogen. Soluble P loss in the surface runoff is predicted according to the concept of partitioning pesticides into the solution and sediment phases (Arnold et al., 1998; Santhi et al., 2001). Similar to Organic-N transport, sediment transport of P is estimated by a loading function. SWAT is also able to simulate instream nutrient dynamics including the kinetics of algae growth, nutrient cycling, carbonaceous biological oxygen demand, and dissolved oxygen. This ability is based on the fact that the kinetic routines from an instream water quality model QUAL2E (Brown and Barnwell, 1987) are embedded into SWAT (Abbaspour et al., 2007; Gassman et al., 2007; Santhi et al., 2001).

The required inputs for SWAT model can be categorized under the following basic categories: topography, land use/land cover, soil properties, land management practices occurring in the watershed, and meteorological inputs. Introduction of model inputs of topographic, land use, soil, and other digital data into SWAT can be enhanced via Geographic Information System (GIS) and other interface tools (Chaubey et al., 2005; Gassman et al., 2007). Due to the fact that majority of input data used by SWAT has spatial characters, several GIS interfaces have been developed so far to write SWAT input files and to build, analyze and display spatial information. For instance, Srinivasan and Arnold (1994) integrated SWAT with GRASS (Geographic Resources Analysis Support System) to develop model inputs and to facilitate the analysis of model outputs. Furthermore, Luzio et al. (1998) developed ArcView interface for SWAT comprising three main components. The first component is the preprocessor which produces the sub-basin topographic parameters and model input parameters. The second component is used for modifying input data and performing model runs. Finally, the last component is the postprocessor showing model outputs graphically and in tabular format (Arnold and Fohrer, 2005; Ogden et al, 2001; Olivera et al., 2006). The interface was further developed by Luzio et al. (2002) and the terrain analysis based on digital elevation model (DEM) became available. Another interface, ArcGIS-SWAT, was developed by Olivera et al., (2006). This interface allows user to enter geographic, numeric, and text input data in the ArcGIS environment, and the model results are presented to the user in an organized manner.

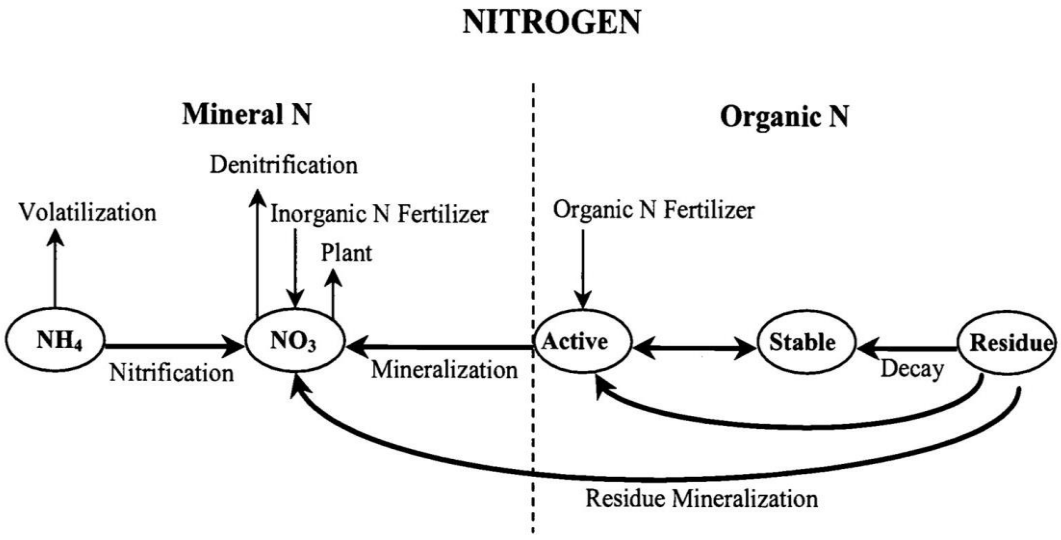

Figure 2. Nitrogen forms and transformations simulated by SWAT (Santhi et al., 2001)

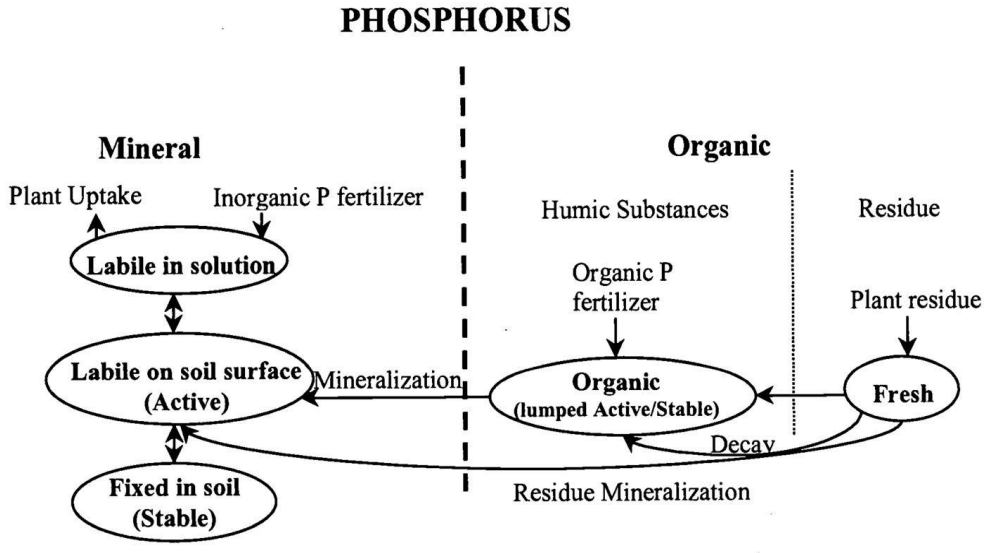

Figure 3. Nitrogen forms and transformations simulated by SWAT (Santhi et al., 2001)

Since the model inputs are of spatial characteristics, GIS data quality with respect to the spatial resolution of data becomes significant. According to Cotter et al. (2003), data resolution may impact the uncertainty in the model outputs and the implementation of the model results. In order to assess the effects of data resolution on the uncertainty of model results, Cotter et al. (2003) used DEM, land use, and soil

data with different spatial resolutions. It was found that the model results are influenced most by the resolution of input DEM. Another important outcome of this study is the suggested resolution ranges for model inputs to achieve less than 10 percent model output error. Minimum resolutions for DEM, land use, and soil data required to attain less than 10 percent errors in the flow, sediment, NO_3-N, and TP predictions are indicated in Table 4.

Table 4. Minimum GIS input data resolutions to attain less than 10 percent error in model predictions (Cotter et al., 2003)

	Minimum Input Data Resolution (m)		
Output	**DEM**	**Land Use**	**Soils**
Flow	300	1000	1000
Sediment	30	30	500
NO_3-N	200	500	500
TP	30	300	500

Luzio et al. (2005), made input combinations with the several available DEM, land use/land cover, and soil maps for their study area. The purpose was to evaluate the effects of input GIS variation on model results; i.e., water runoff and sediment yield. It was found that realistic representation of watershed, the boundaries of the sub-basins, and the topographic input is closely related to DEM selected. Moreover, runoff and sediment yield outputs are affected considerably according to the details of land use map utilized in the model simulations. The model predictions are not altered very much when the format and scale of the soil map is changed. Kim et al. (2012) carried out a study in the Imha watershed in Korea with the purpose of evaluating model predictions with different resolutions of input data; i.e., DEM, land use/land cover, and soil map. The study revealed that the most efficient model predictions of runoff and suspended sediment were obtained when the highest resolution (30 m) DEM was used in the model simulations. Yet, detailed land use and soil maps did not affect the simulated results significantly. Zhang et al. (2014) examined the sediment yield, dissolved oxygen (DO) load, total nitrogen (TN), nitrate nitrogen (NO_3-N) and total phosphorus (TP) loads, flow, and ammonia nitrogen (NH_4-N) outputs from SWAT by performing simulations with different DEMs having a range of spatial resolutions from 30 to 1000 m. Moreover, the effects of DEM resolutions on the temporal

distribution of the mentioned model outputs were also taken into account. Optimum DEM resolutions obtained within the scope of this study are indicated in Table 5.

Table 5. Optimum DEM Resolutions given by Zhang et al. (2014)

Output	**DEM Resolution (m)**
Flow	30 – 200
Sediment and TP	30 – 100
DO and NO_3-N	30 – 300
NH_4-N	30 – 70
TN	30 – 150

Chaplot (2005) claimed that in order to decide on the optimum resolution for a DEM, the scale of the soil map should also be considered. In other words, GIS input data resolutions relate to one another. Furthermore, the author added that it is crucial to realize the mechanisms behind the changes in the model prediction errors.

The capability of a watershed model to simulate the watershed processes is evaluated via calibration and validation process (White and Chaubey, 2005). Calibration is a process of parameterization of a model so that the model predicts the given conditions well and the model prediction uncertainty is low. Validation, on the other hand, is the evaluation of model performance by running a model with the parameters determined in the calibration, and assessing the results with the observed data not used in the calibration (Arnold et al., 2012b). Sensitivity analysis is the first step before the calibration, and it is the process of determining the most sensitive parameters. Sensitivity of a parameter is assessed by measuring the response of an output variable to a change in an input parameter (White and Chaubey, 2005).

Since SWAT is a physically-based model, it is crucial to note that the calibration of SWAT is not a process of fit to data (Santhi et al., 2001). The values of the parameters must be kept within a realistic uncertainty range (Arnold et al., 2012b). Model calibration can be divided into several steps (Neitsch et al., 2002). In the first step calibration of hydrological processes; i.e. water balance and streamflow, is completed. After the desired results are obtained with the streamflow calibration, the parameters associated with the sediment and nutrients are calibrated respectively. In many studies performed with SWAT, it can be seen that the SWAT calibration is carried out in this order (Engel et al., 2007; Santhi et al., 2001; Santhi et al., 2008). SWAT model can be

calibrated through manual calibration, via auto calibration tools in SWAT, or by using SWAT-CUP (SWAT Calibration and Uncertainty Programs) (Abbaspour et al., 2007).

For the manual calibration of flow, sediment, and nutrients in SWAT model Moriasi et al. (2007) provided a general calibration flowchart based on Santhi et al. (2001). According to this flowchart surface runoff and base flow are separated from each other initially. Then, model outputs; e.g. surface runoff, sediment and nutrients, are calibrated by perturbing the proper model parameters and assessing the regression statistics. The flowchart is shown Figure 4. Engel et al. (2007) stated that it is not appropriate to strictly follow the procedure in some cases due to interactions of model parameters. Therefore, it may be possible to deviate from the calibration procedure given by Santhi et al. (2001). The modeler should determine the approach to be followed before beginning model calibration (Engel et al., 2007).

The number of parameters to be adjusted during model calibration in SWAT are various. It is possible to find numerous studies in the literature reporting the SWAT calibration parameters with their respective calibration ranges (Costa et al., 2015; Dechmi et al., 2012; Güngör and Göncü, 2013; Ndomba et al., 2008; Qiu and Wang, 2013) . For instance, Santhi et al. (2001) described input parameters for different model processes used in model calibration. The author reported fifteen different calibration parameters with respect to diverse model processes; i.e. flow, sediment, organic N and P, and mineral N and P. Arnold et al. (2012b) reviewed 64 studies carried out with SWAT model, and summarized the model calibration parameters used in these studies. The table showing the parameters classified by process is given in Table 6.

Prior to model calibration, model performance assessment criteria should be developed. In order to evaluate SWAT model performance during the model calibration and validation process, several graphical and statistical procedures are utilized (Arnold et al., 2012b). After a detailed literature review Nash-Sutcliffe (NS) (Nash & Sutcliffe, 1970), percent bias (PBIAS) (Gupta et al., 1999), and coefficient of determination (R^2) were found to be among the most commonly used criteria to evaluate the model calibration and prediction performance (Dechmi et al., 2012; Faramarzi et al., 2009; Moriasi et al., 2007; Ndomba et al., 2008; Qiu and Wang, 2013; Sahu and Gu, 2009; Santhi et al., 2001; Tuppad et al., 2010). In order to evaluate the

model performance with these statistics there are no explicit standards (Santhi et al., 2001). Nevertheless, Moriasi et al. (2007), provided general performance ratings for a monthly time step, and the ratings are shown in Table 7.

Table 6. Calibration parameters reported in 64 selected SWAT watershed studies (adapted from Arnold et al., (2012b))

Process	Input Parameters						
Surface Runoff	CN2	AWC	ESCO	EPCO	SURLAG	OV_N	
Baseflow	GW_ALPHA	GW_REVAP	GW_DELAP	GW_QWN	REVAPMN	RCHARG_DP	
Snow	SFTMP	SMFMN	SMFMX	SMTMP	TIMP	SNO50COV	SNOCOVMX
Sediment from channels	PRF	APM	SPEXP	SPCON	CH_EROD	CH_COV	
Sediment from landscape	USLE_P	USLE_C	USLE_K	LAT_SED	SLSOIL	SLOPE	
N from landscape	RCN	UBN	GWNO3	ERORGN	NPERCO	ANOIN_EXCL	
P from landscape	PSP	PHOSKD	UBP	PPERCO	GWQMINP	ERORGP	
Pesticides	KOC	HL_SOIL	HL_FOL	WSOL	WOFFW		
Subsurface tile	TDRAIN	GDRAIN	DEP_IMP				
N and P from channels	BC1	BC2	BC3	BC4	RS4	RS5	
Plant growth	GSI	HI	BLAI	PHU	CN_YLD		
Bacteria	BACTRDQ	BACTMIX	BCNST	CFRT_KG	WDPRCH	WDPQ	
Other	BIOMIX	SOL_ROC	MSK_COL	MSK_CO2	CBNINT	SOL_BD	ALPHA_BNR

Table 7. General performance ratings for NS and PBIAS for a monthly time step adapted from Moriasi et al. (2007)

	NS	**PBIAS (%)**		
Performance rating		**Streamflow**	**Sediment**	**N,P**
Very good	$0.75 < NS \leq 1.00$	$PBIAS < \pm 10$	$PBIAS < \pm 15$	$PBIAS < \pm 25$
Good	$0.65 < NS \leq 0.75$	$\pm 10 \leq PBIAS \leq \pm 15$	$\pm 15 \leq PBIAS \leq \pm 30$	$\pm 25 \leq PBIAS \leq \pm 40$
Satisfactory	$0.50 < NS \leq 0.65$	$\pm 15 \leq PBIAS \leq \pm 25$	$\pm 30 \leq PBIAS \leq \pm 55$	$\pm 40 \leq PBIAS \leq \pm 70$
Unsatisfactory	$NS \leq 0.50$	$PBIAS \geq \pm 25$	$PBIAS \geq \pm 55$	$PBIAS \geq \pm 70$

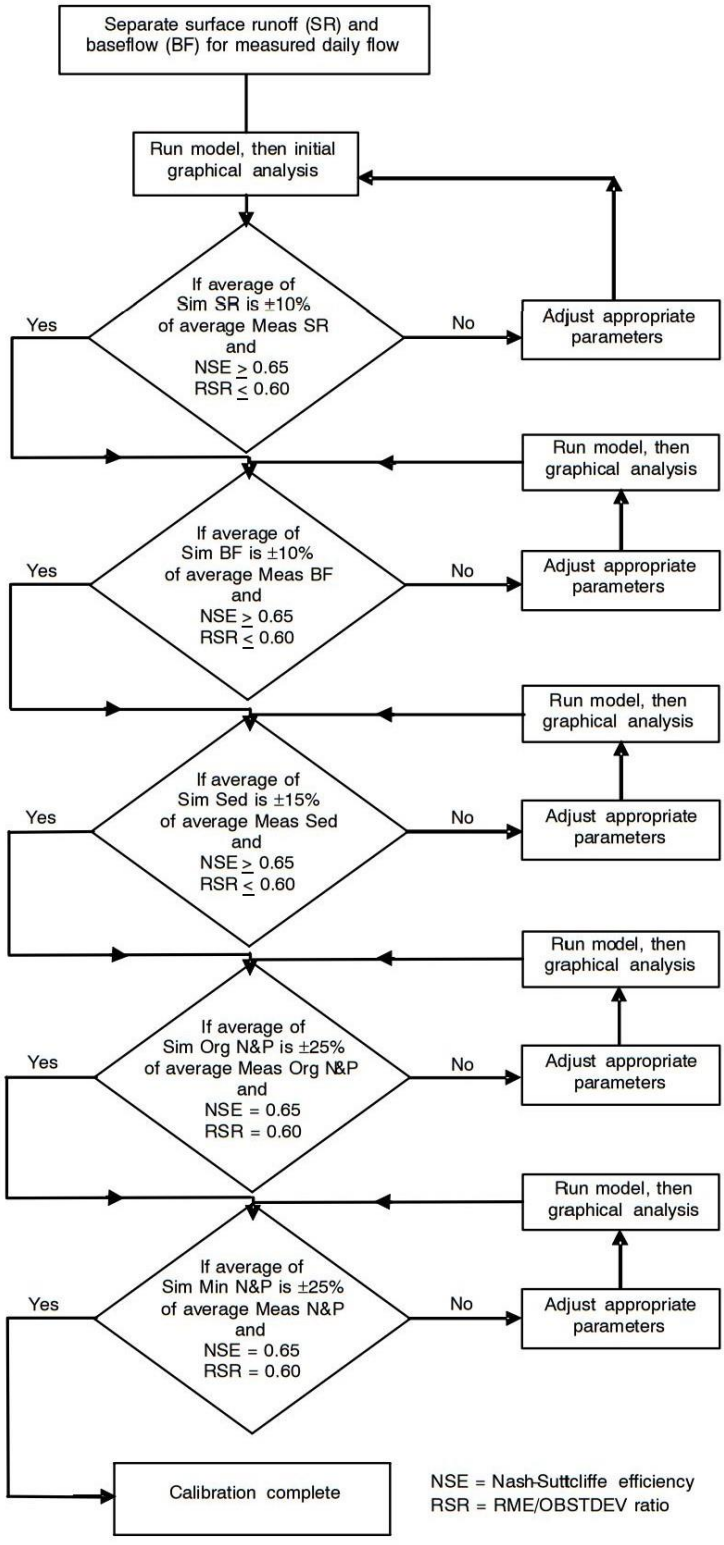

Figure 4. Flowchart for the calibration of flow, sediment, and nutrients in SWAT model adapted from Moriasi et al. (2007)

In addition to manual calibration, SWAT model can be calibrated via auto calibration tools, and SWAT-CUP. SWAT-CUP (Abbaspour et al., 2007) is a public domain

computer program developed for calibration of SWAT model. SWAT-CUP program allows sensitivity analysis, calibration, validation, and uncertainty of SWAT models by using the Sequential Uncertainty Fitting ver. 2 (SUFI-2), Particle Swarm Optimization (PSO), the Generalized Likelihood Uncertainty Estimation (GLUE) (Beven and Binley, 1992), Parameter Solution (ParaSol) (Griensven and Meixner, 2006), and Markov Chain Monte Carlo (MCMC) (Kuczera and Parent, 1998) procedures. SUFI-2 method takes into consideration of all sources of uncertainties, i.e. input data (e.g. precipitation), conceptual model, model parameters and observed data (Abbaspour et al., 2007). In SUFI-2, model output uncertainty is computed by the 95% prediction uncertainty (95PPU). 95PPU is determined at the '2.5% and 97.5% levels of the cumulative distribution of an output variable' which is obtained through Latin hypercube sampling (Abbaspour et al., 2007). The goodness of fit is determined by the p-factor and the r-factor. While the p-factor is 'the percentage of measured data bracketed by the 95% prediction uncertainty', r-factor is 'the average thickness of the 95PPU band divided by the standard deviation of the measured data'. An ideal model simulation in which 100% of the observed data is bracketed within the model prediction uncertainty is with a p-factor of 1 and r-factor of 0 (Abbaspour et al., 2007; Abbaspour, 2015). Rocha et al., (2015) used SWAT model to evaluate the sustainable agricultural practices in the Vouga catchment in Portugal. In order to carry out model calibration and uncertainty analysis SUFI-2 method within SWAT-CUP was utilized. The authors stated that SUFI-2 method was preferred since this algorithm is very efficient for both small and large watersheds. Meaurio et al., (2015) performed a study in the Aixola, a small forested watershed, to assess SWAT model's capability to simulate the runoff generation processes. SWAT-CUP was adapted for auto calibration of the model. In their study Liu et al. (2016) aimed to identify critical source areas (CSAs) for controlling nonpoint source pollution in the Xiangxi River watershed in China. For this purpose they used SWAT model, and SUFI-2 algorithm provided by SWAT-CUP was selected for the calibration and validation of the model. It is possible to find numerous studies in the literature in which calibration and validation of the SWAT model was performed with SWAT-CUP (Costa et al., 2015; Vilaysane et al., 2015; Yesuf et al., 2015).

2.3.2. SWAT Model Applications

The first major application of SWAT model was in the context of the Hydrologic Unit Model of the U.S. (HUMUS) Project (Arnold et al., 1999). In this project, SWAT model was used with the purpose of predicting the hydrological and pollutant losses due to agricultural and municipal water use, tillage trends, cropping systems and some other scenarios (Williams et al., 2008). In their study Arnold and Fohrer (2005) compiled the papers published in the first International SWAT Conference held in August 2001 in Germany. They stated that SWAT applications within the USA addressed the effects of land use change management and climate change on water supply and water quality. In addition, they specified that in Europe SWAT model was generally applied within the scope of the suitability for the European Framework Directive. Gassman et al. (2007) grouped SWAT applications reported in the literature into nine categories as calibration and/or sensitivity analysis, climate change impacts, GIS interface descriptions, hydrologic assessments, variation in configuration or data input effects, comparison with other models or techniques, interfaces with other models, and pollutant assessments. The authors also provided the number of studies carried out under each category. Gassman et al. (2014) overviewed 22 different SWAT-related studies, and presented the summary of these studies in their paper. The studies were collected under four major categories. The first category was named as hydrologic foundations. Most of the studies presented in this category performed hydrologic testing by performing sensitivity and/or uncertainty analyses, manual and/or automatic calibration, and model validation. Then, the model performance was assessed by means of statistical and/or graphical methods. The second category, sediment transport and routing analyses, includes the studies reporting sediment yield and/or transport results, and the factors affecting the model results such as input data resolution and variations in landscape features. The third category is nutrient and pesticide transport. The studies placed in this category applied SWAT model to perform nutrient and/or pesticide transport simulations. The last category, scenario analyses, involves a number of studies evaluating climate change impacts and the impact of BMPs on water quality. Application of SWAT model to assess the impacts of BMPs is a common practice. The number of studies reporting the results of BMP scenario analysis with SWAT is quite high. For instance, Bracmort et al. (2006) used SWAT model to determine the long-term impacts of structural BMPs on sediment and

phosphorus loads in Black Creek watershed in northeastern Indiana. Santhi et al. (2006) assessed the long-term impact of water quality management plans on sediment and nutrient loadings at the farm level and watershed level in West Fork Watershed of Trinity River Basin in Texas, USA. Lam et al. (2011) aimed to evaluate the impact of agricultural BMPs on water quality in a North German lowland catchment. Boithias et al. (2014) used SWAT model to assess a 20% nitrogen application rate reduction scenario in an agricultural watershed in France. Liu and Lu (2014) evaluated the effects of individual and combined BMPs including no tillage, reduced fertilizer application rates and treating domestic sewage on total nitrogen and total phosphorus loads.

CHAPTER 3

APPLICATION OF SWAT MODEL IN LAKE MOGAN WATERSHED

The objective of this study was to evaluate and compare the impacts and effectiveness of several agricultural BMPs on pollution removal in a semi-arid watershed, Lake Mogan. With this purpose, a continuous, long-term, distributed parameter model, SWAT, was used. The model was calibrated at Yavrucak monitoring station and validated at Sukesen monitoring station for the time period between 2007 and 2010. SWAT model input requirements substantial input information. Digital Elevation Model (DEM), soil map, land use/land cover (LULC) map, meteorological data and information about agricultural practices are required to build the model. The sources and definitions of data for Lake Mogan watershed are summarized in Table 8. In the following sub-sections in this chapter, detailed information about the model inputs and the calibration procedure is provided. The calibrated and validated model was used to compare different BMPs. To this end, 11 BMP scenarios were created including fertilizer management, different tillage practices, contouring and terracing. Description of the scenarios and the procedure to represent them in SWAT were explained in the following sub-sections.

Table 8. Model Input Data for Lake Mogan Watershed: Sources and Descriptions

Data Type	Source	Data Description/Properties
Topography	General Command of Mapping	SWAT uses DEM to create sub-basins.
Soil	Field survey (Alp et al. 2014)	Soil physical properties like bulk density, hydraulic conductivity, texture etc. are used by SWAT to estimate the amount of surface runoff and its content.
Agricultural Practices Information	• Gölbaşı District Directorate of Food, Agriculture and Livestock • Central Research Institute of Soil Fertilizer and Water Resources	Agricultural crops grown in the watershed, all types of agricultural practices used during the cultivation of the products (tillage, fertilizers, pesticides etc.) are required by SWAT.
Land use	RAPIDEYE (Alp et al. 2014) (May 7th 2013)	Land use classification (agricultural land, pasture, forest etc.) is required for the definition of HRUs.
Meteorology	General Directorate of Meteorology	Precipitation, temperature, relative humidity, wind speed and solar radiation data are used in the model.

3.1. Study Area

Lake Mogan (39 °47'N 32°47'E) is one of the important natural lakes found within the boundaries of Ankara, the capital city of Turkey. The lake is located in Gölbaşı District 20 km south of Ankara. The watershed (Figure 5) has a drainage area of 970 km^2 with elevations ranging from 960 to 1700 m. The surface area of Lake Mogan is reported as 5.67 km^2 in Ankara Provincial Environment Status Report (Çevre ve Şehircilik İl Müdürlüğü, 2013). Average depth of the lake is around 3 – 5 meters. Lake Mogan is an alluvial dam lake which was formed as a result of the collapse caused by the tectonic events (Karakaya et al., 2007).

Lake Mogan is one of the most significant recreational areas for the inhabitants of Ankara. The lake in which the commercial fishery is prohibited offers opportunities for activities like bird watching, sport fishing, oarsmanship, sailing, and outdoor photography. In addition, it is one of the two lakes in Ankara which are the wetlands of international importance. Moreover, the lake is used by more than 200 bird species for housing and reproduction (Özesmi, 1999). In fact, the lake was declared as special

environmental protection region in 1990. In the south of the lake, there are Çökek and Gölcük marshes which cover approximately of 750 hectares. These marshes consist of seasonal wet meadows, deltas, and agricultural lands. Non-arable hydromorphic alluvial area located in the south of the lake is home to rich aquatic life and wildlife (Çevre ve Şehircilik İl Müdürlüğü, 2013).

Water entry to Lake Mogan is irregular and it is through seasonal transient creeks which are usually dry in summer seasons. The most important creeks feeding the lake are Sukesen, Başpınar, Çölova, Yavrucak, Çolakpınar, Tatlım, Kaldırım and Gölcük and they are located in the east-north-west regions of the watershed. Among them Sukesen, Yavrucak, and Çölova creeks are the main creeks supplying water to the lake (Tabiat Varlıklarını Koruma Genel Müdürlüğü, n.d.). Two reservoirs, İkizce and Dikilitaş, located upstream of the lake have a significant impact on the water level of the lake. Moreover, the lake water is flowing to the Lake Eymir via the regulator located in the northeast part of Lake Mogan. Relative contributions of different processes to water input and output in Lake Mogan are shown in Table 9. On average, the most significant contribution to lake water input belongs to surface runoff having 77% ratio. Second major water entry to the lake is through precipitation. Groundwater, on the other hand, has the lowest impact on the lake water with a share of 4%.

The area of the Lake Mogan watershed is large, and the surface area and water capacity of Lake Mogan are quite small compared to that of the watershed area. These are natural factors increasing the pollution pressure on the lake (Tabiat Varlıklarını Koruma Genel Müdürlüğü, n.d.). Furthermore, Lake Mogan has become a kind of water-meadow with large reeds around it and with bottom plants. The pollutants generated from the diffuse and point sources located in the large watershed area are carried to the lake through the creeks drained into the lake. In addition, the creeks feeding the lake and local flows has resulted in sediment accumulation which in turn has created a serious threat for the lake. As a result, biological activities in the lake have accelerated, and eutrophication process has been observed in the lake for the past 20 years. Besides, secondary residence construction, industrial facilities, and illegal hunting are the other factors threatening the ecological life and water quality of Lake Mogan (Karakaya et al., 2007). Since the dominant land use type in the basin is agriculture, diffuse agricultural pollution is another severe problem in the watershed (Karakoç et al., 2003). Within the Lake Mogan watershed, Gölbaşı District is the most

densely populated area. There are 30 settlements in the watershed and the total population is around 122000 (TÜİK, 2015). In short, the ecological integrity of Lake Mogan is under threat due to high level of urbanization, industrial and agricultural activities. Due to its aesthetic, recreational, and ecological values, the long-term sustainability of Lake Mogan is of concern. Thus, several research, planning, and implementation projects are being conducted to develop conservation plans, to protect the integrity of the ecosystem in coordination and cooperation with the relevant public institutions and organizations. In order to improve the quality in Lake Mogan, some measures have been taken, and some measures have been proposed by evaluating their effects with modelling studies. In 2008, for instance, the municipality implemented flow augmentation strategy to increase the lake water level since the depth of the water dropped to 3 meters due to an extended dry season. The water quality model proposed by Muhammetoğlu and Soyupak (2000) was used to evaluate different macrophyte growth control scenarios such as harvesting of macrophyte, and removal of the sediment layer from the lake bottom.

Table 9. Proportions of inflow and outflow components in the water budget of Lake Mogan (Yagbasan and Yazicigil, 2012; Yağbasan and Yazıcıgil, 2009)

Inflow (%)		
Precipitation	Runoff	Groundwater
19	77	4
Outflow (%)		
Evapotranspiration	Withdrawal	Groundwater
53	43	4

3.1.1. Climate

The continental climate is the dominant climate in Lake Mogan watershed. Winters are cold and rainy/snowy, and summers are hot and dry. The average annual precipitation and evapotranspiration were reported as 375 mm and 1476 mm, respectively (Özesmi, 1999). The precipitation falls in the winter and it is mostly in the form of snow and rain. In their study, Yağbasan and Yazıcıgil (2009) reported the average annual precipitation as 334 mm. Yağbasan and Yazıcıgil (2009) also stated that the annual average evapotranspiration was 1092.2 mm. The average values of the climatic characteristics of several years are given in Table 10 which is adapted from Karakaya et al. (2007).

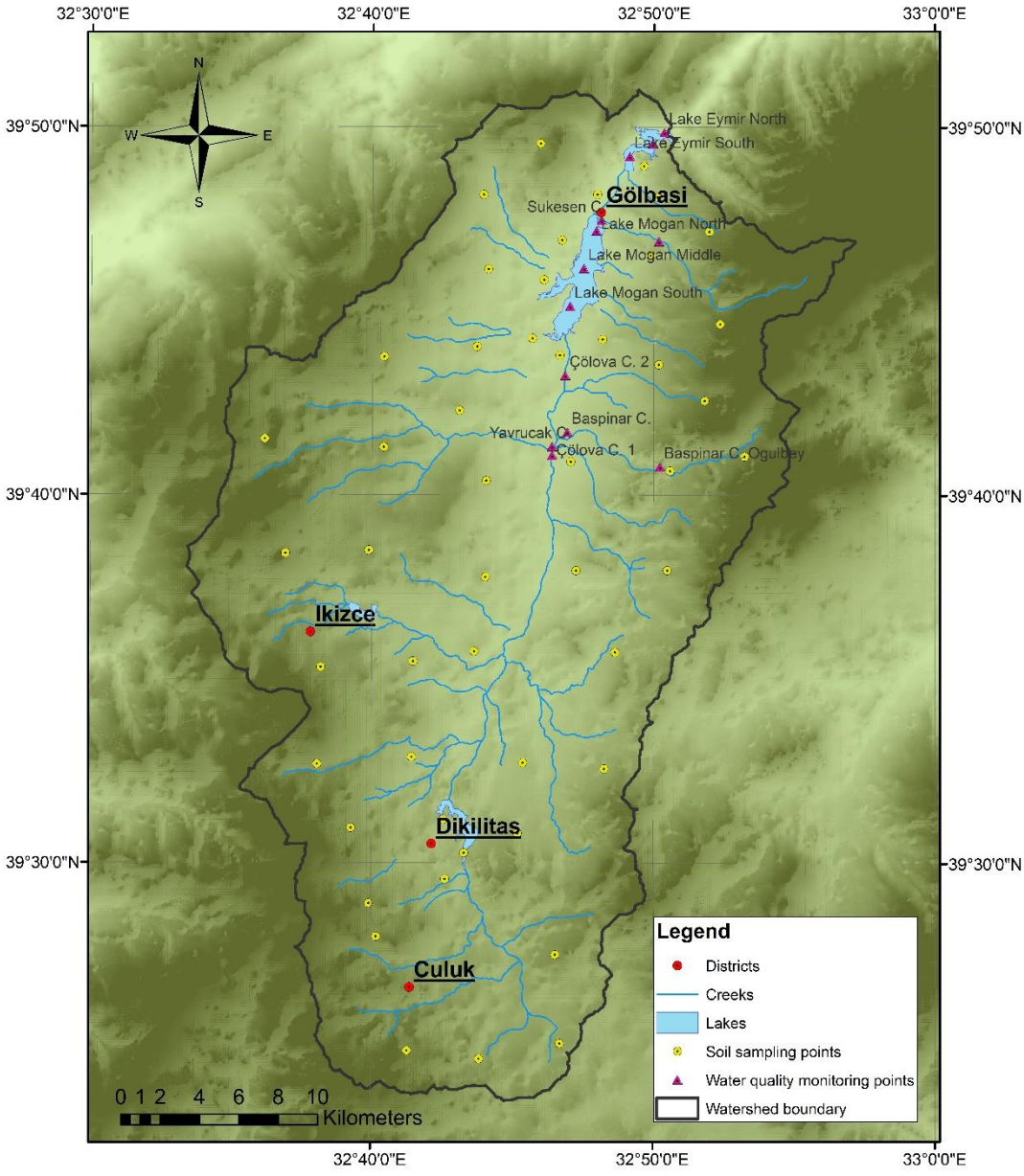

Figure 5. Lake Mogan watershed

As it can be seen from Table 10 the average temperatures in summer months are high while the average amount of precipitation is low in these months. The highest amount of precipitation is observed in April and May. The meteorological data used within the scope of this thesis study was obtained from the General Directorate of Meteorology. Within the boundaries of Lake Mogan watershed there are two automatic meteorological observation stations namely Ufuk Danışment and Haymana

Tarım. The elevation, latitude, longitude information of these stations are provided in Table 11. The weather input data used in the SWAT model belongs to the period of 2007 – 2012 and includes daily precipitation, maximum and minimum daily air temperature, relative humidity, solar radiation, and wind speed. Daily precipitation, maximum and minimum daily temperature data of Ufuk Danışment and Haymana Tarım meteorological stations are shown graphically in Figure 6 and Figure 7, respectively.

Table 10. Average meteorological data for Lake Mogan watershed (Karakaya et al. (2007))

Meterological Data		**Month**												
		1	**2**	**3**	**4**	**5**	**6**	**7**	**8**	**9**	**10**	**11**	**12**	**Yearly**
Temp. (°C)	**Max.**	4.4	6.4	11.3	17	22	26.2	29.8	29.7	26.1	19.8	12	6.6	17.6
	Min.	-2.9	-2.2	0.6	5.6	9.5	12.8	15.8	15.7	11.7	7.4	2	-0.4	6.3
	Ave.	0.4	0.6	5.6	11.1	15.8	19.8	23.1	22.8	18.6	12.9	6.4	2.7	11.8
Precipitation (mm)		41.8	34	38.1	51.3	48.2	36.2	18.9	15	13.7	32.7	38.3	42.3	410.5
Relative humidity (%)		73	71	64	61	58	54	47	47	50	62	70	76	61
Wind speed (m/sec)		1.7	1.8	1.9	1.8	1.9	1.9	2.3	2.2	1.7	1.6	1.5	1.6	1.8
Ave. evaporation (mm)		-	-	-	86.5	146.3	182.1	237.3	222	157.9	87.9	21.6	-	1141.6

Table 11. Information about the automatic meteorological observation stations

Station Number	**Station Name**	**Elevation (m)**	**Latitude**	**Longitude**
17134	Ufuk Danışment	1115	39,8032 N	32,8434 E
17733	Haymana Tarım	1070	39,6130 N	32,6720 E

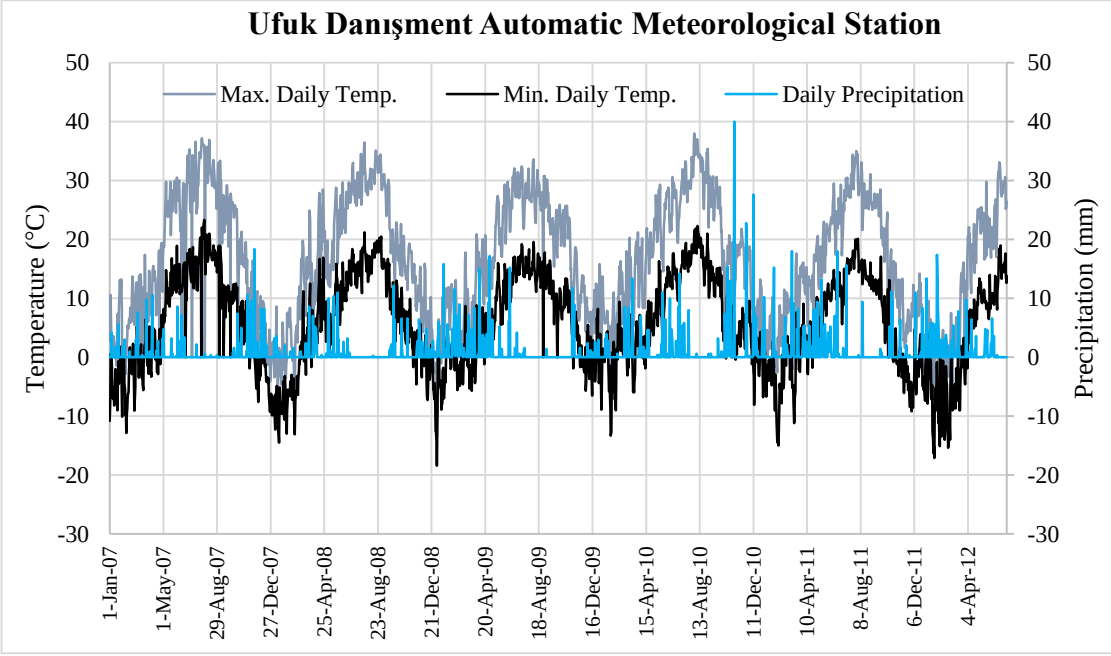

Figure 6. Ufuk Danışment Station: Daily precipitation, max. and min. daily air temperature

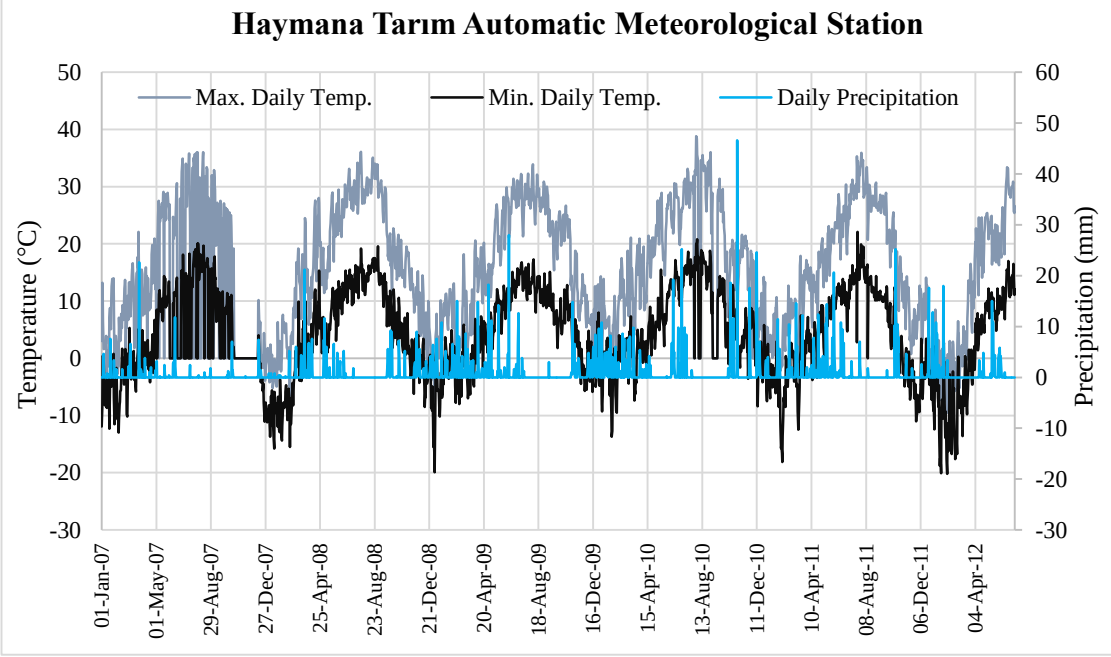

Figure 7. Haymana Tarım Station: Daily precipitation, max. and min. daily air temperature

3.1.2. Topography and Digital Elevation Model (DEM) of the Watershed

Lake Mogan watershed slopes from south to north. The large southern part of the watershed with 972 meters elevation turns into a deep narrow valley in the north at approximately 967 meters elevation. This narrow valley where Lake Eymir is located is connected to Imrahor valley. Lakes Mogan and Eymir were formed as a result of accumulation of stream water behind the natural set which was formed due to aggregation of alluvial materials carried by the rivers into the main valley (Uğur, 2009). Lake Mogan discharges into Lake Eymir with nearly 5 meters elevation difference. Therefore, approximately 98% of water entry to Lake Eymir is provided by Lake Mogan (Tabiat Varlıklarını Koruma Genel Müdürlüğü, n.d.).

Lake Mogan watershed is surrounded by Elmadağ and Küre mountain in the east, by İdris Mountain in the northeast, Mürted lowland and Çile mountain in the west, and Haymana and Sakarya highlands in the south (Uğur, 2009). The watershed has a very low slope in general. Yağbasan and Yazıcıgil (2009) specified the highest and the lowest elevations in the watershed as 1,560 and 980 meters, respectively.

Alp et al. (2014) created the Digital Elevation Model (DEM) of the region covering the whole watershed. In order to generate the DEM, thirty pieces of vector maps in 1/25000 scale were obtained from Turkish General Command of Mapping. These vector maps were used to obtain the DEM by using a geo-statistical method; i.e., simple kriging. The DEM generated is shown in Figure 8. In the map, white and black represents the highest and the lowest elevations, respectively. The highest elevation in the map which also includes the areas outside the watershed boundary is 1,860 meters while the lowest elevation is 798 meters.

3.1.3. Land Use/Land Cover (LULC)

In Lake Mogan watershed, approximately 40% of the total watershed area is used for agricultural purposes. In the agricultural lands, mostly dry farming is practiced. LULC map used in this study was created within the scope of the TÜBİTAK project, namely "Evaluation of Agricultural Diffuse Pollution and its Control Alternatives with SWAT model in Lake Mogan Watershed" with the project number of 111Y284 (Alp et al., 2014). The LULC classification process was accomplished via remote sensing algorithms by using Rapid Eye satellite images. The satellite image dated May 7th, 2013 has five spectral bands. The image with spatial resolution of 5 meters covers the

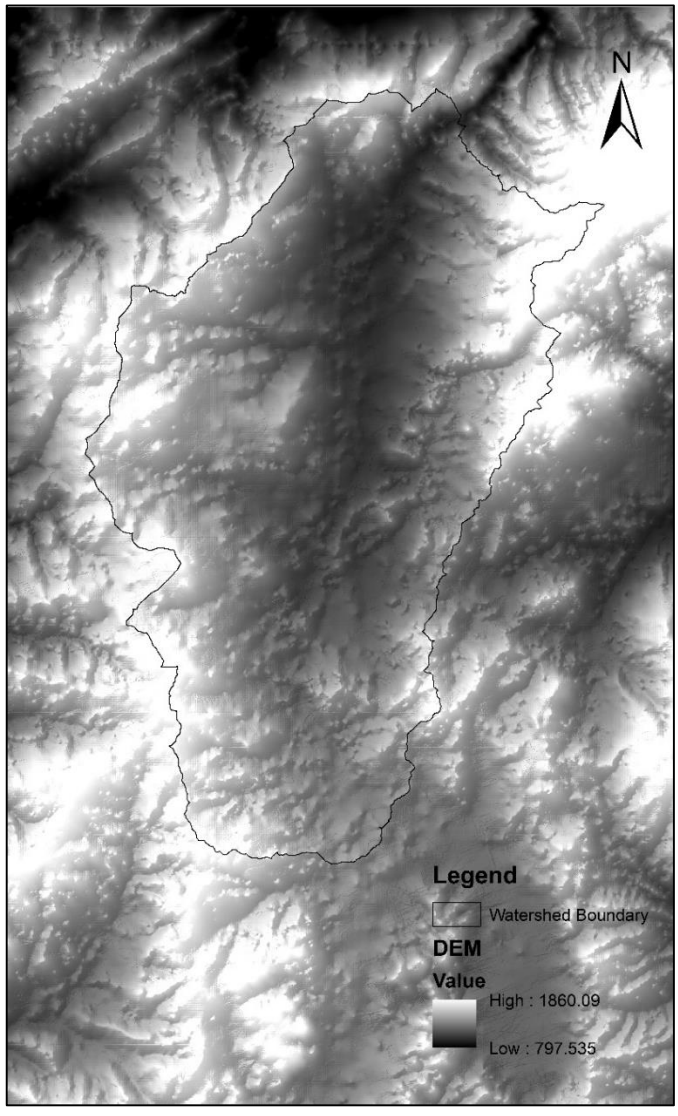

Figure 8. Digital Elevation Model (DEM) of Lake Mogan watershed

whole study area. Nine LULC classes, namely, water bodies, forest, agriculture, road, settlement, mine site, fallowing land, rangeland, and bare land, were used in the classification. Total classification accuracy for the Rapid Eye image data was determined as 70%. Digital Elevation Model (DEM) and its products like slope and aspect were added to image data as additional bands to increase the accuracy. As a result, total accuracy was increased to 80%. Detailed information about the LULC classification of Lake Mogan watershed can be obtained from Alp et al. (2014). In Table 12, the percentages of LULC classes after classification are indicated. As it can be seen from Table 12, total percentage of agricultural lands together with fallowing

and rangelands is nearly 81% while residential areas comprise only 10% of the total watershed area. In Figure 9, LULC map of Lake Mogan watershed is shown.

Table 12. LULC percentages of Lake Mogan watershed

LULC class	Area (km^2)	Ratio (%)
Water	11.74	1.21
Forest	18.62	1.92
Agriculture	297.69	30.69
Fallowing land	79.25	8.17
Road	18.82	1.94
Settlement	100.8	10.39
Mine site	0.29	0.03
Rangeland	408.95	42.16
Bare land	33.85	3.49
TOTAL	**970**	**100.00**

3.1.4. Soil Properties

The soil map used in this study was created within the context of the project "Evaluation of Agricultural Diffuse Pollution and its Control Alternatives with SWAT model in Lake Mogan Watershed" (Alp et al., 2014). Alp et al. (2014) conducted a field study in which the soil surface (0 – 20 cm) samples were collected. The analysis of these samples were performed by the Central Research Institute of Soil Fertilizer and Water Resources Laboratory. In the analysis, the physical, chemical, and hydrological characteristics of the samples were determined. At the end, sixteen different parameters including pH, organic carbon, clay, sand, and silt were analyzed. With the results of the soil analysis the spatial soil map of Lake Mogan watershed was created with Thiessen Polygons or Voronoi Polygons method. The spatial soil map of the watershed was created with the results obtained from the soil sample analyses. The location of 49 soil sampling points are shown in Figure 10.

According to the result of soil sample analysis, in the sampling points where the soil profile depth is high, the plant root depth is also high. Moreover, differences in land use, plant cover, and soil tillage status causes a change in the amount of organic matter and bulk density values. Bulk densities of the soil samples showed significant

differences in arable and fallowing lands. Compared to arable lands, the bulk densities are generally low in fallowing lands where the soil is loosened by tillage. The bulk density values of samples collected from pastures and stubble covered fields were found high. Water transmission rates of hydrologic soil groups were determined as medium (B) and low (C) in all sampling points except for one sampling point which is located in an agricultural land. The percentage of dry aggregates was found low in fallowing lands due to soil tillage. Soil water characteristic values vary in accordance with the soil texture. The field capacity, wilting point, and water saturation values were found high, especially in the soil samples with high clay ratio. Soil sample characteristics as a result of soil analyses are given in Table 13.

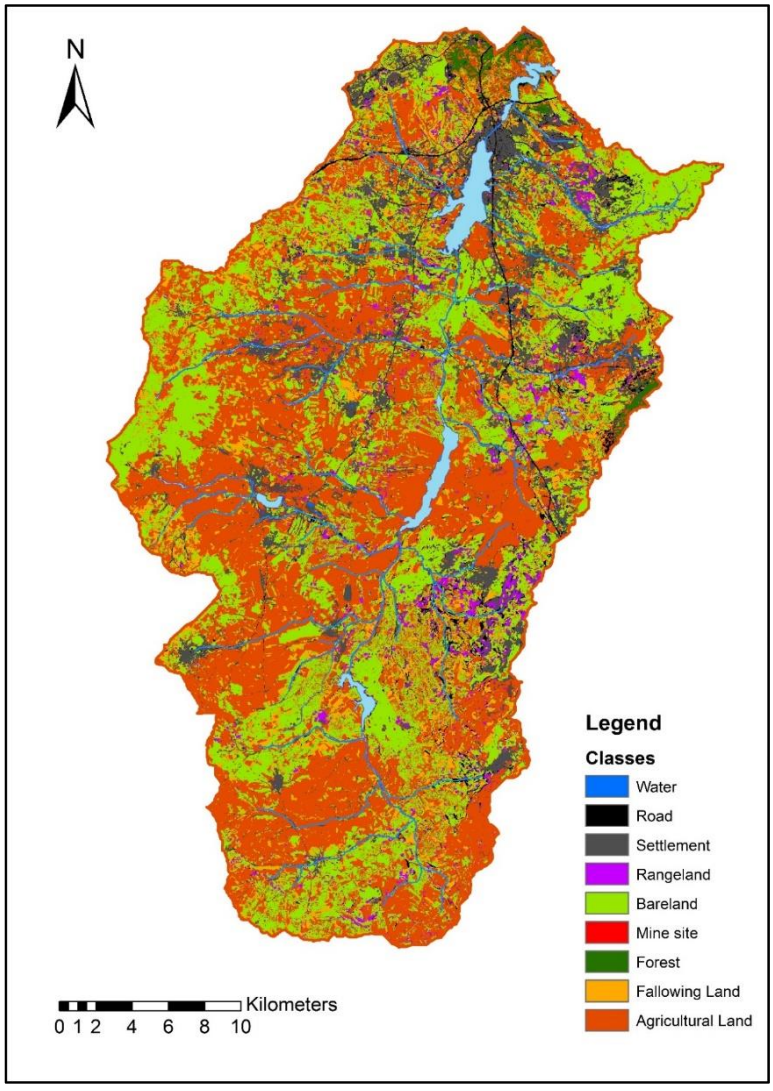

Figure 9. LULC classes in Lake Mogan watershed

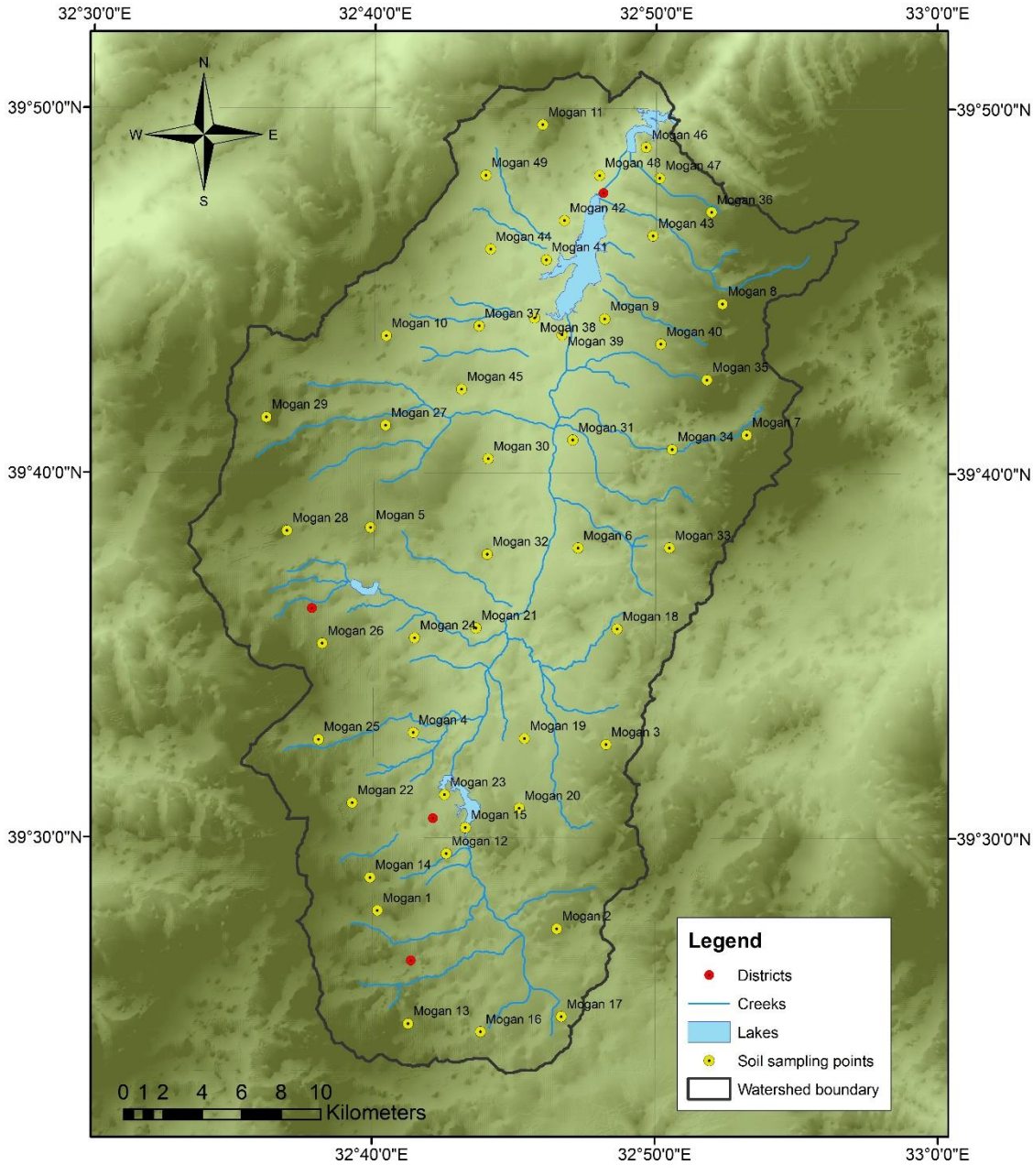

Figure 10. Location of soil sampling points

Table 13. The results of soil sample analyses in Lake Mogan watershed (Alp et al., 2014)

Sample	Maximum Root Depth (cm)	Profile Depth (cm)	Wet Bulk Density (g)	2 mm Sieve Residue Weight (%)	Sand (%)	Silt (%)	Clay (%)	Structure	F.C (%)	W.P (%)	K (cm/h)	Saturation with water (%)	Hydrologic Group	EC (dS m^{-1})*	Total Salt (%)	pH	Lime (%)	Organic Material (%)	Nitrate Nitrogen (%)
1	77	93	1.29	43.05	37.4	18.6	44.0	C	36.20	18.60	0.59	60	C	0.703	0.027	7.61	16.52	1.1	
2	43	62	1.11	58.02	40.1	22.6	37.3	CL	35.70	17.89	1.38	60	C	0.661	0.025	7.7	20.23	1.27	
3	23	23	1.51	46.08	54.8	19.7	25.5	SCL	26.83	14.31	6.52	49	B	0.473	0.015	7.77	10.7	0.36	
4	54	54	1.30	59.42	42.8	25.1	32.1	CL	33.42	16.68	1.37	57	B	0.446	0.016	7.6	10.63	1.65	
5	46	84	1.14	72.82	36.4	23.7	39.9	CL	36.70	18.39	0.34	56	C	0.714	0.026	7.72	6.62	0.7	
6	67	72	1.41	57.01	34.9	18.9	46.2	C	37.50	20.80	0.43	55	C	0.732	0.026	7.69	16.09	0.99	
7	42	118	1.06	54.34	35.5	33.8	30.7	CL	28.09	17.39	0.72	66	C	0.867	0.037	7.66	3.06	0.93	
8	65	102	1.20	38.85	30.8	19.9	49.3	C	33.18	16.62	0.15	67	C	0.696	0.030	7.72	8.44	1.08	0.0086
9	29	29	1.40	57.22	50.1	21.2	28.7	SCL	24.77	12.11	6.52	57	B	0.504	0.018	7.61	7	1.77	
10	48	48	1.08	42.24	32.7	20.8	46.5	C	42.28	18.21	0.22	58	C	0.339	0.013	7.73	11.75	0.91	
11	58	102	1.21	61.36	29.4	18.0	52.6	C	42.70	21.42	0.11	63	C	0.913	0.037	8.16	15.03	0.42	
12	36	74	1.06	51.63	32.4	17.2	50.4	C	43.21	21.58	0.14	68	C	0.816	0.036	7.68	11.53	1.29	0.0158
13	39	49	1.21	55.30	32.7	24.7	42.6	C	35.17	17.38	0.86	56	C	0.644	0.023	7.63	10.8	0.87	
14	56	59	1.32	53.28	49.6	26.0	24.4	SCL	27.12	14.44	2.89	57	B	0.53	0.019	7.71	24.95	1.39	
15	26	43	1.18	45.98	52.5	23.1	24.4	SCL	22.09	11.58	3.78	55	B	0.884	0.031	7.68	12.48	1.03	
16	23	23	1.24	78.55	38.8	27.6	33.6	CL	27.40	14.28	0.35	74	C	0.975	0.046	7.53	13.79	1.86	
17	44	121	1.21	87.66	32.0	25.9	42.1	C	31.85	17.32	0.22	66	C	0.76	0.032	7.58	11.89	1.07	
18	52	107	1.29	72.47	27.6	23.5	48.9	C	41.81	20.89	0.12	64	C	0.823	0.034	7.78	12.4	0.86	
19	25	42	1.30	74.78	39.1	16.9	44.0	C	34.70	16.91	0.43	60	C	0.581	0.022	7.82	48.45	1.37	
20	47	97	1.23	48.72	42.2	25.6	32.2	CL	34.60	17.48	3.02	59	B	0.587	0.022	7.54	8.24	1.15	
21	78	112	1.43	38.41	46.5	27.2	26.3	SCL	26.31	14.21	2.75	62	B	0.705	0.028	7.72	28.67	1.5	0.0157
22	54	92	1.30	68.58	42.2	20.1	37.7	CL	34.18	17.08	1.59	58	B	0.652	0.024	7.68	9.05	1.06	
23	28	98	1.17	73.04	35.7	23.7	40.6	C	33.59	16.78	0.20	62	C	0.831	0.033	7.57	7.88	1.11	0.0079
24	38	48	1.31	59.31	39.9	25.5	34.6	CL	32.10	16.09	1.48	65	C	0.636	0.026	7.54	41	1.86	
25	35	35	1.37	69.87	37.2	11.9	50.9	C	42.41	21.22	0.17	59	C	0.792	0.030	7.55	22.03	1.34	0.0086

Table 13. The results of soil sample analyses in Lake Mogan watershed (Alp et al., 2014)

Sample	Maximum Root Depth (cm)	Profile Depth (cm)	Wet Bulk Density (g)	2 mm Sieve Residue Weight (%)	Sand (%)	Silt (%)	Clay (%)	Structure	F.C (%)	W.P (%)	K (cm/h)	Saturation with water (%)	Hydrologic Group	EC (dS m^{-1})*	Total Salt (%)	pH	Lime (%)	Organic Material (%)	Nitrate Nitrogen (%)
26	64	92	1.31	67.67	38.4	25.9	35.7	CL	35.19	17.84	1.34	59	C	0.604	0.023	7.55	21.67	2.15	
27	36	40	1.39	75.85	48.6	18.3	33.1	SCL	30.55	13.59	3.11	57	B	0.483	0.018	7.65	15.1	0.98	
28	41	98	1.06	61.89	27.4	21.0	51.6	C	42.29	21.09	0.11	60	C	0.85	0.033	7.63	2.26	1.15	
29	34	39	1.28	52.33	46.1	22.6	31.3	SCL	37.12	18.61	2.02	61	B	0.687	0.027	7.61	28.02	3.21	
30	24	57	1.37	53.59	34.3	33.3	32.4	CL	33.52	16.78	0.23	60	C	0.473	0.018	7.72	54.43	0.84	
31	48	77	1.11	63.29	33.8	20.4	45.8	C	41.41	20.25	0.48	63	C	0.662	0.027	7.59	32.18	2.11	
32	29	46	1.18	47.70	33.6	27.4	39.0	CL	33.31	16.30	0.20	57	C	0.512	0.019	7.71	39.11	1.63	
33	22	90	1.50	59.10	51.5	26.0	22.5	SCL	22.39	12.63	4.16	59	B	0.607	0.023	7.71	7.04	1.03	
34	29	42	1.09	67.59	27.7	20.8	51.5	C	42.28	21.22	0.11	65	C	0.824	0.034	8.07	22.18	1.34	
35	52	71	1.42	60.94	22.1	20.8	57.1	C	42.72	21.42	0.09	82	C	0.837	0.044	7.79	19.77	1.02	
36	68	96	1.57	57.40	36.7	21.5	41.8	C	40.23	17.69	0.19	64	C	0.634	0.026	7.67	12.33	1.58	
37	22	27	1.30	57.22	25.0	21.3	53.7	C	42.11	21.12	0.11	74	C	0.797	0.038	7.69	10.8	1.44	
38	64	106	1.06	54.58	26.1	17.3	56.6	C	42.62	21.29	0.09	77	C	0.78	0.038	7.64	8.83	1.73	
39	62	103	1.05	49.50	26.4	23.9	49.7	C	41.72	20.89	0.12	72	C	0.76	0.035	7.65	18.75	1.24	
40	32	81	1.00	35.81	18.2	14.6	67.2	C	42.80	21.40	0.07	79	D	0.735	0.037	7.78	13.21	0.78	
41	33	107	1.37	84.62	39.5	17.8	42.7	C	41.39	14.56	0.49	64	C	0.781	0.032	7.65	3.06	1.17	
42	39	92	1.32	75.22	28.7	14.4	56.9	C	44.41	21.68	0.11	71	C	1.064	0.048	7.87	2.99	1.2	
43	35	98	1.15	70.12	21.9	19.1	59.0	C	42.89	21.54	0.08	79	C	1.035	0.052	7.71	16.27	1.33	
44	57	110	1.23	44.44	29.9	22.9	47.2	C	41.25	18.89	0.13	72	C	0.938	0.043	7.65	15.39	1.55	
45	38	88	1.50	78.21	44.0	28.1	27.9	CL	33.68	17.64	1.57	67	C	0.634	0.027	7.47	13.21	1.79	
46	28	35	1.49	79.82	39.1	20.7	40.2	C	41.49	20.71	0.39	63	C	0.815	0.033	7.54	12.18	1.87	
47	50	64	1.29	60.49	18.5	27.3	54.2	C	41.87	21.04	0.19	59	C	0.682	0.026	7.65	26.85	1.58	
48	39	80	1.33	80.65	17.0	24.0	59.0	C	42.06	20.98	0.09	59	C	1.196	0.045	7.98	15.47	0.74	
49	50	70	1.18	57.59	20.8	20.8	58.4	C	41.89	20.99	0.08	62	C	1.155	0.046	7.97	15.03	0.94	

3.1.5. Agricultural Activities

According to Gölbaşı District Directorate of Food, Agriculture and Livestock, wheat and barley are the most commonly cultivated agricultural crops in Lake Mogan watershed. In the watershed cultivation of rye, oats, vetch, caraway, corn, alfalfa, sainfoin, beans, lentils, chickpeas, and sunflower (for oil) is also carried out on a limited scale compared to wheat and barley. Furthermore, cattle and sheep breeding and beekeeping are other sources of livelihood in the region.

As it can be seen in Table 14 agricultural crops are planted in September, and harvested between July 15th and August 1st. Dry farming is carried out in the region but water is supplied from the wells if necessary. First tillage is carried out between the end of March and beginning of April, and the plow depth is between 18 and 25 cm. Second tillage starts in May 15th and performed for a week. In this tillage, duck foot and disk-harrow are used and the depth of the tillage is between 10 and 12 cm. Third tillage is done between June 21st and July 7th by using duck foot and disk-harrow in 10 cm depth. Final tillage is carried out between September 10th and 30th with duck foot and disk-harrow in 7-8 cm depth.

Table 14. Lake Mogan watershed times of harvesting and plowing

Date	**Type of application**
July 15th – August 1st	Harvesting
end of March – beginning of April	First tillage (with plow – 18-25cm)
May 15th	Second tillage (duck foot – 10-12 cm)
June 21st – July 7th	Third tillage (duck foot – 10 cm)
September 10th and 30th	Fourth tillage (duckfoot – 7-8 cm)

In Lake Mogan watershed, fertilizers and pesticides used in agricultural lands are supplied from the dealers located in the region. The information regarding the fertilizer application during wheat cultivation was obtained from the Gölbaşı District Directorate of Food, Agriculture and Livestock, Assoc. Prof. Dr. Oğuz Başkan from Soil, Fertilizer and Water Resources Institute, and Prof. Dr. Ayten Namlı from Ankara University. The information including the type, timing, and amount of fertilizer is provided in Table 15. Four different types of fertilizers namely urea, ammonium nitrate, ammonium sulfate, and diammonium phosphate (DAP) are used for wheat

growing. In the table N (nitrogen) – P (phosphorus) – K (potassium) ratios of the fertilizers are given below their names.

Table 15. The type of fertilizer applied to wheat, the timing and the amount

Type of fertilizer	Time of application	Amount (kg/da)
Urea (46-00-00)	end of February – beginning of March	8-10
Ammonium Nitrate (33-00-00)	end of March – beginning of April	10-15
Ammonium Sulfate (21-00-00)	October	20-25
DAP (Diammonium phosphate) (18-46-00)	Before planting or with planting	25

3.2. Model Construction

In the context of this thesis study, ArcSWAT 2012 which is an ArcGIS extension (ArcGIS Desktop Service Pack 5) was used for performing SWAT simulations. ArcSWAT extension generates an ArcMap project file containing links to the retrieved data and incorporates all customized GIS functions into the ArcMap project file (Srinivasan, 2014). Model inputs can be categorized under five main categories as topography, soil, agricultural practices, land use, and meteorology. The summary of the model inputs; related sources and descriptions are given in Table 16. Detailed information about each data category can be found in Section 3.

In SWAT; which is run via ArcGIS interface in this study, there are five steps to be completed in order to run the model. The steps to set up a SWAT model project are summarized in Figure 11. The first step is 'Watershed Delineation'. Determination of the watershed boundary; creation of the tributaries and the subbasins; definition of point sources and reservoirs, if any, are performed by using this menu. This step is followed by the 'HRU Analysis'. In this step, definition of hydrologic response units (HRUs) are carried out by defining the land use, soil, and slope classes. The next step is 'Write Input Tables' menu. Via this menu, the meteorological data is introduced to the model. In addition, all SWAT database tables; e.g. soil, groundwater, management data etc., required to run the model are created. The last step before running the SWAT model is 'Edit SWAT Input' menu. In this step agricultural practices carried out in the

watershed can be defined, and the information regarding the reservoirs and inlets, if any, can be adjusted. When all of these steps are completed, the SWAT model can be run. In order to run the model 'Run SWAT' button under the 'SWAT Simulation' menu is used. Please see Appendix A for the detailed procedure on how SWAT model was constructed for Lake Mogan watershed.

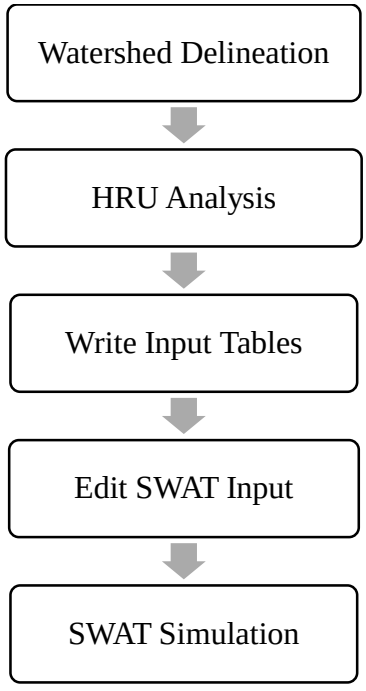

Figure 11. Steps to setup a SWAT model project

3.3. Model Calibration and Validation

Within the scope of this study, SWAT model was calibrated for the Lake Mogan watershed based on the monthly observed data obtained from the Yavrucak monitoring station. The simulation period was 2007 – 2010 where the first year was used as the warm-up period. According to Arnold et al. (2012) warm-up period can also be named as equilibration period. Warm-up period is used when initial conditions are unknown and it is aimed at stabilizing initial conditions (Pereira et al., 2014). Warm-up period becomes more important as the simulation period gets shorter. Furthermore, one year warm-up period is usually sufficient to get the hydrologic cycle fully operational (Arnold et al. 2012). A longer warm-up period would have been better but shortening the already short calibration period was avoided. On the other

hand, using a one-year warm-up period was preferred in several studies in the literature (Abraham et al., 2007; El-Sadek and Irvem, 2014; Ficklin et al., 2013; Tibebe et al., 2013; Vilaysane et al., 2015). The data from the Sukesen monitoring station was used to validate the model performance for the same period. The model was calibrated for streamflow, sediment, nitrogen and phosphorus. Monthly flow rate data of Yavrucak and Sukesen stations were obtained from the METU Limnology Laboratory. Within the framework of the Environment Plan prepared by General Directorate of Natural Heritage Protection, water quality monitoring activities in Lake Mogan watershed are ongoing since 2006. Thus, the water quality data including total suspended solids (TSS), nitrate (NO_3), total nitrogen (TN), and total phosphorus (TP) were acquired from the directorate for the same monitoring stations. The locations of the Yavrucak and Sukesen water quality monitoring stations can be seen in Figure 5.

Table 16. Model input data for Lake Mogan watershed: Sources and Descriptions

Data Type	**Source**	**Data Description/Properties**
Topography	Turkish General Command of Mapping	Digital Elevation Model (DEM), 15 m x 15 m resolution
Soil	Field survey, soil analysis by the Central Research Institute of Soil Fertilizer and Water Resources Laboratory (Alp et al., 2014)	Soil physical properties like bulk density, hydraulic conductivity, texture etc.
Agricultural Practices Information	• Gölbaşı District Directorate of Food, Agriculture and Livestock • Central Research Institute of Soil Fertilizer and Water Resources	Agricultural crops grown in the watershed, all types of agricultural practices
Land use	RAPIDEYE satellite image (Alp et al., 2014) (May 7th, 2013)	Land use classification
Meteorology	General Directorate of Meteorology	Precipitation, temperature, relative humidity, wind speed and solar radiation data

In this study the SWAT model was calibrated though SWAT-CUP (SWAT Calibration and Uncertainty Procedures) software. SWAT-CUP is a computer program developed for the calibration of SWAT models (Abbaspour, 2015). The program allows the user to perform sensitivity analysis, calibration, validation, and uncertainty analysis. There

are several different procedures offered by SWAT-CUP to carry out the mentioned tasks (Section 2.3.1). Within the scope of this study, Sequential Uncertainty Fitting ver. 2 (SUFI-2) method was adopted. SUFI-2 algorithm provides good prediction uncertainty ranges with a small number of model runs. This characteristic becomes more noteworthy if the model is computationally demanding (Yang et al., 2008). SWAT-CUP allows the user to simultaneously calibrate all SWAT parameters comprising all water quality parameters, crop parameters, crop rotation and management parameters, and weather generator parameters in the calibration process (Arnold et al., 2012b). In Appendix B, detailed information about SWAT-CUP is provided.

3.3.1. Sensitivity Analysis

Sensitivity analysis is defined as the determination of the model output response to changes in the model inputs or the parameters (White and Chaubey, 2005). SWAT-CUP allows performing two types of sensitivity analysis namely, one-at-a-time and global. One-at-a-time sensitivity analysis is the modification of a parameter while all other parameters are kept constant. The problem with the one-at-a-time sensitivity analysis is that accurate values of other parameters that are kept constant are never known (Arnold et al., 2012b). This problem should be considered before performing the analysis since the values of the fixed parameters have an effect on the sensitivity of a changing parameter (Abbaspour, 2015). Global sensitivity analysis, on the other hand, allows all parameter values to change simultaneously. However, it requires a large number of simulations (Arnold et al., 2012b). The sensitivity rankings of the parameters are determined according to the t-stat and the p-value. The t-stat is defined as "the coefficient of a parameter divided by its standard error". The second parameter sensitivity statistics, the p-value, indicates the significance of sensitivity. The larger the absolute value of the t-stat, and the smaller the p-value, the more sensitive the parameter is (Abbaspour, 2015). In this study, the most sensitive parameters were deduced from the literature. Therefore, no sensitivity analysis was performed before model calibration. However, after the model simulations were completed, one-at-a-time function in SWAT-CUP was used to rank the parameters selected from the literature according to their sensitivity.

3.3.2. Evaluation of Model Prediction

The strength of calibration through the SUFI-2 algorithm in SWAT-CUP is determined by using two criteria; the p-factor and the r-factor. Furthermore, SWAT-CUP permits the evaluation of the best simulation of the current iteration by using ten different model performance evaluation criteria (Abbaspour, 2015). In this study, the objective function was selected as the Nash-Sutcliffe (NS) efficiency factor but percent bias (PBIAS) and coefficient of determination (R^2) were also taken into consideration while assessing the model performance. The guidelines provided by Moriasi et al. (2007), Table 7, were considered to decide whether the performance was satisfactory or not. In the following subsections detailed information about NS, PBIAS, and R^2 is given.

Nash – Sutcliffe (NS)

The Nash-Sutcliffe (NS) is a normalized statistic that determines the relative magnitude of the residual variance ("noise") compared to the measured data variance ("information") (Nash and Sutcliffe, 1970). NS is formulated as given below:

$$NS = 1 - \frac{\sum_i (Q_m - Q_s)_i^2}{\sum_i \left(Q_{m,i} - \bar{Q}_m\right)^2} \qquad (2)$$

where Q_m and Q_s represent the measured and the simulated variables, respectively. The $\bar{Q}_m$ is the average of the measured values. NS ranges from - ∞ to 1. The optimum condition is reached when NS is 1. If the value of NS is between 0.0 and 1.0, the model performance can be evaluated as acceptable. The values of NS smaller than 0 shows that the mean observed value is better predictor than the simulated value. Thus, the model performance is not satisfactory when NS $\leq$ 0 (Moriasi et al., 2007).

Percent bias (PBIAS)

PBIAS measures the average tendency of the simulated data to be larger or smaller than their observed counterparts (Gupta et al., 1999). PBIAS is calculated with the following equation:

$$PBIAS = \left[\frac{\sum_{i=1}^{n} (Q_m - Q_s)_i}{\sum_{i=1}^{n} Q_{m,i}}\right] \qquad (3)$$

where Q_m and Q_s represent the measured and the simulated variable respectively. When PBIAS is 0, it means that simulated and observed data perfectly match with each other. Lower PBIAS values correspond to better simulations. Negative values point to model overestimation while positive values show that the model underestimates the observed values (Abbaspour, 2015).

Coefficient of determination (R^2)

Coefficient of determination defines the degree of collinearity between simulated and measured data (Moriasi et al., 2007). R^2 is calculated with the following equation:

$$R^2 = \frac{\left[\sum_i (Q_{m,i} - \bar{Q}_m)(Q_{s,i} - \bar{Q}_s)\right]^2}{\sum_i (Q_{m,i} - \bar{Q}_m)^2 \sum_i (Q_{s,i} - \bar{Q}_s)^2} \qquad (4)$$

where Q_m and Q_s represent the measured and the simulated variable respectively, and i represents the i^{th} measured or simulated data. R^2 ranges from 0 to 1. Higher R^2 values mean less error variance, and the values higher than 0.5 are acceptable (Moriasi et al., 2007).

3.3.3. Streamflow Calibration

Data from Yavrucak monitoring station comprising the monthly flow rates between the period 2007 and 2010 were used to calibrate the stream flow. The year 2007 was used as the warm-up period to make the hydrological cycle fully operational (Neitsch et al., 2002). The observed flow rates from January 2008 to September 2010 at the Yavrucak monitoring station is shown graphically in Figure 12. As it can be seen from Figure 12, Yavrucak is a seasonal creek, and the streamflow is very low, always smaller than 0.5 m^3/sec. The average monthly streamflow within the simulation period is 0.097 m^3/sec.

The streamflow calibration parameters and their value ranges were determined after a detailed literature survey (Akhavan et al., 2010; Arnold et al., 2012a; Lam et al., 2012; Oeurng et al., 2011; Pisinaras et al., 2010; Sahu and Gu, 2009; Santhi et al., 2001; Strauch et al., 2012). Twenty parameters were selected for the streamflow calibration, and a total of 1500 simulations were conducted for streamflow calibration. The objective function was selected as Nash – Sutcliffe (NS) efficiency coefficient.

However, the values of R^2 and PBIAS were also evaluated to identify the best simulation. In order to assess the performance of the model as successful NSE > 0.5, PBIAS ≤ ± 25%, R^2> 0.5 was required. All of the 20 parameters used during the streamflow calibration, their explanations and value ranges are given in Table 17. The parameter modifications were made globally which means that hydrological group, soil texture, land use, and subbasin identifiers were omitted. In Table 17, the column 'Method' indicates the type of modification made on the parameter. Relative (r) means that the existing parameter value is multiplied by (1+ a given value). Replace (v), on the other hand, specifies that the existing parameter value is to be replaced by the given value. Table 17 is actually the *par_inf.txt* file (see Appendix B) prepared as an input to SWAT-CUP.

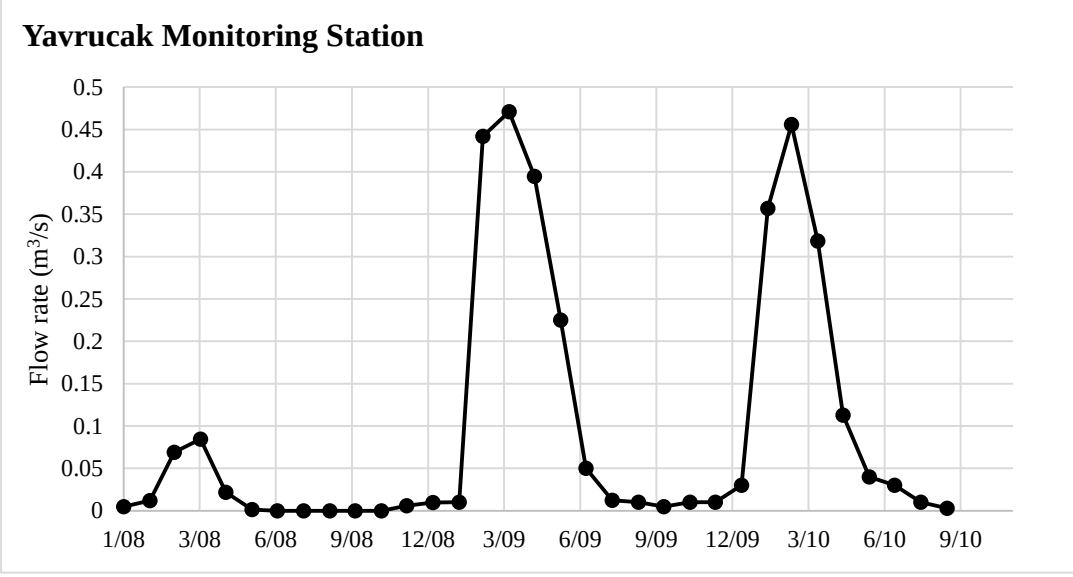

Figure 12. Observed streamflow values at Yavrucak monitoring station

In Table 17, CN2 is the initial SCS runoff curve number for moisture condition II. This parameter is located in the management input file. CN2 is used to calculate runoff depth as a function of total rainfall depth (Liew et al., 2005). It is one of the parameters commonly used in the calibration of hydrological parameters (Arnold et al., 2012b). The baseflow recession factor (ALPHA_BF), the deep aquifer percolation fraction (RCHRG_DP), the groundwater "revap" coefficient (GW_REVAP), the threshold depth of water in the shallow aquifer required for return flow (REVAPMN), and the

groundwater delay (GW_DELAY) are the variables found in the groundwater input file. They control the water movement into and out of the aquifers (Arnold et al., 2012a). Plant uptake compensation factor (EPCO) and soil evaporation compensation factor (ESCO) are the two of the parameters located in the basin input file. EPCO is used to control the amount water uptake by the plants while ESCO enables the user to adjust the soil depth distribution of evapotranspiration. The values of EPCO and ESCO can be also modified in the HRU level. Surface lag coefficient (SURLAG) regulates the fraction of the total available water that will be allowed to enter the reach on any one day (Arnold et al., 2012a). Melt factor for snow on June 21 (SMFMX), melt factor for snow on December 21 (SMFMN), snowfall temperature (SFTMP), snow melt base temperature (SMTMP), snow pack temperature lag factor (TIMP), minimum snow water content that corresponds to 100% snow cover (SNOCOVMX), and fraction of snow volume represented by SNOCOVMX that corresponds to 50% snow cover (SNO50COV) are located in the basin input file. These parameters control the snow related processes. Available water capacity of the soil layer (SOL_AWC) is located in the soil input file. SOL_AWC is also referred to as the plant available water; i.e., the volume of water that is available to plants at field capacity. Manning's "n" value for the tributary channels (CH_N(1)) and manning's "n" value for the main channel (CH_N(2)) are found in the main channel input file. Detailed descriptions about each parameter can be obtained from Arnold et al. (2012a).

Table 17. Streamflow calibration parameters and their value ranges

#	Parameter Name	File Ext.	Method	Min	Max	Hydro Grp	Soil Text.	Landuse	Sub basins
1	CN2	.mgt	r Relative	-0.1	0.1	-	-	-	All
2	ALPHA_BF	.gw	v Replace	0	1	-	-	-	All
3	RCHRG_DP	.gw	v Replace	0	1	-	-	-	All
4	GW_REVAP	.gw	v Replace	0.02	0.2	-	-	-	All
5	GWQMN	.gw	v Replace	0	5000	-	-	-	All
6	REVAPMN	.gw	v Replace	0	500	-	-	-	All
7	GW_DELAY	.gw	v Replace	0	500	-	-	-	All
8	EPCO	.hru	v Replace	0.01	1	-	-	-	All
9	ESCO	.hru	v Replace	0	1	-	-	-	All
10	SURLAG	.bsn	v Replace	1	24	-	-	-	All
11	SMFMX	.bsn	v Replace	0	9	-	-	-	All
12	SMFMN	.bsn	v Replace	0	9	-	-	-	All
13	SFTMP	.bsn	v Replace	-5	5	-	-	-	All
14	SMTMP	.bsn	v Replace	-5	5	-	-	-	All
15	TIMP	.bsn	v Replace	0	0.9	-	-	-	All
16	SNOCOVMX	.bsn	v Replace	0	500	-	-	-	All
17	SNO50COV	.bsn	v Replace	0	0.9	-	-	-	All
18	SOL_AWC	.sol	r Relative	-0.1	0.1	-	-	-	All
19	CH_N1	.sub	v Replace	0.01	1	-	-	-	All
20	CH_N2	.rte	v Replace	0	0.3	-	-	-	All

*v__means the existing parameter value is to be replaced by the given value, r__means the existing parameter value is multiplied by (1+ a given value).

3.3.4. Sediment and Water Quality Calibration

After the model was calibrated for streamflow, the parameters related to hydrology were fixed and then the model was calibrated for sediment. In order to calibrate the sediment, monthly total suspended solids (TSS) data from the Yavrucak monitoring station were used. The simulation period was between 2007 and 2010 together with a one year warm-up period. The observed monthly total suspended solids (TSS) concentrations from January 2008 to September 2010 at the Yavrucak monitoring station is shown graphically in Figure 13. As it can be seen from Figure 13, not all monthly TSS concentration are available between January 2008 and September 2010; there is considerable amount of missing data. The maximum TSS concentration was observed at March 2008 as 71.2 mg/L. The average monthly observed TSS concentration in this period was 26.4 mg/L.

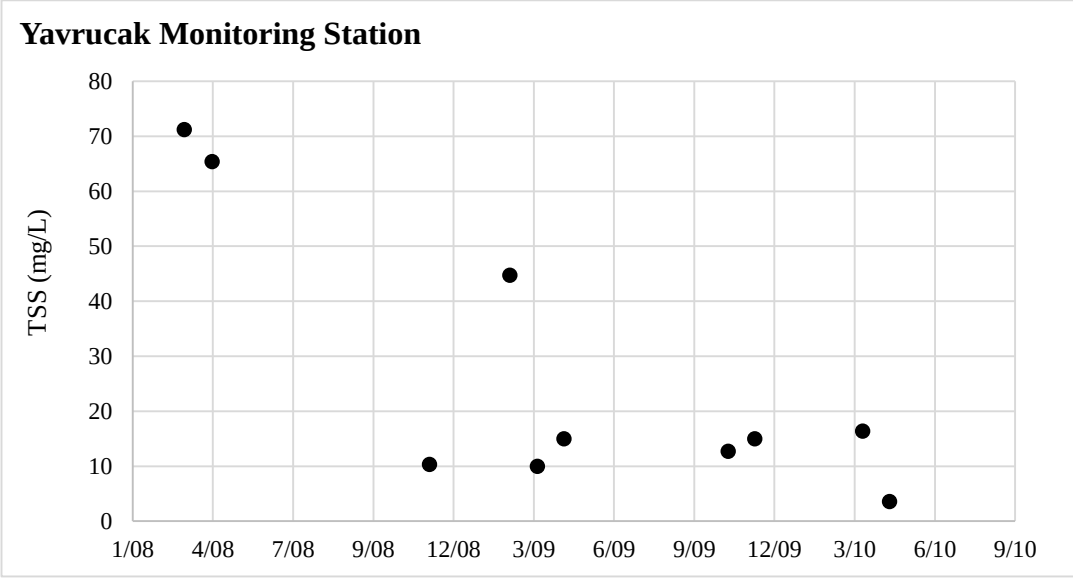

Figure 13. Observed TSS concentrations at the Yavrucak monitoring station

Through literature review and according to the suggestions of the SWAT's user manual (Neitsch et al., 2002) and SWAT Input/output documentation (Arnold et al., 2012a), twenty parameters related to sediment processes were determined (Akhavan et al., 2010; Almendinger et al., 2014; Lam et al., 2012; Oeurng et al., 2011; Pisinaras et al., 2010; Sahu and Gu, 2009; Strauch et al., 2012). The parameters obtained through literature review and used in the sediment calibration, and their ranges are shown in Table 18. A total of 1500 simulations were carried out through SWAT-CUP. Similar to streamflow calibration, the objective function was selected as the Nash – Sutcliffe (NS) efficiency coefficient. To evaluate the model performance as successful NSE > 0.5, R^2 >0.5, and PBIAS ≤ ±55% was required (Moriasi et al., 2007). Hydrological group, soil texture, land use, and subbasin identifiers were not considered, and the parameters were modified globally. The observed TSS concentrations (mg/L) were converted to loads (tons) by multiplying with the corresponding measured streamflow values in order to be able to compare them with the SWAT output values.

In Table 18, SPEXP is the exponent parameter for calculating sediment reentrained in channel sediment routing. SPEXP is found in the basin input file (.bsn). SPCON is the linear parameter for calculating the maximum amount of sediment that can be reentrained during channel sediment routing and it is located in the basin input file. CH_ERODMO is a parameter found in the main channel input file (.rte), and ranges

between 0 and 1. When CH_ERODMO takes the value of 0, it indicates non-erosive channel, while 1 indicates no resistance to erosion. CH_COV1 and CH_COV2 located in the main channel input file are the channel erodibility and the channel cover factor, respectively. ADJ_PKR is the peak rate adjustment factor for sediment routing in the tributary channels. C_FACTOR is the scaling parameter for cover and management factor for overland erosion. USLE_P and USLE_K are the parameters controlling the sediment yield landscape. USLE_P is the support practice factor and USLE_K is the soil erodibility (K) factor of USLE equation. RSDCO is the residue decomposition coefficient and it determines the fraction of residue which will decompose in a day. BIOMIX is the biological mixing efficiency. CH_WDR is the channel width-depth ratio. CH_BED_KD, CH_BNK_KD, CH_BNK_D50, CH_BNK_TC, CH_BNK_BD, CH_BED_BD, and CH_BED_D50 are parameters related to the channel bank and channel bed sediment. They are found in the main channel input file. SOL_ROCK is located in the soil input file, and it is the rock fragment content of the soil layer. Arnold et al. (2012a) can be consulted for more information about these parameters.

Table 18. Sediment calibration parameters and their value ranges

#	Parameter Name	File Ext.	Method	Min	Max	Hydro Grp	Soil Text.	Land use	Sub-basins
1	SPEXP	.bsn	v Replace	1	1.5	-	-	-	All
2	SPCON	.bsn	v Replace	0.001	0.01	-	-	-	All
3	CH-ERODMO	.rte	v Replace	0	1	-	-	-	All
4	CH_COV1	.rte	v Replace	-0.05	0.6	-	-	-	All
5	CH_COV2	.rte	v Replace	-0.001	1	-	-	-	All
6	ADJ_PKR	.bsn	v Replace	0	2	-	-	-	All
7	C_FACTOR	.bsn	v Replace	0.001	0.45	-	-	-	All
8	USLE_P	.mgt	v Replace	0	1	-	-	-	All
9	USLE_K	.sol	v Replace	0	0.65	-	-	-	All
10	RSDCO	.bsn	v Replace	0.02	0.1	-	-	-	All
11	BIOMIX	.mgt	v Replace	0	1	-	-	-	All
12	CH_WDR	.rte	r Relative	-0.1	0.1	-	-	-	All
13	CH_BED_KD	.rte	v Replace	0.001	3.75	-	-	-	All
14	CH_BNK_KD	.rte	v Replace	0.001	3.75	-	-	-	All
15	CH_BNK_D50	.rte	v Replace	1	10000	-	-	-	All
16	CH_BNK_TC	.rte	v Replace	0	400	-	-	-	All
17	CH_BNK_BD	.rte	v Replace	1.1	1.9	-	-	-	All
18	CH_BED_BD	.rte	v Replace	1.1	1.9	-	-	-	All
19	CH_BED_D50	.rte	v Replace	1	10000	-	-	-	All
20	SOL_ROCK	.sol	r Relative	-0.1	0.1	-	-	-	All

*v__means the existing parameter value is to be replaced by the given value, r__means the existing parameter value is multiplied by (1+ a given value).

After sediment calibration, nutrients (N and P) calibration was performed. To calibrate nitrogen loads, monthly total nitrogen (TN) and nitrate (NO_3) measurements carried out in Yavrucak monitoring station were utilized. For total nitrogen, only 3, and for nitrate, only 7 monthly measurements in mg/L were available from January 2008 to September 2010. Therefore, nutrient calibration was problematic due to limited data availability. Since the simulated results for TN and NO_3 are given in kg/month, it was required that the observed TN and NO_3 concentrations (mg/L) in Yavrucak were converted to loads in kg/month. For this reason, observed concentrations were multiplied with the corresponding streamflow values and since the simulations were performed on a monthly time step, the result was multiplied by 30 days. For phosphorus calibration, total phosphorus (TP) concentrations measured at Yavrucak monitoring station were utilized. During the period from January 2008 to September 2010, total phosphorus measurements were carried out in 10 months. The average of TN, NO_3, and TP concentrations are given in Table 19. Similar to the nitrogen calibration, observed concentrations (mg/L) were converted to loads (kg/month) by multiplying the corresponding streamflow values with 30 days (monthly time step). To assess the simulation results, NS, PBIAS, and R^2 were used. The model results were identified as successful when NSE > 0.5, R^2 >0.5, and PBIAS $\leq \pm 70\%$ (Moriasi and Arnold, 2007).

Similar to streamflow and sediment calibration, the parameters and the ranges for nitrogen and phosphorus calibration were determined through literature survey. The recommendations from the SWAT's user manual, and SWAT input/output documentation (Arnold et al., 2012a; Neitsch et al., 2002) were also taken into consideration. Fifteen parameters used in nutrient calibration are given in Table 20.

In Table 20, SOL_ORGN, SOL_NO3, and SOL_ORGNP is the initial organic nitrogen, initial nitrate, and initial organic phosphorus concentration in the soil layer, respectively. These parameters are found in the chemical input file. NPERCO and PPERCO are the nitrate and phosphorus percolation coefficient, respectively. They are located in the basin input file. BC1_BSN, BC2_BSN, and BC3_BSN are the rate constants for the biological oxidation of NH_3, biological oxidation of NO_2 to NO_3, and hydrolysis of organic nitrogen to ammonia, respectively. BC4_BSN is the rate constant for decay of organic phosphorus to dissolved phosphorus. These rate constants are found in the basin input file. CDN is the denitrification exponential rate

coefficient located in the basin input file. SDNCO is the fraction of field capacity water content above which denitrification takes place. PHOSKD and PSP are the phosphorus soil partitioning coefficient and phosphorus availability index, respectively. RS5 is the organic phosphorus settling rate in the reach. Lastly, ERORGP, found in the HRU input file, is the phosphorus enrichment ratio for loading with sediment. Detailed information about these parameters can be obtained from Arnold et al. (2012a).

Table 19. Average observed nutrient concentrations at Yavrucak monitoring station

Variable	Unit	Period	Value
TSS	mg/L	January 2008 to September 2010 (10 monthly values available)	26.43
NO_3	mg/L	January 2008 to September 2010 (7 monthly values available)	2.33
TN	mg/L	January 2008 to September 2010 (3 monthly values available)	2.69
TP	mg/L	January 2008 to September 2010 (10 monthly values available)	0.12

Table 20. Nutrient calibration parameters and their value ranges

#	Parameter Name	File Ext.	Method	Min	Max	Hydro Grp	Soil Text.	Land use	Sub-basins
1	SOL_ORGN	.chm	v Replace	0	100	-	-	-	All
2	NPERCO	.bsn	v Replace	0	1	-	-	-	All
3	BC1_BSN	.bsn	v Replace	0.1	1	-	-	-	All
4	BC2_BSN	.bsn	v Replace	0.2	2	-	-	-	All
5	BC3_BSN	.bsn	v Replace	0.2	0.4	-	-	-	All
6	BC4_BSN	.bsn	v Replace	0.01	0.7	-	-	-	All
7	CDN	.bsn	v Replace	0	3	-	-	-	All
8	SDNCO	.bsn	v Replace	0	1	-	-	-	All
9	SOL_NO3	.chm	v Replace	0	100	-	-	-	All
10	SOL_ORGP	.chm	v Replace	0	100	-	-	-	All
11	PPERCO	.bsn	v Replace	10	17.5	-	-	-	All
12	PHOSKD	.bsn	v Replace	100	200	-	-	-	All
13	PSP	.bsn	v Replace	0.01	0.7	-	-	-	All
14	RS5	.swq	v Replace	0.001	0.1	-	-	-	All
15	ERORGP	.hru	v Replace	0	5	-	-	-	All

*v__means the existing parameter value is to be replaced by the given value

3.3.5. Model Validation

Model validation is the process of evaluation of the model performance in periods and areas outside the calibration data and areas. In the literature, it is observed that the validation is commonly carried out at the same monitoring site used in the calibration process at a different time period. However, validation can also be performed in the same time period as calibration but at a different spatial location (Assegahegn and Zemadim, 2013; Benaman et al., 2005; Chekol et al., 2007).

In this study the calibration period was selected from 2007 to 2010 including a one-year warm-up period due to data restrictions. Since the duration of the available data is short, it was decided not to divide the data between calibration and validation. Instead, validation was performed for the same time interval of calibration from 2007 to 2010 for at a different location, Sukesen, in the same watershed. The location of Yavrucak and Sukesen subbasins are shown in Figure 14. As can be seen in the figure, Sukesen is located downstream of Yavrucak. Detailed comparison of these two subbasins in terms of land use classifications, slope etc. is provided in Section 4.2.1. In the validation, the parameters modified through the calibration were kept constant, and the simulated streamflow, total nitrogen, nitrate, and total phosphorus loads were compared with the observed loads at Sukesen monitoring station.

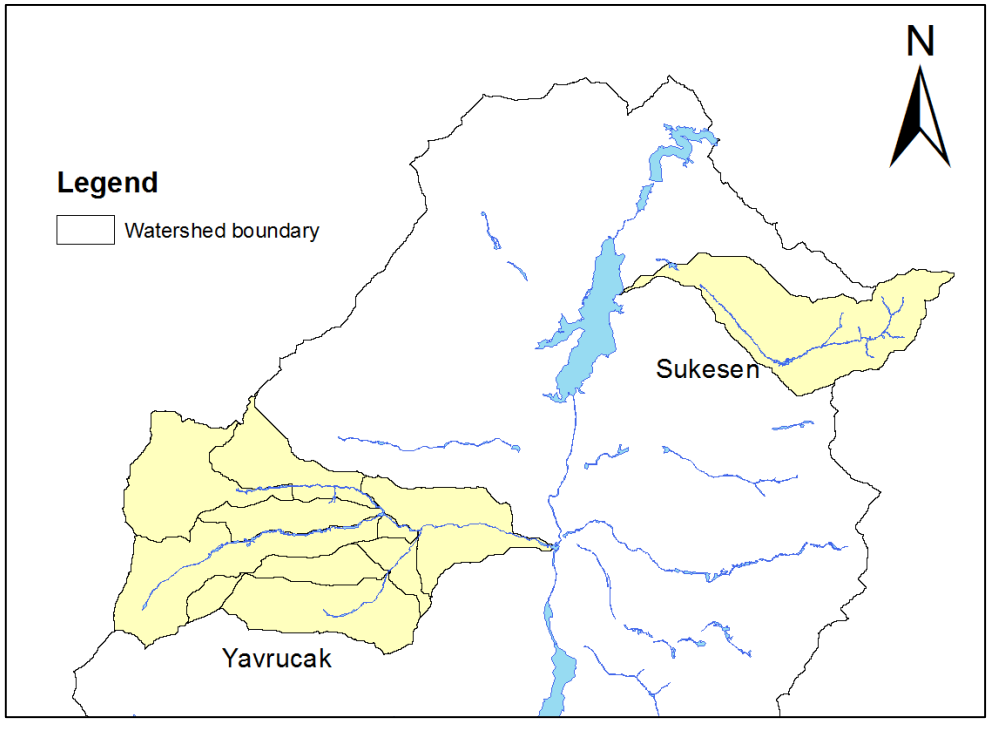

Figure 14. The locations of Yavrucak and Sukesen subbasins

3.4. Representation of BMPs in SWAT (Scenario Development)

In the context of this study, 11 different BMP scenarios were developed, and the efficiencies of these scenarios were compared in terms of reducing the amount of transported sediment and nutrient loads. The changes in the amount of pollutants were evaluated at the Yavrucak and Sukesen subbasin outlets. To evaluate the results, the changes in the amount of pollutants were compared with a baseline scenario which is based on the current practices carried out in the watershed. The BMPs evaluated includes nutrient management by reducing fertilizer amounts, land use management by replacing conventional tillage methods with conservation or no tillage, contouring, and terracing. All of the mentioned scenarios simulated for the Lake Mogan watershed are listed in Table 21 with their descriptions.

Table 21. Description of BMPs simulated for the Lake Mogan watershed

BMP Scenario	**Descriptions**
Baseline Scenario	Model simulation after streamflow, sediment, and nutrient load calibration was finalized.
Scenario-1	Fertilizer application rates were decreased by 10%.
Scenario-2	Fertilizer application rates were decreased by 20%.
Scenario-3	Fertilizer application rates were decreased by 30%.
Scenario-4	Conventional tillage operations were replaced by conservation tillage.
Scenario-5	Conventional tillage operations were replaced by no tillage.
Scenario-6	Conservation tillage was applied at low clay (<30%) agricultural lands.
Scenario-7	No tillage was applied at low clay (<30%) agricultural lands.
Scenario-8	Contouring was applied at agricultural lands.
Scenario-9	Terracing was applied at agricultural lands.
Scenario-10	Combination of Scenario 3 and 5
Scenario-11	Combination of Scenario 3, 5 and 7

3.4.1. Nutrient Management

It is important to evaluate the efficiency of nutrient management plans in terms of the economic and environmental sustainability of the agricultural system (Lam et al., 2011). Nutrient management plans generally involve performing soil tests, adjusting timing of fertilizer application, and keeping records (Merrill et al., 2011; Sharpley et al., 2006). Reducing the fertilizer application rates to control the loss of nutrients in surface runoff is one of the commonly applied methods in agricultural watersheds

(Lam et al., 2011; Liu and Lu, 2014; Schilling and Wolter, 2009; Thodsen et al., 2015). In these studies, the percentages of fertilizer reductions range from 10% to 30%. Therefore, three fertilizer management scenarios were developed in the context of this study. In Scenario-1, Scenario-2, and Scenario-3, current fertilizer amounts applied in agricultural lands in Lake Mogan watershed were reduced by 10%, 20%, and 30%, respectively. The impact of these scenarios on the sediment and nutrient loads were assessed at Yavrucak and Sukesen subbasin outlets. The results of the fertilizer management scenarios are given in Section 4.3.

Scenario-1

In this scenario, the fertilizer application rates in agricultural lands were reduced by 10% compared to the Baseline Scenario. The fertilizer application rates in the Baseline Scenario and Scenario-1 are given in Table 22.

Scenario-2

The fertilizer application rates were reduced by 20% compared to Baseline Scenario. The fertilizer application rates in Baseline Scenario and Scenario-2 are given in Table 22.

Scenario-3

The fertilizer application rates were reduced by 30% compared to Baseline Scenario. The fertilizer application rates in Baseline Scenario and Scenario-3 are given in Table 22.

Table 22. Fertilizer application rates in Scenario-1, Scenario-2 and Scenario-3

	Application Rate (kg/ha)			
Fertilizer Type	**Baseline Scenario**	**Scenario-1**	**Scenario-2**	**Scenario-3**
Urea (46-00-00)	100	90	80	70
Amonium Nitrate (33-00-00)	150	135	120	105
Amonium Sulfate (21-00-00)	200	180	160	140
DAP (18-46-00)	250	225	200	175

*Parentheses below represents the N-P-K ratio of the fertilizers

3.4.2. Conservation Tillage / No Tillage

To assess the impacts of different tillage treatments on sediment and nutrient loads, four different scenarios were created. The conventional (baseline) tillage operations are being carried out with duck foot cultivator in Lake Mogan watershed. In Scenario-4 and Scenario-5, conventional tillage operations were replaced with conservation tillage and no tillage, respectively. In Scenario-6 and Scenario-7, the impacts of conservation and no tillage scenarios were tested on agricultural lands with low clay ratio (<%30) according to the expert opinion from Soil, Fertilizer and Water Resources Central Research Institute. The detailed information about the mentioned scenarios are given in the following subsections.

Scenario-4

Conservation tillage is any tillage method that leaves at least 30% of the soil surface covered with crop residue after planting (Novotny, 2003). In Scenario-4, the conventional tillage operation performed with duck foot cultivator was replaced with conservation tillage, and the impacts on sediment and nutrient loads were evaluated. The related tillage parameters; i.e., the mixing efficiency and the depth of mixing, for conventional and conservation tillage are given in Table 23. As it can be seen from the Table 23, both the mixing efficiency and the depth of mixing is lower in conservation tillage compared to the conventional tillage. Therefore, the soil is disturbed less and nutrient loss gets lower. The tillage parameter values were taken from SWAT's tillage database.

Table 23. Tillage parameters: Conventional tillage vs. Conservation tillage

Tillage Operation Name	Mixing Efficiency (fraction)	Depth of mixing (mm)
Duck foot Cultivator (Conventional Tillage)	0.55	150
Conservation Tillage	0.25	100

Scenario-5

In Scenario-5, conventional tillage operations were replaced with the no tillage case. No tillage planting is carried out by placing seeds in the soil without tillage and maintaining previous plant residues (Novotny, 2003). The related tillage parameters are given in Table 24. As shown in the Table 24, the mixing efficiency and the depth

of mixing in no tillage are much lower compared to conventional tillage. For this reason, the disturbance of soil and nutrient loss in surface runoff is much lower. The tillage parameter values were taken from SWAT's tillage database.

Table 24. Tillage parameters: Conventional tillage vs. No tillage

Tillage Operation Name	Mixing Efficiency (fraction)	Depth of mixing (mm)
Duck foot Cultivator (Conventional Tillage)	0.55	150
No Tillage	0.05	25

Scenario-6

In Scenario-6, conservation tillage was applied in agricultural lands where the soil clay ratio is smaller than 30%. This was a suggestion of an expert from Soil, Fertilizer and Water Resources Central Research Institute. As it was mentioned before in Section 4.3, 49 soil types were determined in Lake Mogan watershed. Seven of them were determined as having clay ratio smaller than 30%. Therefore, conservation tillage was applied in agricultural lands with the specified soil classes.

Scenario-7

Similar to Scenario-6, Scenario-7 is the simulation of no tillage applied in agricultural lands where the soil clay ratio is smaller than 30%.

3.4.3. Contouring and Terracing

Contour farming or contouring is farming in which plowing and crop rows follow field contours across the slope (Novotny, 2003). Contouring reduces soil erosion and increases infiltration. Terrace, on the other hand, is defined as an earthen embankment, channel, or a combination ridge and channel constructed across the slope to intercept runoff (Novotny, 2003). Terracing reduces soil erosion since it allows using more intensive cropping systems. Terraces are also very effective in moisture conservation to increase crop production (Georgia Soil & Water Conservation Commission, 1994). In Scenario-8 and Scenario-9, application of contouring and terracing in agricultural lands in the watershed were simulated, respectively. The impacts of the scenarios were

evaluated at Yavrucak and Sukesen subbasin outlets by comparing the estimated sediment and nutrient loads with the ones estimated in Baseline Scenario.

Scenario-8

In Scenario-8, contouring was applied in agricultural lands. As mentioned previously, contouring reduces soil erosion and increases infiltration. To simulate these effects, curve number (CN2) and the USLE Practice factor (USLE_P) are adjusted in SWAT (Arabi et al., 2008). As suggested by Arabi at al. (2008), the calibrated value of CN2 was reduced by 3 units. The USLE_P values were multiplied with the suggested values varying according to percent slope (see Table 25) to represent contouring. These values for the corresponding percent slopes were adapted from Wischmeier and Smith (1978). USLE_P values for the remaining percent slopes were left with their default values.

Table 25. USLE_P values for contouring

Land Slope (%)	Contouring USLE_P
1 – 3	0.6
3 – 5	0.5
5 – 10	0.5

Scenario-9

In Scenario-9, terracing was applied in agricultural lands. Terracing reduces soil erosion and provides moisture conservation. Terracing in SWAT is simulated by adjusting both erosion and runoff parameters (Arnold et al., 2012a). For this reason, curve number (CN2) and USLE Practice factor (USLE_P) are modified. The parameter SLSUBBSN (i.e. the average slope length) was also adjusted to represent terracing in several studies (Arabi et al., 2008; Kaini et al., 2012; Shao et al., 2013) but SLSUBBSN was not modified in this study. According to Strauch et al. (2013), reducing SLSUBBSN could cause increased peak runoff rates and thus prevent the desired impacts of terraces. Based on the literature (Kaini et al., 2012; Strauch et al., 2013; Tuppad et al., 2010), CN2 was reduced by 5 units, and USLE_P was multiplied with the suggested values according to the land slope (Wischmeier and Smith, 1978) as shown in Table 26.

Table 26. USLE_P values for terracing

Land Slope (%)	Terracing
1 – 3	0.12
3 – 5	0.1
5 – 10	0.1

3.4.4. Combined Scenarios

Combined Scenarios are the scenarios in which the management practices achieving the most effective pollutant reduction were combined. The decision on the most effective scenarios was based on the percent change in the pollutant loads compared to the Baseline Scenario. Two combination scenarios namely Scenario-10 and Scenario-11 were created.

Scenario-10

The most effective nutrient management scenario, in which the fertilizer application rates were decreased by 30% (Scenario-3), was combined with the no tillage scenario (Scenario-5).

Scenario-11

Scenario-11 is the combination of 30% reduction in the fertilizer application rate (Scenario-3), no tillage (Scenario-5), and terracing (Scenario-9). These three scenarios are the most effective scenarios among others. In fact, no tillage is among the suggested conservation practices in conjunction with the terrace systems (ASAE, 2012).

CHAPTER 4

RESULTS AND DISCUSSION

In this chapter the results of model calibration and validation, sensitivity analysis, and the BMP scenarios are provided.

4.1. Model Calibration and Validation

The model calibration and validation was performed using data between 2007 and 2010. One year of this range was used as the warm-up period. The calibration was carried out with the data of the Yavrucak monitoring station while the validation was performed at an upstream monitoring station, Sukesen. The comparison of observed and simulated streamflow, sediment and nutrient loads and the performance evaluation statistics i.e., NS, PBIAS, and R^2 for the simulations carried out *before* the model calibration at Yavrucak and Sukesen monitoring stations are given in Appendix C in detail.

4.1.1. Number of Data Used in the Calibration and Validation

The calibration period was from 2007 to 2010. Calibration was carried out at Yavrucak monitoring station. Since 2007 was used as the warm-up period, only the monthly streamflow and water quality data between 2008 and 2010 was used in the calibration and validation process. The validation was carried out for the same period but at a different monitoring station, the Sukesen monitoring station, located in the Lake Mogan watershed. Within this simulation period there are missing monthly water quality data. As it can be seen from Table 27, the number of monthly data available for water quality calibration and validation processes ranges between 3 and 18. The limited number of data was the greatest difficulty in this study. Thus, the calibration and validation processes, and the interpretation of the results were challenging.

Table 27. Number of available monthly available data for calibration and validation of the model

	Streamflow (m^3/sec)	
	Period	Number of Data
Yavrucak (Calibration)	2008 - 2010	33
Sukesen (Validation)	2008 - 2010	33
	Total Nitrogen (kg/month)	
	Period	Number of Data
Yavrucak (Calibration)	2008 - 2010	3
Sukesen (Validation)	2008 - 2010	9
	Nitrate (kg/month)	
	Period	Number of Data
Yavrucak (Calibration)	2008 - 2010	7
Sukesen (Validation)	2008 - 2010	7
	Total Phosphorus (kg/month)	
	Period	Number of Data
Yavrucak (Calibration)	2008 - 2010	10
Sukesen (Validation)	2008 - 2010	16
	Total Suspended Solids (tons/month)	
	Period	Number of Data
Yavrucak (Calibration)	2008 - 2010	10
Sukesen (Validation)	2008 - 2010	16

4.1.2. Streamflow Calibration Results

In the streamflow calibration process, the SUFI-2 method was adopted, and 1500 iterations were performed with 20 streamflow related parameters (see Section 3.3.3). For the simulation period between 2007 and 2010, approximately 21.5 hours was required to complete 1500 iterations. To assess the model performance as successful NS>0.5, PBIAS ± 25%, and R^2>0.5 were required. Streamflow calibration parameters are given in Table 28 with their calibration ranges and final calibrated values.

SWAT-CUP calibration results for streamflow at Yavrucak monitoring station is shown in Figure 15 and in Figure 16, the correlation between observed and simulated streamflow is demonstrated. In Figure 15, 95PPU represents the 95% prediction uncertainty (see Section 2.3.1 and Appendix B). When the monthly simulated and observed streamflow values are compared, it is seen that the model simulates the streamflow successfully. For the best simulation the p-factor and the r-factor values are 0.67 and 0.71, respectively while NSE, R^2 and PBIAS values are 0.74, 0.8 and -19.1, respectively (Table 29). Obtained p-factor and r-factor values are acceptable (Abbaspour, 2015).

Table 28. Streamflow calibration parameters and their final calibrated values

Parameter Name*	Calibration Range	Final Value
v__SNO50COV.bsn	0 to 0.9	0.47
v__GW_DELAY.gw	0 to 500	100.83
v__GWQMN.gw	0 to 5000	3188.33
v__RCHRG_DP.gw	0 to 1	0.06
v__SNOCOVMX.bsn	0 to 500	375.17
v__SFTMP.bsn	-5 to 5	4.14
r__CN2.mgt	-0.1 to 0.1	-0.08
v__SMFMX.bsn	0 to 9	2.14
v__CH_N1.sub	0.01 to 1	0.73
r__SOL_AWC(..).sol	-0.1 to 0.1	-0.09
v__CH_N2.rte	0 to 0.3	0.01
v__ALPHA_BF.gw	0 to 1	0.42
v__SMFMN.bsn	0 to 9	5.72
v__GW_REVAP.gw	0.02 to 0.2	0.11
v__SURLAG.bsn	1 to 24	7.68
v__EPCO.hru	0.01 to 1	0.48
v__SMTMP.bsn	-5 to 5	-4.85
v__ESCO.hru	0 to 1	0.85
v__REVAPMN.gw	0 to 500	142.50
v__TIMP.bsn	0 to 0.9	0.59

* v__means the existing parameter value is to be replaced by the given value, r__means the existing parameter value is multiplied by (1+ a given value).

According to Moriasi et al. (2007), the model performance can be rated as good with respect to NSE and satisfactory according to PBIAS and R^2 (Table 7). Even though the model performance is satisfactory based on the suggested statistical criteria, it is observed that the model slightly overestimates the streamflow in some months. The highest discrepancy seems to occur in April 2009 where the simulated and observed streamflow is 0.75 and 0.47 m^3/sec, respectively. Such differences may be observed due to the limitation of the curve number method (Yuan, 2010). The author also specified that the curve number method does not take into account the impacts of duration and intensity of precipitation. Since only the daily total rainfall depth is used as an input, the uncertainties may be high. Another reason for the differences between simulated and observed streamflow values at the Mogan watershed may be due to the fact that spatial variability of precipitation cannot be truly represented with only two rain gauges, namely Gölbaşı and Haymana, found in the study area. Similarly, David

and Davidova (2015) discussed the significance of the number of precipitation gauging stations across the watershed and they concluded that significant under or overestimations can occur when network of gauging station is not dense enough.
When the simulated streamflow at the Yavrucak monitoring station are compared before (Figure 64 in Appendix C) and after (Figure 15) the calibration, it is seen that the unreal peaks simulated by the uncalibrated model are eliminated after calibration. For instance, before calibration the model was significantly overestimating the streamflow in January and February 2009, and January 2010. After calibration these overestimated points are removed. The calibrated model successfully simulates the increasing and the decreasing trend in the streamflow.

It is hard to predict the response of streamflow to precipitation in the semi-arid Lake Mogan watershed where the observed streamflow is around 0.5 m^3/sec at most (between Jan. 2008 and Sept. 2010). However, the conclusion which can be drawn from Figure 17 is that the streamflow peaks when the precipitation peaks especially during winter and spring months. However, the same conclusion cannot be drawn for the rest of the months. For instance, although a relatively high amount of precipitation (48 mm) is observed in May 2008 at Gölbaşı gauging station, the streamflow observed in Yavrucak creek at that time is nearly zero (0.023 m^3/sec). Therefore, the contribution of rainfall to streamflow is being prevented by another process. It is known that approximately 53% of the water loss is attributed to evapotranspiration in Lake Mogan (Yagbasan and Yazicigil, 2012; Yağbasan and Yazıcıgil, 2009). Taking this fact into account, the comparison of precipitation and simulated evapotranspiration in Yavrucak subbasin is performed (see Figure 18). In May 2008, the evapotranspiration is nearly 38 mm. Thus, approximately 87% of precipitation is lost due to evapotranspiration which in turn results in lower streamflow contribution of the precipitation in the creek. The same situation is observed in Sept. 2008, June 2009 and May 2010, and it can again be explained with high evapotranspiration rates. As a result, it can be said that the streamflow response to precipitation is highly depended on the evapotranspiration rates in Lake Mogan watershed where the groundwater contribution to streamflow is relatively low.

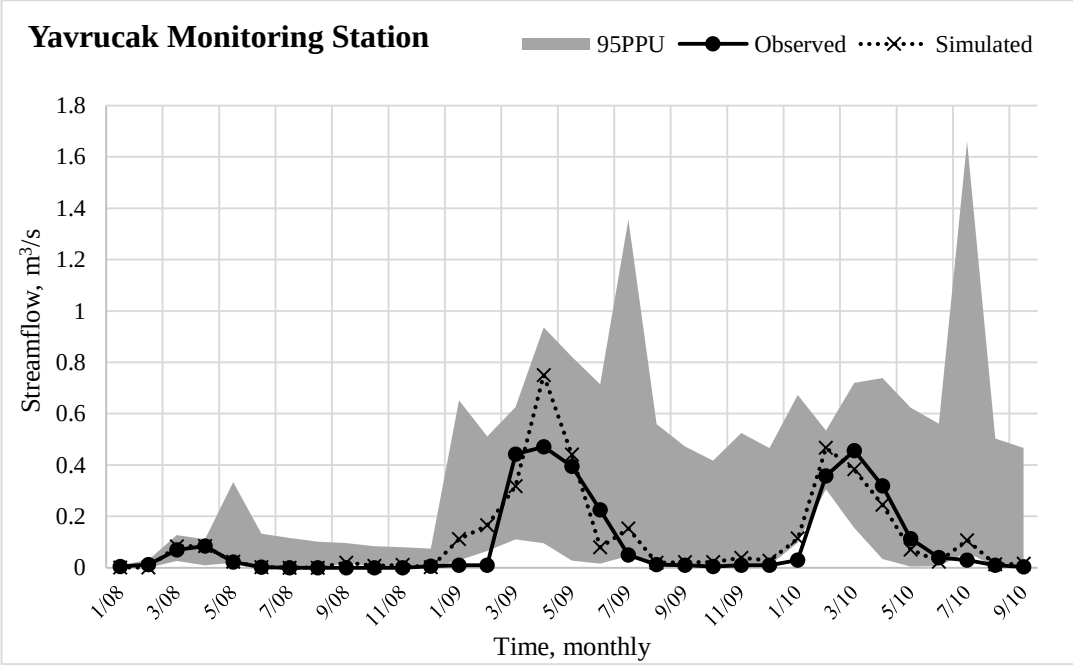

Figure 15. Simulated vs. observed streamflow values after calibration at Yavrucak monitoring station (1)

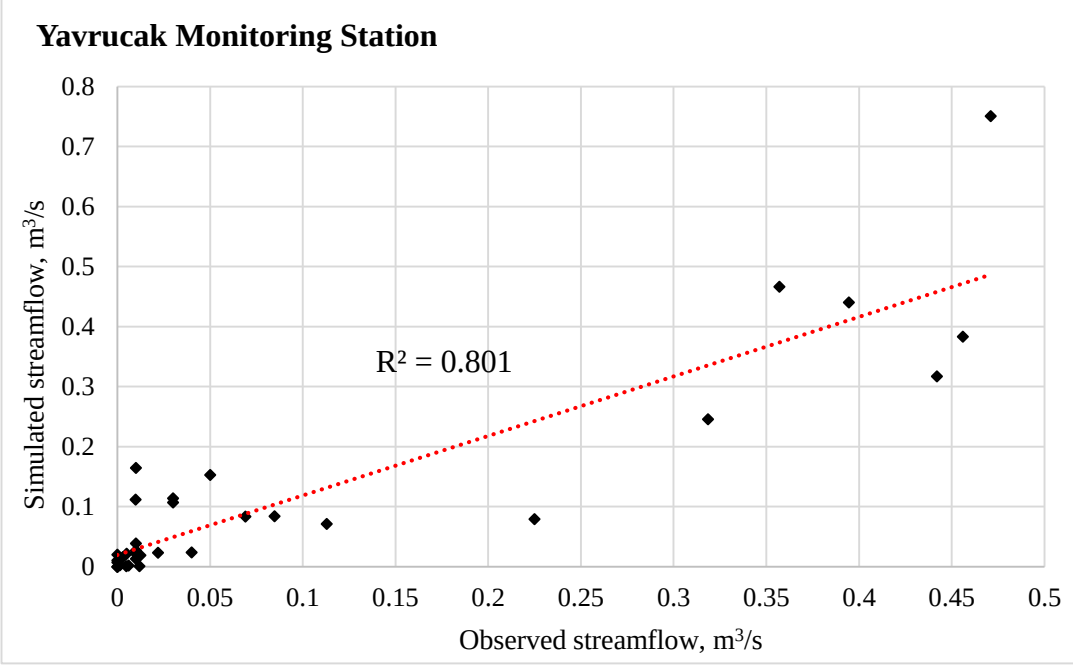

Figure 16. Simulated vs. observed streamflow values after calibration at Yavrucak monitoring station (2)

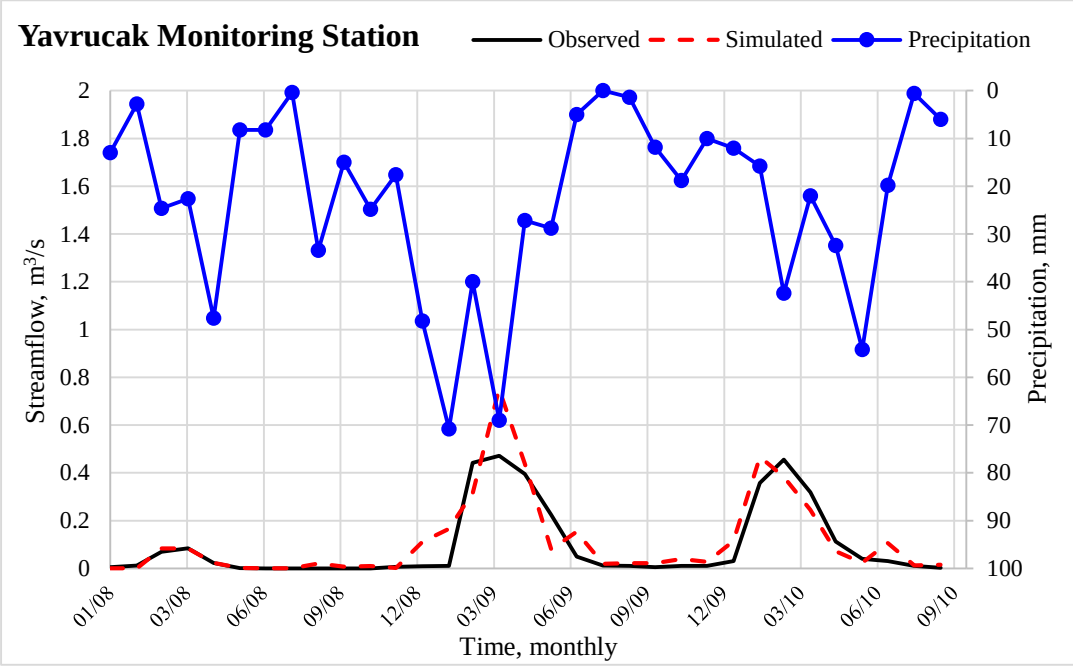

Figure 17. Simulated vs. observed streamflow values after calibration with precipitation at Yavrucak monitoring station

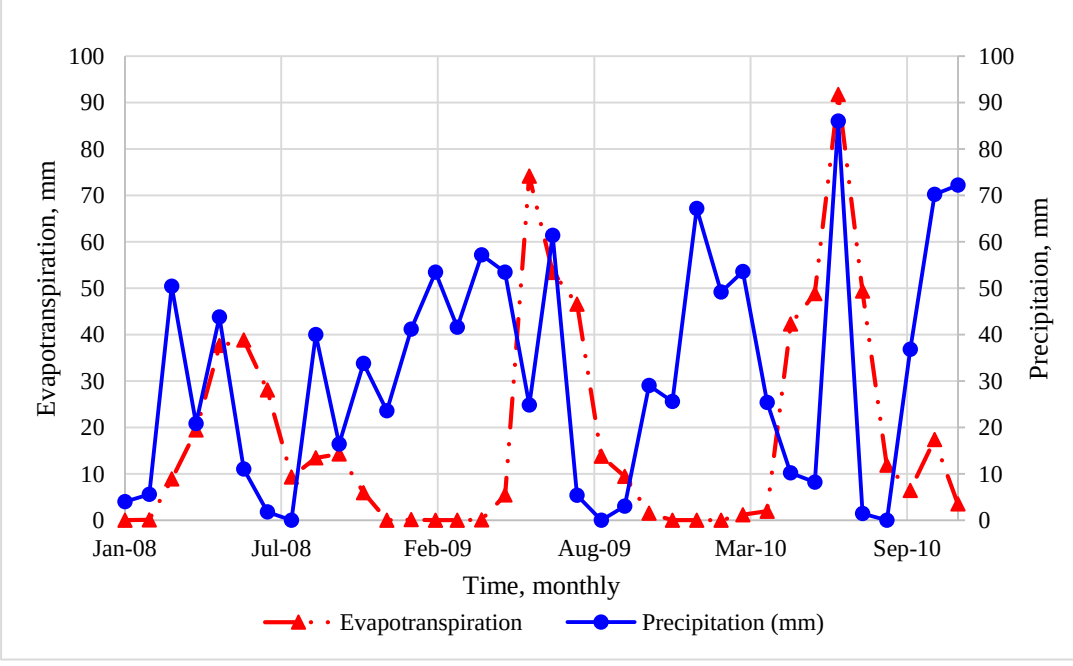

Figure 18. Comparison of precipitation and evapotranspiration in Yavrucak subbasin

Table 29. Summary statistics of streamflow calibration

Summary of statistics	
Number of simulations	1500
Best simulation number	1121
p-factor	0.67
r-factor	0.71
NS	0.74
PBIAS	-19.1
R^2	0.8

4.1.3. Sediment Calibration Results

After streamflow was calibrated, additional 1500 runs were performed with 20 sediment related parameters (see Section 3.3.4). Similar to streamflow calibration, to assess the model performance, NS, PBIAS and R^2 was used. As it was mentioned before, the model performance was identified as successful when NS > 0.5, R^2 >0.5, PBIAS ≤ ±55% for sediment. Sediment calibration parameters are given in Table 30 with their calibration ranges and final calibrated values.

SWAT-CUP calibration result for sediment at Yavrucak monitoring station is shown in Figure 19. There is a reasonable agreement between the simulated and observed sediment loads. However, significant under- and overestimation in sediment load occurred in March 2009 and April 2009, respectively. The first reason may be inaccurate simulated streamflow values at these months. The observed sediment load in March 2009 is 51.2 tons while the simulated load is 8.84 tons. When the observed and simulated streamflows in this month are compared, it is seen that there is approximately 30% underestimation. Similarly, the streamflow in April 2009 is overestimated nearly 34%, and the observed and simulated sediment loads are 12.2 and 24.9 tons, respectively. Moreover, as it can be seen from Figure 19, the number of monthly observed sediment loads within the calibration period (from January 2008 to September 2010) is 12. Three of these observations belong to winter while the others were measured in spring. The total average of observed sediment load is 12.1 tons, and the averages of sediment load in spring and winter months are 17.2 and 0.29 tons, respectively. Figure 15 shows that the streamflow in the spring months are comparably higher than the streamflow observed in other months. Thus, it seems like that the sediment load accumulated within the river bed during the low flow months are transported in the spring.

Table 30. Streamflow calibration parameters and their final calibrated values

Parameter Name	Calibration Range	Final Value
v__USLE_K(..).sol	0 to 0.65	0.18
v__USLE_P.mgt	0 to 1	0.09
r__SOL_ROCK(..).sol	-0.1 to 0.1	-0.02
v__BIOMIX.mgt	0 to 1	0.98
v__CH_BNK_D50.rte	1 to 10000	9735.03
v__CH_BED_BD.rte	1.1 to 1.9	1.73
v__SPEXP.bsn	1 to 1.5	1.41
v__CH_BED_KD.rte	0.001 to 3.75	1.76
v__ADJ_PKR.bsn	0 to 2	1.28
v__CH_COV2.rte	-0.001 to 1	0.11
v__SPCON.bsn	0.001 to 0.01	0.01
v__RSDCO.bsn	0.02 to 0.1	0.04
v__CH_BNK_BD.rte	1.1 to 1.9	1.68
v__C_FACTOR.bsn	0.001 to 0.45	0.44
r__CH_WDR.rte	-0.1 to 0.1	0.03
v__CH_BED_D50.rte	1 to 10000	2045.80
v__CH_BNK_KD.rte	0.001 to 3.75	3.45
v__CH_COV1.rte	-0.05 to 0.6	0.03
v__CH_BNK_TC.rte	0 to 400	308.20
v__CH_ERODMO(..).rte	0 to 1	0.90

Chahinian et al. (2011) specified that MUSLE equation is inadequate to reproduce anything but average erosion rates over long periods. Therefore, the second reason for the underestimations of sediment load occurred in March and April 2008 and in March 2009 may be because of the mentioned constraint of MUSLE equation. However, since there is no available information about the sediment loads observed in the fall and summer months, it is hard to comment on the sediment transport trend and the actual reasons for the under- and overestimation of sediment loads in Lake Mogan watershed.

Among 1500 iterations, the best simulation has Nash-Sutcliffe (NS) simulation efficiency of -0.01, which is not a satisfactory result. The PBIAS and R^2 values of the best simulation are 31.7 and 0.1, respectively (see Table 31). According to Table 7, the model performance for sediment can be rated as satisfactory based on PBIAS. However, typical success criteria for R^2 was not achieved. Although success criteria was not achieved for each measure for sediment, the statistics was considerably

improved after calibration. Before calibration, NS, PBIAS, and R^2 values were -44.1, -460.4 and 0.05, respectively (see Table 68). After calibration these statistics (see Table 31) were improved to -0.01, 31.7 and 0.1, respectively.

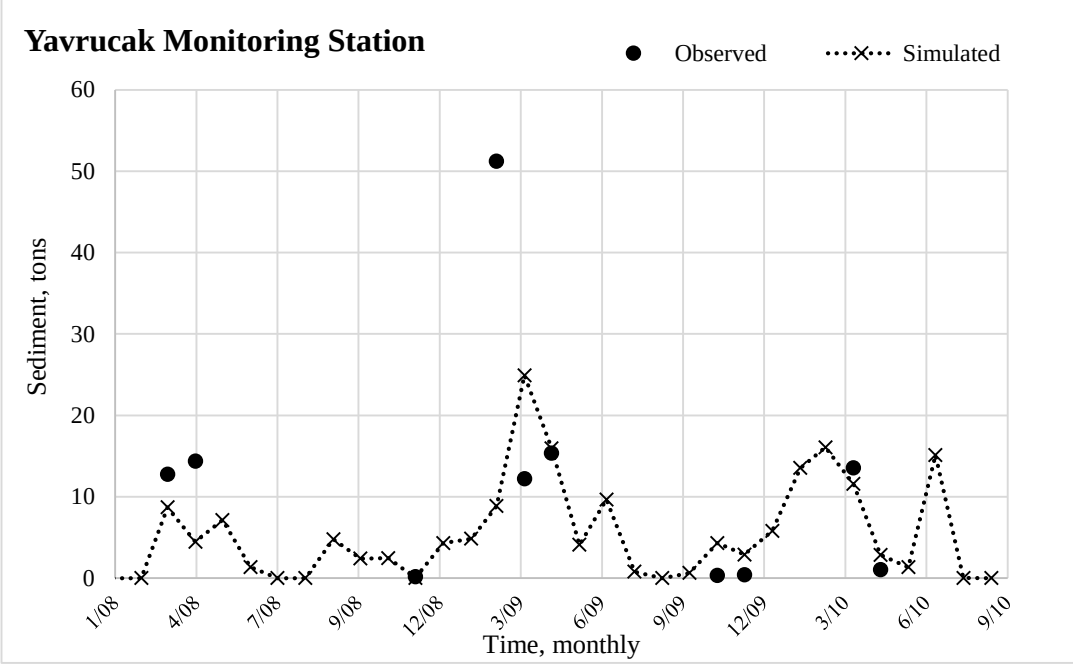

Figure 19. Simulated vs. observed sediment loads after calibration at Yavrucak monitoring station

Table 31. Summary statistics of sediment calibration

Summary of statistics	
Number of simulations	1500
Best simulation number	419
p-factor	0.6
r-factor	7.19
NS	-0.01
PBIAS	31.7
R^2	0.1

4.1.4. Water Quality (NO_3, TN and TP) Calibration Results

After sediment parameters were calibrated, water quality (N and P) calibration was carried out. A total of 1500 runs were performed with 15 parameters by fixing hydrology and sediment calibration parameters (see Section 3.3.4). To assess the model performance NS, PBIAS and R^2 was used. NS > 0.5, R^2 >0.5 and PBIAS ≤

±70% was required to conclude that the model performance is satisfactory. Water quality calibration parameters are given in Table 32 with their calibration ranges and final calibrated values.

Table 32. Water quality calibration parameters and their final calibrated values

Parameter Name	Calibration Range	Final Value
v__NPERCO.bsn	0 to 1	0.57
v__CDN.bsn	0 to 3	0.08
v__SOL_NO3(..).chm	0 to 100	95.81
v__SOL_ORGN(..).chm	0 to 100	0.45
v__BC4_BSN.bsn	0.01 to 0.7	0.21
v__SDNCO.bsn	0 to 1	0.02
v__SOL_ORGP(..).chm	0 to 100	62.40
v__RS5.swq	0.001 to 0.1	0.06
v__PHOSKD.bsn	100 to 200	120.09
v__ERORGP.hru	0 to 5	3.99
v__PPERCO.bsn	10 to 17.5	11.67
v__BC3_BSN.bsn	0.02 to 0.4	0.39
v__BC2_BSN.bsn	0.2 to 2	1.47
v__PSP.bsn	0.01 to 0.7	0.53
v__BC1_BSN.bsn	0.1 to 1	0.25

SWAT-CUP calibration results for nitrate (NO_3), total nitrogen (TN) and total phosphorus (TP) are shown in Figure 20, Figure 21 and Figure 22, respectively. NS, PBIAS and R^2 values are correspondingly -0.2, 37.9 and 0 for NO_3; 0.64, 11.7, and 0.68 for TN; 0.26, -1.5 and 0.27 for TP (see Table 33). Based on PBIAS, the model performance can be rated as satisfactory (Table 7) but for NSE and R^2 success criteria was not achieved in water quality calibration except for TN. As shown in Figure 20, the model is not able to catch the peak NO_3 loads in March and April 2009, and there is an overestimation in May 2009. Uncontrolled discharges to the water bodies from the industries located in the watershed may be the cause of large errors in peak NO_3 loads. It is hard comment on TN calibration results since there are only three monthly TN load data available within the simulation period (see Figure 21). The most problematic point in TP calibration is May 2009 (see Figure 22). There is a significant underestimation of TP load in this month. The most likely explanation of this error is the uncontrolled discharge of a pollutant to Yavrucak causing a jump in the TP

concentration in the river. Except for May 2009, the model is able to follow the increasing and decreasing trends in TP loads. The primary reason for the poor model performance in nutrient simulations is the insufficient data availability.

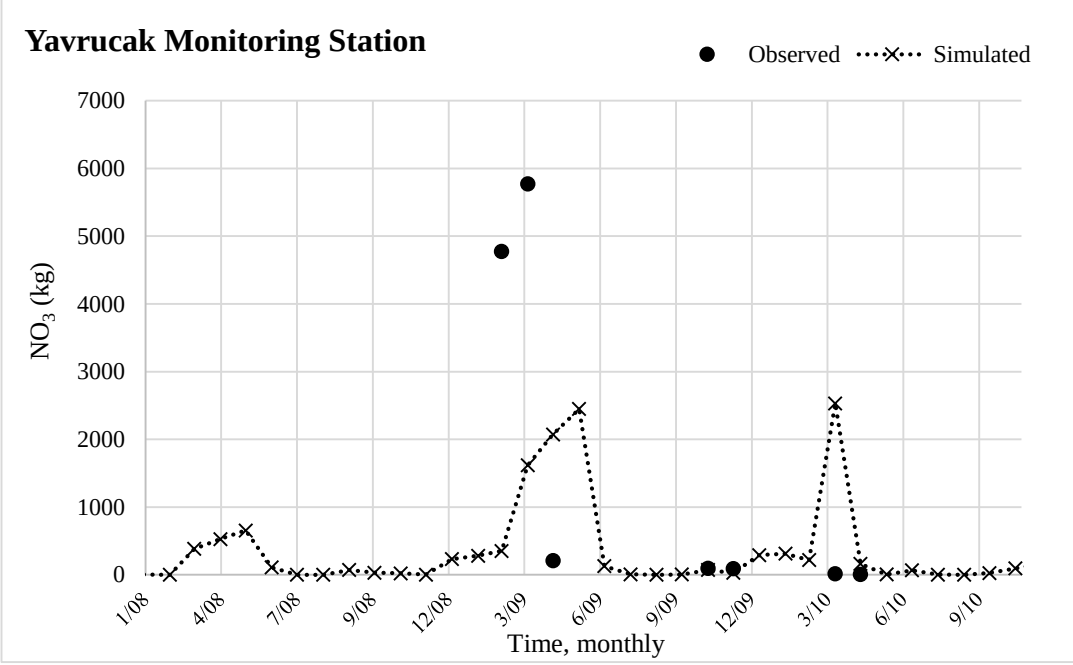

Figure 20. Simulated vs. observed NO_3 loads after calibration at Yavrucak monitoring station

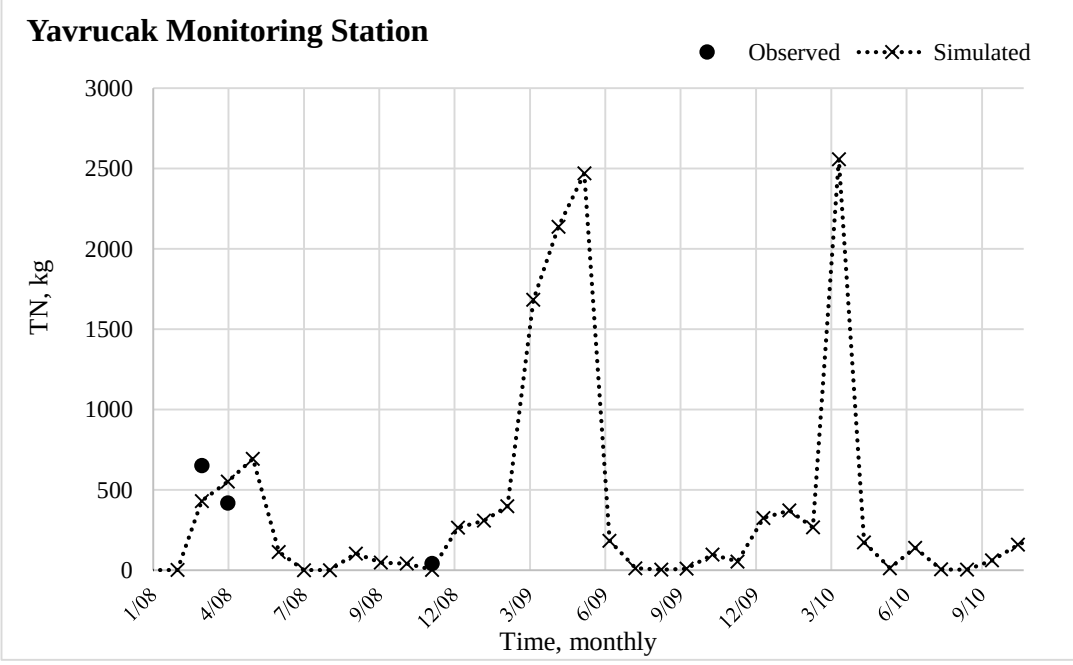

Figure 21. Simulated vs. observed TN loads after calibration at Yavrucak monitoring station

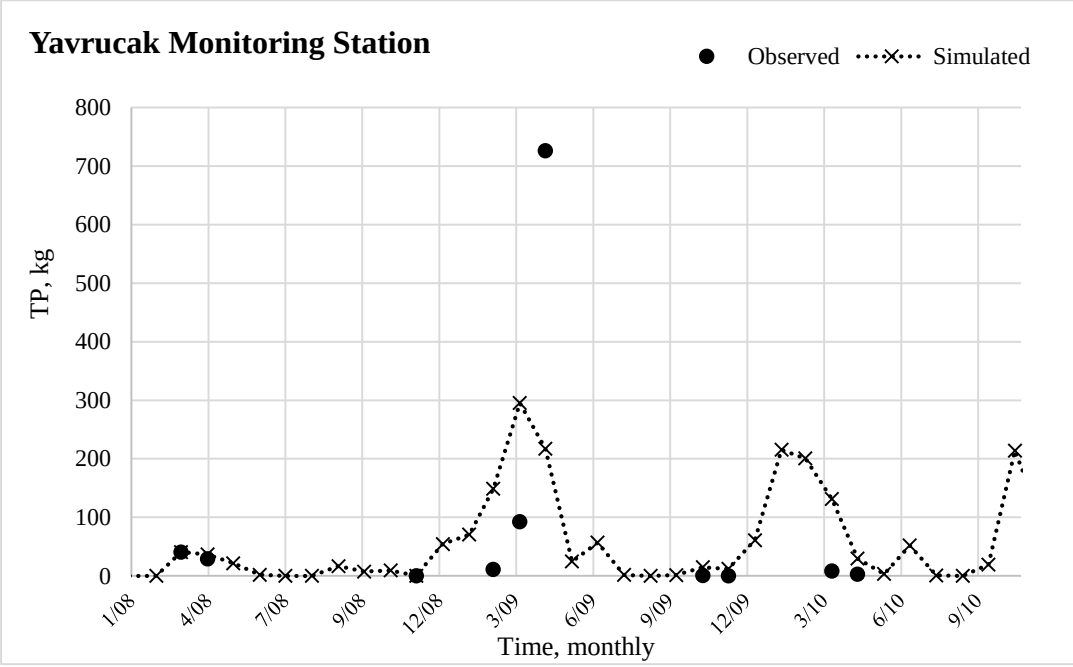

Figure 22. Simulated vs. observed TP loads after calibration at Yavrucak monitoring station

Table 33. Summary statistics of water quality calibration

Summary of statistics			
Number of simulations	1500		
Best simulation number	409		
	NO_3	**TN**	**TP**
p-factor	0.14	0.67	0.2
r-factor	1.33	2.08	0.15
NS	-0.20	0.64	0.26
PBIAS	37.9	11.7	-1.5
R^2	0.0	0.68	0.27

In Table 34, the means of monthly observed and simulated (from January 2008 to September 2010) streamflow, sediment and nutrient loads are given. The results show that when the long term monthly averaged values are of concern, the model performance is quite satisfactory except for NO_3. As it can be seen in Table 34, the mean of NO_3 mass transported monthly is quite high compared to other nutrient loads. The reason can be due to the fact that the fertilizers used to enhance the growth of wheat in the watershed is mainly nitrogen based (see Table 15). Four types of fertilizers namely urea, ammonium nitrate, ammonium sulfate and diamonium phosphate are used in agricultural lands. The percentage of nitrogen included in these

fertilizers are 46%, 33%, 21%, and 18%, respectively. Therefore, the source of such high amount of NO_3 is most probably the fertilizers.

Table 34. Observed and simulated means of monthly streamflow and nutrient loads at Yavrucak monitoring station

	Mean	
	Observed	**Simulated**
Streamflow (m^3/s)	0.10	0.12
Sediment (tons)	12.1	8.3
NO_3-N (kg)	1567.1	973.7
TN (kg)	369.4	326.1
TP (kg)	91.3	92.7

As it was mentioned in Section 3.3, the calibration and validation period excluding the warm-up was between January 2008 and September 2010. Within the specified period, all monthly streamflow values were available at Yavrucak and Sukesen monitoring stations. However, water quality calibration was troublesome due to data limitation. For instance, total nitrogen concentration was available only for three months at Yavrucak monitoring station. For total phosphorus and total suspended solids, 10 and 12 monthly data were available within the calibration period, respectively (see Section 4.1.1). Data availability at Sukesen monitoring station was slightly better compared to Yavrucak monitoring station. The model performance evaluation statistics; i.e., NSE, PBIAS and R^2, show that (see Section 4.1.3 and Section 4.1.4), the model does not simulate the sediment and water quality parameters satisfactorily. Although the general performance ratings suggest that the model performance is poor, the statistics for Lake Mogan watershed are not very meaningful because of the limited number of data. Therefore, long-term observed data (from January 2008 to September 2010) are compared with the mean ± 2 standard deviation (STD) range of the simulated data (see Figure 24). Two STD range corresponds to 95% probability. Figure 24 shows that all sediment loads observed in Yavrucak monitoring station remain within 95% probability range of the simulated data. In Sukesen, only one sediment load measurement stays outside the 2 STD range. Both at Yavrucak and Sukesen, only one total phosphorus measurement remains out of the range. These months are May and March, respectively. Similarly, all measured total nitrogen loads in Yavrucak are comprised within the 95% probability range. Lastly, only one total nitrogen load observation in March is outside the range in Sukesen. As a result, nearly all of the

observed water quality data were encompassed by the 95% probability range of the simulated data apart from few exemptions both in Yavrucak and Sukesen monitoring stations.

4.1.5. Model Validation Results

The model was validated at Sukesen monitoring station (see Section 3.3.5). The simulated and observed streamflow comparison for the validation is shown in Figure 23. NSE, PBIAS and R^2 values of the streamflow validation simulation are 0.4, 62.4 and 0.35, respectively. The results show that the model performance was poor according to Table 7. Although the general trend in the streamflow of Sukesen is simulated acceptably, the model is not able to catch the peak values in March and April 2009, and Jan., Feb. and March 2010. Sukesen is a quite different subbasin than Yavrucak especially in terms of land use classification (see Section 4.2.1). Therefore, the validation results imply that model is not capable of simulating spatial variability of the watershed. To represent spatial variability better and thus to improve model reliability, it could have been healthier to prefer multi-gauge calibration. In fact, there are numerous studies emphasizing the importance of multi-gauge calibration in arid and semi-arid watersheds (Niraula et al., 2012; Shrestha et al., 2016). Consequently, the results highlighted the importance of increasing monitoring campaigns in Lake Mogan watershed.

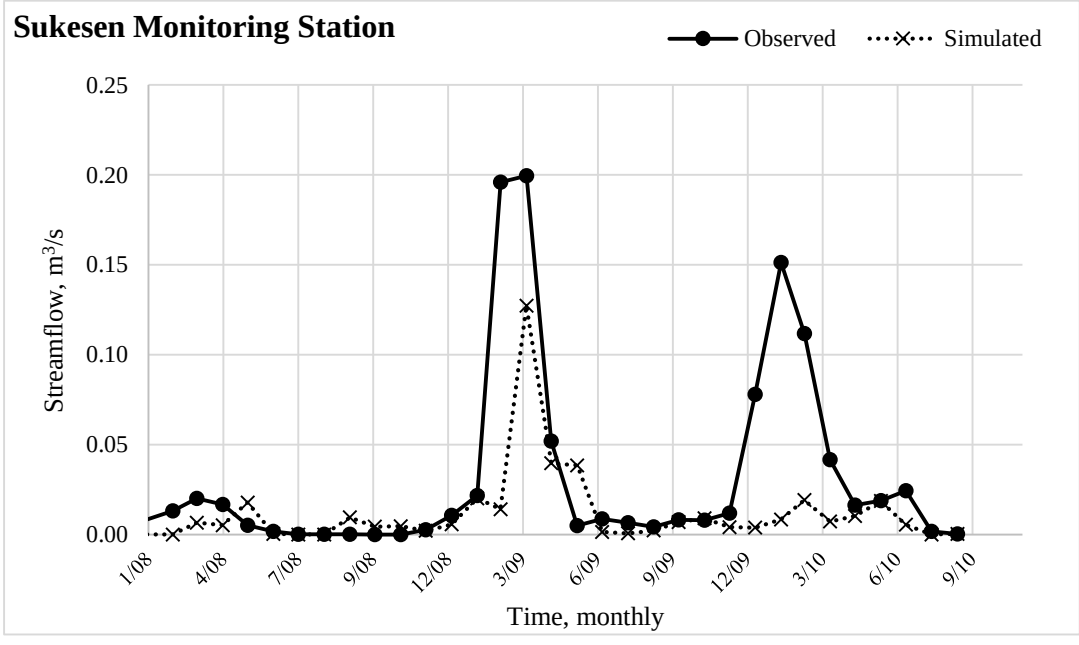

Figure 23. Simulated vs. observed streamflow values at Sukesen monitoring station

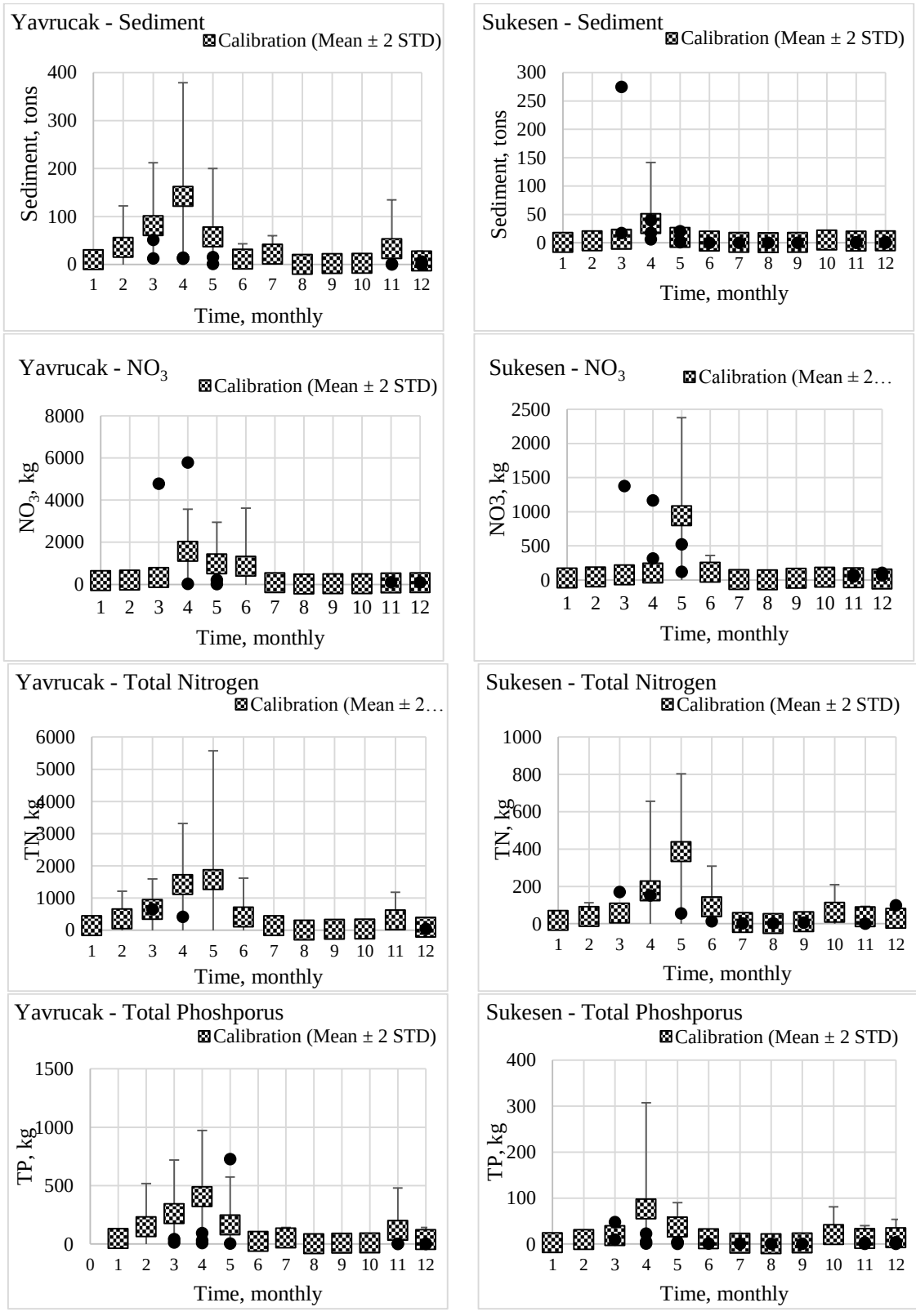

Figure 24. The comparison of observed sediment and water quality data with the mean ±2 STD range of simulated data on a monthly basis

The mean values of observed and simulated streamflow, and nutrient loads at Sukesen monitoring station are given in Table 35. As can be seen from Table 35, Yavrucak creek is exposed to higher nutrient loads compared to Sukesen creek. This is because Yavrucak and Sukesen subbasins are different from each other in terms of land/land cover characteristics. Detailed comparison of Yavrucak and Sukesen subbasins in terms of landuse, soil and slope is given in the following section (Section 4.2.1).

Table 35. Observed and simulated means of monthly streamflow and nutrient loads at Sukesen and Yavrucak monitoring station

	Sukesen		**Yavrucak**	
	Mean		**Mean**	
	Observed	**Simulated**	**Observed**	**Simulated**
Streamflow (m^3/s)	0.03	0.01	0.10	0.12
Sediment (tons)	23.9	1.8	12.1	8.3
NO_3-N (kg)	514.9	361.7	1567.1	973.7
TN (kg)	55.3	112.9	369.4	326.1
TP (kg)	6.2	14.2	91.3	92.7

4.2. Sensitivity Analysis

One-at-a-time sensitivity analysis was performed after calibration to see the overall effect of each calibration parameter on the model outputs. There are two parameter sensitivity statistics, the t-stat and the p-value. While the smaller values of p-value shows higher sensitivity, the sensitivity increases with higher values of t-stat.

A total of 20 parameters were used in streamflow calibration (see Section 3.3.3). Table 36 lists the streamflow calibration parameters with their sensitivity statistics. The groundwater and snow related parameters were found as the most sensitive variables for the semi-arid region, Lake Mogan watershed. The six most sensitive parameters are SNO50COV, GW_DELAY, GWQMN, RCHRG_DP, SNOCOVMX, and SFTMP. Greater sensitivity of the snow related parameters was not surprising since the snowmelt has a substantial effect on the streamflow in Lake Mogan watershed. Furthermore, the groundwater supply in Lake Mogan watershed being quite low may result in higher sensitivity of groundwater parameters. Even small changes in groundwater supply may result in considerable impacts on the flowrates of the seasonal creeks located in the Lake Mogan watershed.

The results obtained in this study show that the streamflow parameters that are found to significantly affect simulations in the Lake Mogan are consistent with those specified in the studies carried out in regions showing similar characteristics with Lake Mogan watershed. For instance, Yang et al. (2014) performed a study in Amur river where the stream hydrograph is dominated by spring snowmelt. They found that the parameters SNOCOVMX and SNO50COV were found as the top-ranked sensitive parameters. CN2, curve number, which is generally the most sensitive streamflow calibration parameter came after the snow parameters in sensitivity ranking. Likewise, CN2 was found as the 7th sensitive parameter, less sensitive than snow parameters, in Lake Mogan watershed. Lévesque et al. (2008) carried out a study in two agricultural watersheds located in southeastern Canada. They stated that among the 10 most sensitive parameters, the top four were snowmelt related parameters. Noor et al. (2014) performed a study in a semi-arid mountainous watershed, Taleghan, and specified that the calibration of five snow related parameters, SMFMN, SMFMX, SNOCOVMX, SNO50COV, and TIMP had the greatest effect on the model performance. Moreover, Stratton et al. (2009) modeled the water balance processes in a semi-arid mountainous watershed of Idaho. They found that the groundwater related parameters namely ALPHA_BF, RCHRG_DP, REVAPMIN, and two snow parameters SMTMP and TIMP were among the top eleven sensitive parameters. Our results are in good agreement with the result of these studies. A total of 20 parameters were used in the sediment calibration. Table 37 shows the sediment calibration parameters with their sensitivity statistics. The most sensitive parameter was found to be USLE_K which is the soil erodibility factor. USLE_K is followed by USLE_P, support practice factor. USLE_P and USLE_K are two parameters of Modified Universal Soil Loss Equation (MUSLE) which is defined by the following equation:

$$sed = 11.8 \,.\, (Q_{surf}.q_{peak}.area_{hru})^{0.56}.K_{USLE}.C_{USLE}.P_{USLE}.LS_{USLE}.CFRG \quad (5)$$

where sed = sediment yield on a given day (metric tons), Q_{surf}= surface runoff volume (mm H_2O/ha), q_{peak} = peak runoff rate (m^3/s), $area_{hru}$ = area of the HRU (ha), K_{USLE} = USLE soil erodibility factor, C_{USLE} = USLE cover and management factor, P_{USLE} = USLE support practice factor, LS_{USLE} = USLE topographic factor, $CFRG$ = coarse fragment factor.

Table 36. Streamflow calibration parameters' sensitivity statistics

Parameter Name	t-stat	p-value
SNO50COV.bsn	-34.76	0.00
GW_DELAY.gw	10.82	0.00
GWQMN.gw	9.63	0.00
RCHRG_DP.gw	-9.42	0.00
SNOCOVMX.bsn	-7.88	0.00
SFTMP.bsn	-6.98	0.00
CN2.mgt	-5.04	0.00
SMFMX.bsn	4.13	0.00
CH_N1.sub	2.56	0.01
SOL_AWC(..).sol	1.82	0.07
CH_N2.rte	1.46	0.14
ALPHA_BF.gw	-1.45	0.15
SMFMN.bsn	1.34	0.18
GW_REVAP.gw	1.20	0.23
SURLAG.bsn	0.65	0.52
EPCO.hru	0.64	0.52
SMTMP.bsn	-0.64	0.52
ESCO.hru	0.60	0.55
REVAPMN.gw	-0.35	0.73
TIMP.bsn	0.27	0.79

USLE_P is normally used to represent support practices including contour tillage, strip-cropping on the contour, and terrace systems (Arnold et al., 2012a). Its default value is 1. However, it can be used as a scaling parameter to further reduce sediment yield as needed (Almendinger et al., 2014). Initially, USLE_P was not included among the sediment calibration parameters since there is no support practice implemented in Lake Mogan watershed. However, the simulated sediment yield was overestimated with default sediment parameters (see Figure 66 in Appendix C), and the best sediment simulation result was obtained when USLE_P was calibrated. Therefore, it was included in the calibration. SOL_ROCK, rock fragment content; BIOMIX, biological mixing efficiency; CH_BNK_D50, median particle size diameter of channel bank sediment, comes sequentially after USLE_P in the sensitivity ranking.

Table 37. Sediment calibration parameters' sensitivity statistics

Parameter Name	t-stat	p-value
USLE_K(..).sol	-25.73	0.00
USLE_P.mgt	-24.88	0.00
SOL_ROCK(..).sol	11.59	0.00
BIOMIX.mgt	-3.07	0.00
CH_BNK_D50.rte	-2.26	0.02
CH_BED_BD.rte	-1.73	0.08
SPEXP.bsn	-1.51	0.13
CH_BED_KD.rte	-1.16	0.25
ADJ_PKR.bsn	1.00	0.32
CH_COV2.rte	0.93	0.35
SPCON.bsn	0.85	0.40
RSDCO.bsn	-0.64	0.52
CH_BNK_BD.rte	0.62	0.54
C_FACTOR.bsn	0.49	0.63
CH_WDR.rte	-0.35	0.72
CH_BED_D50.rte	0.35	0.73
CH_BNK_KD.rte	0.31	0.76
CH_COV1.rte	0.21	0.83
CH_BNK_TC.rte	0.19	0.85
CH_ERODMO(..).rte	0.10	0.92

In nitrogen and phosphorus calibration a total of 15 parameters were used. Table 38 lists the nitrogen and phosphorus calibration parameters according to their sensitivity statistics. The six most sensitive parameters are found to be the ones related to nitrogen processes. NPERCO, nitrate percolation coefficient, was the most sensitive parameter. In their study Santhi et al. (2001) explained the calibration procedure of SWAT which was applied in the Bosque River watershed. According to the calibration procedure given in this study, for nutrients, after adjusting initial soil concentrations of organic nitrogen (SOL_ORGN) and phosphorus (SOL_ORGP), NPERCO, phosphorus percolation coefficient (PPERCO), and phosphorus soil partitioning coefficient (PHOSKD) should be adjusted (Santhi et al., 2001). For Lake Mogan watershed, as well as SOL_ORGN and SOL_ORGP, initial nitrate concentration in the soil layer (SOL_NO3) which was found as the third sensitive parameter, was also adjusted. Among the parameters controlling the phosphorus processes, SOL_ORGP was found as the most sensitive one. RS5 and PHOSKD were the second and third sensitive parameter, respectively.

Table 38. Nitrogen and phosphorus calibration parameters' sensitivity statistics

Parameter Name	t-stat	p-value
NPERCO.bsn	-5.44	0.00
CDN.bsn	4.13	0.00
SOL_NO3(..).chm	-2.24	0.03
SOL_ORGN(..).chm	-1.50	0.13
BC4_BSN.bsn	1.38	0.17
SDNCO.bsn	1.29	0.20
SOL_ORGP(..).chm	-1.28	0.20
RS5.swq	1.05	0.29
PHOSKD.bsn	-0.96	0.34
ERORGP.hru	-0.61	0.54
PPERCO.bsn	-0.52	0.60
BC3_BSN.bsn	-0.35	0.73
BC2_BSN.bsn	-0.15	0.88
PSP.bsn	-0.09	0.93
BC1_BSN.bsn	-0.02	0.98

4.2.1. Landuse, Soil and Slope Characteristics of Yavrucak and Sukesen Subbasins

Yavrucak and Sukesen subbasins' land use/land cover areas and percentages are given in Table 39. Figure 25 shows the percentages of each landuse class. Figure 26 is the landuse/landcover map of Yavrucak and Sukesen subbasins. As shown in Table 39, Yavrucak subbasin is mostly covered with agricultural land (47%). Pastures also occupy a significant part (31%) of the basin. Sukesen, on the other hand, is mainly covered with pastures (55.2%). Residential areas (21.6%) comprise other significant part of the basin (see Table 39, Figure 25). When the pollutant loads in Yavrucak and Sukesen are compared (see Table 35), the nutrient loads are relatively higher in Yavrucak than Sukesen. The difference is, in fact, because of the differences in land use percentages. The fact that the agricultural lands cover large portion of the Yavrucak basin results in higher amounts of nutrient loads transported in this stream.

Table 39. Areas and percentages of land use classes in Sukesen and Yavrucak subbasins

	Sukesen		Yavrucak	
Land use class	**Area (ha)**	**Area (%)**	**Area (ha)**	**Area (%)**
Water	2.8	0.1	3.0	0.0
Forest	0.8	0.03	0.2	0.0
Agricultural land	325.8	11.1	4339.1	47.0
Transportation	60.9	2.1	39.5	0.4
Residential area	631.2	21.6	1059.8	11.5
Mining site	0.2	0.01	4.8	0.1
Fallowing land	134.1	4.6	781	8.5
Pasture	1616.7	55.2	2853.9	30.9
Range land	155.3	5.3	151.5	1.6
Total area	2927.7		9232.7	

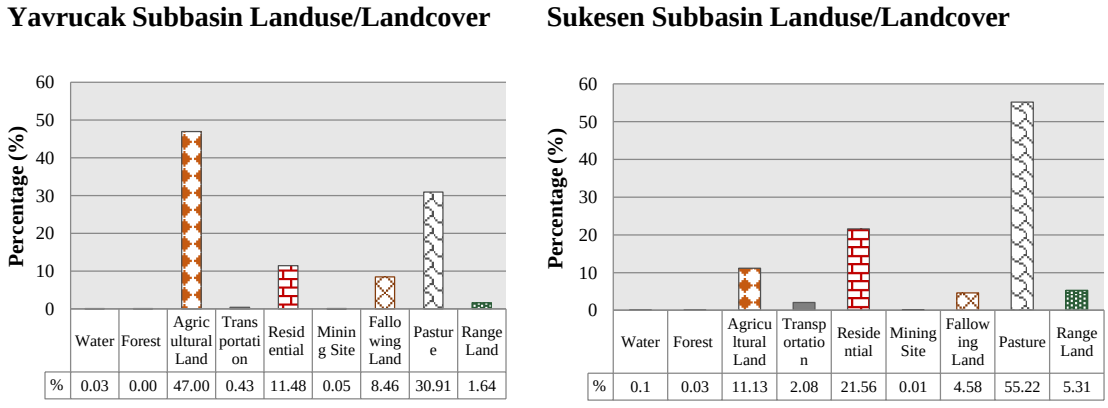

Figure 25. Sukesen and Yavrucak subbasins' landuse percentages

Yavrucak and Sukesen subbasins were also compared in terms of soil and slope classes. The percentages of soil and slope classes in both subbasins are given in Table 40 and Table 41, respectively. Soil and slope maps of the subbasins are given in Figure 27 and Figure 28, respectively. As it was mentioned in Section 3.1.4, 49 soil classes were determined in Lake Mogan watershed. The properties of the soil classes were previously given in Table 13. As it can be seen from Table 40, the majority of Yavrucak subbasin is composed of two classes namely Mogan 28 (33.9%) and Mogan 30 (27.06%). In Sukesen subbasin, on the other hand, Mogan 7 is the main soil class constituting 52.1% of the basin. See Table 13 for the properties of the mentioned soil classes.

As can be seen from Figure 28, Yavrucak is not a very sloping subbasin. The largest percentage (36.05%) belongs to the slope class of 3 – 5% while the lowest percentage (2.12%) is of >10% soil class. In contrast to Yavrucak, Sukesen is a more sloping subbasin. At Sukesen subbasin, 54.13% of the area has slopes greater than 10%. As can be seen from Figure 28, the steep region is located in the eastern part of the basin.

Table 40. Soil class percentages in Yavrucak and Sukesen subbasins

Soil Class	**Yavrucak Subbasin (10336 ha)**	**Sukesen Subbasin (2928 ha)**
	Area (%)	**Area (%)**
Mogan 5	-	0.17
Mogan 6	-	33.59
Mogan 7	-	52.08
Mogan 8	-	14.02
Mogan 10	-	0.15
Mogan 19	0.00	-
Mogan 22	0.58	-
Mogan 24	5.99	-
Mogan 25	9.17	-
Mogan 27	7.08	-
Mogan 28	34.86	-
Mogan 29	4.75	-
Mogan 30	27.06	-
Mogan 31	10.49	-

Table 41. Slope class percentages in Yavrucak and Sukesen subbasins

Slope (%)	**Yavrucak Subbasin (10336 ha)**	**Sukesen Subbasin (2928 ha)**
	Area (%)	**Area (%)**
0-1	4.46	0.55
1-3	31.93	5.45
3-5	36.05	12.23
5-10	25.43	27.64
10-9999	2.12	54.13

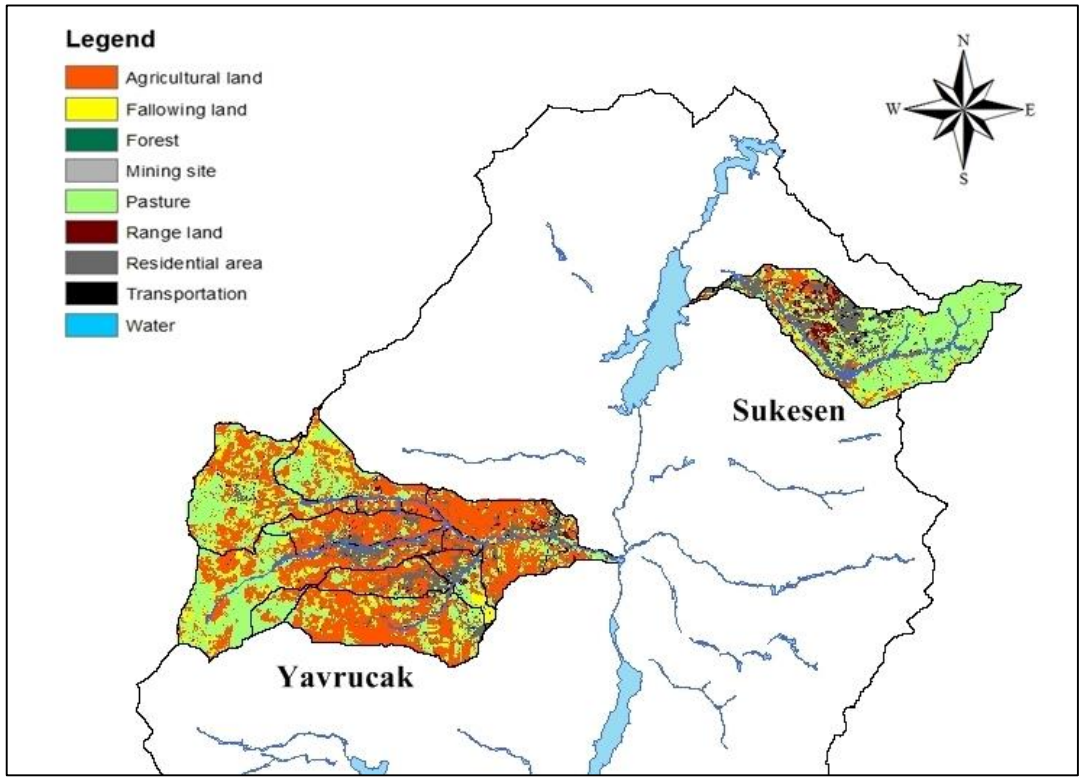

Figure 26. Land use map of Yavrucak and Sukesen subbasins

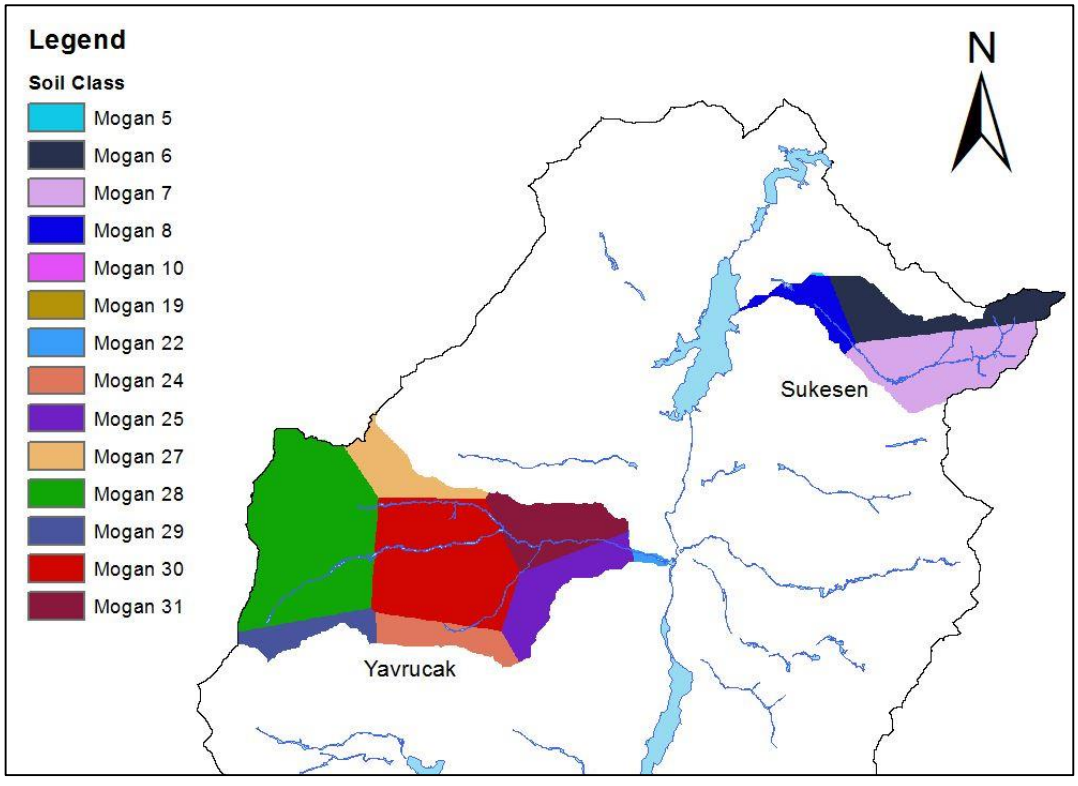

Figure 27. Soil map of Yavrucak and Sukesen subbasins

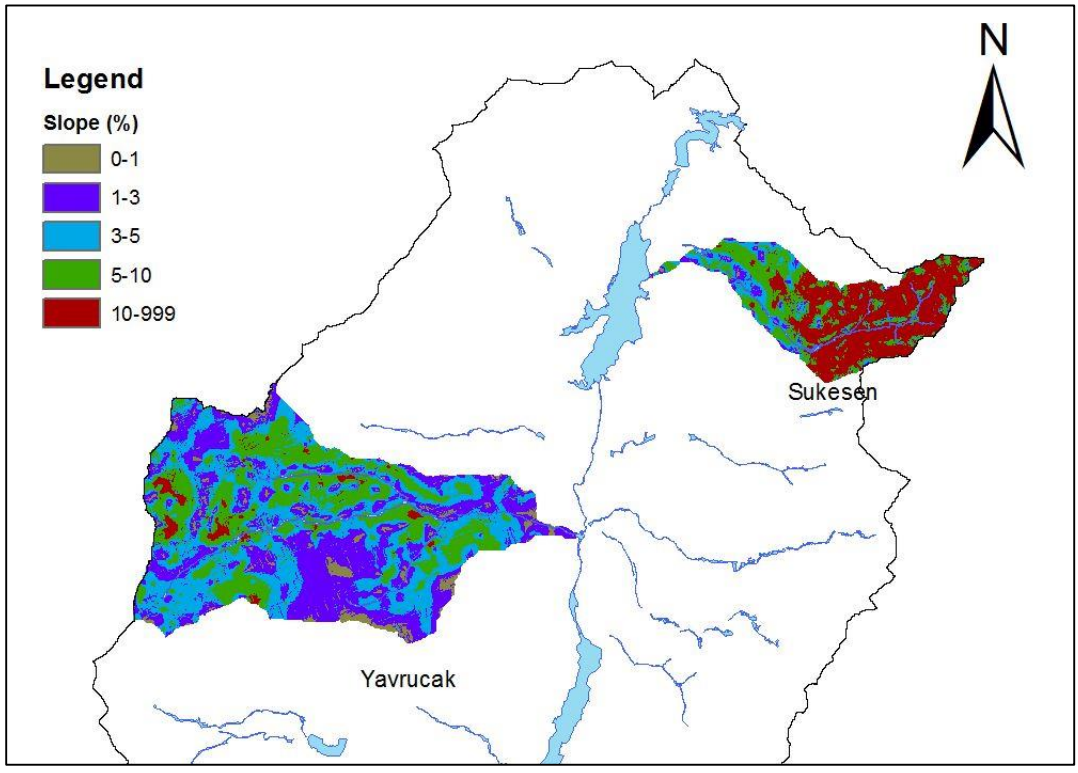

Figure 28. Slope map of Yavrucak and Sukesen subbasins

4.2.2. Overall Evaluation of Calibration Results and Model Performance

Application of deterministic models in semi-arid regions is a challenging task. The challenges in modelling these regions are mainly due to varying hydrological characteristics and lack of observed data. Schneider et al. (2007) mentioned that there can be unexpected challenges in modelling the hydrology of semi-arid watersheds compared to similar efforts made in humid environments. Moreover, the author added that differing precipitation and temperature patterns together with the differences in soil and vegetation properties cause alterations in the distribution of runoff processes. Wheater (2008) pointed out that modelling methods have been used for decades but nearly all of them were developed for humid regions. The author also mentioned that the challenges experienced in arid and semi-arid area modelling have received little attention so far. Pilgrim et al. (1988) specified that the major problem for runoff modelling in arid regions is the lack of observed data. Similarly, Hughes (2008) stated that a lack of spatial and temporal detail in rainfall data is among the main constraints of modelling in arid and semi-arid regions. Furthermore, data on evapotranspiration, another significant component of water balance, is generally less available compared to rainfall in these regions. The limited availability of data on evapotranspiration is,

therefore, another challenge in modeling semi-arid and arid hydrology. According to Croke and Jakeman (2008), poor raingauge density is another issue limiting the capacity of any rainfall-runoff model to simulate the observed flow. Mirshahi (2010) listed the features of semi-arid and arid regions making hydrological modelling challenging as poor data quality, data paucity, poor raingauge density, rainfall spatial variability, low frequency of events, highly non-linear relationships between rainfall and runoff, and less documentation for rainfall-runoff modelling in such regions compared to humid watersheds. In Lake Mogan, a semi-arid watershed located in Turkey, almost all of the mentioned limitations of semi-arid regions for modelling are encountered. Firstly, there are only two raingauges found within a watershed area of 970 km^2. Therefore, the spatial variability of rainfall cannot be reflected truly. Next, available rainfall data period is really short in these raingauges. Only the data between 2007 and 2010 are available for the modelling study. When the temporal variability of rainfall in semi-arid regions is taken into account, the limited rainfall data becomes another significant problem for the hydrological modeling in Lake Mogan watershed. In addition to limited data availability, evaporation data, a critical component of water balance, is not available. Finally, it is know that there are several irrigation wells located in the watershed, however, no information is available about them. Consequently, it is really challenging to represent the actual water balance in Lake Mogan watershed.

Although SWAT is widely used all over the world, its application in the arid/semi-arid regions like Lake Mogan watershed is not so common but increasing (Yuan, 2010). In addition, the majority of these studies focused on the calibration of streamflow. Thus, the calibration of water quality parameters are not reported frequently. Niraula et al. (2012) used SWAT model in the semi-arid Santa Cruz watershed to simulate the streamflow and to evaluate the impacts of multi-gauge calibration on flow predictions. The calibration of water quality parameters was not carried out in this study. Chahinian et al. (2011) modelled the flow and water quality dynamics of a coastal Mediterranean intermittent river via SWAT 2005. Within the scope of this study, sediment, nitrogen and phosphorus simulations were also carried out together with streamflow. The authors reported that the model performed well in streamflow simulation but the sediment and nutrient simulations were less satisfactory. Yuan (2010) assessed the applicability of SWAT model on a semi-arid watershed in Arizona. The model was calibrated and validated satisfactorily for

streamflow. The water quality calibration was not carried out. The author reported that the model can be used to evaluate the current conditions in the watershed, and to assess different management scenarios. Shrestha et al. (2016) compared the single and multi-site calibration by using SWAT in terms of flow and nutrient loads simulations in the semi-arid Onkaparinga catchment in South Australia. The success criteria were met for the streamflow calibration. However, sediment and nutrient loadings were not simulated satisfactorily. The model performance statistics reported in the mentioned studies are summarized in Table 42. The studies given in Table 42 were carried out in semi-arid areas, and the statistics given are for the monthly time-step.

Table 42. The summary of the model performance statistics for the selected studies

	Streamflow (Calibration)			**Streamflow (Validation)**		
	NS Min/Max	PBIAS Min/Max	R^2 Min/Max	NS Min/Max	PBIAS Min/Max	R^2 Min/Max
Shrestha et al. (2016)	0.64/0.84	-27.3/8.1	0.7/0.85	0.69/0.87	-	-
Niraula et al. (2012)	0.61/0.90	-18/72	0.62/0.91	0.41/0.85	-51/26	0.61/0.85
Chahinian et al. (2011)	0.89/0.94	-1.31/4.32	-	0.67/0.79	-13.7/3.77	-
Yuan (2010)	0.52/0.56	-1.29/24.63	0.55/0.57	0.55/0.57	-9.23/3.00	0.70/0.70
This study	0.74	-19.1	0.8	0.4	62.4	0.35
	Sediment (Calibration)			**Sediment (Validation)**		
	NS Min/Max	PBIAS Min/Max	R^2 Min/Max	NS Min/Max	PBIAS Min/Max	R^2 Min/Max
Shrestha et al. (2016)	0.06/0.36	-221.9/39.3	0.07/0.38	-	-	-
Niraula et al. (2012)	-	-	-	-	-	-
Chahinian et al. (2011)	-2.06/0.09	-65.02/101.11	-	-1.5/0.01	-84.98/-24.68	-
Yuan (2010)	-	-	-	-	-	-
This study	-0.01	31.7	0.1	-0.1	92.5	0.0
	Nitrate (Calibration)			**Nitrate (Validation)**		
	NS Min/Max	PBIAS Min/Max	R^2 Min/Max	NS Min/Max	PBIAS Min/Max	R^2 Min/Max
Shrestha et al. (2016)	-	-	-	-	-	-
Niraula et al. (2012)	-	-	-	-	-	-
Chahinian et al. (2011)	-2.86/-2.07	-98.83/-97.59	-	-5.82/-1.59	-100/-100	-
Yuan (2010)	-	-	-	-	-	-
This study	-0.20	37.9	0.0	-2.05	29.7	0.06
	Total Nitrogen (Calibration)			**Total Nitrogen (Validation)**		
	NS Min/Max	PBIAS Min/Max	R^2 Min/Max	NS Min/Max	PBIAS Min/Max	R^2 Min/Max
Shrestha et al. (2016)	-0.10/0.39	23.5/55.9	0.04/0.41	-	-	-
Niraula et al. (2012)	-	-	-	-	-	-
Chahinian et al. (2011)	-	-	-	-	-	-
Yuan (2010)	-	-	-	-	-	-
This study	0.64	11.7	0.68	-8.8	-104.3	0.02
	Total Phosphorus (Calibration)			**Total Phosphorus (Validation)**		
	NS Min/Max	PBIAS Min/Max	R^2 Min/Max	NS Min/Max	PBIAS Min/Max	R^2 Min/Max
Shrestha et al. (2016)	0.13/0.40	-30.1/49.2	0.17/0.4	-	-	-
Niraula et al. (2012)	-	-	-	-	-	-
Chahinian et al. (2011)	-	-	-	-	-	-
Yuan (2010)	-	-	-	-	-	-
This study	0.26	-1.5	0.27	-3.7	-129.1	0.15

The calibration results revealed that the model performance is quite satisfactory in streamflow simulations. However, sediment and especially nitrogen and phosphorus simulations are not as successful as streamflow. At this point, judgment of whether the model can be used effectively for the comparison of agricultural BMPs should be made. In other words, is the calibrated SWAT model performance is sufficient for the purpose of the study? Harmel et al. (2014) divided the intended model uses into three category; Exploratory, Planning, and Regulatory/Legal. The studies falling into the Exploratory category aim to carry out initial or approximate comparisons. The Planning category includes modelling projects for planning purposes such as urban development and watershed planning. The Regulatory/Legal category comprises the studies with regulatory, legal, and/or human health implications. The required accuracy in model predictions becomes more critical towards the Regulatory/Legal category. The authors stated that reduced confidence in predictions is acceptable in the Exploratory category. Similar comparison regarding the models' intended use was carried out by Moriasi et al. (2007). The authors mentioned that stricter model performance ratings are required in studies involving potentially large consequences such as development of new laws and regulations and congressional testimony. The studies in which there is no regulatory action is required, the accuracy in model simulations is less significant. Furthermore, the authors specified that basic exploratory studies will require even lower performance ratings. Arabi et al. (2012) stated that "exploratory models are used to provide insights about potential outcomes, opportunities, and risks associated with alternative management strategies". Given the objective of this thesis study is to compare different agricultural best management practices, the study can be placed on the exploratory category. Therefore, it can be said that the model accuracy is not very critical. Finally, a spectrum showing the relationship between required model accuracy and model's intended use was created based on literature to emphasize that when the model is to be used for screening purposes then there is no need for strict accuracy (see Figure 29). As a conclusion, although the SWAT model performance for *water quality* simulations was assessed as unsatisfactory in Lake Mogan watershed, the model can be used for the evaluation and comparison of agricultural best management practices.

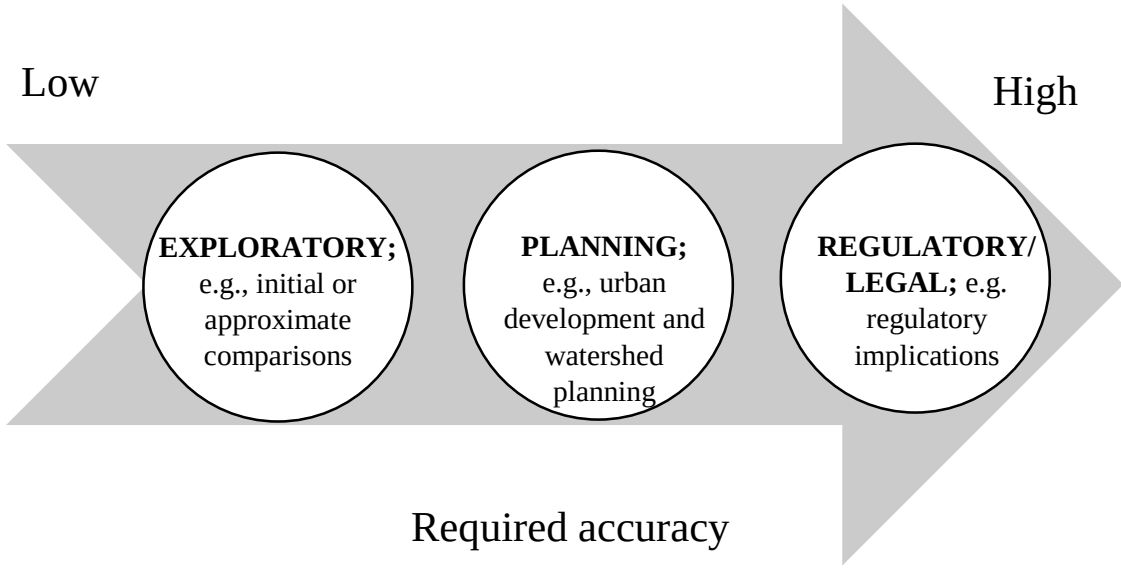

Figure 29. Continuum of model's intended use from least accuracy to most required accuracy

4.3. Evaluation of BMP Scenarios

As mentioned in Section 3.4, 11 BMP scenarios were developed within the scope this study. To evaluate and compare the impacts of BMP scenarios on water quality, model simulations were performed over a three year period from 2008 to 2010. SWAT requires daily input data but the model results can be printed daily, monthly and annually. For instance, if monthly print-out option is selected, the model is still run on a daily time-step but the results are aggregated to evaluate monthly yields. Therefore, the model was run and the results were printed out both on a monthly and yearly basis. The average monthly and annual loads for each pollutant (sediment, NO_3, TN and TP) were calculated at Yavrucak and Sukesen subbasin outlets. The percent changes in the amounts of average monthly and annual pollutant loads obtained for each scenario were compared with the ones simulated in the baseline scenario to evaluate the effectiveness of each BMP. The percent change in the pollutant loads was calculated with the following formula:

$$percent\ change,\ \% = \frac{(postBMP - preBMP)}{preBMP} * 100 \qquad (6)$$

where preBMP and postBMP are the average monthly or yearly pollutant loads before and after BMP is applied, respectively.

4.3.1. Nutrient Management

As it was mentioned in Section 3.4.1, three different nutrient management scenarios were developed by reducing the fertilizer amount by 10%, 20% and 30% compared to current fertilizer application rates in agricultural lands. The results showed that reduction in fertilizer application for agricultural lands provided considerable decrease in nitrogen (NO_3 and TN) loads at the Yavrucak subbasin outlet. There was not a significant change in the TP and sediment loads which is most probably due to the fact that the fertilizers applied in agricultural lands are mainly nitrogen based (see Section 3.1.5). As the reduction ratio increased, the amount of transported pollutant loads decreased, as expected. Among the nutrient management scenarios the highest pollutant load reduction was achieved with the alternative in which fertilizer application rates were decreased by 30%. Other scenarios did not lead to a significant change in the sediment and nutrient loads. The effect of changes in fertilizer application at Yavrucak is observed more prominently compared to Sukesen monitoring station. The reason is that the percentage of agricultural lands in Yavrucak subbasin is much higher compared to Sukesen subbasin (see Section 4.2.1).

In some months, increases in nutrient loads were calculated. These increases are most probably due to fluctuations in numeric calculations and approximations in the model.

The monthly percent changes in pollutant loads in Scenario-1, Scenario-2 and Scenario-3 are given in the following sub-headings in detail. The comparison of scenario results on a yearly basis is given in Section 4.4.

Scenario-1

The monthly percent changes in sediment and nutrient (NO_3, TN and TP) loads at Yavrucak and Sukesen monitoring stations when the fertilizer application rates in agricultural lands are reduced by 10% is shown in Figure 30 and Figure 31, respectively. The averages of percent changes in NO_3, TN, TP and sediment loads are -1.6%, -1.1%, -0.02% and -0.06%, respectively in Yavrucak. The monthly percent changes in NO_3 and TN loads range from -14.5% to 0.25% and -8.4% to 0.13%, respectively. The magnitude of maximum monthly percent change in NO_3 load is -

14.5. The highest load change in TN, on the other hand, is -8.4%. TP and sediment loads are less affected by the changes in the fertilizer application rates compared to NO_3 and TN. The utmost reductions in TP and sediment loads are -1.5% and -1.5%, respectively.

In Sukesen monitoring station, the averages of monthly percent changes in NO_3, TN, TP and sediment loads are -0.23%, -0.15%, -0.03% and -0.01%, respectively. The magnitude of highest NO_3 and TN load reductions are -3.3% and -1.9%, respectively. Similar to Yavrucak, there is not a considerable reduction in TP and sediment loads in Sukesen. The maximum load reductions in TP and sediment loads are -0.5% and -0.1%, respectively.

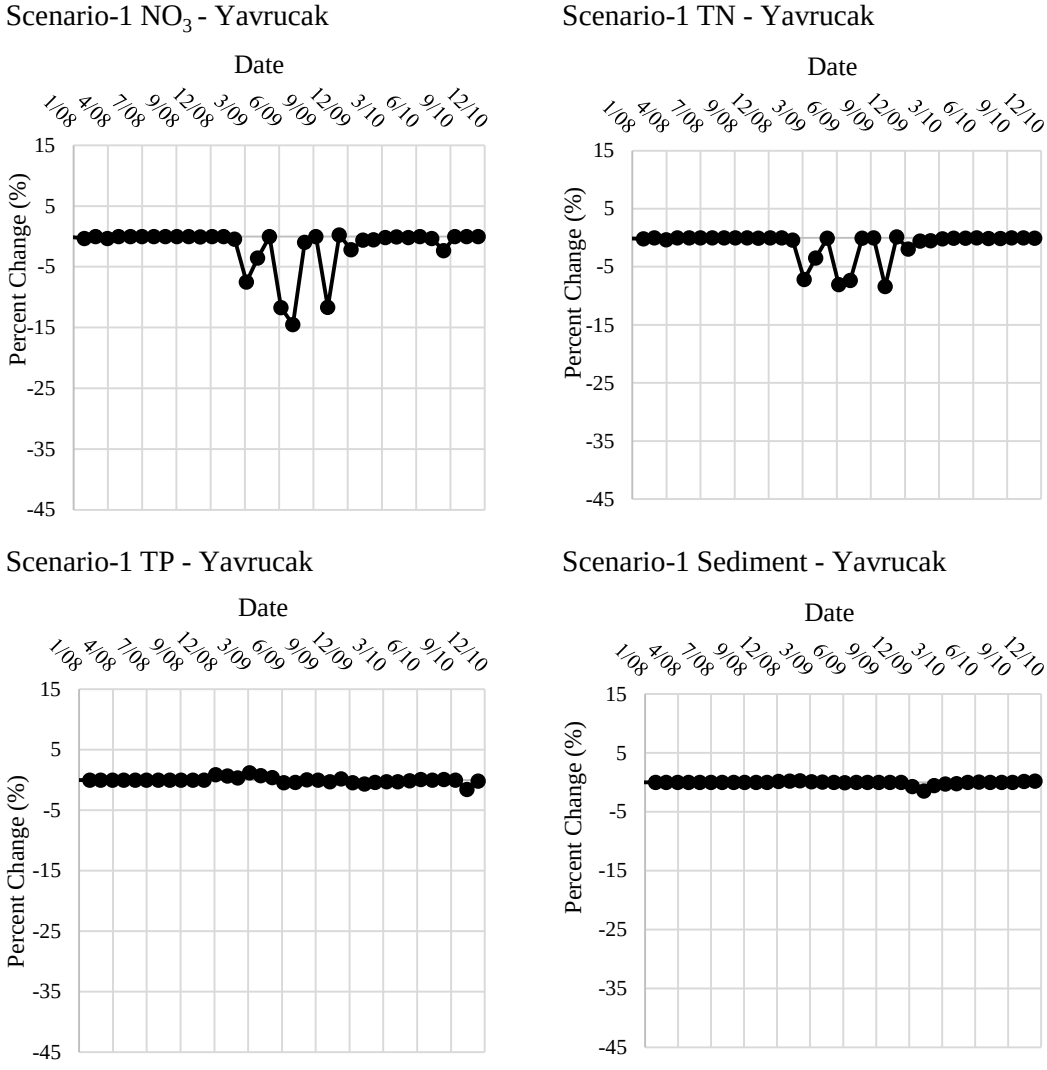

Figure 30. The results of Scenario-1 at Yavrucak monitoring station: Percent changes in NO_3, TN, TP and sediment loads

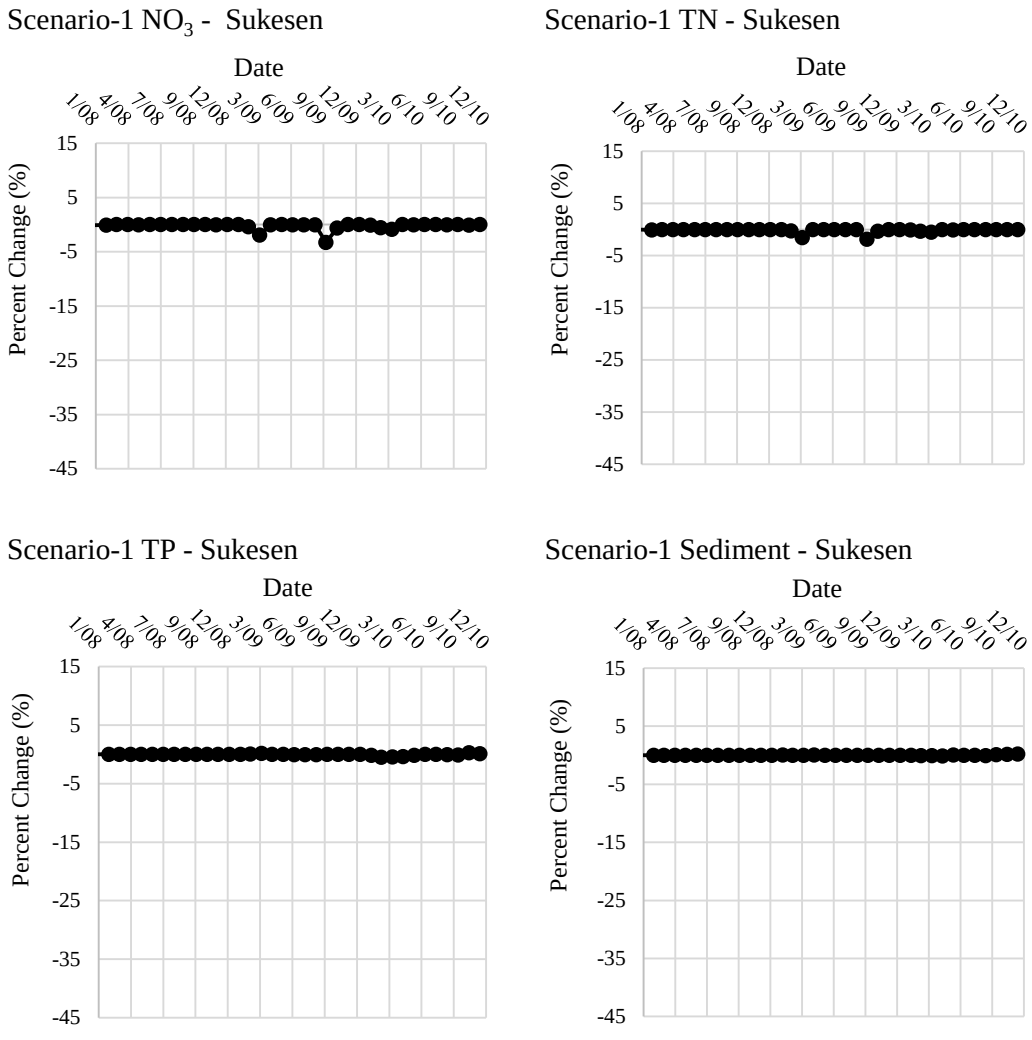

Figure 31. The results of Scenario-1 at Sukesen monitoring station: Percent changes in NO_3, TN, TP and sediment loads

Scenario-2

The monthly percent changes in sediment and nutrient (NO_3, TN and TP) loads at Yavrucak and Sukesen monitoring stations when the fertilizer application rates in agricultural lands are reduced by 20% is shown in Figure 32 and Figure 33, respectively. The simulated average monthly loads for NO_3, TN, TP and sediment are reduced by -4%, -2.8%, -0.2% and -0.02%, respectively, compared to the baseline scenario in Yavrucak monitoring station. Similar to Scenario-1, Scenario-2 shows that NO_3 and TN loads are affected more by the reductions in fertilizer application rates than TP and sediment loads. The percent changes in NO_3 and TN loads range from -29.2% to 0% and -17.1% to 0.3%, respectively. The highest monthly percent

reductions in TP and sediment loads, on the other hand, are -2.7% and -1.9%, respectively.

In Sukesen monitoring station, the averages of monthly percent changes in NO_3, TN, TP and sediment loads are -0.42%, -0.28%, -0.08% and 0.03%, respectively. The percent reductions in monthly NO_3 and TN loads are higher compared to TP and sediment loads. The percent changes in NO_3 and TN ranges from -5.5% to 0% and -3.2% to 0%, respectively. The highest reductions in TP and sediment loads are -1.1% and -0.17, respectively.

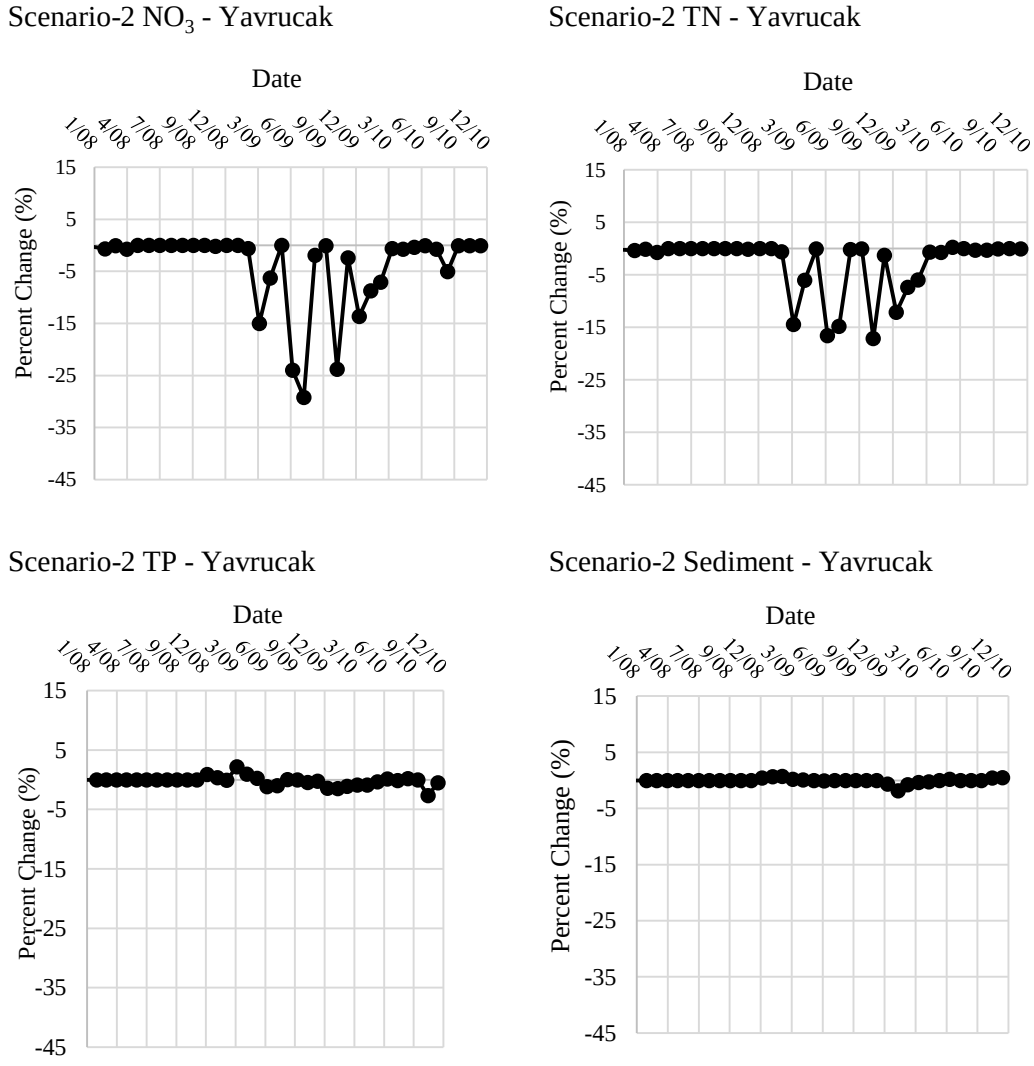

Figure 32. The results of Scenario-2 at Yavrucak monitoring station: Percent changes in NO_3, TN, TP and sediment loads

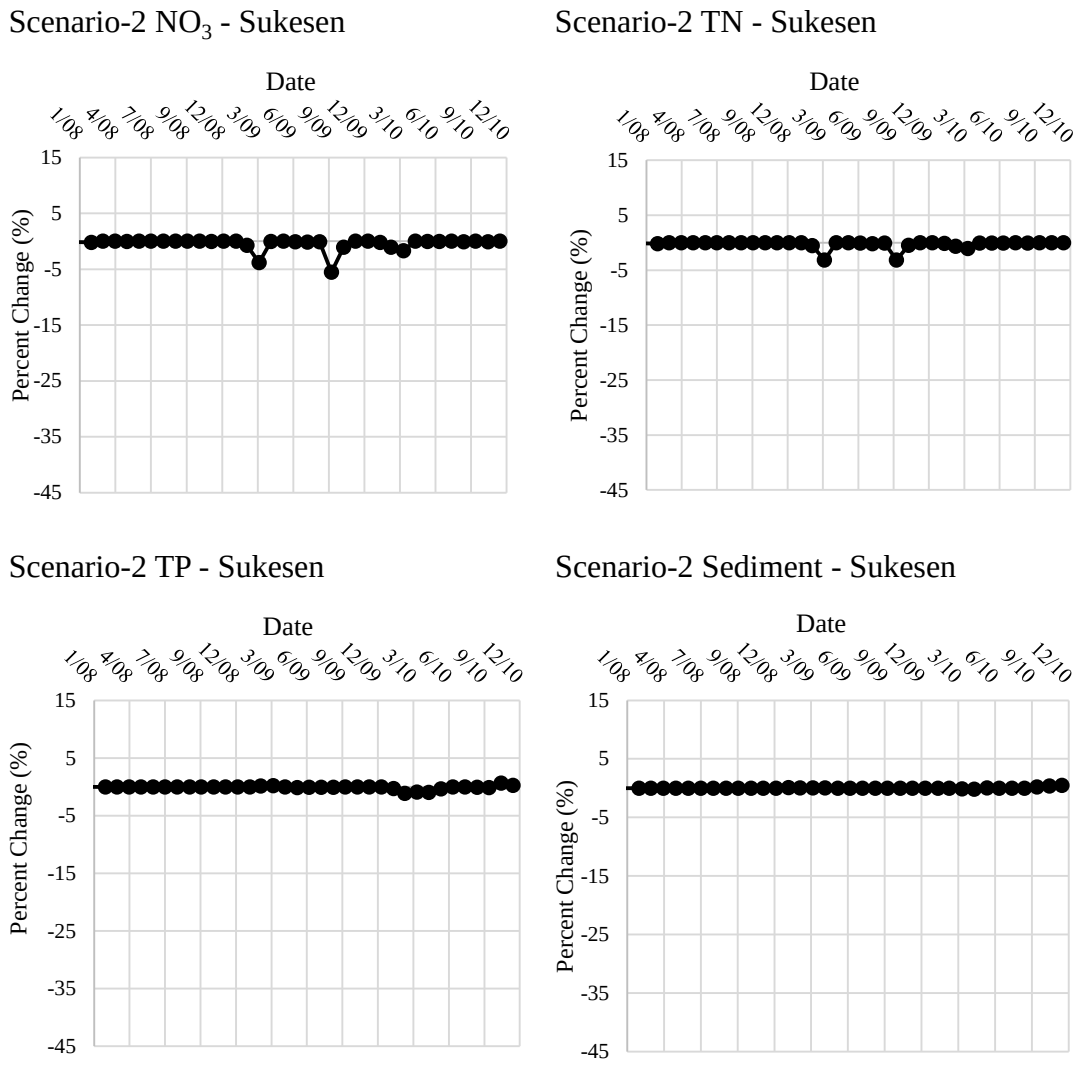

Figure 33. The results of Scenario-2 at Sukesen monitoring station: Percent changes in NO_3, TN, TP and sediment loads

Scenario-3

The monthly percent changes in sediment and nutrient (NO_3, TN and TP) loads at Yavrucak and Sukesen monitoring stations when the fertilizer application rates in agricultural lands are reduced by 30% is shown in Figure 34 and Figure 35, respectively. The averages of percent changes in monthly NO_3, TN, TP and sediment loads are -6.2%, -4.4%, -0.38% and -0.04%, respectively in Yavrucak. The percent changes in monthly NO_3 and TN loads range from -39% to 0% and -24.2% to 0.17%, respectively. The magnitude of highest percent reductions in TP and sediment loads are -4.8% and -11.2%, respectively.

In Sukesen, the averages of percent changes in monthly NO_3, TN, TP and sediment loads are -0.58%, -0.4%, -0.11% and 0.11%, respectively. The reduction of monthly NO_3 and TN loads range from -6.64% to 0% and -4.78% to 0%, respectively. The maximum percent reductions in TP and sediment loads were calculated as -1.55% and -0.29%, respectively. The results show that the most effective scenario among the three nutrient management scenarios was Scenario-3. In addition, it can be concluded that nitrogen (NO_3 and TN) loads are more effectively controlled compared to TP and sediment loads via reduction in fertilizer application. Furthermore, reduction in fertilizer application rate does not result in considerable impacts on pollutant loads in Sukesen. The reason is most probably due to the fact that Sukesen is a more urbanized subbasin, and thus agricultural activities are not as intense as they are in Yavrucak.

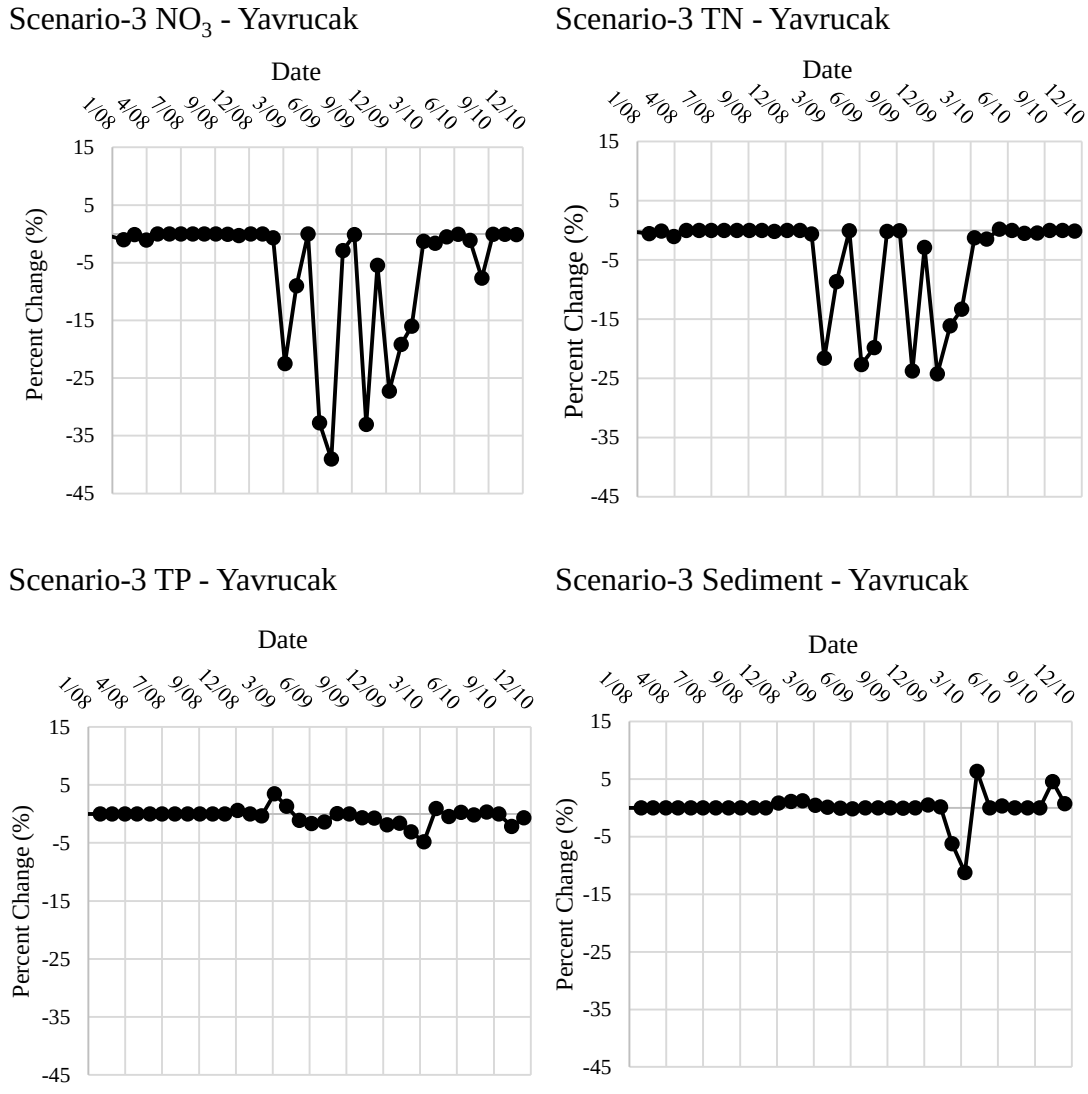

Figure 34. The results of Scenario-3 at Yavrucak monitoring station: Percent changes in NO_3, TN, TP and sediment loads

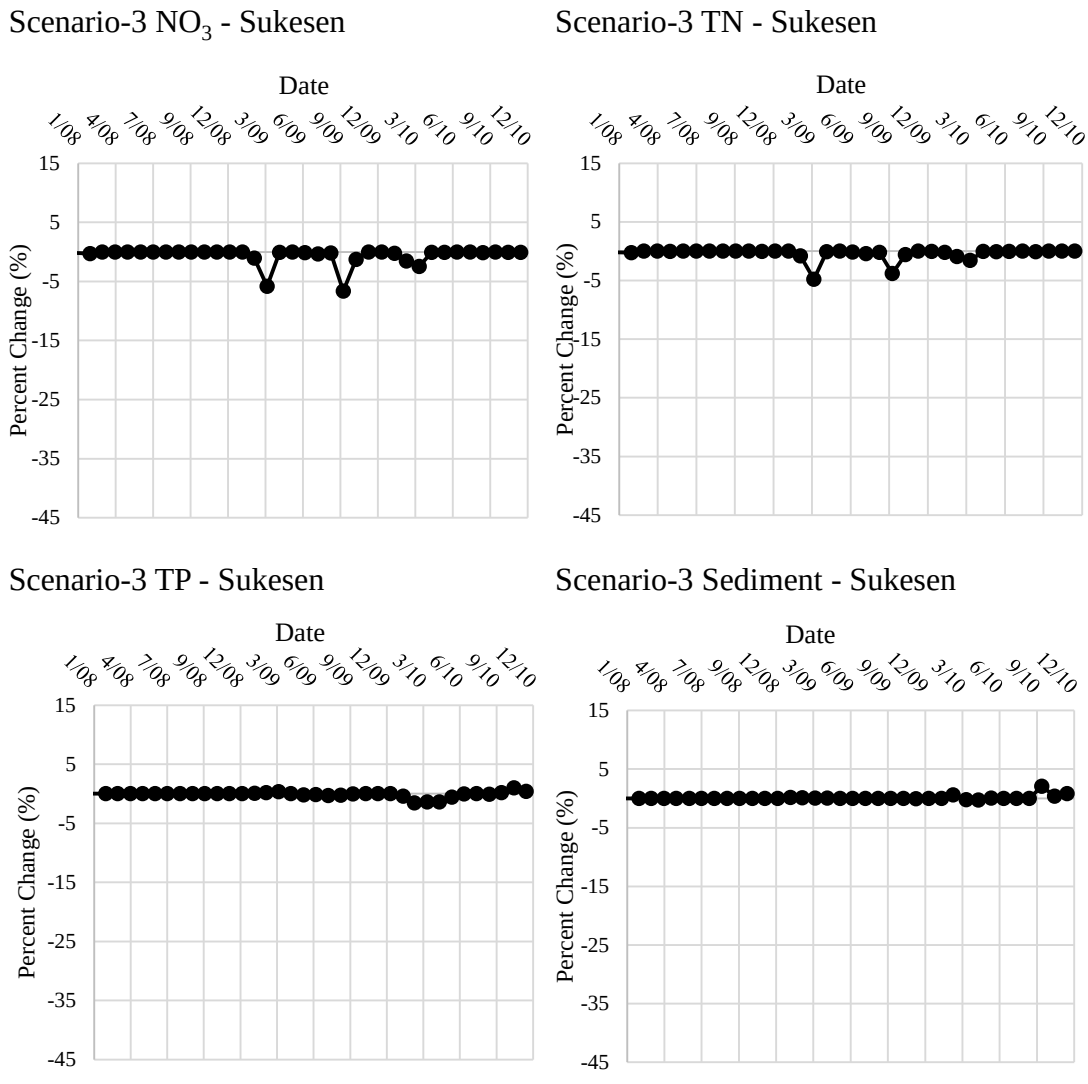

Figure 35. The results of Scenario-3 at Sukesen monitoring station: Percent changes in NO_3, TN, TP and sediment loads

4.3.2. Conservation Tillage / No Tillage

As it was mentioned in Section 3.4.2, four different tillage scenarios were developed to assess the impacts of different tillage methods on pollutant loads. Application of tillage scenarios did not have significant impacts on sediment and nutrient loads. There was also no significant difference between the conservation tillage and no tillage scenarios. Still, no tillage operation was more successful in terms of nutrient load reduction compared to conservation tillage. This was expected since the soil is mixed to a depth of 25 mm with 5% efficiency in no tillage operation involving minimum disturbance of soil. If the soil is tilled with conservation tillage, on the other hand, the soil will be mixed to a depth of 100 mm with a mixing efficiency of 25%. As in the

nutrient management scenarios, the pollutant loads were more effectively reduced in Yavrucak where the agricultural lands are dominated. The monthly percent changes in pollutant loads in Scenario-4, Scenario-5, Scenario-6 and Scenario-7 are given in the following sub-headings in detail. The comparison of scenario results on a yearly basis is given in Section 4.4.

Scenario-4

In Scenario-4, the conventional tillage applications carried out in agricultural lands with duck-foot cultivator was replaced with conservation tillage. The monthly percent changes in sediment and nutrient (NO_3, TN and TP) loads at Yavrucak and Sukesen monitoring stations when conservation tillage is implemented are shown in Figure 36 and Figure 37, respectively. The results showed that conservation tillage scenario reduced the average monthly NO_3, TN, TP and sediment loads -0.53%, -0.53%, -0.86% and -0.11%, respectively. The utmost percent reductions for monthly NO_3, TN, TP and sediment loads were calculated as -23.6%, -22.5%, -4.2% and -2.5%, respectively.

In Sukesen, application of conservation tillage resulted in -0.07%, -0.05%, -0.56% and -0.02% reduction on average in the monthly NO_3, TN, TP and sediment loads, respectively. The highest percent reductions in NO_3, TN, TP and sediment loads were -2.5%, -1.6%, -4.3% and -0.35%, respectively.

The results show that conservation tillage application was more effective in reducing TP load compared to nitrogen and sediment loads.

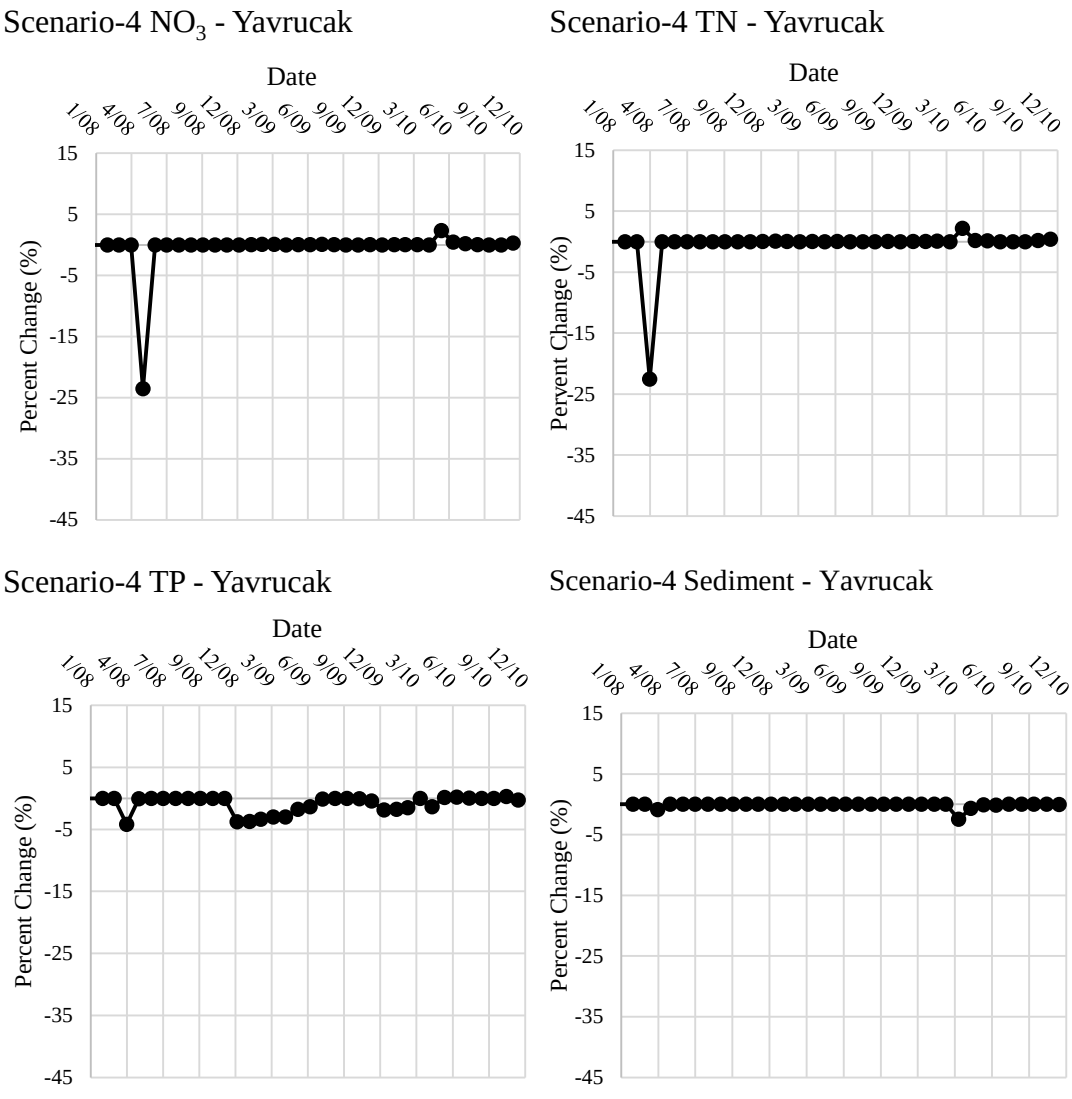

Figure 36. The results of Scenario-4 at Yavrucak monitoring station: Percent changes in NO_3, TN, TP and sediment loads

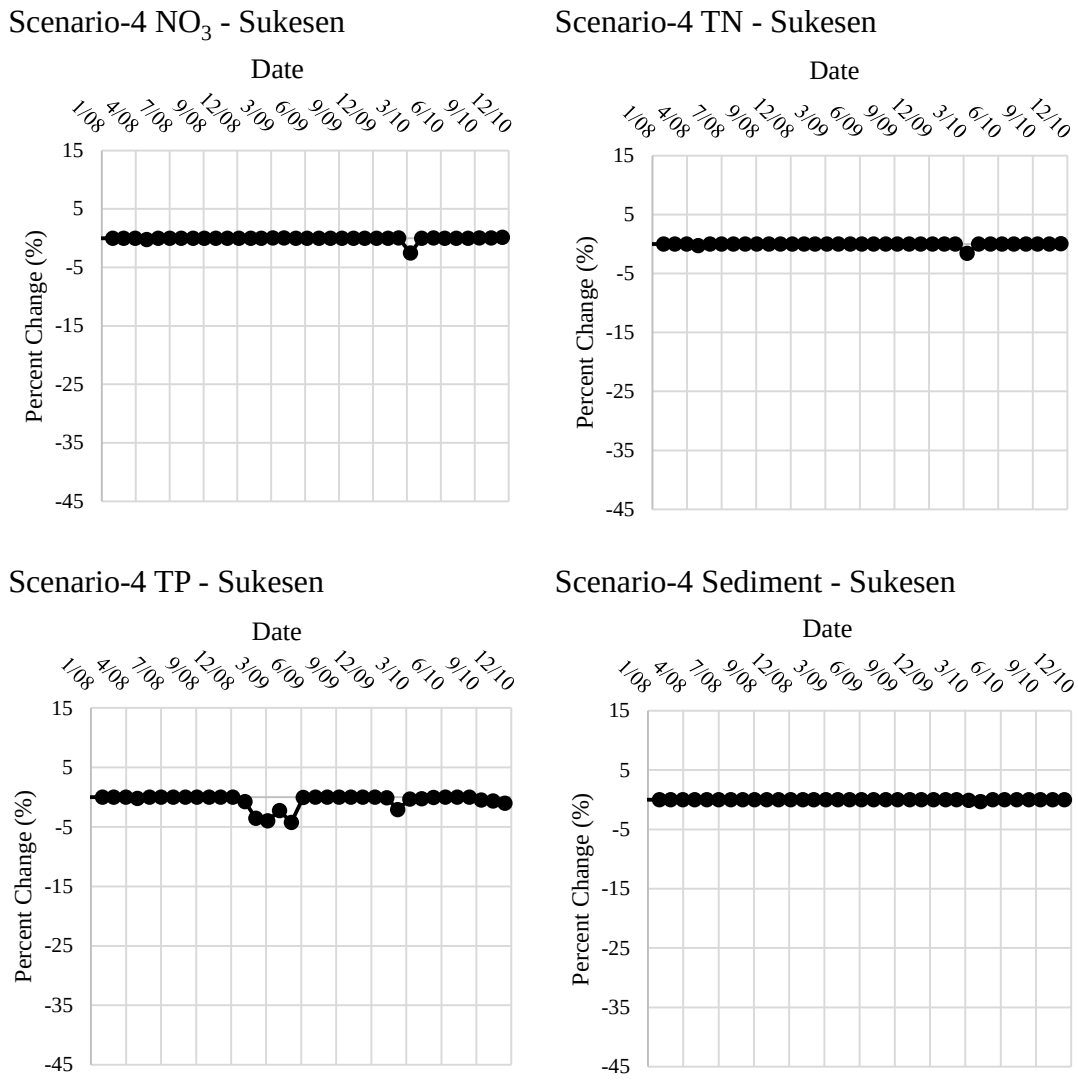

Figure 37. The results of Scenario-4 at Sukesen monitoring station: Percent changes in NO_3, TN, TP and sediment loads

Scenario-5

In Scenario-5, the impact of no tillage on pollutant loads was evaluated. The monthly percent changes in sediment and nutrient (NO_3, TN and TP) loads at Yavrucak and Sukesen monitoring stations when no tillage is implemented in agricultural lands are shown in Figure 38 and Figure 39, respectively. In Yavrucak, the averages of monthly percent changes in NO_3, TN, TP and sediment loads are -0.83%, -0.84%, -2.2% and -0.19%, respectively. The magnitude of maximum reductions calculated for NO_3, TN, TP and sediment loads are -38.6%, -37%, -9.3% and -3.9%, respectively.

In Sukesen, Scenario-5 resulted in average reductions of -0.1%, -0.07%, -1.3% and -0.03% in NO_3, TN, TP and sediment loads, respectively. The highest monthly

reductions calculated for NO_3, TN, TP and sediment loads within the simulation period are -4%, -2.5%, -8.5% and -0.58%, respectively.

Similar to Scenario-4, no tillage scenario was more effective in reducing TP load compared to nitrogen and sediment loads. Furthermore, no tillage operation was more successful in terms of nutrient load reduction compared to conservation tillage.

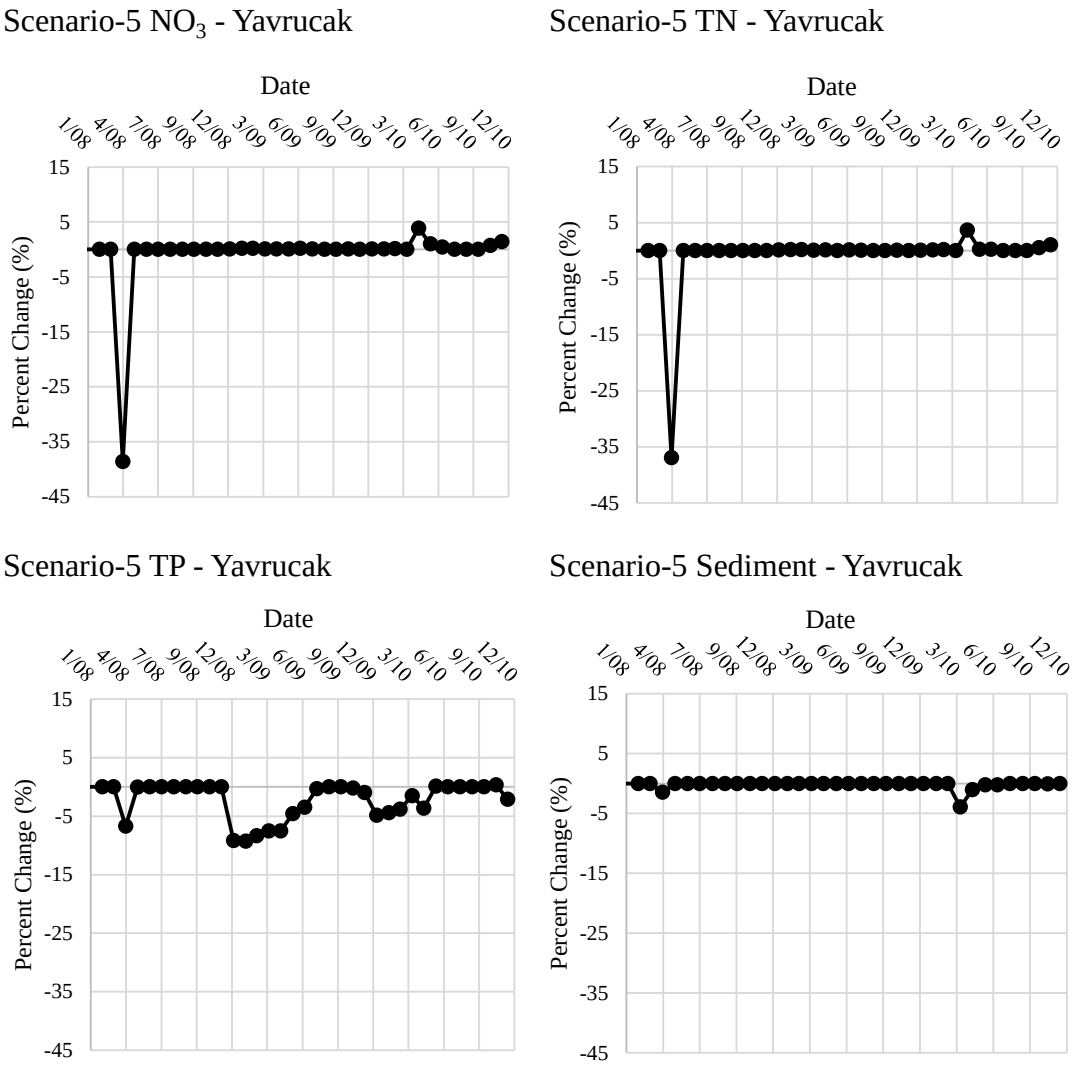

Figure 38. The results of Scenario-5 at Yavrucak monitoring station: Percent changes in NO_3, TN, TP and sediment loads

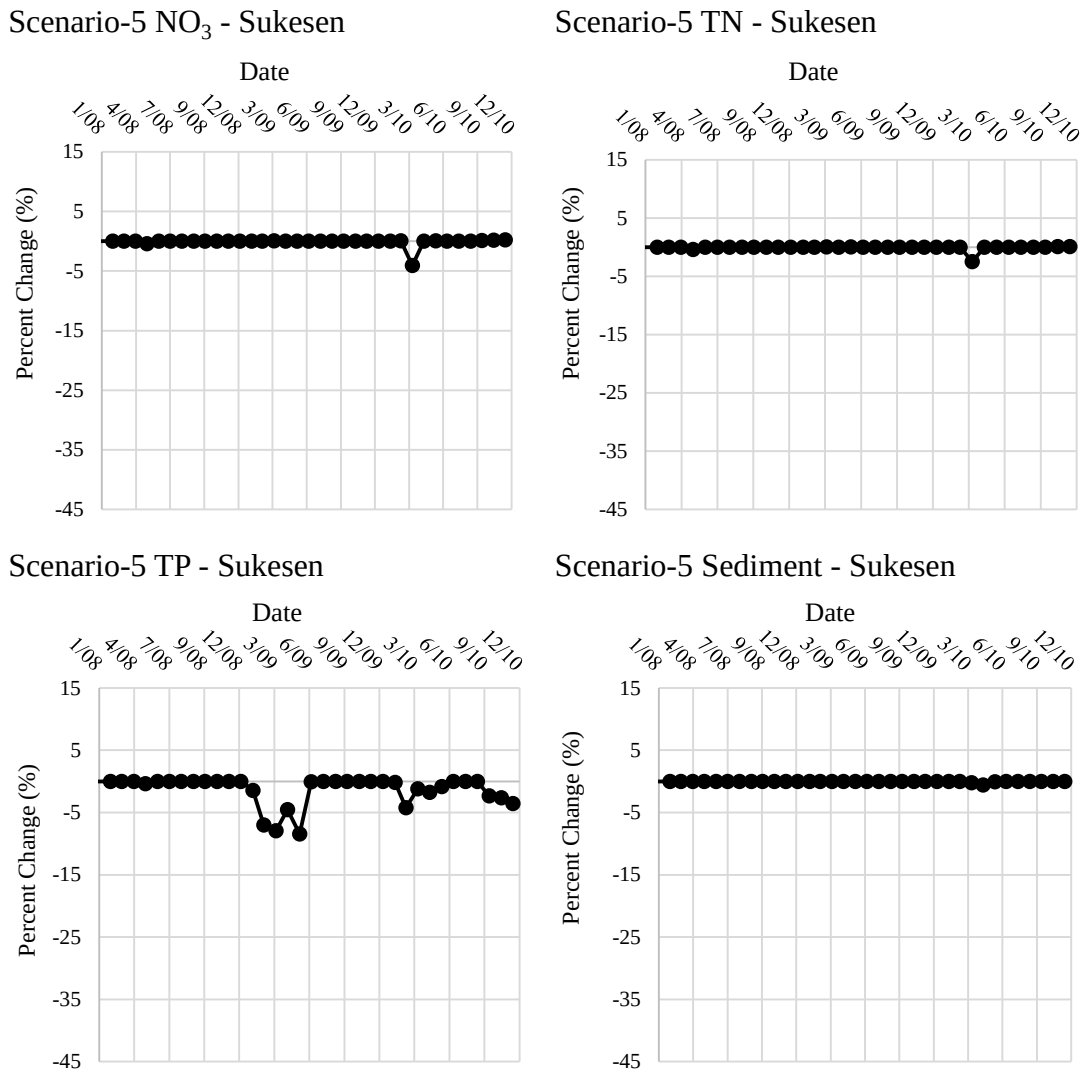

Figure 39. The results of Scenario-5 at Sukesen monitoring station: Percent changes in NO_3, TN, TP and sediment loads

Scenario-6

In Scenario-6, conservation tillage was applied in agricultural lands with low clay ratio (< 30%). The monthly percent changes in sediment and nutrient (NO_3, TN and TP) loads at Yavrucak and Sukesen monitoring stations are shown in Figure 40 and Figure 41, respectively. As it can be seen from Figure 40 and Figure 41, implementation of Scenario-6 did not result in considerable impacts on pollutant loads both in Yavrucak and Sukesen subbasins. The average change in the amount of all pollutant loads was approximately zero or zero. Based on the soil analyses 49 soil types were determined in Lake Mogan watershed (see Section 3.1.4). The soil types having clay ratio smaller than 30% were determined as Mogan 6, Mogan 14, Mogan 15, Mogan 25, Mogan 38, Mogan 46 and Mogan 48. Among these soil classes only two of them namely Mogan

6 and Mogan 25 are found on agricultural lands. Therefore, it is not surprising that Scenario-6 has negligible impacts on pollutant loads.

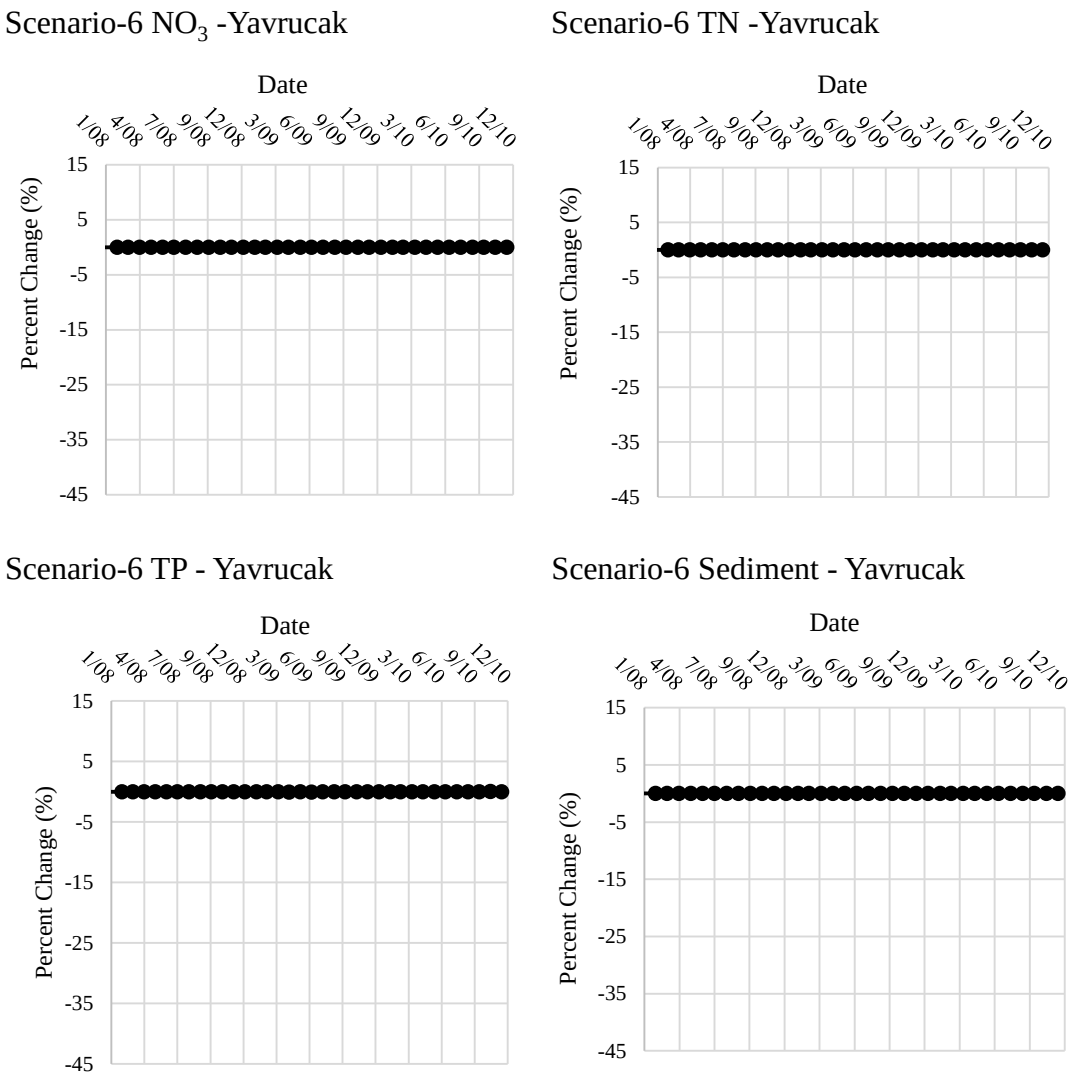

Figure 40. The results of Scenario-6 at Yavrucak monitoring station: Percent changes in NO_3, TN, TP and sediment loads

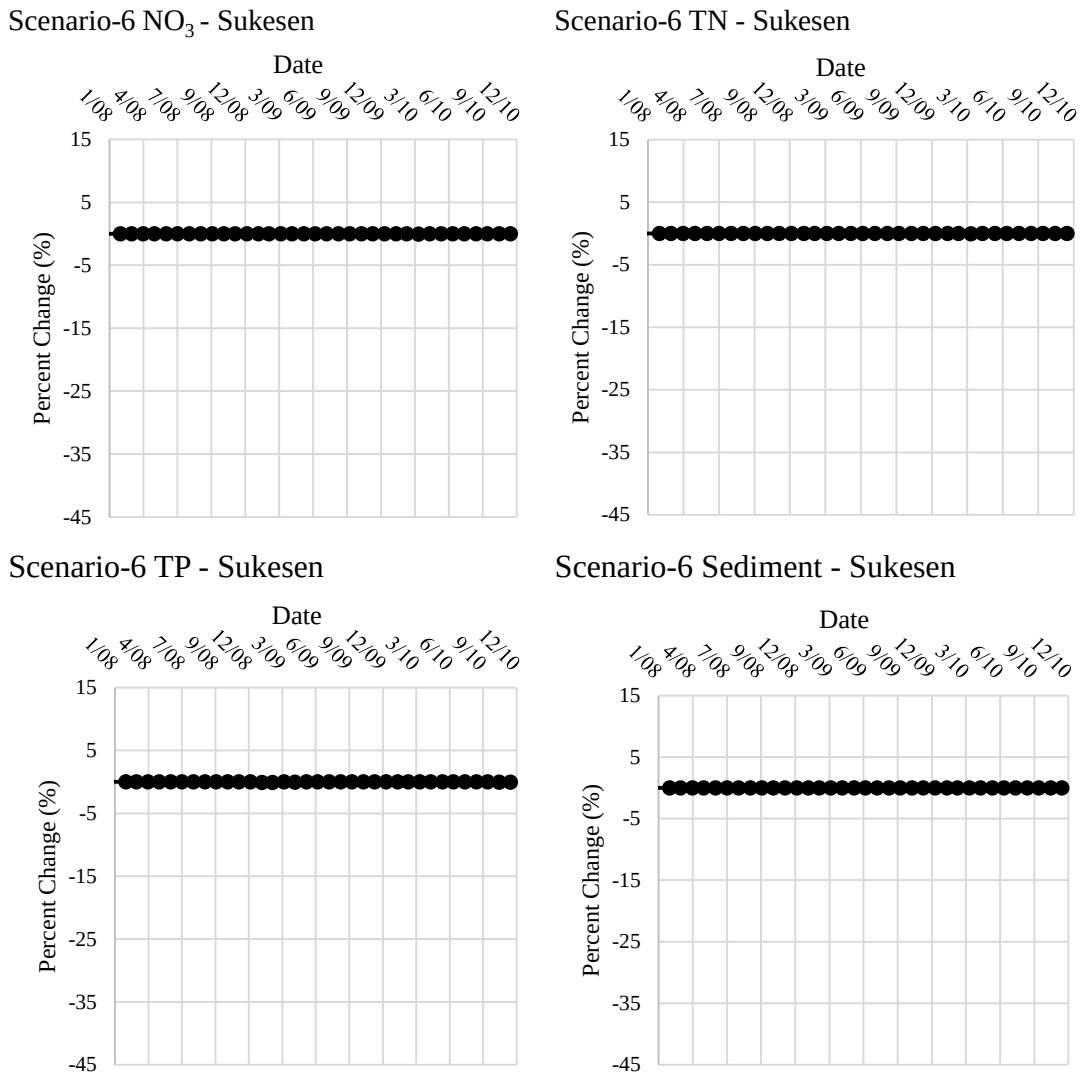

Figure 41. The results of Scenario-6 at Sukesen monitoring station: Percent changes in NO_3, TN, TP and sediment loads

Scenario-7

Scenario-7 is the application of no tillage in agricultural lands having soils with a low clay ratio. The monthly percent changes in sediment and nutrient (NO_3, TN and TP) loads at Yavrucak and Sukesen monitoring stations are shown in Figure 42 and Figure 43, respectively. Similar to Scenario-6, Scenario-7 was not an effective scenario for pollution reduction. The average of percent changes in nutrient and sediment loads was nearly zero. The highest percent reduction, -0.12%, was calculated in TP load. As it was mentioned in Scenario-6, since only two soil classes with low clay ratios are found in agricultural lands, the impact of Scenario-7 on pollutant loads was not considerable.

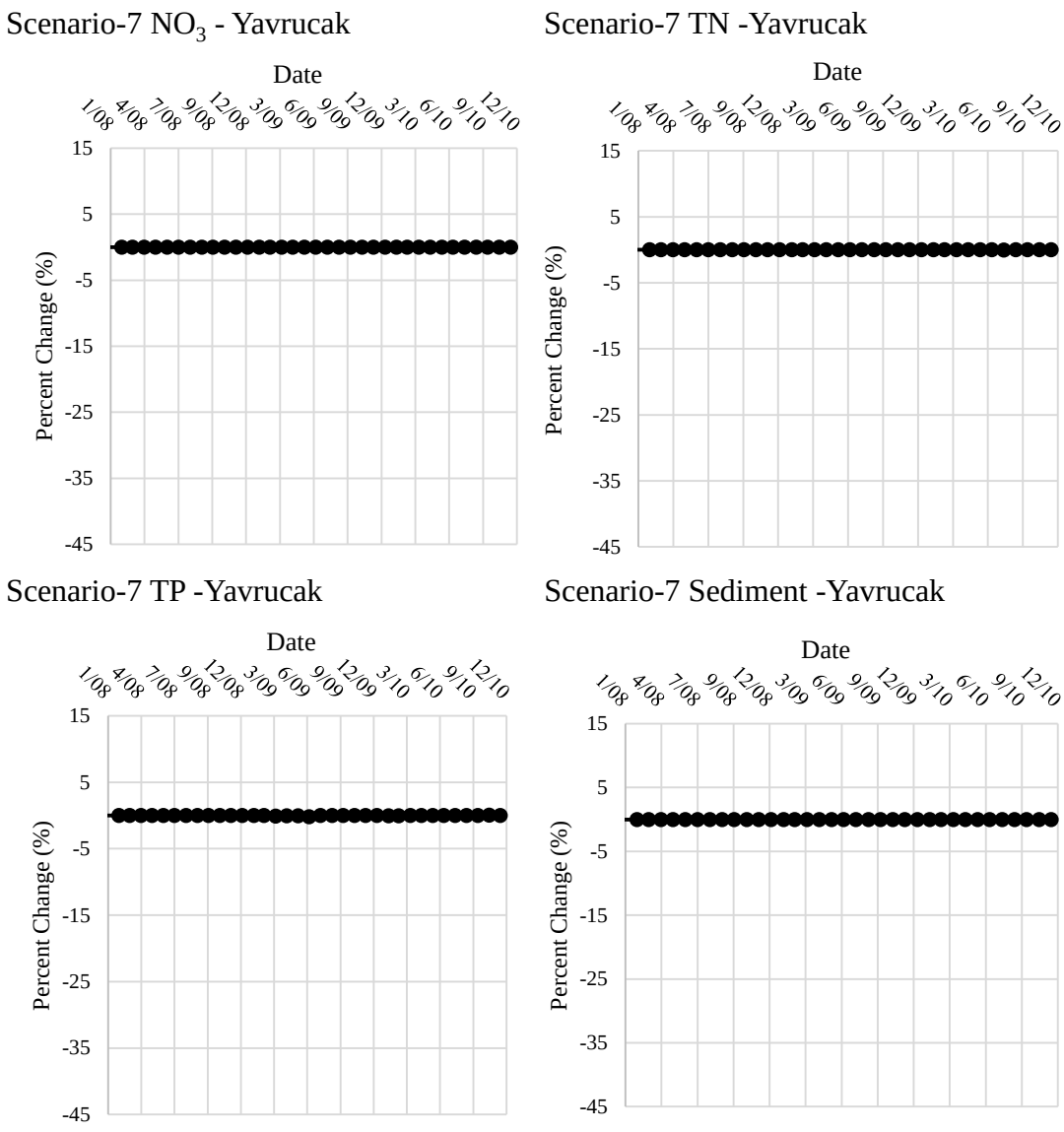

Figure 42. The results of Scenario-7 at Yavrucak monitoring station: Percent changes in NO_3, TN, TP and sediment loads

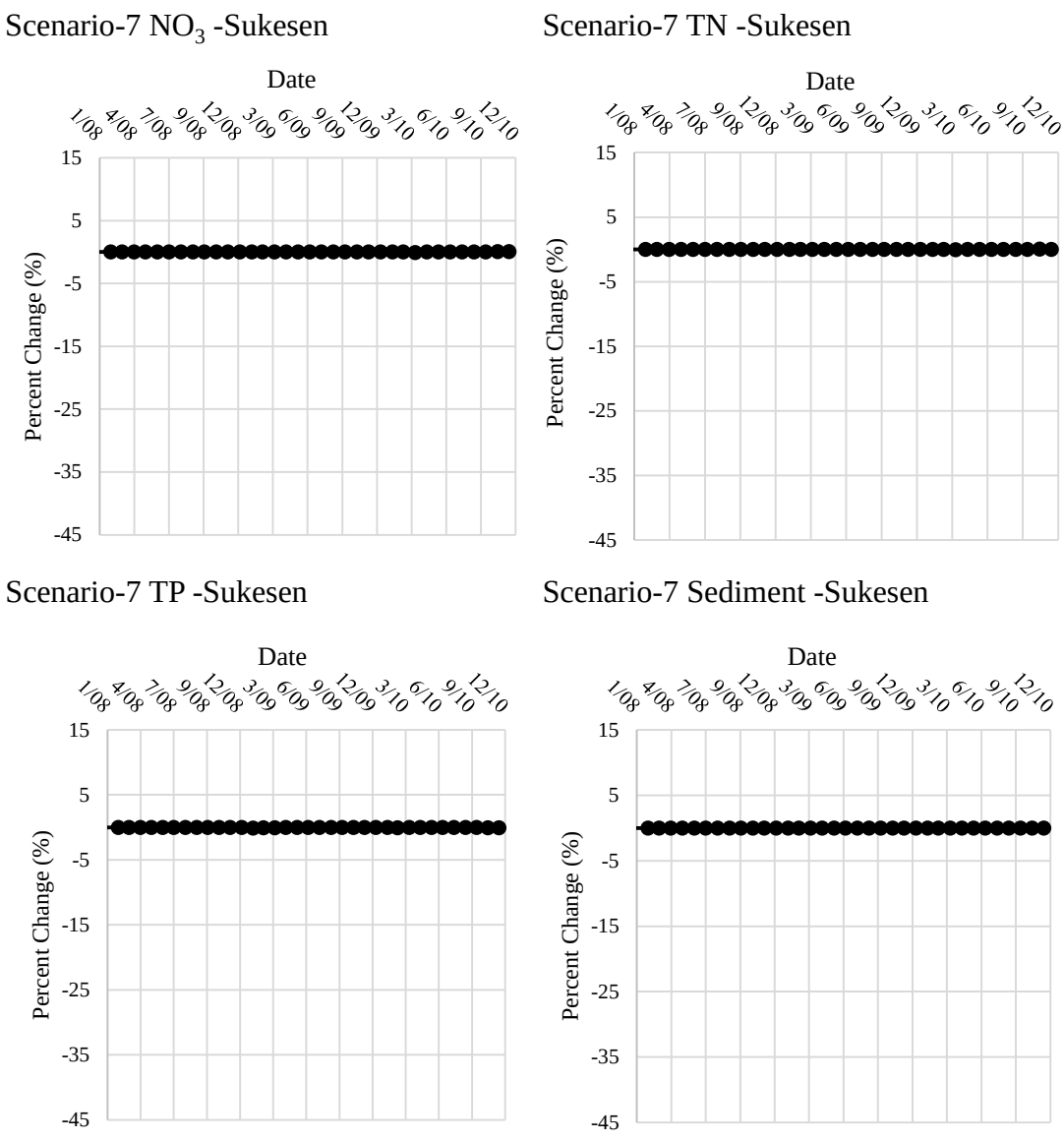

Figure 43. The results of Scenario-7 at Sukesen monitoring station: Percent changes in NO_3, TN, TP and sediment loads

4.3.3. Contouring and Terracing

As it was mentioned in Section 3.4.3, application of contouring and terracing in the agricultural lands were simulated in Scenario-8 and Scenario-9, respectively. The results indicate that contouring and terracing scenarios achieved remarkable pollutant load reduction at the Yavrucak and Sukesen subbasin outlets. In addition, the terracing scenario was the most effective scenario among the individual scenarios developed. The average monthly reductions achieved in Sukesen subbasin was comparably lower. The difference was not surprising since the percentage of agricultural lands in Yavrucak (47%) is more than 4 times that of Sukesen (11%) (see Section 4.3.3).

Moreover, since the adjustment of parameters to represent contouring and terracing was carried out according to percent slope (Table 25 and Table 26), there occurred differences in the results obtained in the two subbasins. The monthly percent changes in pollutant loads in Scenario-8 and Scenario-9 are given in the following sub-headings in detail. The comparison of scenario results on a yearly basis is given in Section 4.4.

Scenario-8

Scenario- 8 is the application of contouring in agricultural lands. The monthly percent changes in sediment and nutrient (NO_3, TN and TP) loads at Yavrucak and Sukesen monitoring stations are shown in Figure 44 and Figure 45, respectively. In Yavrucak subbasin, the average monthly percent reductions in NO_3, TN, TP and sediment loads are -2.3%, -1.5%, -2.4% and -3.3%, respectively. The highest percent reductions are -27.6%, -19.9%, -10.6% and -24.5% for NO_3, TN, TP and sediment, respectively.

The pollution reductions obtained in Sukesen subbasin was lower compared to that of Yavrucak subbasin. The average percent reductions were calculated as -0.5%, -0.3%, -1.1% and -0.36% for NO_3, TN, TP and sediment, respectively. The utmost percent reductions in NO_3, TN, TP and sediment loads were -6.8%, -3.9%, -5.4 and -2.9%, respectively.

Scenario-8 NO_3 -Yavrucak

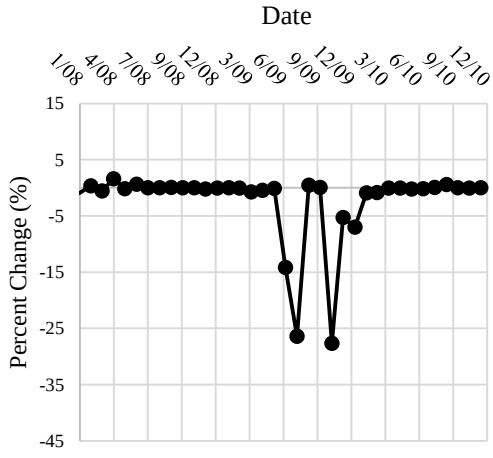

Scenario-8 TN -Yavrucak

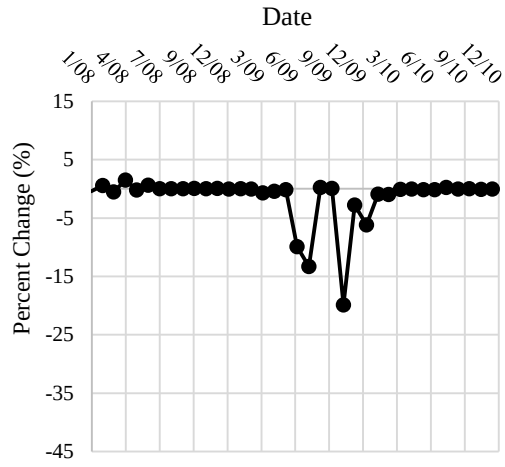

Scenario-8 TP -Yavrucak

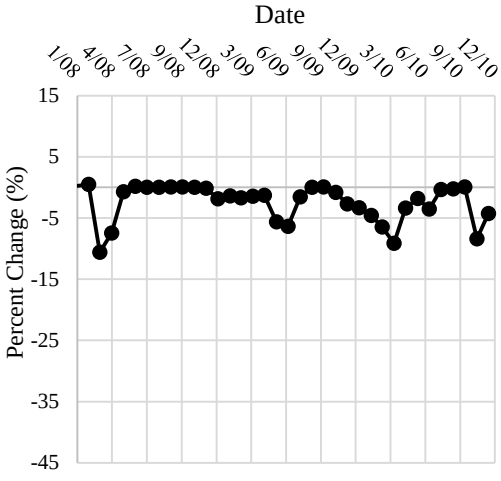

Scenario-8 Sediment -Yavrucak

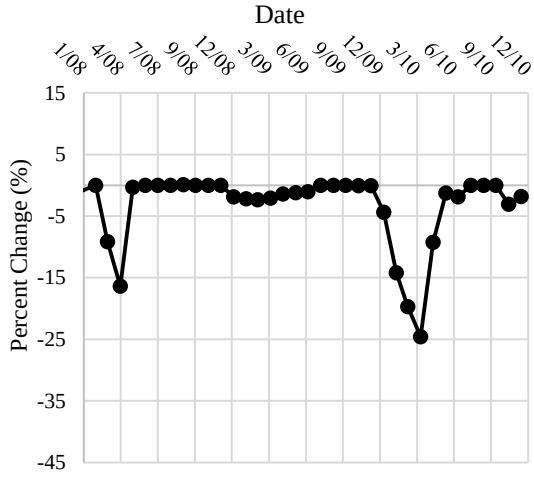

Figure 44. The results of Scenario-8 at Yavrucak monitoring station: Percent changes in NO_3, TN, TP and sediment loads

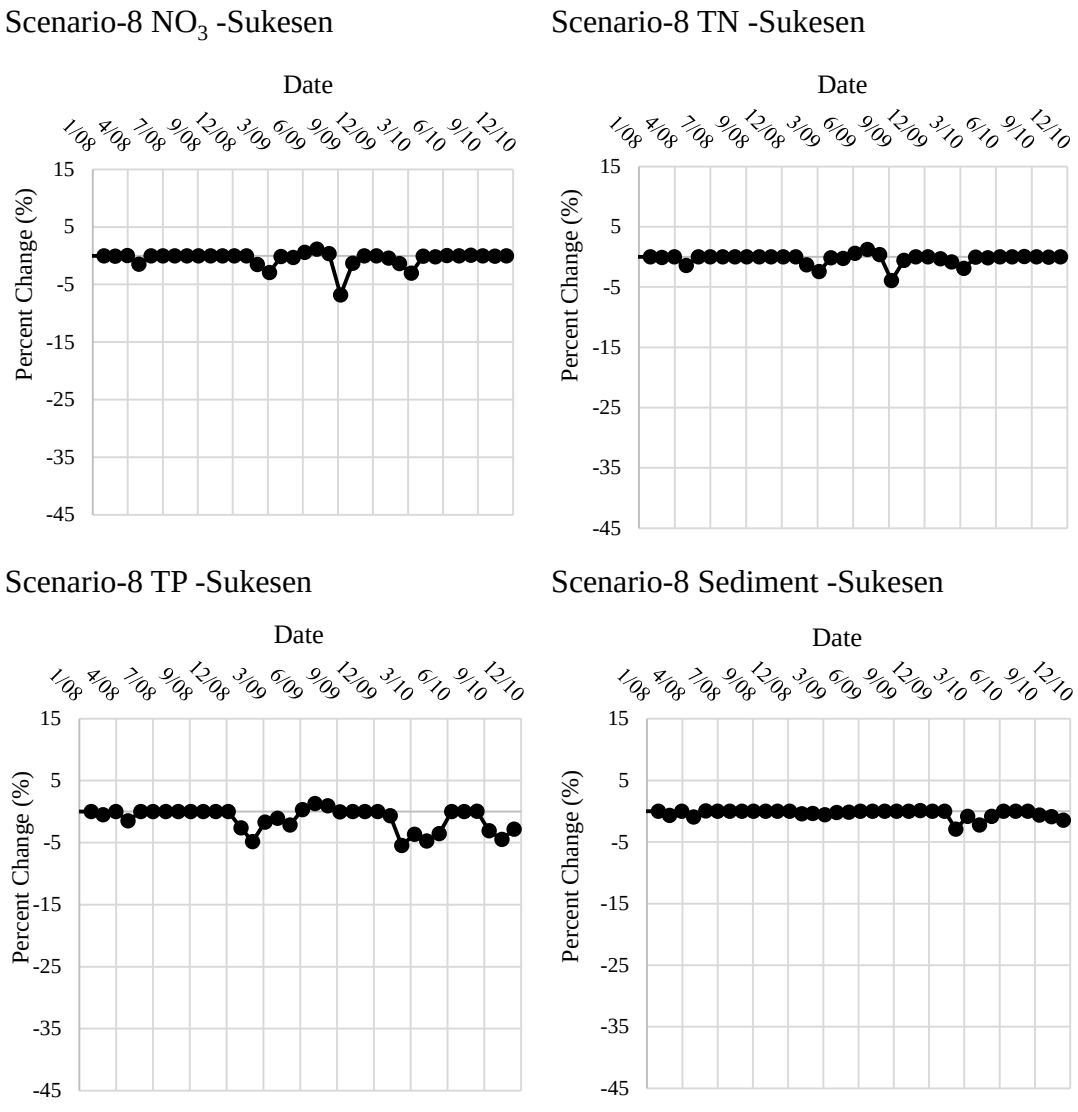

Figure 45. The results of Scenario-8 at Sukesen monitoring station: Percent changes in NO_3, TN, TP and sediment loads

Scenario-9

In Scenario-9, terracing on agricultural lands in Lake Mogan watershed was simulated. The monthly percent changes in NO_3, TN, TP and sediment loads in Yavrucak and Sukesen subbasins are shown in Figure 46 and Figure 47, respectively. The results revealed that the terracing scenario can visibly improve the environmental conditions in the watershed. In Yavrucak, the average percent changes in the monthly NO_3, TN, TP and sediment loads are -3.4%, -2.2%, -3.8% and -5.2%, respectively. The highest percent reductions for NO_3, TN, TP and sediment were calculated as -41.6%, -29.9%, -15.5% and -39.7%, respectively.

In Sukesen, a more urbanized subbasin, the pollutant reductions were lower compared to Yavrucak as in the other scenarios. The terracing scenario resulted in average percent reductions of -0.58%, -0.44%, -1.6% and -0.48% in NO_3, TN, TP and sediment loads, respectively. The maximum percent reductions for NO_3, TN, TP and sediment loads were -6.8%, -6.1%, -8.1% and -4%, respectively.

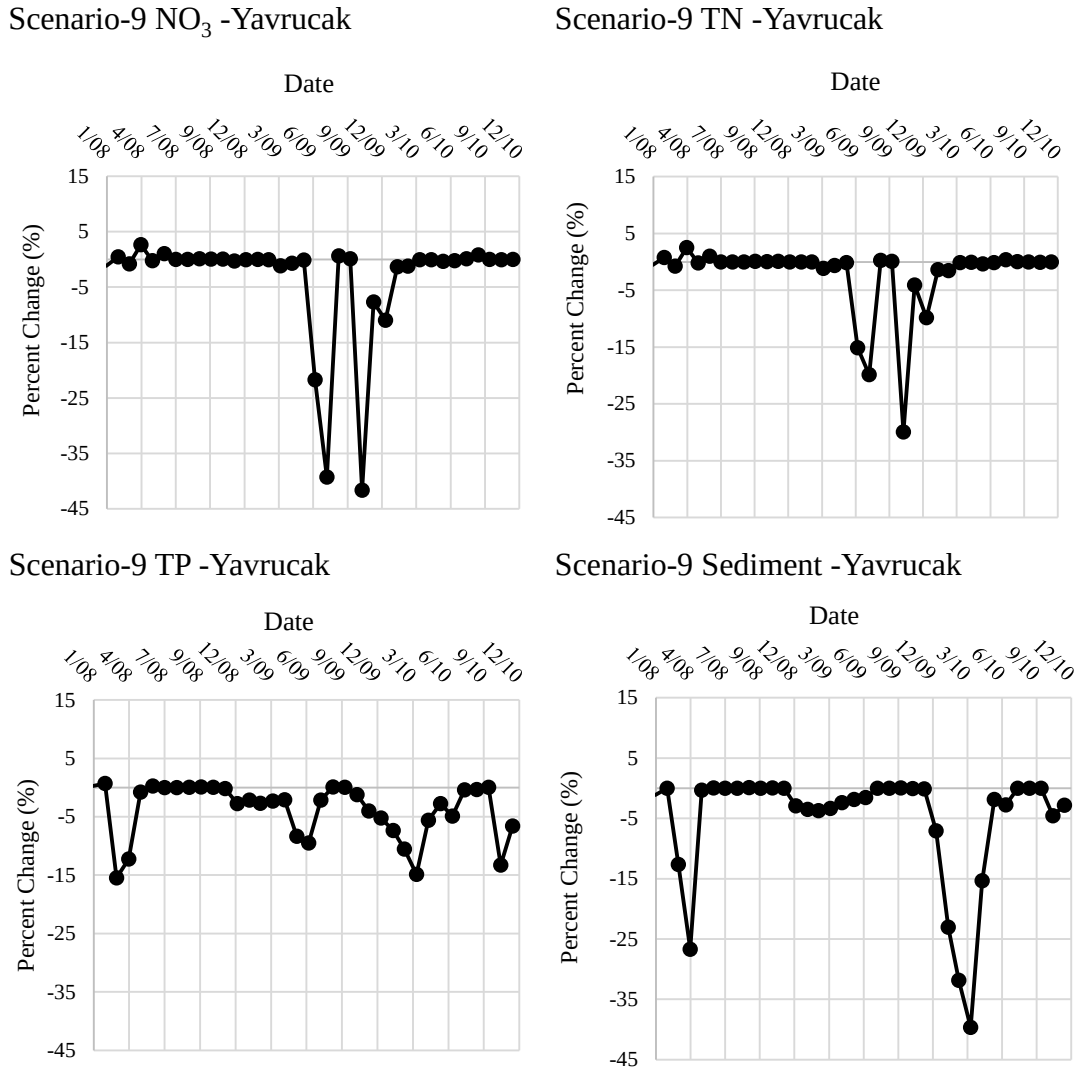

Figure 46. The results of Scenario-9 at Yavrucak monitoring station: Percent changes in NO_3, TN, TP and sediment loads

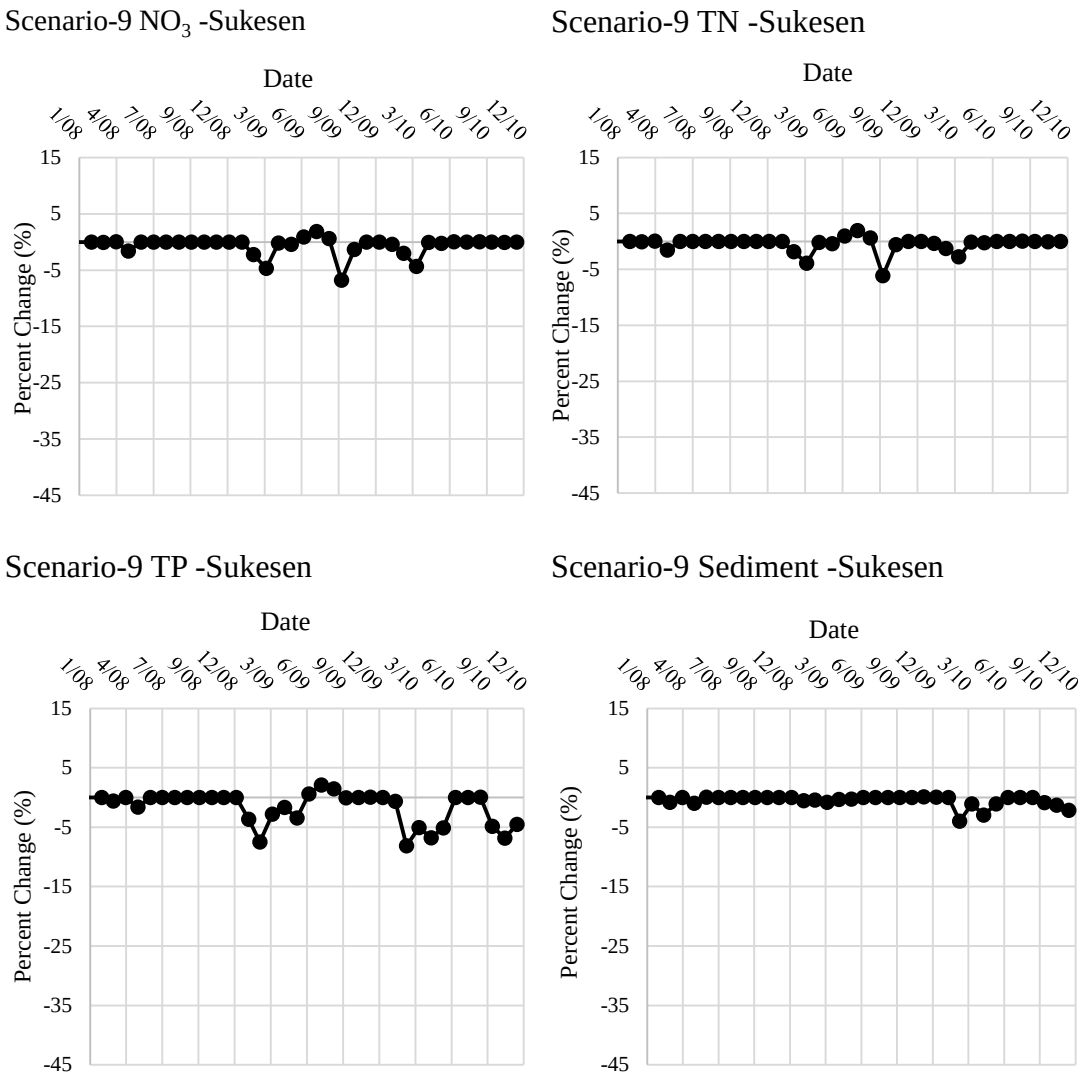

Figure 47. The results of Scenario-9 at Sukesen monitoring station: Percent changes in NO_3, TN, TP and sediment loads

4.3.4. Combined Scenarios

The results indicate that each class of BMPs is more effective in controlling certain types of diffuse pollution. For instance, Scenario-3, a fertilizer management scenario, was the most effective scenario in reducing nitrogen loads in both Yavrucak and Sukesen subbasins. TN and NO_3 loads on average were nearly 5% lower compared to the baseline scenario in Yavrucak. Total phosphorus and sediment loads were most effectively reduced by the terracing scenario in both subbasins. Application of individual BMP scenarios achieved pollutant load reductions at a certain level but they did not significantly contribute to water quality improvement. Thus, instead of individual BMPs, the combinations; i.e. Scenario-10 and Scenario-11, were simulated to achieve more effective pollution load reductions. Scenario-10 is the combination of

the 30% fertilizer reduction scenario and the no tillage scenario. In Scenario-11, on the other hand, nutrient management (30% reduction in the fertilizer application rates) and no tillage were combined with terracing. Scenario-11 provided better reductions in pollutant loads than Scenario-10. The monthly percent changes in pollutant loads in Scenario-10 and Scenario-11 are given in the following sub-headings in detail. The comparison of scenario results on a yearly basis is given in Section 4.4.

Scenario-10

Scenario-10 is the combination of the most effective nutrient management scenario with the no tillage scenario. The monthly percent changes in sediment and nutrient (NO_3, TN and TP) loads at Yavrucak and Sukesen monitoring stations are shown in Figure 48 and Figure 49, respectively. In Yavrucak, the average percent reductions in monthly NO_3, TN, TP and sediment loads are -7.1%, -5.3%, -2.5% and -0.2%, respectively. The utmost percent reductions for NO_3, TN, TP and sediment were -39%, -37%, -9.1% and -14.3%, respectively.

In Sukesen, Scenario-10 resulted in average percent changes of -0.64%, -0.44%, -1.4% and 0.1% in NO_3, TN, TP and sediment loads, respectively. The highest percent reductions were calculated as -6.6%, -4.7%, -8.6% and -0.7% for NO_3, TN, TP and sediment, respectively.

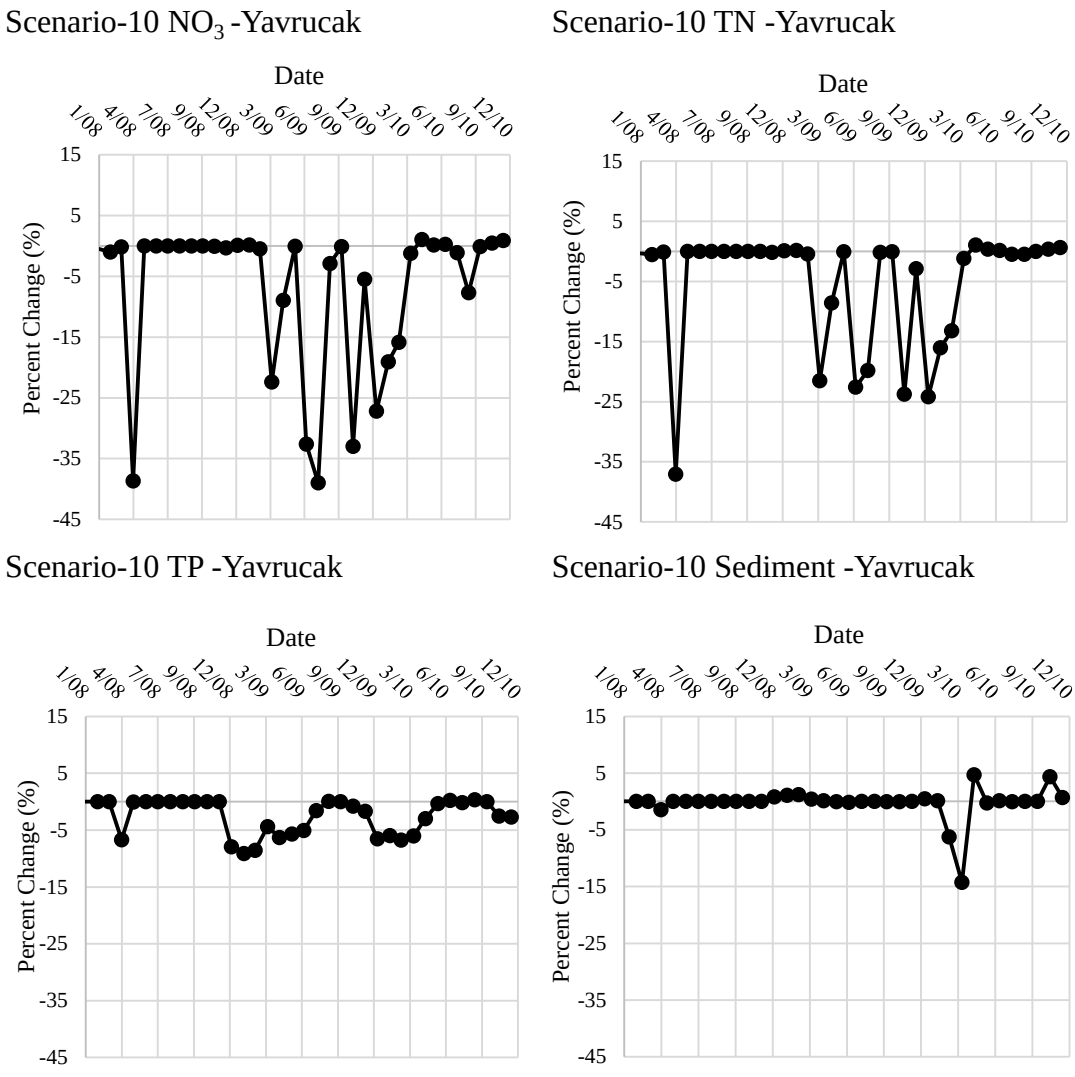

Figure 48. The results of Scenario-10 at Yavrucak monitoring station: Percent changes in NO_3, TN, TP and sediment loads

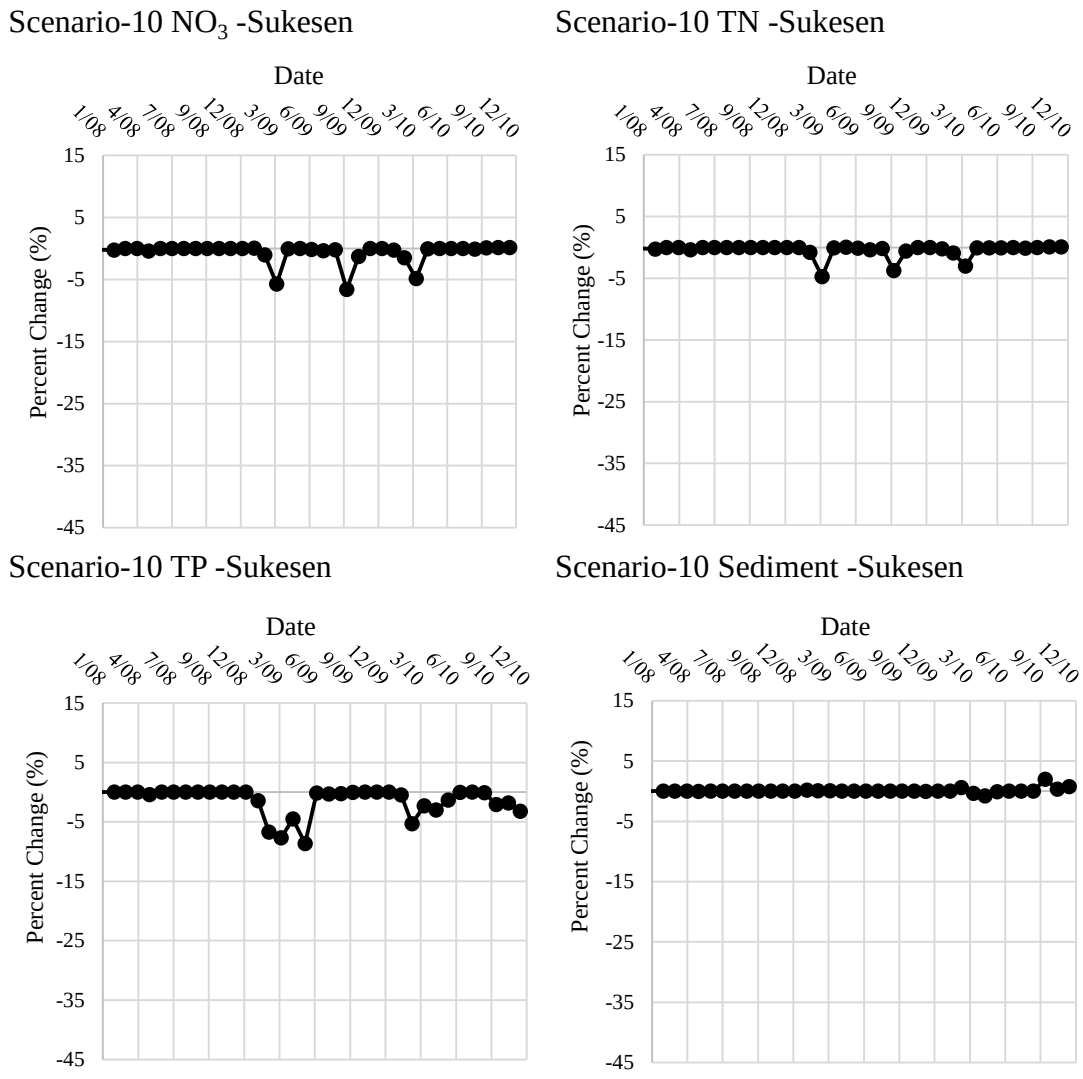

Figure 49. The results of Scenario-10 at Sukesen monitoring station: Percent changes in NO_3, TN, TP and sediment loads

Scenario-11

Scenario-11 is the combination of 30% reduction in the fertilizer application rate, no tillage and terracing. The monthly percent changes in sediment and nutrient (NO_3, TN and TP) loads at Yavrucak and Sukesen monitoring stations are shown in Figure 50 and Figure 51, respectively. In Yavrucak, the average percent reductions in NO_3, TN, TP and sediment loads were -9.1%, -6.7%, -6.0% and -5.3%, respectively. The highest reductions for NO_3, TN, TP and sediment loads were calculated as -60.0%, -42.2%, -16.7% and -41.3%, respectively.

The results revealed that even the most efficient scenario; i.e. Scenario-11, could not achieve significant pollution reduction in Sukesen subbasin. The average percent

reductions in NO_3, TN, TP and sediment loads were determined as -0.82%, -0.63%, -2.5% and -0.45%, respectively. The highest monthly percent reductions for NO_3, TN, TP and sediment were -9.1%, -7.5%, -11.3% and -3.9%, respectively.

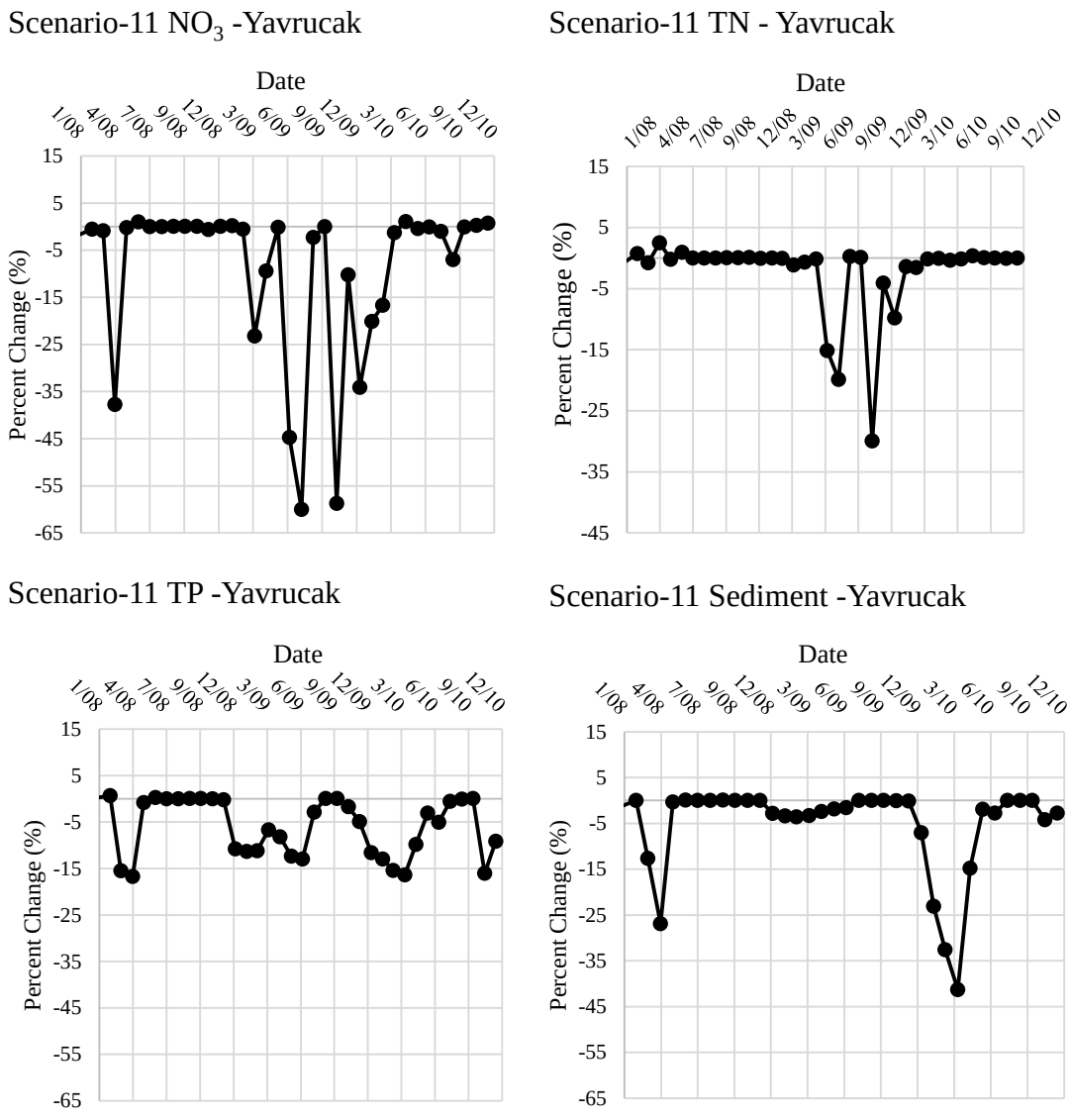

Figure 50. The results of Scenario-11 at Yavrucak monitoring station: Percent changes in NO_3, TN, TP and sediment loads

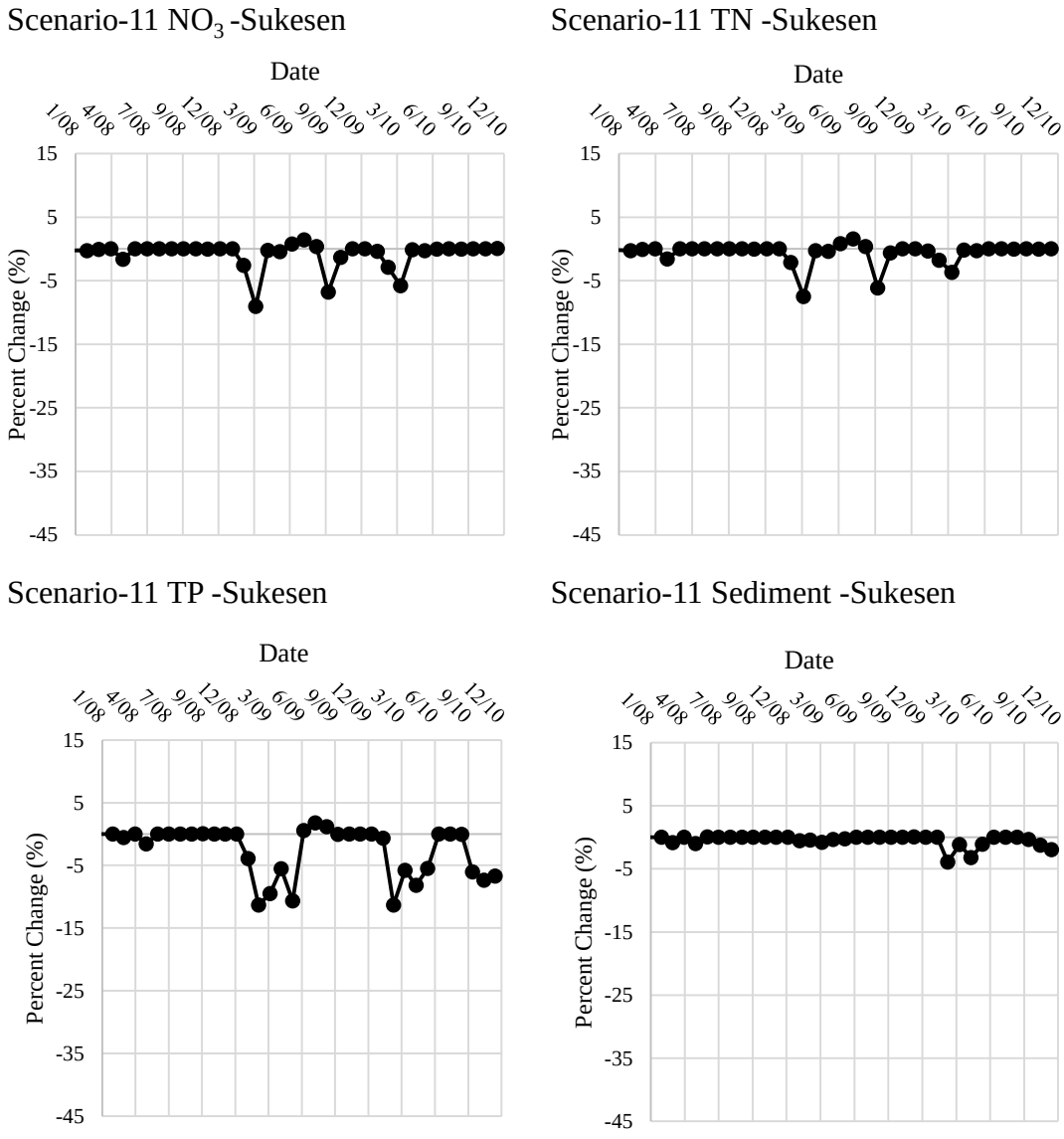

Figure 51. The results of Scenario-11 at Yavrucak monitoring station: Percent changes in NO_3, TN, TP and sediment loads

4.4. Comparison of Scenario Results on a Yearly Basis and Overall Evaluation of the BMP Scenarios

In Section 4.3, the impacts; i.e. the changes in *monthly* nutrient and sediment loads, of each BMP scenario are given in detail. In this section, the average *annual* pollutant loads reductions are evaluated. For this purpose, the model was run on a yearly basis and the average annual loads for each pollutant (sediment, NO_3, TN and TP) were calculated at Yavrucak and Sukesen subbasin outlets. The simulation time period was from January 2007 to December 2010 and 2007 was used as the warm-up period. The simulated annual loads in each scenario were compared with the loads simulated in

the baseline scenario. The average annual loads were calculated by taking the average of loads simulated in 2008, 2009 and 2010. The percent changes in the amounts of average annual pollutant loads were calculated with *Eqn. 6*. The results of each BMP scenario are summarized in Table 43, Figure 52 and Table 44, Figure 53 for Yavrucak and Sukesen subbasins, respectively.

In Scenario-1, Scenario-2 and Scenario-3, the reduction in fertilizer application rate led to reduction in NO_3 and TN loads. The sediment and TP loads were not affected significantly. As mentioned in Section 4.3.1, the reason why the reductions in the nitrogen load is more pronounced is most probably because of the types of fertilizer used in the watershed. The fertilizers applied in the agricultural lands (ammonium sulfate, 21-00-00; ammonium nitrate, 33-00-00; urea, 46-00-00; diammonium phosphate (DAP), 18-46-00) are mainly nitrogen based. Furthermore, as the rate of reduction in the fertilizer application increased, the reduction in the amount of pollutants improved. In the Yavrucak subbasin, annual NO_3 and TN loads were reduced approximately 5% when the fertilizer application rate was decreased by 30%. A very similar study was carried out by Lam et al. (2011) in a watershed of 50 km^2 in Northern Germany. The study revealed that when the fertilizer application rate in arable lands were reduced by 20%, the simulated values of average annual loads for TN, NO_3, TP and sediment were decreased by 8.6%, 9.9%, 1.1% and 0.82%, respectively. Although the average annual nitrogen load reduction was slightly higher than the reductions obtained in the Yavrucak subbasin, TP and sediment loads were not affected significantly similar to the Yavrucak subbasin. Another study performed by Park et al. (2015) in a watershed of 50 km^2 where 55% of the watershed is an agricultural area. The authors found that reducing nutrient application resulted in 8.6%, 1.1% and 0.8% reductions in the annual TN, TP and sediment loads. Similar to the results obtained in Lake Mogan, TP and sediment load reductions were lower compared to TN.

In Scenario-4, all tillage operations carried out with duck foot cultivator in agricultural lands were replaced by conservation tillage. Scenario-4 led to reduction in NO_3, TN and TP loads. In addition, the reduction rate achieved in NO_3 and TN loads was higher than the TP load. However, conservation tillage did not affect the sediment load significantly. Annual average NO_3, TN and TP loads were decreased by 2.3%, 2.0% an 1.6%, respectively. Scenario-5, no tillage scenario, seems to be better than

Scenario-4 since the calculated percent reductions were on average higher to some extent. Average annual percent reductions were calculated as 3.7%, 3.3% and 3.8% for NO_3, TN and TP loads, respectively. When Scenario-5 and Scenario-3 are compared, it is seen that the no tillage scenario is more effective in reducing the TP load. On the other hand, reduction in fertilizer application achieved higher percent reductions in NO_3 and TN loads. Similarly, Lam et al. (2011) reported that application of tillage scenarios did not result in considerable impacts on nitrogen load at the watershed outlet. Tuppad et al. (2010) assessed that the impacts of several BMPs including conservation tillage in the Bosque River watershed in Texas. The authors stated that the application of conservation tillage resulted in 3.6% reduction in the annual average TN load at the sub-watershed level which is very close to the percent reduction calculated in the Lake Mogan watershed.

In Scenario-6 and Scenario-7, the impacts of conservation tillage and no tillage operations were tested when they are applied on agricultural lands with low lay ratio. The implementation of these two scenarios did not have any impact on the average annual nutrient and sediment loads.

Contour farming was expected to result in reduction of sheet and rill erosion by decreasing the erosive capacity of surface runoff and minimizing the development of rills (Mazdak Arabi et al., 2008). In Scenario-8, contouring was simulated and the results revealed that it achieved a considerable annual average percent reduction (around 5%) in the sediment load, as expected. Moreover, contour farming brought about 4.4% reduction in the TP load. However, average annual NO_3 and TN loads were not affected considerably by contour farming.

Scenario-9 is the simulation of terraces in all agricultural lands. The results demonstrated that the terracing application reduced the TP and sediment loads quite successfully. In Yavrucak subbasin, TP and sediment loads were decreased by 6.9% and 8.4%, respectively. The annual percent reductions in NO_3 and TP loads, on the other hand, were 0.6% and 0.6%, respectively. Regarding the individual BMP scenarios, the results revealed that terracing provided more efficient TP and sediment load reduction than the others in Yavrucak subbasin. Thus, terraced agriculture can obviously enhance the environmental quality in the Lake Mogan watershed. Strauch et al. (2013) used SWAT model to assess the impacts of BMPs including terracing on

streamflow and sediment loads in the Pipiripau River Basin. The terracing scenario led to sediment load reductions of up to 31%. The authors reported that, the terraces were implemented in approximately 74% of the watershed area. Considering the extent of implementation in Yavrucak subbasin (up to 47% of the total subbasin area), the predicted reduction in sediment loads in Yavrucak is reasonable. Tuppad et al. (2010) stated that the long-term annual average sediment percent reduction at the watershed outlet was estimated as 17.2% when the terraces implemented on 10% of the catchment area. Gassman et al. (2006) specified that terraces achieved the greatest sediment reduction among the simulated BMPs. Up to 60% reduction in sediment loads provided when terraces implemented on 80% of the total watershed area.

The results demonstrated that each individual BMP scenario is effective in controlling certain types of pollutant. For instance, reducing fertilizer rate can play an important role in enhancing environmental quality by lessening NO_3 and TN loads in river. The outcomes obtained from tillage scenarios show that replacing the conventional tillage operations by no tillage can clearly reduce TP loads in addition to NO_3 and TN loads. Neither nutrient management scenarios nor changing tillage practices resulted in effective sediment control in the watershed. The highest percent reductions in sediment loads were simulated in the terracing scenario. As the results revealed, none of the scenarios was effective in reducing all kind of pollutant. Thus, the combined effects of the scenarios were tested. In Scenario-10, 30% fertilizer reduction and no tillage scenario were combined. Scenario-10 achieved 0.5%, 8.4%, 7.7%, and 4.2% reductions at sediment, NO_3, TN, and TP loads, respectively in Yavrucak. In Scenario-11, nutrient management and no tillage were combined with terracing. The highest reductions in pollutant loads among all BMP scenarios were obtained in this scenario. The annual average pollutant load reductions in Yavrucak subbasin were 8.4%, 8.9%, 8.2%, and 10.5% for sediment, NO_3, TN, and TP respectively.

The annual average percent reductions achieved in each BMP scenario were discussed based on the results obtained in the Yavrucak subbasin. The reason is that this subbasin is more representative of whole Lake Mogan watershed. Pastures and agricultural lands occupy a significant part of Lake Mogan watershed, 31% and 42%, respectively (see Table 12). The watershed has a very low slope in general. Similarly, Yavrucak subbasin is mostly covered with agricultural lands (47%). Pastures also occupy a significant part (31%) of the basin. The subbasin is flat, and only 2% of the total area

has a slope higher than 10%. Thus, it is assumed that the results obtained in Yavrucak subbasin can be adapted for whole Lake Mogan watershed. As expected, the impacts of agricultural BMP scenarios on pollutant loads at Yavrucak subbasin were more obvious compared to Sukesen subbasin. In Sukesen, even the most efficient BMP scenario achieved 0.72%, 1.13%, 1.04% and 5.01% reductions in sediment, NO_3, TN and TP loads, respectively. The reason is that the agricultural lands in Sukesen occupy only 11% of the total subbasin area. Therefore, the differences obtained between the results in the two subbasins were reasonable.

The results of this study suggest that the combination of reducing fertilizer rate by 30%, changing tillage practice from duckfoot cultivator to conservation tillage and implementation of terraces in agricultural lands in Lake Mogan watershed is a viable solution for controlling the agricultural diffuse pollution and improving the environmental quality in the area. However, it is important to consider that the required fertilizer rates and tillage measures may change depending on different soil types, climate, and landscape (Liu and Lu, 2014). Moreover, the cost-effectiveness of BMPs at the watershed scale should be evaluated. Thus, the farmers and the decision-makers should take into account all the benefits and drawbacks before implementing the BMPs which seem to be as effective solution for the pollution.

Table 43. Percent changes in annual average loads at Yavrucak monitoring station

Scenario	**Sediment (%)**	**NO_3 (%)**	**TN (%)**	**TP (%)**
Scenario-1: 10% reduction in fertilizer application rate	-0.08	-1.2	-1.1	0.04
Scenario-2: 20% reduction in fertilizer application rate	-0.04	-2.9	-2.7	-0.14
Scenario-3: 30% reduction in fertilizer application rate	-0.23	-4.8	-4.5	-0.3
Scenario-4: Conservation tillage scenario	-0.15	-2.3	-2.0	-1.6
Scenario-5: No tillage scenario	-0.30	-3.7	-3.3	-3.8
Scenario-6: Conservation tillage scenario (at low clay (<30%) agricultural lands)	0.00	0.00	0.00	-0.01
Scenario-7: No tillage scenario (at low clay (<30%) agricultural lands)	0.00	0.00	0.00	-0.02
Scenario-8: Contouring scenario	-5.3	-0.4	-0.4	-4.4
Scenario-9: Terracing scenario	-8.4	-0.6	-0.6	-6.9
Scenario-10: Combination of Scenario 3 and 5	-0.5	-8.4	-7.7	-4.2
Scenario-11: Combination of Scenario 3, 5 and 9	-8.4	-8.9	-8.2	-10.5

Table 44. Percent changes in annual average loads at Sukesen monitoring station

Scenario	Sediment (%)	NO_3 (%)	TN (%)	TP (%)
Scenario-1: 10% reduction in fertilizer application rate	0.03	-0.15	-0.14	0.02
Scenario-2: 20% reduction in fertilizer application rate	0.07	-0.32	-0.27	-0.01
Scenario-3: 30% reduction in fertilizer application rate	0.27	-0.48	-0.44	0.06
Scenario-4: Conservation tillage scenario	-0.01	-0.05	-0.06	-1.31
Scenario-5: No tillage scenario	-0.03	-0.05	-0.09	-2.96
Scenario-6: Conservation tillage scenario (at low clay (<30%) agricultural lands)	0.00	0.00	0.00	-0.01
Scenario-7: No tillage scenario (at low clay (<30%) agricultural lands)	0.00	0.00	0.00	-0.04
Scenario-8: Contouring scenario	-0.60	-0.60	-0.56	-1.91
Scenario-9: Terracing scenario	-0.79	-0.80	-0.76	-2.86
Scenario-10: Combination of Scenario 3 and 5	0.25	-0.53	-0.52	-2.91
Scenario-11: Combination of Scenario 3, 5 and 9	-0.72	-1.13	-1.04	-5.01

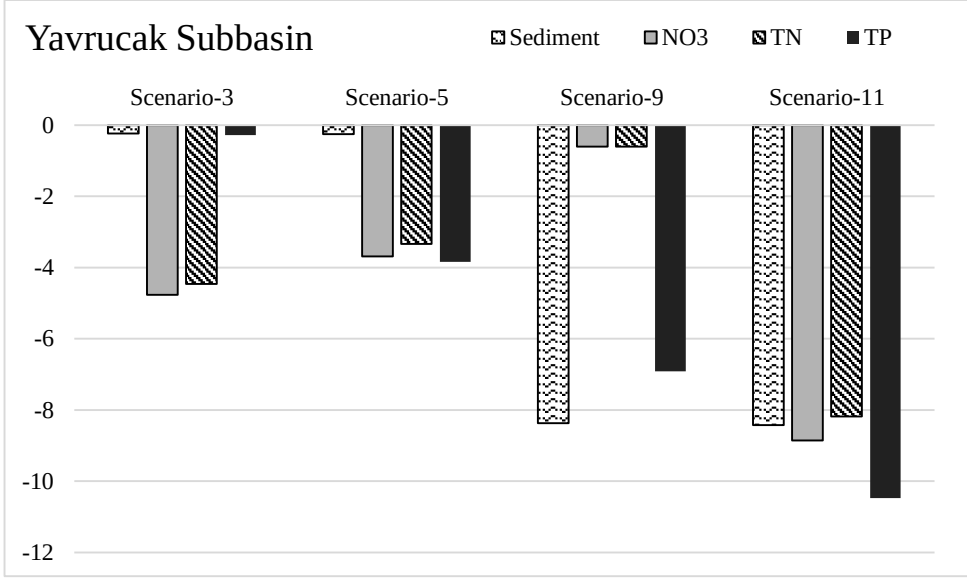

Figure 52. Percent changes in annual average loads at Yavrucak monitoring station

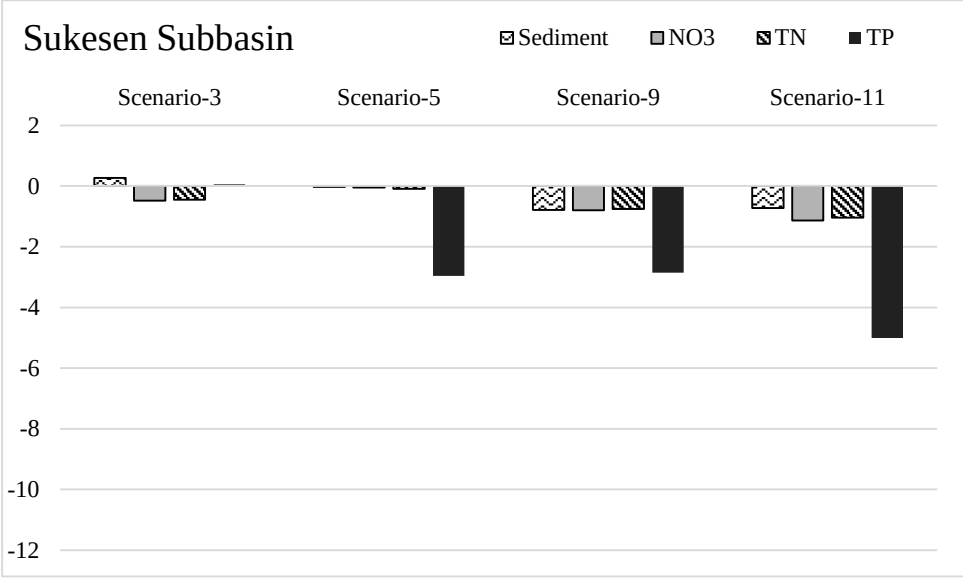

Figure 53. Percent changes in annual average loads at Yavrucak monitoring station

4.5. Evaluation of the Scenario Results for Wet Periods

As it was mentioned before in Section 3.1, the amount of streamflow in rivers is either very low or zero in Lake Mogan watershed. When there is no or negligible flow in the rivers, transport of pollutants and thus modelling of this process are not possible. In other words, there must be advection in order to talk about transport of pollutants. To this end, the hydrographs of Yavrucak and Sukesen creeks were analyzed. It was decided that when the streamflow rate is smaller than 5% and 10% of the maximum streamflow values simulated respectively for Yavrucak and Sukesen, the pollutant loads are negligible. Thus, the pollutant loads in Yavrucak and Sukesen were ignored when the streamflow is smaller than 0.03 m^3/sec and 0.02 m^3/sec, respectively.

The percent changes in the pollutant loads calculated in the best BMP scenario (Scenario-11) in Yavrucak is shown in together with the baseline streamflow values in Figure 54. The red line seen in the figure represents the streamflow of 0.03 m^3/sec. As it can be seen from Figure 54, when the streamflow is smaller than or equal to 0.03 m^3/sec, the percent changes in the pollutant loads are either negligible or zero. Therefore, evaluating dry and wet periods together may be misleading since the pollutant transport model may not be functioning properly when there is no or negligible flow in the rivers.

The percent changes in the pollutant loads calculated for wet periods (Yavrucak > 0.03 m^3/sec; Sukesen > 0.02 m^3/sec) in each BMP scenario are given in Table 45 and Table 46 for Yavrucak and Sukesen subbasins, respectively. The results revealed that when the wet periods are considered, the percent reductions in the pollutant loads get higher. For instance, the percent reductions in sediment, NO_3, TN and TP were 8.4, 8.9, 8.2 and 10.5, respectively when the dry and wet conditions were considered together for the best simulation (Scenario-11) in Yavrucak. On the other hand, the percent reductions increases to 9.84, 12.9, 10.7 and 10.7, respectively when the wet conditions are taken into account separately.

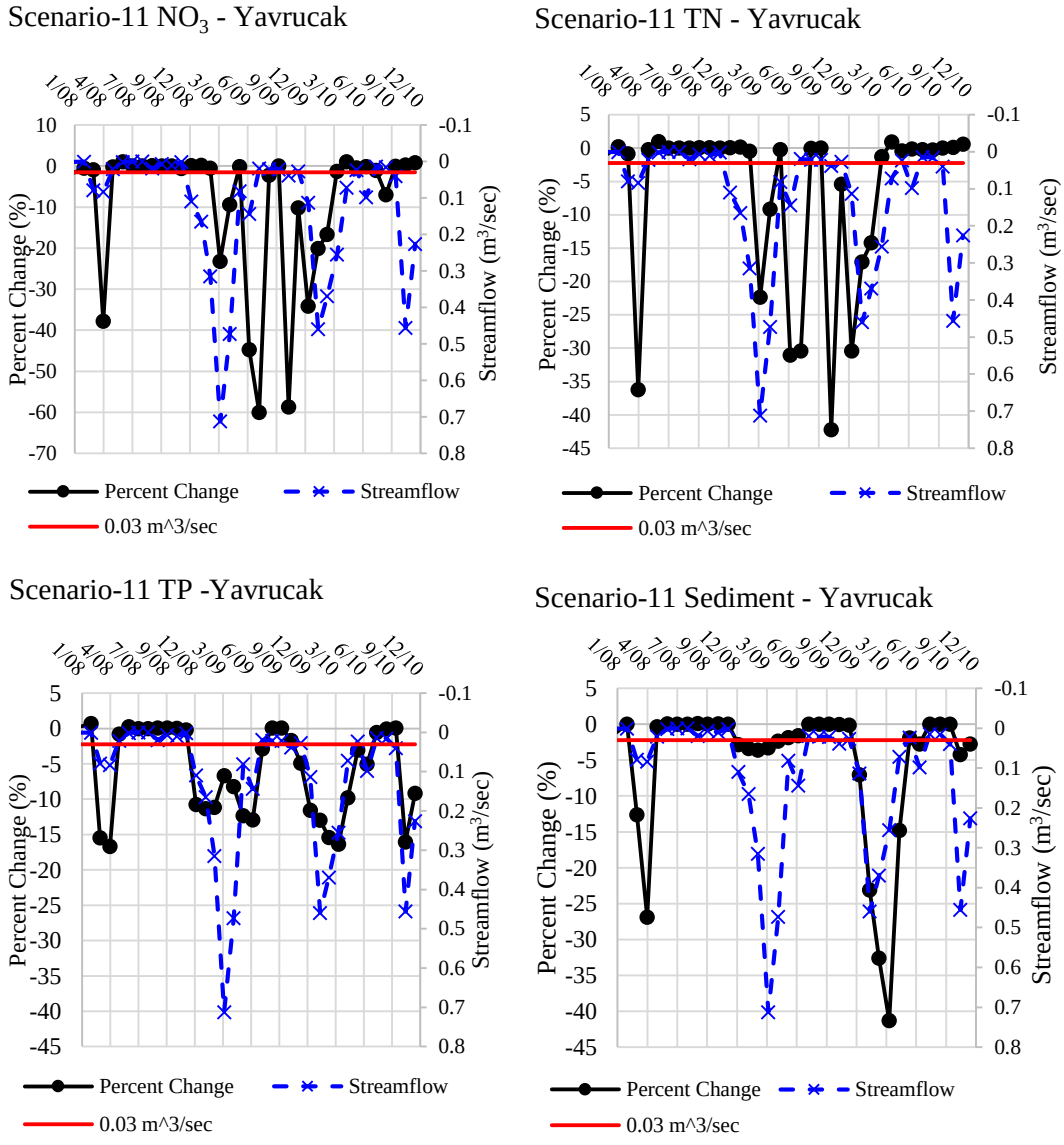

Figure 54. Comparison of the percent changes in the pollutant loads with the baseline streamflow

Table 45. Percent changes in annual average loads at Yavrucak monitoring station for wet conditions

Scenario	Sediment (%)	NO_3 (%)	TN (%)	TP (%)
Scenario-1: 10% reduction in fertilizer application rate	-0.11	-2.05	-1.64	-0.01
Scenario-2: 20% reduction in fertilizer application rate	-0.04	-5.34	-4.33	-0.31
Scenario-3: 30% reduction in fertilizer application rate	-0.07	-8.67	-7.11	-0.60
Scenario-4: Conservation tillage scenario	-0.22	-1.04	-1.01	-1.61
Scenario-5: No tillage scenario	-0.35	-1.63	-1.60	-4.04
Scenario-6: Conservation tillage scenario (at low clay (<30%) agricultural lands)	0.00	0.00	0.00	0.00
Scenario-7: No tillage scenario (at low clay (<30%) agricultural lands)	0.00	0.00	0.00	-0.02
Scenario-8: Contouring scenario	-6.14	-2.68	-2.03	-4.29
Scenario-9: Terracing scenario	-9.77	-4.09	-3.08	-6.69
Scenario-10: Combination of Scenario 3 and 5	-0.41	-10.4	-8.75	-4.62
Scenario-11: Combination of Scenario 3, 5 and 9	-9.84	-12.9	-10.7	-10.7

Table 46. Percent changes in annual average loads at Sukesen monitoring station for wet conditions

Scenario	Sediment (%)	NO_3 (%)	TN (%)	TP (%)
Scenario-1: 10% reduction in fertilizer application rate	0.09	-0.33	-0.27	0.09
Scenario-2: 20% reduction in fertilizer application rate	0.19	-0.66	-0.53	0.14
Scenario-3: 30% reduction in fertilizer application rate	0.56	-1.00	-0.81	0.31
Scenario-4: Conservation tillage scenario	0.00	0.05	0.02	-2.11
Scenario-5: No tillage scenario	0.00	0.10	0.05	-4.90
Scenario-6: Conservation tillage scenario (at low clay (<30%) agricultural lands)	0.00	0.00	0.01	-0.01
Scenario-7: No tillage scenario (at low clay (<30%) agricultural lands)	0.00	0.02	0.01	-0.05
Scenario-8: Contouring scenario	-0.65	-0.56	-0.48	-2.55
Scenario-9: Terracing scenario	-0.96	-0.90	-0.76	-4.02
Scenario-10: Combination of Scenario 3 and 5	0.53	-0.92	-0.77	-4.66
Scenario-11: Combination of Scenario 3, 5 and 9	-0.82	-1.61	-1.36	-7.63

CHAPTER 5

CONCLUSIONS AND RECOMMENDATIONS

In this study, SWAT model was used to estimate the effectiveness of several BMPs at subbasin level in Lake Mogan watershed. Lake Mogan is a semi-arid watershed located in Ankara, Turkey. Since agricultural activities are carried out intensively, agricultural diffuse pollution is a significant concern in the region. The quality of water bodies found in the region are under threat. Thus, this study aimed to identify efficient BMPs in terms of reducing diffuse pollution loads. For this purpose, the SWAT model was utilized to simulate the streamflow, sediment and nutrient loads in Lake Mogan watershed. The model was calibrated for streamflow, sediment and water quality (nitrogen and phosphorus) with SWAT-CUP. The model performance was quite satisfactory in simulating monthly streamflow. The statistical performance evaluation criteria NS, PBIAS and R^2 values are 0.74, -19.1 and 0.8, respectively, demonstrating a reasonable model simulations. The results for sediment and water quality were not as successful as streamflow simulations. The statistical coefficients NS, PBIAS and R^2 pointed out poor model performance. The main reason behind the unsatisfactory sediment and water quality simulations is the limited data availability which is actually one of the commonly experienced problems in semi-arid regions. The conclusion which is frequently mentioned in the literature and supported by the results of this study is that application of deterministic models like SWAT in semi-arid regions is a challenging task. Most reported reasons for the difficulties encountered in these regions are varying hydrological characteristics, lack of spatial and temporal detail in rainfall data and poor rain gauge density. In addition, less documentation for rainfall-runoff modeling compared to humid watersheds is another problem. Moreover, the number of studies reporting the water quality modelling results is even lower. The ones performing water quality calibration generally reported to demonstrate less satisfactory model performance compared to that of streamflow (see Table 42).

Based on literature, it was concluded that the intended use of SWAT model in this study which is to compare different BMPs falls into the exploratory category. Thus,

strict model accuracy in model simulations is not very critical. Therefore, it was decided that SWAT model can be used to assess and compare agricultural best management practices in Lake Mogan watershed even though the model performance is not very successful in water quality simulations.

The calibrated and validated SWAT model was used to develop 11 different BMP scenarios. Simulated BMPs included fertilizer management, conservation/no tillage, contouring and terracing, and combined scenarios. The results were evaluated at the two subbasins of Lake Mogan watershed namely Yavrucak and Sukesen. Average monthly and annual sediment, nitrate, total nitrogen, and total phosphorus loads were calculated for each scenario in both subbasins. The scenarios were compared with the baseline scenario which represents the current situation in the watershed. The results indicate that each BMP is effective in controlling certain type of diffuse source pollutant. In addition, individual BMP scenarios are not very effective in reducing pollutant loads. Therefore, combined BMP scenarios were developed and simulated. The most successful scenario (Scenario-11) was the one in which the amount of fertilizers reduced by 30% together with no tillage and parallel terraces applied in agricultural lands. It achieved 8.4%, 8.9%, 8.2%, and 11% reductions in average annual sediment, nitrate, total nitrogen, and total phosphorus loads, respectively in Yavrucak subbasin. However, there was not a significant impact on pollutant loads in Sukesen with the implementation of Scenario-11 due to high urbanization. The scenario results were also evaluated for wet periods since the pollutant transport model may not be functioning properly when there is no or negligible flow in the rivers. The results showed that the percent reductions in the pollutant loads get higher when the wet conditions are considered separately. For instance, the percent reductions in annual average sediment, NO_3, TN and TP loads increased to 9.84%, 12.9%, 10.7% and 10.7%, respectively under wet conditions for the best simulation (Scenario-11) in Yavrucak.

The results of this study suggest that the combination of reducing fertilizer rate by 30%, changing tillage practice from duckfoot cultivator to no tillage and implementation of terraces in agricultural lands in Lake Mogan watershed is a viable solution for controlling agricultural diffuse pollution and improving the environmental quality in the area. However, it is important to consider that the required fertilizer rates and tillage measures may change depending on different soil types, climate, and

landscape (Liu and Lu, 2014). Moreover, the cost-effectiveness of BMPs at the watershed scale should be evaluated. Thus, the farmers and the decision-makers should take into account all the benefits and drawbacks before implementing the BMPs which seem to be as effective solution for the pollution.

Evaluating the impacts of different management alternatives on pollution control is one of the steps of integrated watershed management plans which is proposed by the European Union Water Framework Directive. The goal of this study was to provide guidance for decision makers to implement effective best management practices in terms of controlling agricultural diffuse pollution in Lake Mogan watershed, and in watersheds showing similar characteristics with Lake Mogan. Hence, the proposed practices can help to protect the environment and increase the economic value of the agricultural activities due to cost and time related benefits.

Recommendations

Based on the challenges encountered and the results obtained in this study, it can be suggested that the monitoring studies carried out in the Lake Mogan watershed should be improved. To this end, the number of monitoring stations, and the frequency and the number of parameters monitored should be increased. The greatest difficulty experienced in this study was due to data limitation. Especially, the sediment and water quality calibration of SWAT model was challenging because of limited data availability. Moreover, the calibration and validation of the model could not be carried out in the same monitoring station since available data was not long enough to do so. In other words, there was not enough data for warm-up, calibration and validation at a single station.

In this study, only 1 year warm-up period has been used due to data limitation. Longer warm-up period would have been healthier. Thus, the available data series could have been copied at the beginning of the real one in order to allow for longer warm-up period.

Model validation results show that it could have been healthier to prefer multi-gauge calibration to represent spatial variability of the watershed better and thus to increase model reliability. This actually depends on the availability of continuous data in other monitoring stations located in the watershed.

Point sources were not considered in this study since there is no available information about the point sources located in the watershed. Once the information about them is available, their impacts on the water bodies should also be included.

Within the scope of this study, it was assumed that winter wheat is the only crop type cultivated in the agricultural lands. The effects of different crop patterns should also be assessed when detailed information about them is available.

In the context of this study, only sediment and nutrient simulations were carried out. If the monitoring of pesticides is performed in the future, it is recommended to carry out pesticide simulations as well.

It is recommended that the effects of climate change on diffuse pollution in Lake Mogan watershed is also evaluated.

Regarding the BMPs, it is important to consider that each BMP evaluated within the scope of this study has a different economic cost. For instance, while reducing fertilizer application rate is economically favorable, initial investment cost of implementation of terraces may become an important limiting parameter at the decision phase. Therefore, cost-effectiveness analyses should be performed before selecting the BMPs for the study area.

As a future study, development of the water quality model of Lake Mogan should be beneficial. SWAT model should be integrated with the lake water quality model, and holistic solution proposals should be developed.

REFERENCES

Abbaspour, K. C. (2015). SWAT-CUP SWAT Calibration and Uncertainty Programs - A User Manual. Retrieved from http://www.neprashtechnology.ca/wp-content/uploads/2015/06/Usermanual_SwatCup.pdf

Abbaspour, K. C., Johnson, C. A., & van Genuchten, M. T. (2004). Estimating Uncertain Flow and Transport Parameters Using a Sequential Uncertainty Fitting Procedure. *Vadose Zone Journal*, *3*, 1340–1352.

Abbaspour, K. C., Rouholahnejad, E., Vaghefi, S., Srinivasan, R., Yang, H., & Kløve, B. (2015). A continental-scale hydrology and water quality model for Europe: Calibration and uncertainty of a high-resolution large-scale SWAT model. *Journal of Hydrology*, *524*, 733–752. doi:10.1016/j.jhydrol.2015.03.027

Abbaspour, K. C., Vejdani, M., Haghighat, S., & Yang, J. (2007). SWAT-CUP Calibration and Uncertainty Programs for SWAT. In *The fourth International SWAT conference* (pp. 1596–1602). doi:10.1007/s00402-009-1032-4

Abbaspour, K. C., Yang, J., Maximov, I., Siber, R., Bogner, K., Mieleitner, J., … Srinivasan, R. (2007). Modelling hydrology and water quality in the pre-alpine/alpine Thur watershed using SWAT. *Journal of Hydrology*, *333*(2-4), 413–430. doi:10.1016/j.jhydrol.2006.09.014

Abraham, L. Z., Roehrig, J., & Chekol, D. A. (2007). Calibration and Validation of SWAT Hydrologic Model for Meki Watershed, Ethiopia. In *Conference on International Agricultural Research for Development*. University of Kassel-Witzenhausen and University of Göttingen.

Akhavan, S., Abedi-Koupai, J., Mousavi, S. F., Afyuni, M., Eslamian, S. S., & Abbaspour, K. C. (2010). Application of SWAT model to investigate nitrate leaching in Hamadan-Bahar Watershed, Iran. *Agriculture, Ecosystems and Environment*, *139*, 675–688. doi:10.1016/j.agee.2010.10.015

Almendinger, J. E., Murphy, M. S., & Ulrich, J. S. (2014). Use of the Soil and Water Assessment Tool to Scale Sediment Delivery from Field to Watershed in an Agricultural Landscape with Topographic Depressions. *Journal of Environment Quality*, *43*(1), 9. doi:10.2134/jeq2011.0340

Alp, E., Özcan, Z., Hatipoğlu, A., Başkan, O., Düzgün, H. Ş., & Kentel, E. (2014). *Evaluation of Agricultural Diffuse Pollution and its Control Alternatives with SWAT model in Lake Mogan Watershed*. Ankara, Turkey.

Arabi, M., Frankenberger, J. R., Engel, B. A., & Arnold, J. G. (2008). Representation of agricultural conservation practices with SWAT. *Hydrological Processes*, *22*, 3042–3055. doi:10.1002/hyp.6890

Arabi, M., Govindaraju, R. S., Hantush, M. M., & Engel, B. a. (2006). Role of Watershed Subdivision on Modeling the Effectiveness of Best Management Practices with SWAT. *Journal of the American Water Resources Association*, *42*, 513–528. doi:10.1111/j.1752-1688.2006.tb03854.x

Arabi, M., Meals, D. W., & Hoag, D. L. (2012). Watershed Modeling: National Institute of Food and Agriculture-Conservation Effects Assessment Project. In *How to Build Better Agricultural Conservation Programs to Protect Water Quality* (pp. 84–119). Soil and Water Conservation Society.

Arheimer, B., & Olsson, J. (2003). *Integration and Coupling of Hydrological Models with Water Quality Models: Applications in Europe*. Norrköping.

Arnold, J. . G., Srinivasan, R., Muttiah, R. S., & Allen, P. . M. (1999). Continental Scale Simulation of the Hydrologic Balance. *Journal of the American Water Resources Association*, *35*(5), 1037–1051. doi:10.1111/j.1752-1688.1999.tb04192.x

Arnold, J. G., & Fohrer, N. (2005). SWAT2000: current capabilities and research opportunities in applied watershed modelling. *Hydrological Processes*, *19*(3), 563–572. doi:10.1002/hyp.5611

Arnold, J. G., Kiniry, J. R., Srinivasan, R., Williams, J. R., Haney, E. B., & Neitsch, S. L. (2012a). *Soil & Water Assessment Tool: Input/output documentation*. *Texas Water Resources Institute*, *TR-439*. Retrieved from http://swat.tamu.edu/media/69296/SWAT-IO-Documentation-2012.pdf

Arnold, J. G., Moriasi, D. N., Gassman, P. W., Abbaspour, K. C., White, M. J., Srinivasan, R., … Jha, M. K. (2012b). SWAT: Model Use, Calibration, and Validation. *ASABE*, *55*, 1491–1508.

Arnold, J. G., Srinivasan, R., Muttiah, R. S., & Williams, J. R. (1998). LARGE AREA HYDROLOGIC MODELING AND ASSESSMENT PART I : MODEL DEVELOPMENT. *American Water Resources Association*, *34*(1), 73–89. doi:10.1111/j.1752-1688.1998.tb05961.x

ASAE. (2012). Design , Layout , Construction , and Maintenance of Terrace Systems. *American Society of Agricultural and Biological Engineers*, 1–6.

Assegahegn, M. A., & Zemadim, B. (2013). Erosion modelling in the upper Blue Nile basin: The case of Mizewa watershed in Ethiopia. In W. Mekuria (Ed.), *Rainwater management for resilient livelihoods in Ethiopia: Proceedings of the Nile Basin Development Challenge*. Nairobi, Kenya.

Bagnold, R. A. (1977). Bedload Transport in Natural Rivers. *Water Resources Research*, *13*(2), 303–312.

Benaman, J., Shoemaker, C. A., & Haith, D. A. (2005). Calibration and Validation of Soil and Water Assessment Tool on an Agricultural Watershed in Upstate New York. *Journal of Hydrologic Engineering*, *10*(5), 363–374. doi:10.1061/(ASCE)1084-0699(2005)10:5(363)

Beven, K., & Binley, A. (1992). The future of distributed models: model calibration and uncertainty prediction. doi:10.1002/hyp.3360060305

Bicknell, B. R., Imhoff, J. C., Kittle, Jr., J. L., Jobes, T. H., & Donigian, Jr., A. S. (2005). *Hydrological Simulation Program-Fortran: HSPF Version 12.2 User's Manual*. *Water science and technology : a journal of the International Association on Water Pollution Research* (Vol. 56). doi:EPA/68/C-01/037

Boithias, L., Srinivasan, R., Sauvage, S., Macary, F., & Sánchez-Pérez, J. M. (2014).

Daily nitrate losses: Implication on long-term river quality in an intensive agricultural catchment of southwestern france. *Journal of Environmental Quality*, *43*(1), 46–54. doi:10.2134/jeq2011.0367

Borah, D. K., & Bera, M. (2003). Watershed-Scale Hydrologic and Nonpoint-Source Pollution Models: Review of Mathematical Bases. *Transactions of the ASAE*, *46*(6), 1553–1566.

Bozkurt, O. Ç. (2013). *Operation of the Water Control Structure*. *Middle East Technical University*. Middle East Technical University.

Bracmort, K. S., Arabi, M., Frankenberger, J. R., Engel, B. A., & Arnold, J. G. (2006). Modeling Long-Term Water Quality Impact of Structural BMPs, *49*(2), 367–374.

Brown, L., & Barnwell, T. (1987). *The enhanced water quality models: QUAL2E and QUAL2E-UNCAS Documentation and User Manual*. Athens, Georgia.

Cestti, R., Srivastava, J., & Jung, S. (2003). Agriculture Non-Point Source Pollution Control Good Management Practices The Chesapeake Bay Experience, 44. Retrieved from http://books.google.ca/books?id=YQNcztHzpv4C&pg=PA33&lpg=PA33&dq=BMP+adoption+factor&source=bl&ots=hTRbgr2dIY&sig=ZDVi6MII94Bb2zF3SVsZK9QeM5g&hl=fr&sa=X&ei=mFQET8uMMYHn0QHwi_yuAg&ved=0CB4Q6AEwAA#v=onepage&q=BMP adoption factor&f=false

Çevre ve Şehircilik İl Müdürlüğü. (2013). *2012 Yılı Ankara İl Çevre Durum Raporu*. Ankara.

Chahinian, N., Tournoud, M.-G., Perrin, J.-L., & Picot, B. (2011). Flow and nutrient transport in intermittent rivers: a modelling case-study on the Vène River using SWAT 2005. *Hydrological Sciences Journal*, *56*(2), 268–287. doi:10.1080/02626667.2011.559328

Chaplot, V. (2005). Impact of DEM Mesh Size and Soil Map Scale on SWAT Runoff, Sediment, and NO3–N Loads Predictions. *Journal of Hydrology*, *312*(1-4), 207–222. doi:10.1016/j.jhydrol.2005.02.017

Chaplot, V., Saleh, A., Jaynes, D. B., & Arnold, J. (2004). Predicting water, sediment and NO3-N loads under scenarios of land-use and management practices in a flat watershed. *Water, Air, and Soil Pollution*, *154*, 271–293. doi:10.1023/B:WATE.0000022973.60928.30

Chaubey, I., Cotter, A. S., Costello, T. A., & Soerens, T. S. (2005). Effect of DEM data resolution on SWAT output uncertainty. *Hydrological Processes*, *19*(3), 621–628. doi:10.1002/hyp.5607

Chekol, D. A., Tischbein, B., Eggers, H., & Vlek, P. (2007). Application of SWAT for assessment of spatial distribution of water resources and analyzing impact of different land management practices on soil erosion in Upper Awash River Basin watershed. *Catchment and Lake Research*, 110–117.

Costa, D., Avelino, R., Sára, S., Thomazini, L., Aurélio, M., & Caiado, C. (2015). Application of the SWAT hydrologic model to a tropical watershed at Brazil. *Catena*, *125*, 206–213. doi:10.1016/j.catena.2014.10.032

Cotter, A. S., Chaubey, I., Costello, T. A., Soerens, T. S., & Nelson, M. A. (2003).

Water Quality Model Output Uncertainity as Affected by Spatial Resolution of Input Data. *Journal of American Water Resources Association*, *39*(4), 977–986.

Crawford, N. H., & Linsley, R. K. (1966). *Digital Simulation in Hydrology: Stanford Watershed Model IV*. California.

Croke, B. F. W., & Jakeman, A. J. (2008). Use of the IHACRES rainfall-runoff model in arid and semi arid regions. In H. Wheater, S. Sorooshian, & K. D. Sharma (Eds.), *Hydrological Modelling in Arid and Semi-Arid Areas*. Cambri. doi:10.1017/CBO9780511535734.005

Daniel, E. B., Camp, J. V., LeBoeuf, E. J., Penrod, J. R., Dobbins, J. P., & Abkowitz, M. D. (2011). Watershed Modeling and its Applications: A State-of-the-Art Review. *The Open Hydrology Journal*, *5*(1), 26–50. doi:10.2174/1874378101105010026

David, V., & Davidova, T. (2015). PRECIPITATION ASSESSMENT FROM THE VIEWPOINT DATA AVAILABILITY FOR PURPOSES OF FLOOD MODELLING. In *Proceedings of the 14th International Conference on Environmental Science and Technology*. Rhodes, Greece.

Dechmi, F., Burguete, J., & Skhiri, A. (2012). SWAT application in intensive irrigation systems: Model modification, calibration and validation. *Journal of Hydrology*, *470-471*, 227–238. doi:10.1016/j.jhydrol.2012.08.055

Dechmi, F., & Skhiri, a. (2013). Evaluation of best management practices under intensive irrigation using SWAT model. *Agricultural Water Management*, *123*(2013), 55–64. doi:10.1016/j.agwat.2013.03.016

Di Luzio, M., Srinivasan, R., & Arnold, J. G. (1998). Watershed Oriented Non-Point Pollution Assessment Tool. In F. S. Zazueta & J. Xing (Eds.), *Proceedings of the 7th International Conference on Computers in Agriculture* (pp. 233–241).

Di Luzio, M., Srinivasan, R., & Arnold, J. G. (2002). Integration of Watershed Tools and SWAT Model into Basins. *JAWRA Journal of the American Water Resources Association*, *38*(4), 1127–1141. doi:10.1111/j.1752-1688.2002.tb05551.x

El-Sadek, A., & Irvem, A. (2014). Evaluating the impact of land use uncertainty on the simulated streamflow and sediment yield of the Seyhan River basin using the SWAT model. *Turkish Journal of Agriculture and Forestry*, *38*(4), 515–530. doi:10.3906/tar-1309-89

Engel, B. A., Storm, D., White, M., Arnold, J. G., & Arabi, M. (2007). A hydrologic/water quality model application protocol. *Journal of the American Water Resources Association*, *43*, 1223–1236. doi:10.1111/j.1752-1688.2007.00105.x

Faramarzi, M., Abbaspour, K. C., Schulin, R., & Yang, H. (2009). Modelling blue and green water resources availability in Iran. *Hydrological Processes*, *23*, 486–501. doi:10.1002/hyp.7160

Ficklin, D. L., Stewart, I. T., & Maurer, E. P. (2013). Climate Change Impacts on Streamflow and Subbasin-Scale Hydrology in the Upper Colorado River Basin. *PLoS ONE*, *8*(8). doi:10.1371/journal.pone.0071297

Gassman, P., Osei, E., Saleh, A., Rodecap, J., Norvell, S., & Williams, J. (2006).

Alternative practices for sediment and nutrient loss control on livestock farms in northeast Iowa. *Agriculture, Ecosystems & Environment*, *117*(2-3), 135–144. doi:10.1016/j.agee.2006.03.030

Gassman, P. W., Balmer, C., & Siemers, M. (2014). The SWAT Literature Database : Overview of Database Structure and Key SWAT Literature Trends. In *SWAT 2014 Conference Pernambuco, Brazil*.

Gassman, P. W., Reyes, M. R., Green, C. H., & Arnold, J. G. (2007). The Soil and Water Assessment Tool: Historical Development, Applications, and Future Research Directions. *Transactions of the Asabe*, *50*, 1211–1250. doi:10.1.1.88.6554

Gassman, P. W., Sadeghi, A. M., & Srinivasan, R. (2014). Applications of the SWAT Model Special Section: Overview and Insights. *Journal of Environmental Quality*, 1–8. doi:10.2134/jeq2013.11.0466

Georgia Soil & Water Conservation Commission. (1994). *Agricultural Best Management Practices to Control Water Quality in Georgia*. Atlanta. Retrieved from http://infohouse.p2ric.org/ref/34/33252.pdf

Glavan, M., & Pintar, M. (2012). Strengths, Weaknesses, Opportunities and Threats of Catchment Modelling with Soil and Water Assessment Tool (SWAT) Model. *Water Resources Management and Modeling*, 39–64. doi:10.5772/34539

Green, W., & Ampt, G. (1911). Studies on soil physics: 1. The flow of air and water through soils. *J Agric Sci*, *4*, 11–24.

Güngör, Ö., & Göncü, S. (2013). Application of the soil and water assessment tool model on the Lower Porsuk Stream Watershed. *Hydrological Processes*, *27*(March 2012), 453–466. doi:10.1002/hyp.9228

Gupta, H. V., Sorooshian, S., & Yapo, P. O. (1999). Status of Automatic Calibration for Hydrologic Models: Comparison with Multilevel Expert Calibration. *Journal of Hydrologic Engineering*. doi:10.1061/(ASCE)1084-0699(1999)4:2(135)

Harmel, R. D., Smith, P. K., Migliaccio, K. W., Chaubey, I., Douglas-Mankin, K. R., Benham, B., … Robson, B. J. (2014). Evaluating , interpreting , and communicating performance of hydrologic/water quality models considering intended use : A review and recommendations. *Environmental Modelling & Software*, *57*, 40–51. doi:http://dx.doi.org/10.1016/j.envsoft.2014.02.013

Hranova, R. (2006). *Diffuse Pollution of Water Resources: Principles and Case Studies in the Southern African Region*. London: Taylor & Francis Group.

Hughes, D. A. (2008). Modelling Semi-Arid and Arid Hydrology and Water Resources–the Southern African Experience. In H. Wheater, S. Sorooshian, & K. D. Sharma (Eds.), *Hydrological Modelling in Arid and Semi-Arid Areas* (p. 195). Cambridge University Press.

Jayakrishnan, R., Srinivasan, R., Santhi, C., & Arnold, J. G. (2005). Advances in the application of the SWAT model for water resources management. *Hydrological Processes*, *19*(3), 749–762. doi:10.1002/hyp.5624

Kaini, P., Artita, K., & Nicklow, J. (2012). Optimizing Structural Best Management Practices Using SWAT and Genetic Algorithm to Improve Water Quality Goals.

Water Resources Management, *26*(7), 1827–1845. doi:10.1007/s11269-012-9989-0

Karakaya, V., Güner, Ö., Bölük, M., & Uludağ, T. (2007). *Ankara İl Çevre Durum Raporu*. Ankara, Turkey.

Karakoç, G., Ünlü Erkoç, F., & Katircioğlu, H. (2003). Water quality and impacts of pollution sources for Eymir and Mogan Lakes (Turkey). *Environment International*, *29*(1), 21–27. doi:10.1016/S0160-4120(02)00128-9

Kersebaum, K. C., Steidl, J., Bauer, O., & Piorr, H. P. (2003). Modelling scenarios to assess the effects of different agricultural management and land use options to reduce diffuse nitrogen pollution into the river Elbe. *Physics and Chemistry of the Earth*, *28*, 537–545. doi:10.1016/S1474-7065(03)00090-1

Kim, I., Noh, J., Son, K., & Kim, I. (2012). Impacts of GIS Data Quality on Determination of Runoff and Suspended Sediments in the Imha Watershed in Korea. *Geosciences Journal*, *16*(2), 181–192. doi:10.1007/s12303-012-0013-8

Krause, S., Jacobs, J., Voss, A., Bronstert, A., & Zehe, E. (2008). Assessing the impact of changes in landuse and management practices on the diffuse pollution and retention of nitrate in a riparian floodplain. *Science of the Total Environment*, *389*, 149–164. doi:10.1016/j.scitotenv.2007.08.057

Krysanova, V., Müller-Wohlfeil, D. I., & Becker, A. (1998). Development and test of a spatially distributed hydrological/water quality model for mesoscale watersheds. *Ecological Modelling*, *106*, 261–289. doi:10.1016/S0304-3800(97)00204-4

Kuczera, G., & Parent, E. (1998). Monte Carlo assessment of parameter uncertainty in conceptual catchment models: The Metropolis algorithm. *Journal of Hydrology*, *211*, 69–85. doi:10.1016/S0022-1694(98)00198-X

Lam, Q. D., Schmalz, B., & Fohrer, N. (2011). The impact of agricultural Best Management Practices on water quality in a North German lowland catchment. *Environmental Monitoring and Assessment*, *183*(1-4), 351–379. doi:10.1007/s10661-011-1926-9

Lam, Q. D., Schmalz, B., & Fohrer, N. (2012). Assessing the spatial and temporal variations of water quality in lowland areas, Northern Germany. *Journal of Hydrology*. doi:10.1016/j.jhydrol.2012.03.011

Lee, M., Park, G., Park, M., Park, J., Lee, J., & Kim, S. (2010). Evaluation of non-point source pollution reduction by applying Best Management Practices using a SWAT model and QuickBird high resolution satellite imagery. *Journal of Environmental Sciences*, *22*(6), 826–833. doi:10.1016/S1001-0742(09)60184-4

Lévesque, É., Anctil, F., Van Griensven, A., & Beauchamp, N. (2008). Evaluation of streamflow simulation by SWAT model for two small watersheds under snowmelt and rainfall. *Hydrological Sciences Journal*, *53*(5), 961–976. doi:10.1623/hysj.53.5.961

Liew, M. W. Van, Arnold, J. G., & Bosch, D. D. (2005). Problems and Potential of Autocalibrating a Hydrologic Model. *Transactions of the ASAE*, *48*(3), 1025–1040.

Liu, M., & Lu, J. (2014). Predicting the impact of management practices on river water quality using SWAT in an agricultural watershed. *Desalination and Water Treatment*, (May 2014), 1–14. doi:10.1080/19443994.2014.902332

Liu, R., Xu, F., Zhang, P., Yu, W., & Men, C. (2016). Identifying non-point source critical source areas based on multi-factors at a basin scale with SWAT. *Journal of Hydrology*, *533*, 379–388. doi:10.1016/j.jhydrol.2015.12.024

Luzio, M. Di, Arnold, J. G., & Srinivasan, R. (2005). Effect of GIS data quality on small watershed stream fl ow and sediment simulations. *Hydrological Processes*, *19*, 629–650. doi:10.1002/hyp.5612

McElroy, A. D., Chiu, S. Y., Nebgen, J. W., Aleti, A., & Bennet, F. W. (1976). *Loading Functions for Assessment of Water Pollution From Nonpoint Sources*. Washington. doi:EPA 600/2- 76-151

McKay, M. D., Beckman, R. J., & Conover, W. J. (1979). A Comparison of Three Methods for Selecting Values of Input Variables in the Analysis of Output from a Computer Code. *Technometrics*, *21*(2), 239–245. doi:doi:10.2307/1268522

Meaurio, M., Zabaleta, A., Uriarte, J. A., Srinivasan, R., & Antigüedad, I. (2015). Evaluation of SWAT models performance to simulate streamflow spatial origin. The case of a small forested watershed. *Journal of Hydrology*, *525*, 326–334. doi:10.1016/j.jhydrol.2015.03.050

Merrill, L. S., Crawford, S. K., & Hall, T. (2011). *Manual of Best Management Practices (BMPs) for Agriculture in New Hampshire*.

Miller, T., Peterson, J., Lenhart, C., & Nomura, Y. (2012). *The Agricultural BMP Handbook for Minnesota*. Retrieved from http://www.mda.state.mn.us/protecting/cleanwaterfund/research/agbmphandbook.aspx

Mirshahi, B. (2010). *Hydrological modelling in data-sparse snow-affected semiarid areas*. University of London.

Monteith, J. L., & Moss, C. J. (1977). Climate and the Efficiency of Crop Production in Britain [and Discussion]. *Philosophical Transactions of the Royal Society B: Biological Sciences*. doi:10.1098/rstb.1977.0140

Moriasi, D. N., Arnold, J. G., Van Liew, M. W., Bingner, R. L., Harmel, R. D., & Veith, T. L. (2007). Model Evaluation Guidelines for Systematic Quantification of Accuracy in Watershed Simulations. *Transactions of the Asabe*, *50*(3), 885–900. doi:10.13031/2013.23153

Muhammetoğlu, A., & Soyupak, S. (2000). A three-dimensional water quality-macrophyte interaction model for shallow lakes. *Ecological Modelling*, *133*(3), 161–180. doi:10.1016/S0304-3800(00)00297-0

Nash, J. E., & Sutcliffe, J. V. (1970). River flow forecasting through conceptual models part I — A discussion of principles. *Journal of Hydrology*. doi:10.1016/0022-1694(70)90255-6

Ndomba, P., Mtalo, F., & Killingtveit, A. (2008). SWAT model application in a data scarce tropical complex catchment in Tanzania. *Physics and Chemistry of the Earth*, *33*, 626–632. doi:10.1016/j.pce.2008.06.013

Neitsch, S. L., Arnold, J. G., Kiniry, J. R., Srinivasan, R., & Williams, J. R. (2002). Soil and Water Assessment Tool User's Manual. *Temple, TX*, 412. Retrieved from http://swat.tamu.edu/media/1294/swatuserman.pdf

Neitsch, S. L., Arnold, J. G., Kiniry, J. R., & Williams, J. R. (2009). *Soil & Water Assessment Tool - Theoretical Documentation Version 2009*. Texas.

Niraula, R., Norman, L. M., Meixner, T., & Callegary, J. B. (2012). Multi-gauge Calibration for modeling the Semi-Arid Santa Cruz watershed in Arizona-Mexico border area using SWAT. *Air, Soil and Water Research*, *5*, 41–57. doi:10.4137/ASWR.S9410

Noor, H., Vafakhah, M., Taheriyoun, M., & Moghadasi, M. (2014). Hydrology modelling in Taleghan mountainous watershed using SWAT. *Journal of Water and Land Development*, *20*, 11–18. doi:10.2478/jwld-2014-0003

Novotny, V. (2003). *Water Quality: Diffuse Pollution and Watershed Management* (2nd ed.). New York: John Wiley & Sons, Inc.

Oeurng, C., Sauvage, S., & Sánchez-Pérez, J. M. (2011). Assessment of hydrology, sediment and particulate organic carbon yield in a large agricultural catchment using the SWAT model. *Journal of Hydrology*, *401*, 145–153. doi:10.1016/j.jhydrol.2011.02.017

Ogden, F. L., Garbrecht, J., DeBarry, P. a., & Johnson, L. E. (2001). GIS and Distributed Watershed Models. II: Modules, Interfaces, and Models. *Journal of Hydrologic Engineering*, *6*, 515–523. doi:10.1061/(ASCE)1084-0699(2001)6:6(515)

Olivera, F., Valenzuela, M., Srinivasan, R., Choi, J., Cho, H., Koka, S., & Agrawal, A. (2006). ArcGIS-SWAT: A Geodata Model and GIS Interface for SWAT. *Journal of the American Water Resources Association*, *42*(2), 295–309. doi:10.1111/j.1752-1688.2006.tb03839.x

Oogathoo, S. (2006). *Runoff Simulation in the Canagagigue Creek Watershed Using the Mike She Model*. McGill University.

Özesmi, U. (1999). Ecology and Politics of Rehabilitation: Mogan Lake Wetland Ecosystem, Ankara, Turkey. In W. Streever (Ed.), *An International Perspective on Wetland Rehabilitation* (pp. 181 – 187). Kluwer Academic Publishers.

Parajuli, P. B., & Ouyang, Y. (2013). *Watershed-Scale Hydrological Modeling Methods and Applications*. (P. Bradley, Ed.)*Current Perspectives in Contaminant Hydrology and Water Resources Sustainability*. doi:DOI: 10.5772/53596

Park, Y. S., Lim, K. J., Yang, J. E., & Kim, K. (2015). Modelling of Best Management Practices in Agricultural Areas. In Prof. Vytautas Pilipavicius (Ed.), *Agroecology*. InTech. doi:10.5772/59990

Pereira, D. dos R., Martinez, M. A., Almeida, A. Q. de, Pruski, F. F., Silva, D. D. da, & Zonta, J. H. (2014). Hydrological Simulation Using Swat Model in Headwater Basin in Southeast Brazil Simulação Hidrológica Usando O Modelo Swat Em Bacia Hidrográfica De Cabeceira Da Região Sudeste Do Brasil. *Eng. Agríc. Jaboticabal*, *34*(4), 789–799. doi:https://dx.doi.org/10.1590/S0100-

69162014000400018

Pilgrim, D. H., Chapman, T. G., & Doran, D. G. (1988). Problems of rainfall-runoff modelling in arid and semiarid regions. *Hydrological Sciences Journal*, *33*(March 2015), 379–400. doi:10.1080/02626668809491261

Pisinaras, V., Petalas, C., Gikas, G. D., Gemitzi, A., & Tsihrintzis, V. A. (2010). Hydrological and water quality modeling in a medium-sized basin using the Soil and Water Assessment Tool (SWAT). *Desalination*, *250*, 274–286. doi:10.1016/j.desal.2009.09.044

Priestley, C. H. B., & Taylor, R. J. (1972). On the Assessment of Surface Heat Flux and Evaporation Using Large-Scale Parameters. *Monthly Weather Review*, *100*, 81–92. doi:10.1175/1520-0493(1972)100<0081:OTAOSH>2.3.CO;2

Qiu, Z., & Wang, L. (2013). Hydrological and Water Quality Assessment in a Suburban Watershed with Mixed Land Uses Using the SWAT Model. *Journal of Hydrologic Engineering*, *319*(April), 130603185714005. doi:10.1061/(ASCE)HE.1943-5584.0000858

Randall, M. J. (2012). *Best Management Practices Effectiveness to Reduce Sediment Transport to Morro Bay*. California Polytechnic State University.

Ritter, W. F., & Shirmohammadi, A. (2001). *Agricultural Nonpoint Source Pollution: Watershed Management and Hyrdrology*. CRC Press LLC.

Rocha, J., Roebeling, P., & Rial-Rivas, M. E. (2015). Assessing the impacts of sustainable agricultural practices for water quality improvements in the Vouga catchment (Portugal) using the SWAT model. *Science of The Total Environment*, *536*, 48–58. doi:10.1016/j.scitotenv.2015.07.038

Rostamian, R., Jaleh, A., Afyuni, M., Mousavi, S. F., Heidarpour, M., Jalalian, A., & Abbaspour, K. C. (2008). Application of a SWAT model for estimating runoff and sediment in two mountainous basins in central Iran. *Hydrological Sciences Journal*, *53*(5), 977–988. doi:10.1623/hysj.53.5.977

Sahu, M., & Gu, R. R. (2009). Modeling the effects of riparian buffer zone and contour strips on stream water quality. *Ecological Engineering*, *35*, 1167–1177. doi:10.1016/j.ecoleng.2009.03.015

Santhi, C., Arnold, J. G., Williams, J. R., Dugas, W. a., Srinivasan, R., & Hauck, L. M. (2001). Validation of the SWAT model on a large river basin with point and nonpoint sources. *Journal of the American Water Resources Association (JAWRA)*, *37*(5), 1169–1188. doi:10.1111/j.1752-1688.2001.tb03630.x

Santhi, C., Kannan, N., Arnold, J. G., & Di Luzio, M. (2008). Spatial calibration and temporal validation of flow for regional scale hydrologic modeling. *Journal of the American Water Resources Association*, *44*, 829–846. doi:10.1111/j.1752-1688.2008.00207.x

Santhi, C., Srinivasan, R., Arnold, J. G., & Williams, J. R. (2006). A modeling approach to evaluate the impacts of water quality management plans implemented in a watershed in Texas. *Environmental Modelling & Software*, *21*(8), 1141–1157. doi:10.1016/j.envsoft.2005.05.013

Schertz, D. L. (1988). Conservation tillage: An analysis of acreage projections in the

United States. *J. Soil Water Cons.*, *43*, 256–258.

Schilling, K. E., & Wolter, C. F. (2009). Modeling Nitrate-Nitrogen Load Reduction Strategies for the Des Moines River, Iowa Using SWAT. *Environmental Management*, *44*(4), 671–682. doi:10.1007/s00267-009-9364-y

Schneider, K., Ketzer, B., Breuer, L., Vache, K. B., Bernhofer, C., & Frede, H. G. (2007). Evaluation of evapotranspiration methods for model validation in a semi-arid watershed in Northern China. *Advances in Geosciences*, *11*, 37–42. doi:10.5194/adgeo-11-37-2007

Schwab, G. O., Fangmeier, D. D., Elliot, W. J., & Frevert, R. K. (1993). *Soil and Water Conservation Engineering* (4th ed.). John Wiley & Sons, Inc.

Shao, H., Baffaut, C., Gao, J. E., Nelson, N. O., Janssen, K. A., Pierzynski, G. M., & Barnes, P. L. (2013). Development and application of algorithms for simulating terraces within SWAT. *Transactions of the ASABE*, *56*(5), 1715–1730. doi:10.13031/trans.56.10047

Sharpley, A. N., Daniel, T., Gibson, G., Bundy, L., Cabrera, M., Sims, T., … Parry, R. (2006). Best Management Practices To Minimize Agricultural Phosphorus Impacts on Water Quality, *ARS-163*(July). Retrieved from http://www.ars.usda.gov/is/np/BestMgmtPractices/Best Management Practices.pdf

Shen, Z., Liao, Q., Hong, Q., & Gong, Y. (2011). An overview of research on agricultural non-point source pollution modelling in China. *Separation and Purification Technology*, *84*, 104–111. doi:10.1016/j.seppur.2011.01.018

Shrestha, M. K., Recknagel, F., Frizenschaf, J., & Meyer, W. (2016). Assessing SWAT models based on single and multi-site calibration for the simulation of flow and nutrient loads in the semi-arid Onkaparinga catchment in South Australia. *Agricultural Water Management*. doi:10.1016/j.agwat.2016.02.009

Singh, V. P., & Frevert, D. K. (2002). Mathematical Modeling of Watershed Hydrology. *Journal of Hydrologic Engineering*, *7*(4), 270–292.

Singh, V. P., & Frevert, D. K. (2006). *Watershed Models*. Boca Raton: Taylor & Francis Group.

Society, A., & Agricultural, O. F. (1985). Reference Crop Evapotranspiration from Temperature. *Applied Engineering in Agriculture*, *1*, 96–99. doi:10.13031/2013.26773

Soil Conservation Service Engineering Division. (1972). Section 4: Hydrology. In *National Engineering Handbook* (pp. 10–1 – 10–22).

Sood, A., Muthuwatta, L., & McCartney, M. (2013). A SWAT evaluation of the effect of climate change on the hydrology of the Volta River basin. *Water International*, *38*, 297–311. doi:10.1080/02508060.2013.792404

Srinivasan, R. (2014). *Beginner SWAT Training Manual*.

Srinivasan, R., & Arnold, J. G. (1994). Integration of a Basin-Scale Water Quality Model with GIS. *Water Resources Bulletin*, *30*(3), 453–462. doi:10.1111/j.1752-1688.1994.tb03304.x

Stratton, B. T., Sridkar, V., Gribb, M. M., Mcnamara, J. P., & Narasimhan, B. (2009). Modeling the Spatially Varying Water Balance Processes in a Semi- Arid Mountainous Watershed of Idaho Modeling the Spatially Varying Water Balance Processes in a Semi-, *45*(6). doi:10.1111/j.1752-1688.2009.00371.x

Strauch, M., Bernhofer, C., Koide, S., Volk, M., Lorz, C., & Makeschin, F. (2012). Using precipitation data ensemble for uncertainty analysis in SWAT streamflow simulation. *Journal of Hydrology*, *414-415*, 413–424. doi:10.1016/j.jhydrol.2011.11.014

Strauch, M., Lima, J. E. F. W., Volk, M., Lorz, C., & Makeschin, F. (2013). The impact of Best Management Practices on simulated streamflow and sediment load in a Central Brazilian catchment. *Journal of Environmental Management*, *127*, S24–S36. doi:10.1016/j.jenvman.2013.01.014

Tabiat Varlıklarını Koruma Genel Müdürlüğü. (n.d.). Gölbaşı Özel Çevre Koruma Bölgesi. Retrieved January 26, 2016, from http://www.csb.gov.tr/gm/tabiat/index.php?Sayfa=sayfa&Tur=webmenu&Id=195

TAMU. (2016). SWAT Soil & Water Assessment Tool. Retrieved February 19, 2016, from http://swat.tamu.edu/

Thodsen, H., Andersen, H. E., Blicher-Mathiesen, G., & Trolle, D. (2015). The combined effects of fertilizer reduction on high risk areas and increased fertilization on low risk areas, investigated using the SWAT model for a Danish catchment. *Acta Agriculturae Scandinavica, Section B — Soil & Plant Science*, *65*, 217–227. doi:10.1080/09064710.2015.1010564

Tibebe, M., Zemadim, B., Haile, D., & Melesse, A. (2013). Runoff estimation and water management for the Holetta river in Ethiopia Runoff estimation and water management for the Holetta river in Ethiopia. In W. Mekuria (Ed.), *Rainwater management for resilient livelihoods in Ethiopia: Proceedings of the Nile Basin Development Challenge science meeting* (pp. 9–10). Addis Ababa.

Troeh, F. R., Hobbs, J. A., & Donahue, R. L. (2004). *Soil and Water Conservation for Productivity and Environmental Proteciton*. (S. Helba, Ed.) (4th ed.). New Jersey: Pearson Education.

TÜİK. (2015). Adrese Dayalı Nüfus Kayıt Sistemi Sonuçları. Retrieved February 2, 2016, from https://biruni.tuik.gov.tr/medas/?kn=95&locale=tr

Tuppad, P., Kannan, N., Srinivasan, R., Rossi, C. G., & Arnold, J. G. (2010). Simulation of Agricultural Management Alternatives for Watershed Protection. *Water Resources Management*, *24*, 3115–3144. doi:10.1007/s11269-010-9598-8

Uğur, S. (2009). *Study of Big Scale Park Around of Natural Water Surface According to Ecological Criteria: Mogan Park Example*. Ankara University.

USDA-ARS, & Texas A&M. (2015). SWAT Soil and Water Assessment Tool. Retrieved December 1, 2015, from http://swat.tamu.edu/

USEPA. (2012a). Agricultural Nonpoint Source Fact Sheet. Retrieved November 8, 2015, from http://water.epa.gov/polwaste/nps/agriculture_facts.cfm

USEPA. (2012b). What is Nonpoint Source Pollution? Retrieved November 8, 2015,

from http://water.epa.gov/polwaste/nps/whatis.cfm

van Griensven, A., & Meixner, T. (2006). Methods to quantify and identify the sources of uncertainty for river basin water quality models. *Water Science and Technology : A Journal of the International Association on Water Pollution Research*, *53*, 51–59. doi:10.2166/wst.2006.007

Vilaysane, B., Takara, K., Luo, P., Akkharath, I., & Duan, W. (2015). Hydrological Stream Flow Modelling for Calibration and Uncertainty Analysis Using SWAT Model in the Xedone River Basin, Lao PDR. *Procedia Environmental Sciences*, *28*, 380–390. doi:10.1016/j.proenv.2015.07.047

Walter, M. F., Steenhuis, T. S., & Haith, D. A. (1979). Nonpoint Source Pollution Control by Soil and Water Conservation Practices. *Transactions of the ASAE*, 834–840.

Weiner, R. F., & Matthews, R. A. (2003). *Environmental Engineering* (4th ed.). Butterworth - Heinemann.

Wheater, H. (2008). *Hydrological Modeling in Arid and Semi-Arid Areas*. New York: Cambridge University Press.

White, K. L., & Chaubey, I. (2005). Sensitivity Analysis , Calibration, and Validations for a Multisite and Multivariable Swat Model. *Journal Of The American Water Resources Association*, *41*(5), 1077–1089.

Williams, J. R. (1975). Sediment routing for agricultural watersheds. *Water Resources Bulletin*, *11*, 965–974. doi:10.1111/j.1752-1688.1975.tb01817.x

Williams, J. R., Arnold, J. G., Kiniry, J. R., Gassman, P. W., & Green, C. H. (2008). History of model development at Temple, Texas. *Hydrological Sciences Journal*, *53*(January 2015), 948–960. doi:10.1623/hysj.53.5.948

Williams, J. R., & Hann, R. W. (1978). *Optimal Operation of Large Agricultural Watersheds With Water Quality Constraints*. Texas.

Williams, J. R., Jones, C. A., & Dyke, P. T. (1984). A modelling approach to determining the relationship between erosion and soil productivity. *Transactions - American Society of Agricultural Engineers*, *27*, 129–144. Retrieved from http://www.scopus.com/inward/record.url?eid=2-s2.0-0021644951&partnerID=40&md5=c2306c0c16b0a6db86ed12e70567a973

Winchell, M., Srinivasan, R., & Di Luzio, M. (2010). *ArcSWAT Interface for SWAT 2009 User's Guide*. Temple, Texas.

Winchell, M., Srinivasan, R., Di Luzio, M., & Arnold, J. (2013). *ArcSWAT Interface for SWAT2012 User's Guide*. Texas.

Wischmeier, W. H., & Smith, D. D. (1978). *Predicting Rainfall Erosin Losses - A Guide to Conservation Planning*. *U.S. Department of Agriculture*. U.S. Department of Agriculture.

Xie, H., Chen, L., & Shen, Z. (2015). Assessment of Agricultural Best Management Practices Using Models: Current Issues and Future Perspectives. *Water*, *7*(3), 1088–1108. doi:10.3390/w7031088

Yagbasan, O., & Yazicigil, H. (2012). Assessing the impact of climate change on Mogan and Eymir Lakes' levels in Central Turkey. *Environmental Earth Sciences*, *66*(1), 83–96. doi:10.1007/s12665-011-1209-3

Yağbasan, Ö., & Yazıcıgil, H. (2009). Sustainable management of Mogan and Eymir Lakes in Central Turkey. *Environmental Geology*, *56*(6), 1029–1040.

Yang, J., Reichert, P., Abbaspour, K. C., Xia, J., & Yang, H. (2008). Comparing uncertainty analysis techniques for a SWAT application to the Chaohe Basin in China. *Journal of Hydrology*, *358*(1-2), 1–23. doi:10.1016/j.jhydrol.2008.05.012

Yang, Y. (1997). *Evaluating Agricultural Non-Point Source Pollution Using the Soil and Water Assessment Tool (SWAT)*. The University of New Brunswick.

Yang, Y., Onishi, T., & Hiramatsu, K. (2014). Improving the Performance of Temperature Index Snowmelt Model of SWAT by using MODIS Land Surface Temperature Data. *The Scientific World Journal*, *2014*. doi:10.1155/2014/823424

Yesuf, H. M., Assen, M., Alamirew, T., & Melesse, A. M. (2015). Modeling of sediment yield in Maybar gauged watershed using SWAT, northeast Ethiopia. *Catena*, *127*, 191–205. doi:10.1016/j.catena.2014.12.032

Young, F. A., Onstad, C. A., Bosch, D. D., & Anderson, W. P. (1989). AGNPS: A nonpoint-source pollution model for evaluating agricultural watersheds. *Journal of Soil and Water Conservation*, *44*, 168–173. Retrieved from http://www.jswconline.org/content/44/2/168.abstract?sid=75063e10-8665-4f00-ad9d-43731c694e80

Yuan, Y. (2010). Problems and Prospects of Swat Model Application on an Arid / Semiarid Watershed in Arizona.

Zhai, X., Zhang, Y., Wang, X., Xia, J., & Liang, T. (2014). Non-point source pollution modelling using Soil and Water Assessment Tool and its parameter sensitivity analysis in Xin'anjiang catchment, China. *Hydrological Processes*, *28*(February 2013), 1627–1640. doi:10.1002/hyp.9688

Zhang, P., Liu, R., Bao, Y., Wang, J., Yu, W., & Shen, Z. (2014). Uncertainty of SWAT model at different DEM resolutions in a large mountainous watershed. *Water Research*, *53*, 132–144. doi:10.1016/j.watres.2014.01.018

APPENDIX A

SWAT MODEL CONSTRUCTION STEPS

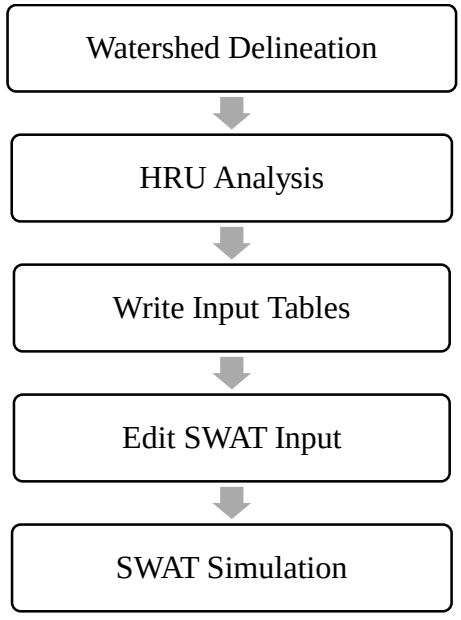

Figure 55. Swat Model Construction Steps

Watershed Delineation

Through Watershed Delineation tool subbasins are delineated via an automatic procedure according to the Digital Elevation Model data provided by the user. The parameters specified by the user determine the size and the number of subbasins generated. Furthermore, it is possible to carry out stream definition by importing pre-defined streams and watersheds (Winchell et al., 2010).

Watershed Delineation tool consists of five sections; DEM Setup, Stream Definition, Outlet and Inlet Definition, Watershed Outlet(s) Selection and Definition, and Calculation of Subbasin Parameters (Srinivasan, 2014). The sections in the Watershed Delineator menu are shown schematically in Figure 56.

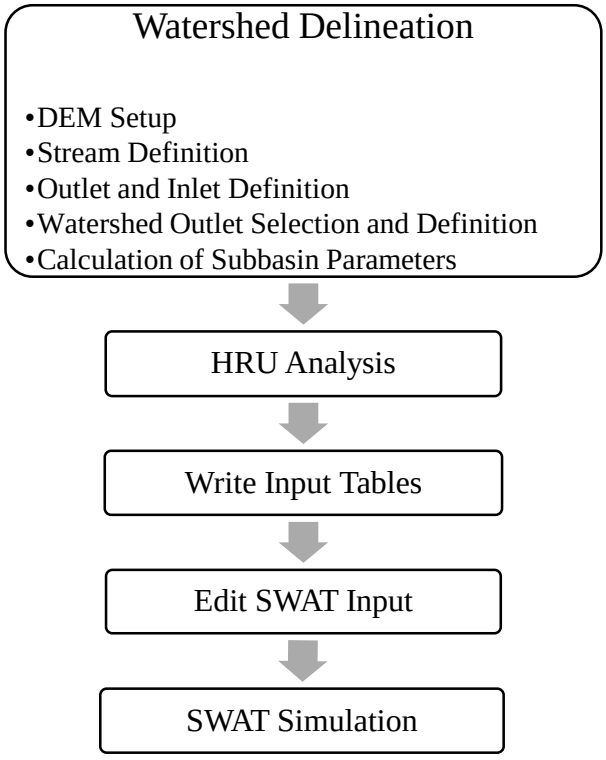

Figure 56. SWAT model construction steps: Watershed Delineation

Input DEM must be in ESRI grid format. If the pre-defined streams network is to be imported, the file can be in ArcView shapefile or geodatabase feature class (PolyLine) format (Winchell et al., 2010).

As it was mentioned before DEM of Lake Mogan watershed used in this thesis study was generated within the scope of the project carried out by Alp et al., (2014). The spatial reference information about the DEM (Figure 8) is given in Table 47. After DEM was loaded in the DEM Setup section of Watershed Delineation tool, DEM properties; vertical and horizontal units, were defined. The Z unit of DEM was edited as meter. In DEM Setup section there are two other steps namely mask and burn-in which are optional. The first option, mask, allows user to specify the watershed area of interest. Via burn-in option, on the other hand, the stream network can be superimposed onto the DEM (Srinivasan, 2014). If the location of the stream network cannot be estimated precisely since the DEM does not provide sufficient detail, burn-in option can be used to deal with this problem. In this study, the mask option was not utilized but the stream network was burned in.

Table 47. Lake Mogan watershed DEM: spatial reference information

Spatial Reference	WGS_1984_UTM_Zone_36N
Linear unit	Meter (1.000000)
Angular unit	Degree (0.0174532925199433299)
False Easting	500000
False Northing	0
Central Meridian	33
Scale Factor	0.9996
Latitude of Origin	0
Datum	D_WGS_1984

After DEM Setup was completed, the stream definition through which the stream network and subbasin outlets are defined was carried out by using the threshold method. Firstly, the Flow Direction and Accumulation was calculated. In the threshold method the model provides a minimum and maximum subbasin area, and suggests a threshold area. The threshold area determines the detail of the stream network and the size and number of subbasins (Winchell et al., 2010). In this study the minimum and maximum subbasin area was estimated as 544 and 108886 hectares respectively by the model. The threshold area was selected as 600 hectares in order to obtain a detailed and a more representative stream network.

The next section in the Watershed Delineation tool is the Outlet and Inlet Definition. In this section the subbasin outlets can be edited manually. New subbasin outlets can be added, if required, and unwanted outlets can be deleted. Moreover, inlets and point sources can be defined. Inlets represent either a point-source discharge or the inlets of drainage into the watershed from an upstream area (Srinivasan, 2014). In this study, one inlet was defined at the outlet of Çölova stream and; therefore, the upstream of Çölova stream is not directly modeled by SWAT. The reason is that the streamflow is really low in Çölova and so the model does not simulate the streamflow well at this outlet. Therefore, discharge data records and available water quality data; i.e. NO_3 and NO_2, at this inlet point were provided to the model. The location of the inlet can be seen in Figure 57. In addition, 'Add point source to each basin' option was selected since it is not possible to define a point source in the subsequent steps of the model construction. The values for water, sediment, and nutrient inputs of added point sources are zero by default. However, the user has the option to define the inputs later on. In this way, the user is able to create scenarios to test the impacts of any point

source located within any subbasins of the watershed. However, within the scope of this study no point source input definition was done since there is no available information about the point sources found in Lake Mogan watershed.

After Outlet and Inlet Definition was completed, the whole watershed outlet was defined. This step is required to define the boundary of the main watershed (Srinivasan, 2014). The location of the whole watershed outlet is indicated in Figure 57. After the whole watershed outlet definition is completed, the watershed can be delineated.

The last step in watershed delineator is the 'Calculation of Subbasin Parameters'. With this function basic watershed characteristics from DEM are estimated. Moreover, definition of the reservoirs found in the watershed is carried out in the section. If there are natural/artificial lakes or reservoirs in watershed, they should be added in this step. Within the boundaries of Lake Mogan watershed there are two natural lakes namely Lake Mogan and Lake Eymir. Therefore, two reservoirs were added to the watershed. The location of the reservoirs; the boundary of the watershed, streams, and subbasins obtained after watershed delineation is shown in Figure 57.

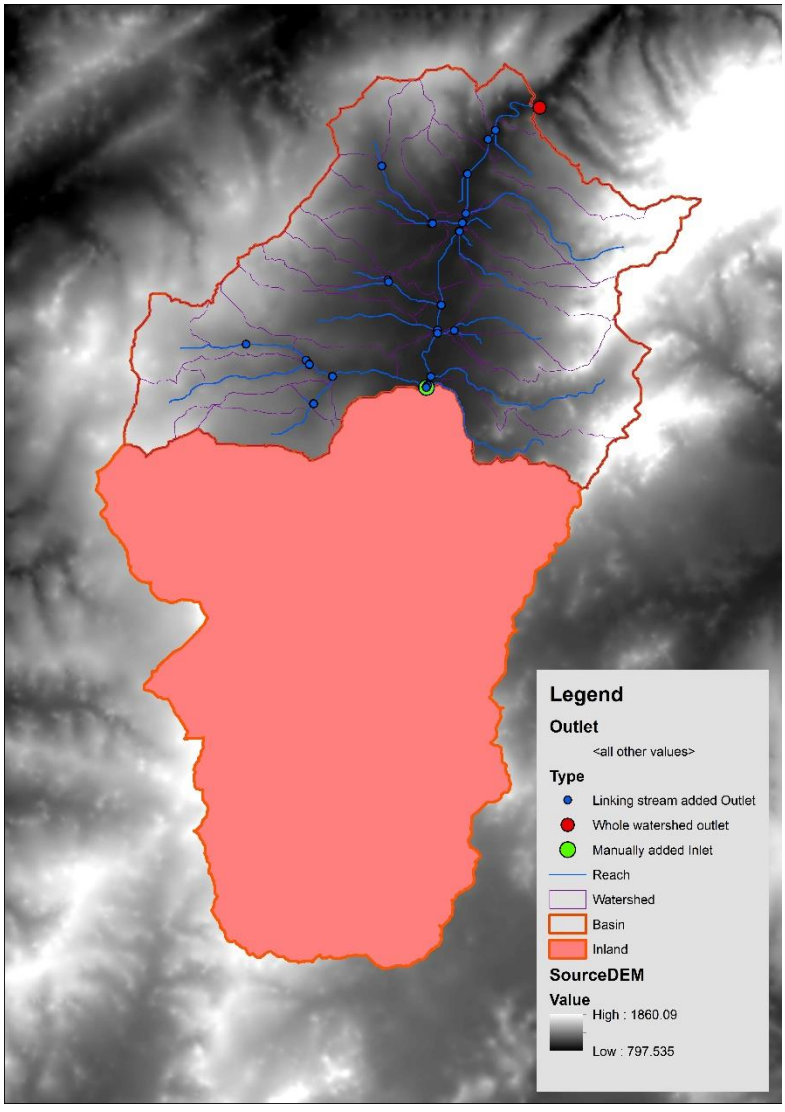

Figure 57. Location of the inlet and whole watershed outlet

Lastly, topographic reports can be viewed under the Watershed Delineator menu. In this report the area and percentage wise distribution of land surface elevations is provided. The statistics of the elevation report for Lake Mogan watershed is given in Table 48.

Table 48. Elevation report statistics of Lake Mogan watershed

Min. Elevation (m)	964
Max. Elevation (m)	1704
Mean. Elevation (m)	1127.35
Std. Deviation (m)	116.53

HRU Analysis

HRU Analysis menu on the ArcSWAT Toolbar allows the characterization of land use, soil, and slope for a watershed (Winchell et al., 2010). There are three options in the HRU Analysis menu: Land use, Soil and Slope Definition, HRU Definition and HRU Analysis Reports (see Figure 58).

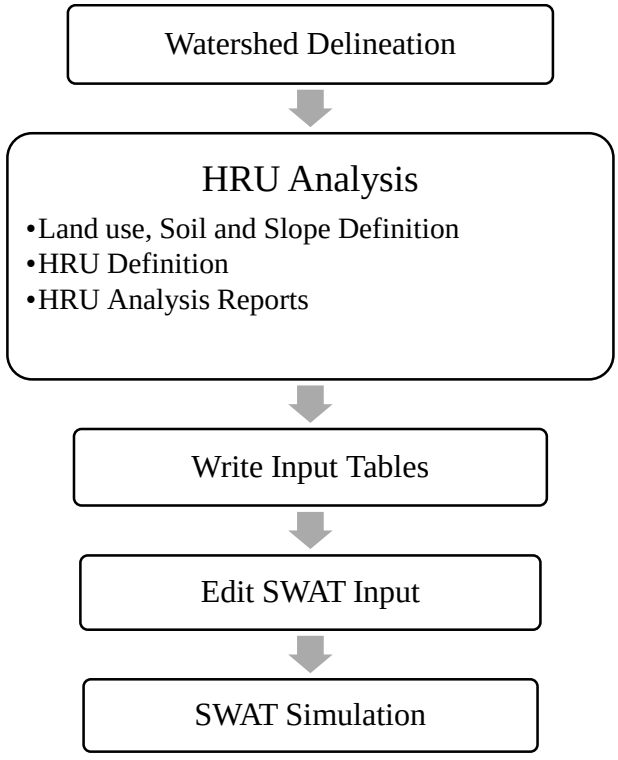

Figure 58. SWAT model construction steps: HRU Analysis

The first option under HRU Analysis menu is Land Use/Soils/Slope Definition. Via this option land use and soil datasets are loaded into the model. Then, the land use/soil/slope class combinations and distributions for the watershed and the subbasins are determined. Land use and soil data can be in either shape or grid format (Srinivasan, 2014). The important thing is that the projections of the datasets must be the same with the DEM used in the watershed projection.

There are three steps in Land Use/Soils/Slope Definition option. The first step is the definition of land use data. After the land use data is loaded into the model, land use classification is carried out. As it was mentioned in Section 3.1.3 nine land use classes were determined in Lake Mogan watershed. These classes are water, forest,

agriculture, fallowing land, road, settlement, mine site, rangeland and bare land. SWAT land use classification table is given in Table 49. The first column includes the unique values in the Grid Field chosen (Srinivasan, 2014) which was chosen as 'Value' in this study. The second column shows the area of each land use class. The last column indicates the land use names in the SWAT database corresponding to each index value. In the last step the land use map was reclassified by clicking on the 'Reclassify' button.

Table 49. SWAT Land Use Classification Table

Value	Area (%)	LandUseSwat
1	1.88	WATR
2	1.64	FRST
3	31.88	AGRL
4	2.95	UTRN
5	17.08	URBN
6	0.03	OAK
7	8.24	AGRR
8	33.02	PAST
9	3.28	RNGE

The next step is the definition of soil data. After the soil file was loaded into the map, the field used as the index to define different soil types was selected as 'Value', and SWAT Soil Classification Table was created automatically. The soil map grid has to be linked to a database. There are two soil database options as ArcSWAT STATSGO and ArcSWAT SSURGO, or UserSoil. Since the available databases within SWAT are valid for United States, the user soil table was created specifically for this study. Detailed information about the soil analysis for Lake Mogan watershed is given in Section 3.1.4, and the user soil table was created accordingly. Then, the new soil types was added to the default user soil table found in the SWAT database. SWAT soil classification table is shown in Table 50. The third column in the table was filled through a look-up table (in .txt or .dbf format). As it can be seen from the table there are forty nine different soil types but not all of them do have area value. The reason is that the outlet of Çölova stream outlet is selected as inlet and so the upstream part of this stream is not modeled. Finally, the soils grid was reclassified using the Reclassify button.

Table 50. SWAT Soil Classification Table

Value	Area (%)	Name	Value	Area (%)	Name
0	4.48	Mogan 1	25	3.34	Mogan 26
1	3.95	Mogan 2	26	6.84	Mogan 27
2	2.55	Mogan 3	27	7.52	Mogan 28
3	4.51	Mogan 4	28	1.02	Mogan 29
4	1.71	Mogan 5	29	5.84	Mogan 30
5	4.26	Mogan 6	30	3.91	Mogan 31
6	5.92	Mogan 7	31	-	Mogan 32
7	3.51	Mogan 8	32	-	Mogan 33
8	3.08	Mogan 9	33	-	Mogan 34
9	2.72	Mogan 10	34	-	Mogan 35
10	2.16	Mogan 11	35	-	Mogan 36
11	3.34	Mogan 12	36	-	Mogan 37
12	3.50	Mogan 13	37	-	Mogan 38
13	0.23	Mogan 14	38	-	Mogan 39
14	-	Mogan 15	39	-	Mogan 40
15	4.98	Mogan 16	40	-	Mogan 41
16	4.79	Mogan 17	41	-	Mogan 42
17	1.34	Mogan 18	42	-	Mogan 43
18	0.00	Mogan 19	43	-	Mogan 44
19	2.71	Mogan 20	44	-	Mogan 45
20	1.89	Mogan 21	45	-	Mogan 46
21	3.56	Mogan 22	46	-	Mogan 47
22	3.07	Mogan 23	47	-	Mogan 48
23	1.29	Mogan 24	48	-	Mogan 49
24	1.98	Mogan 25			

The last step in Land Use/Soils/Slope Definition option is the slope classification. In this step, HRUs are divided according to slope classes together with land use and soils. There are two options for slope discretization as 'Single Slope' and 'Multiple Slope'. If the Single Slope option is selected, then the mean value of slope will be used for the whole watershed. Multiple Slope option, on the other hand, allows the classification of slope into several levels (Srinivasan, 2014). In this study the slope was divided into five classes. SWAT slope classification table is shown in Table 51**.** In order to add the classified soil layer to the map, Reclassify button was used.

Table 51. SWAT Soil Classification Table

Class	Lower Limit (%)	Upper Limit (%)
1	0	1
2	1	3
3	3	5
4	5	10
5	10	9999

After the land use, soil, and slope classification were completed, all these three layers were overlaid by clicking the overlay button.

The next step after Land Use/Soils/Slope Definition is 'HRU Definition'. In this option the user specifies the criteria used in determining the HRU distribution. There are two options to complete the HRU distribution. The user can assign a single HRU to each subbasin by selecting the 'Dominant Land Use, Soils, Slope' option. On the other hand, it is possible to define multiple HRUs in a subbasin by defining the land use, soil class, and soil class percentage (or area) thresholds. The first threshold is 'Land use percentage (%) over subbasin area' which eliminates the minor land uses in each subbasin. The second threshold 'Soil class percentage (%) over land use area' controls the elimination of the minor soils within the land use area. The last threshold 'Slope class percentage (%) over soil area' is used to eliminate the minor slope classes. The threshold levels are up to the modeler's goals. The default values for the thresholds are 20%, 10%, and 20% for land use, soil, and slope respectively (Winchell et al., 2010). In this study, the threshold levels were selected as 5%, 5%, and 10% respectively. According to 'Final HRU Distribution' report created after the HRU Definition was completed, the number of HRUs generated is 1163 and the number of subbasins is 44.

Write Input Tables for SWAT

'Write Input Tables' menu is the next menu after 'HRU Analysis' (see Figure 59). After HRU distribution is completed, weather data can be imported to the model via the first command in 'Write Input Tables' menu. Using the second command 'Write SWAT Input Tables', all the input data files are generated.

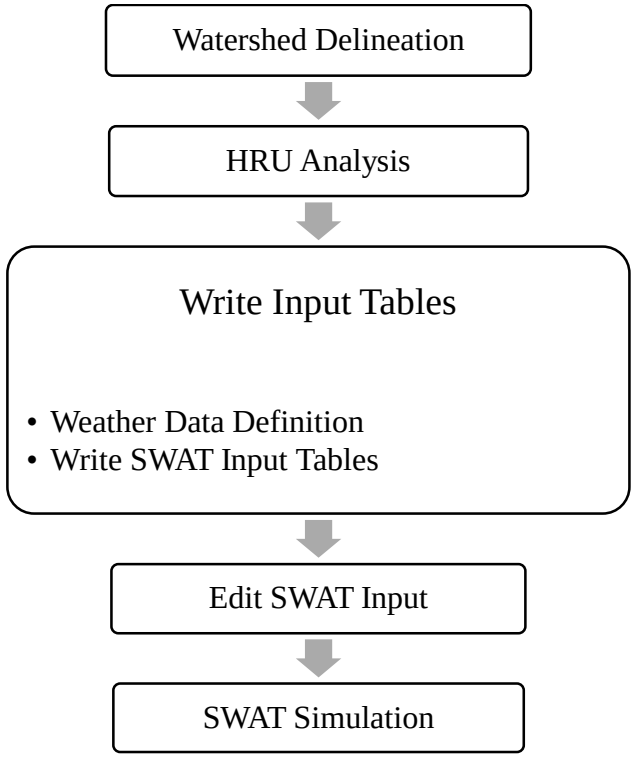

Figure 59. SWAT model construction steps: Write Input Tables

After HRU distribution is completed, weather data can be imported to the model via the first command in 'Write Input Tables' menu. The required weather data by SWAT are daily precipitation, maximum/minimum air temperature, solar radiation, wind speed, and relative humidity. However, the required inputs change according to the evapotranspiration method used in the model as explained in Section 2.3.1. If the observed data for the mentioned parameters is not available, they can be generated with SWAT's weather generator. The weather generator model WXGEN in SWAT is used to produce climatic data or to fill the gaps in the measured data (Neitsch et al., 2009). The weather generator input file includes the statistical data required to produce representative daily climate data for the subbasins (Arnold et al., 2012a).

The weather stations found within the SWAT database are valid for United States. Therefore, in order to introduce the weather stations outside the United States to the model and to create the user weather station files for SWAT, there is an Excel macro called 'WGNmaker4'. This macro can be downloaded from SWAT's website (TAMU, 2016). Microsoft Excel is needed to run the macro. The input files required to run the Excel macro are given in Table 52. In addition to the data given in the Table

52, the station names, latitude, longitude, and elevation of weather stations have to be introduced. If the observed dew point data is not available, it can be estimated via the program provided by the SWAT website. Furthermore, maximum half-hour rainfall is not a usual weather input file required to run SWAT, but this file is needed for the weather generator. The required format for the input files can be found in the pdf file called 'wgen-excel' provided within the excel macro zip file downloaded from the SWAT website.

Table 52. WGNmaker4: Required input files

Data Type	**Units**
Rainfall	millimeters
Temperature	Degrees Celsius
Solar Radiation	$MJ/m^2/day$
Wind Speed	m/s
Dew Point	Degrees Celsius
Max. ½ Hour Rainfall	millimeters

The output files will be generated as the number of weather stations found in the study area. For instance, there are two meteorological stations located in Lake Mogan watershed as Gölbaşı and Haymana (Section 3.1.1). Therefore, after the excel macro was run, two output files which involve all of the calculated statistics were obtained. The description about the variables in the weather generator input file is given in Table 53. The output file involving the statistical data shown in Table 53 was imported to SWAT by updating the default WGEN-user table located in the model's database.

To load the weather data into the model, the 'Weather Stations' option is selected from the 'Write Input Tables' menu. Then, the 'Weather Data Definition' dialog is showed. This dialog consists of six tabs namely; Weather Generator Data, Rainfall Data, Temperature Data, Solar Radiation Data, Wind Speed Data and Relative Humidity Data. Without setting the Weather Generator Data, it is not possible to proceed to define other weather input data. From the Weather Generator Data tab, monthly weather database was selected as 'WGEN-user' which was previously imported to the database. When measured weather data are to be used, the location of the rain gages, the temperature gages etc. have to be provided (Winchell et al., 2010). In the subsequent tabs the gage location tables are selected. The gage location tables contain the name of the individual weather data files, and they have to be located under the

same folder as the weather data files. These tables can be in either dBASE or text format. In this study, the gage location tables were prepared in text format. The table prepared for rain gages is shown in Table 54. Since the format for the remaining location tables is nearly the same, they are not indicated. In the table, pGolbasi and pHayman are the name of the files including the precipitation data for Gölbaşı and Haymana meteorological stations, respectively. In Table 55, the text table format is shown. The data in this table belongs to pGolbasi precipitation file. The first row represents the starting date of data. Please note that not whole recorded data is provided in Table 55.

Table 53. Description of the variables in the weather generator input file

Variable name	**Definition**
Station	Weather station name
WLATITUDE	Latitude of weather station used to create statistical parameters (degrees).
WLONGITUDE	Longitude of weather station (degrees).
WELEV	Elevation of weather station (m).
RAIN_YRS	The number of years of maximum monthly 0.5 h rainfall data used to define values for RAIN_HHMX(1) - RAIN_HHMX(12).
TMPMX (mon)	Average or mean daily maximum air temperature for month (ºC).
TMPMN(mon)	Average or mean daily minimum air temperature for month (ºC).
TMPSTDMX (mon)	Standard deviation for daily maximum air temperature in month (ºC).
TMPSTDMN (mon)	Standard deviation for daily minimum air temperature in month (ºC).
PCPMM (mon)	Average or mean total monthly precipitation (mm H_2O).
PCPSTD (mon)	Standard deviation for daily precipitation in month (mm H_2O/day).
PCPSKW (mon)	Skew coefficient for daily precipitation in month.
PR_W (1,mon)	Probability of a wet day following a dry day in the month.
PR_W (2,mon)	Probability of a wet day following a wet day in the month.
PCPD (mon)	Average number of days of precipitation in month.
RAINHHMX (mon)	Maximum 0.5 hour rainfall in entire period of record for month (mm H_2O).
SOLARAV(mon)	Average daily solar radiation for month (MJ/m^2/day)
DEWPT (mon)	Average daily dew point temperature for each month (ºC) or relative humidity (fraction) can be input.
WNDAV (mon)	Average daily wind speed in month (m/s).

Table 54. Precipitation gage location table

ID	NAME	LAT	LONG	ELEVATION
1	pGolbasi	39.802	32.842	1105.000
2	pHaymana	39.612	32.669	1075.000

Table 55. Daily precipitation data table for Gölbaşı meteorological station

20070101
0
0
0
0.8
4.2
0.6
0
0
0

After the weather data definition is completed, writing the input tables is the next step. In order to generate the input files 'Write SWAT Database Tables' option is selected under the 'Write Input Tables' menu.

Editing SWAT Input

'Edit SWAT Input' menu allows user to adjust the default SWAT databases. Via this menu it is possible to make edits on point source discharges, inlet discharges, reservoirs, and subbasin and watershed data (see Figure 60).

Within the scope of this study no point source discharge was introduced to the model. However, there is an inlet discharge since Çölova stream outlet was selected as inlet during HRU analysis. In order to edit inlet discharge database, 'Inlet Discharges' option was selected from the 'Edit SWAT Input'. When this option was selected, the subbasin number of Çölova stream was displayed. The inlet discharge data can be introduced to the model by one of the following formats; constant daily loadings, average annual loadings, average monthly loadings, and daily loadings. In this study, the inlet input data was loaded to the model as monthly records. The monthly flow data was obtained from METU Limnology Labarotory, and the pollutant loadings (kg/day); i.e. NO_2 and NO_3, were calculated by multiplying the flow rates with the concentration of the pollutants at the corresponding months. The input data have to be

provided to the model in .dbf format. Therefore, the table was prepared in Microsoft Excel, then converted to .dbf format.

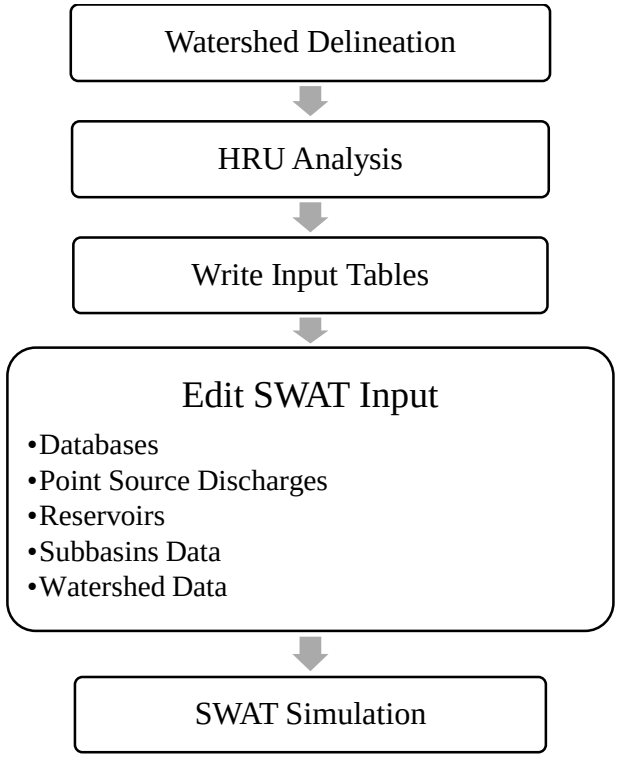

Figure 60. SWAT model construction steps: Edit SWAT Input

In SWAT, there is no distinction between naturally-occurring and man-made structures. Therefore, **t**he natural lakes within the study area have to be introduced to the model as reservoirs. The water balance for a reservoir is calculated with the following equation:

$$V = V_{stored} + V_{flowin} - V_{flowout} + V_{pcp} - V_{evap} - V_{seep}$$

where V is the volume of water in the impoundment at the end of the day (m^3 H_2O), V_{stored} is the volume of water stored in the water body at the beginning of the day (m^3 H_2O), V_{flowin} is the volume of water entering the water body during the day (m^3 H_2O), $V_{flowout}$ is the volume of water flowing out of the water body during the day (m^3 H_2O), V_{pcp} is the volume of water removed from the water body by evaporation during the day (m^3 H_2O), and V_{seep} is the volume of water lost from the water body by seepage (m^3 H_2O)."

Two reservoirs, namely Lake Mogan and Lake Eymir, were defined in this study. The variables in the reservoir input file and their descriptions is given in Table 56.

Table 56. The variables in the reservoir input file (Arnold et al., 2012a)

Variable Name	Definition
MORES	Month the reservoir became operational
IYRES	Year the reservoir became operational
RES_ESA	Reservoir surface area when the reservoir is filled to the emergency spillway (ha).
RES_EVOL	Volume of water needed to fill the reservoir to the principal spillway (10^4 m^3).
RES_PSA	Reservoir surface area when the reservoir is filled to the principal spillway (ha).
RES_PVOL	Volume of water needed to fill the reservoir to the principal spillway (10^4 m^3).
RES_VOL	Initial reservoir volume.
RES_SED	Initial sediment concentration in the reservoir (mg/L).
RES_NSED	Equilibrium sediment concentration in the reservoir (mg/L).
RES_D50	Median particle diameter of sediment (μ).
RES_K	Hydraulic conductivity of the reservoir bottom (mm/hr).
EVRSV	Lake evaporation coefficient. Default = 0.6
IRESCO	Outflow simulation code
RES_RR	Average daily principal spillway release rate (m^3/s).
IFLOD1R	Beginning month of non-flood season
IFLOD2R	Ending month of non-flood season.
NDTARGR	Number of days to reach target storage from current reservoir storage
OFLOWMN_FPS	Minimum reservoir outflow as a fraction of the principal spillway volume (0-1).
STARG_FPS	Target volume as a fraction of the principal spillway volume. This input is needed if ISRECO = 2. Default = 1.0

Although Lake Mogan and Lake Eymir are natural lakes, their water levels are controlled by water control structures to prevent the flood damages in the watershed. For instance, Lake Mogan water control structure is composed of two vertical sluice gates of 3.25 m width. The sill elevation of this structure is 971.00 meters (Bozkurt, 2013). In addition, there is a lined canal between the Mogan and Eymir lakes, and the capacity of this canal is around 7 – 10 m^3/s. Similarly, there is a water control structure at the exit of Lake Eymir. The structure consists of two vertical sluice gates with 1 m wide, and the sill elevation is 966.65 m. Furthermore, Bozkurt (2013) stated that the storage capacity of Lake Eymir is lower compared to Lake Mogan. Therefore, the extra flood volume conveyed through the lined canal should not be accumulated. For

this reason, it was mentioned that what comes to Lake Eymir via this canal has to be discharged. The basic characteristics of Mogan and Eymir lakes including the minimum, normal, and maximum water level, volume, and the surface area is given in Table 57 and Table 58 respectively. According to all these mentioned information, the variables in reservoir input file in SWAT was edited. However, not all of the required information is available for the whole variables. Thus, some of the variables given in Table 56 were left with their default values.

Table 57. Basic characteristics of Lake Mogan (Bozkurt, 2013)

	Minimum	**Normal**	**Maximum**
Water Level (m)	971	972	973.25
Volume (hm^3)	6.2	11.63	20.19
Area (km^2)	4.77	5.43	7.72

Table 58. Basic characteristics of Lake Eymir (Bozkurt, 2013)

	Minimum	**Normal**	**Maximum**
Water Level (m)	967	968.5	969.5
Volume (hm^3)	2.16	3.88	5.2
Area (km^2)	1.05	1.25	1.34

The next command under 'Edit SWAT Input' menu is 'Subbasins Data'. When this command is selected, the dialog containing the list of SWAT input tables and the list of subbasins, land uses, soil types, and slope levels will show up. The tables listed correspond to the file extensions of the SWAT ASCII files required to run the SWAT model (Winchell et al., 2010). The user can select a specific subbasin/land use/soil/slope combination in order to make edits. The list of SWAT input tables is given with their descriptions in Table 59. The definition of the parameters included in each of these input files can be found in the *SWAT Input/Output Documentation Version 2012* (Arnold et al., 2012a). In order to introduce the agricultural activities carried out within the study area to the model, 'Management (.Mgt)' input file should be modified. If this file is selected, a dialog displaying the management data editor will appear. There are two tabs in this dialog; General Parameters and Operations. In the first tab, the general parameters regarding the Initial Plant Growth, General Management, Urban Management, Irrigation Management, and Tile Drain Management can be adjusted. The second tab allows the user to schedule the management operations on the current HRU. The edits can be extended to other HRUs.

The operations can be scheduled either by date or by heat units. Scheduled management operations simulated by SWAT are shown in Table 60.

Table 59. List of SWAT input tables to edit

SWAT Input Table	Description
Soils (.Sol)	to edit soil parameters
Weather (.Wgn)	to edit weather generator data
Subbasin (.Sub)	to edit general subbasin data
HRU (.Hru)	to edit general HRU data
Routing (.Rte)	to edit the main channel input file
Groundwater (.Gw)	to edit the groundwater input file
Water Use (.Wus)	to edit the consumptive water use input data
Management (.Mgt)	to edit the management file input data
Soil Chemical (.Chm)	to edit the soil chemical data
Pond (.Pnd)	to edit pond data
Stream Water Quality (.Swq)	to edit stream water quality input data
Septic (.Sep)	to edit septic input data file
Operations (.Ops)	to edit operations input data file

Table 60. List of scheduled management operations simulated by SWAT

Scheduled Management Operations
Planting/Beginning of Growing Season
Irrigation Operation
Fertilizer Application
Pesticide Application
Harvest and Kill Operation
Tillage Operation
Harvest Only Operation
Kill/End of Growing Season
Grazing Operation
Auto Irrigation Initialization
Auto Fertilization Initialization
Street Sweeping Operation
Release/Impound
Continuous Fertilization
Continuous Pesticide
End of Year Rotation Flag

In the context of this study simulations were performed between 2007 and 2010. In 2007, wheat was planted in agricultural lands in Lake Mogan watershed. Therefore, 'Initial Land Cover' was selected as winter wheat from the General Parameters tab. Other parameters were left with their default values. For detailed information about the parameters found in General Parameters tab, please refer to *Soil and Water*

Assessment Tool Input/Output Documentation Version 2012 (Arnold et al., 2012a). After defining the initial land cover, the management operations carried out in agricultural lands were scheduled. When the Operation tab is selected, the default management operations performed on the selected land cover will be displayed. The default operations were modified according to the operations carried out in Lake Mogan watershed (Section 3.1.5), and they were scheduled by date. The list of operations scheduled is shown in Table 61. In the table, 1, 2, 3, and 4 represent the years 2007, 2008, 2009, and 2010 respectively. In the last column WWHT symbolizes winter wheat.

Table 61. List of management operations scheduled

Year	Month	Day	Operation	Crop
1	2	28	Fertilizer application	-
1	3	30	Fertilizer application	-
1	7	15	Harvest and kill operation	-
2	4	1	Tillage operation	-
2	5	15	Tillage operation	-
2	6	21	Tillage operation	-
2	9	10	Tillage operation	-
2	10	14	Plant/begin. growing season	WWHT
2	10	15	Fertilizer application	-
2	10	15	Fertilizer application	-
3	2	28	Fertilizer application	-
3	3	30	Fertilizer application	-
3	7	15	Harvest and kill operation	-
4	4	1	Tillage operation	-
4	5	15	Tillage operation	-
4	6	21	Tillage operation	-
4	9	10	Tillage operation	-
4	10	14	Plant/begin. growing season	WWHT
4	10	15	Fertilizer application	-
4	10	15	Fertilizer application	-

Planting/beginning of growing season operation initiates the plant growth. The timing of the planting operation, and the type of the land cover to be simulated has to be known to add this operation. Harvest and kill operation, on the other hand, ends plant growth, and leaves the remaining fraction which is not removed from the HRU as yield on the soil surface (Neitsch et al., 2009).

As it was mentioned in Section 3.1.5, there are four types of fertilizers used during wheat cultivation in Lake Mogan watershed. These fertilizers are urea, ammonium

nitrate, ammonium sulfate, and diammonium phosphate. There is a fertilizer database provided with the SWAT model. In this database, the relative fractions of nitrogen and phosphorus pools in the different fertilizers are summarized (Arnold et al., 2012a). Moreover, if the required fertilizer type is not found in the database, it is possible to add a new one by defining the fertilizer parameters. For instance, ammonium sulfate (21-00-00) is not defined in the default SWAT fertilizer database. Therefore, ammonium sulfate was added to the database. The fertilizer parameters are given in Table 62. The values of the parameters for ammonium sulfate definition is shown in Table 63.

Table 62. Fertilizer parameters and their descriptions

Fertilizer Parameter	**Description**
Fertilizer Name	Fertilizer description name.
FERTNM	Name of fertilizer/manure.
FMINN	Fraction of mineral N (NO_3 and NH_4) in fertilizer (kg min-N/kg fertilizer).
FMINP	Fraction of mineral P in fertilizer (kg min-P/kg fertilizer).
FORGN	Fraction of organic N in fertilizer (kg org-N/kg fertilizer).
FORGP	Fraction of organic P in fertilizer (kg org-P/kg fertilizer).
FNH3N	Fraction of mineral N in fertilizer applied as ammonia (kg NH_3-N/ min-N).
BACTPDB	Concentration of persistent bacteria in manure/fertilizer (# cfu/g manure).
BACTLPDB	Concentration of less-persistent bacteria in manure/fertilizer (# cfu/g manure).
BACTFDDB	Bacteria partition coefficient.

Table 63. Ammonium sulfate fertilizer parameter values

Fertilizer Parameter	**Value**
Fertilizer Name	21-00-00
FERTNM	21-00-00
FMINN	0.21
FMINP	0
FORGN	0
FORGP	0
FNH3N	0

Tillage database in SWAT contains various tillage type options. Similar the fertilizer database, the user is able to define a new tillage operation type by describing the required variables. The tillage parameters and the definitions are given in Table 64. In

order to schedule the tillage operations, the user has to provide the timing and the type of the operation. The timing of the tillage operations in Lake Mogan watershed throughout the wheat cultivation can be seen in Table 61. In addition, the duckfoot cultivator is used for the tillage. The tillage parameters for the duckfoot cultivator is shown in Table 65.

Table 64. Tillage parameters and their descriptions

Tillage Parameters	**Description**
Tillage Operation Name	Tillage operation description name
Tillage Name	8-character tillage code
EFTMIX	Mixing efficiency for tillage (fraction)
DEPTIL	Depth of mixing caused by the tillage operation (mm)
RRNS	Random roughness (mm)

Table 65. Duckfoot cultivator tillage parameters

Tillage Parameters	**Value**
Tillage Operation Name	Duckfoot Cultivator
Tillage Name	Duckftc
EFTMIX	0.55
DEPTIL	150
RRNS	15

The last command under 'Edit SWAT Input' menu is 'Watershed Data'. This command allows users to adjust the parameters related to three main groups: (i) water balance, surface runoff, and reaches; (ii) nutrients and water quality; (iii) basin-wide management. No parameter modification was performed in this section.

SWAT Simulation Setup

The last menu in ArcSWAT toolbar is 'SWAT Simulation'. This menu contains commands to setup and run a SWAT simulation (see Figure 61).

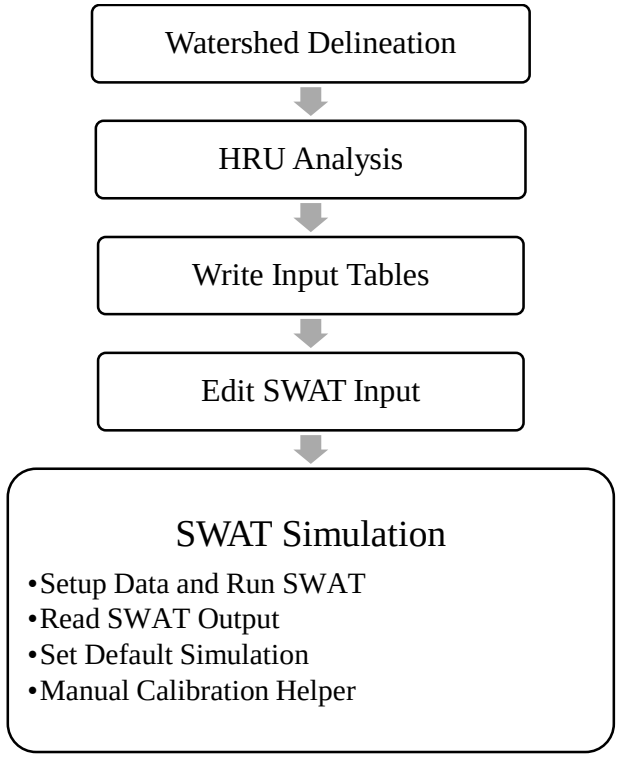

Figure 61. SWAT model construction steps: SWAT Simulation

If the 'Run SWAT' command under 'SWAT Simulation' is selected, SWAT data setup and simulation dialog will be displayed. The simulation period in this study is from 1/1/2007 to 31/12/2010. The simulation period was determined according to the available observed streamflow data so that the calibration is possible. The simulations were performed on a monthly time step. The warm-up period (NYSKIP) was selected as one year. Arnold et al. (2012a) suggested that at least one year warm-up period is used for the simulations covering 5 years or less to make hydrological cycle fully operational. The SWAT simulation commands are summarized in Table 66. After defining the simulation options and commands, the SWAT model was run, and the model outputs were obtained.

Table 66. Summary of commands to set up a SWAT simulation

Period of Simulation	Starting Date: 1/1/2007 Ending Date: 12/31/2010
Rainfall Distribution	Skewed normal
SWAT.exe Version	64-bit, release
Printout Settings	Monthly NYSKIP: 1

APPENDIX B

SWAT-CUP (SWAT Calibration and Uncertainty Procedures)

SWAT-CUP is an interface developed for SWAT. This generic interface enables to link any calibration/uncertainty or sensitivity program to SWAT. SWAT-CUP provides five different optimization procedures to the users, namely PSO, SUFI-2, MCMC, ParaSol, and GLUE. The linkage between SWAT and these procedures is illustrated in Figure 62 schematically. The file exchange between SWAT and the procedures are carried out through text file formats (Abbaspour, 2015).

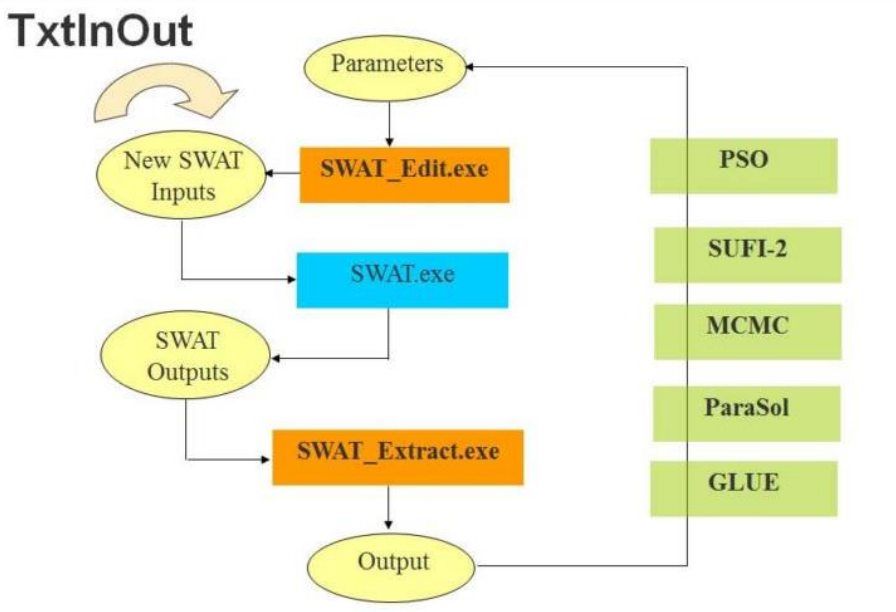

Figure 62. Schematic diagram of the linkage between SWAT-CUP and optimization procedures (Abbaspour, 2015)

The first step to create a SWAT-CUP project is importing the SWAT TxtInOut directory. All of the input and output files which are used and generated by the SWAT2012 model are found in this folder (Winchell et al., 2013). Then, the selected optimization program writes the model parameters to model.in, and SWAT_Edit.exe edits the SWAT text files. The SWAT.exe is run, and then SWAT_Extract.exe extracts the chosen variables from the SWAT output files, and writes the variables to model.out (Rostamian et al., 2008).

Since the SWAT divides the watershed into HRUs, it is possible to define a distributed parameter for each HRU. Therefore, there are large number of input parameters. However, SWAT-CUP provides convenience and flexibility in the calibration process by allowing the parameter aggregation based on the hydrological group, soil texture, land use, and subbasin number (Abbaspour, 2015). The parameter identifiers provided by SWAT-CUP allow the users to adjust parameters based on soil hydrological group, soil texture, land use, subbasin and slope. The parameter identifiers are formulated as shown below:

x__<parname>.<ext>__<hydrogrp>__<soltext>__<landuse>__<subbsn>__<slope>

where

x__ = identifier code to indicate the type of change to be applied to the parameter:

v__ means the existing parameter value is to be replaced by a given value,

a__means a given value is added to the existing parameter value, and

r__means an existing parameter value is multiplied by (1+ a given value).

<parname> = SWAT parameter name

<ext> = SWAT file extension code for the file containing the parameter

< hydrogrp> = (optional) soil hydrological group (‘A’, ‘B’, ‘C’, or ‘D’)

<soltext> = (optional) soil texture as it appears in the header line of SWAT input files

<landuse> = (optional) name of the land use category as it appears in the header line of SWAT input files

<subbsn> = (optional) subbasin number(s) as it appears in the header line of SWAT input files

<slope> = (optional) slope as it appears in the header line of SWAT input files

The identifiers <hydrogrp>, <soltext>, <landuse>, and <subbsn> are optional which means that they can be omitted if the user wants to assign the parameters globally.

As it was mentioned before, the SUFI-2 algorithm was selected as the optimization program in this study. In the SUFI-2 algorithm, the aim is to find the best range for the parameters in concern rather than to find the set of best fit parameters (Abbaspour

et al., 2004). In order to obtain the best range for each parameter, the prediction uncertainties have to bracket most of the measured data, and the prediction uncertainty band has to be as small as possible (Rostamian et al., 2008). Therefore, there are two criteria to confirm the best parameter ranges. Initially, a large parameter uncertainty is assumed, and then this uncertainty is decreased until the two criteria are fulfilled. The first criterion is called the p-factor. The p-factor is the percentage of observed data bracketed by the 95% prediction uncertainty (95PPU). This criteria is met when most of the observations are bracketed by the 95PPU. For instance, it is suggested that the p-factor is larger than 70% for discharge (Abbaspour, 2015). The second one is the r-factor which is defined as the average thickness of the 95PPU band divided by the standard deviation of the measured data. The thickness is the distance between the upper (the 97.5th percentile) and the lower (the 2.5^{th} percentile) parts of the 95PPU (Abbaspour et al., 2007). When the p-factor is 1 and the r-factor is 0, the ideal situation is obtained.

The connection between the SWAT and SUFI2 is shown schematically in Figure 63. In Figure 63, *par_inf.txt* is the text file including the information about the parameters; i.e., the range and the number of parameters, and the number of simulations. *SUFI2_LH_sample.exe* is the executable file generating the Latin hypercube samples (McKay et al., 1979). Latin hypercube sampling is used by the program, and the parameters are sampled from the parameter intervals specified in *par_inf.txt*. The sampled parameters are stored in *par_val.txt* file. *SWAT_Edit.exe* program substitutes the parameters in the SWAT files. The program does not permit modification of the parameters below or above the ranges given in *Absolute_SWAT_Values.txt* file. This file involves nearly all SWAT parameters together with their minimum and maximum ranges. The ranges can be edited by the user, and the missing parameters can be added to the file. *SUFI2-swEdit.def* file includes the starting and ending simulation years. This file is used by the *SWAT_Edit.exe* program. *SWAT.exe* is an executable file which execute the files required to run the model. *SUFI2_extract_rch.exe* extracts the necessary outputs from the SWAT's output.rch file by using the *SUFI2_extract_rch.def*. *SUFI_goal_fn.exe* calculates the objective function. SUFI2 provides ten different objective functions such as Nasch-Sutcliff (NS), mean square error (MSE), and r^2 (Abbaspour et al., 2015). *SUFI2_95ppu.exe* computes the 95% prediction uncertainty (95PPU) band. SUFI2_new_pars.exe calculates the modified

parameters for the next iteration. This process continues until the objective function, the p-factor and the r-factor are satisfied.

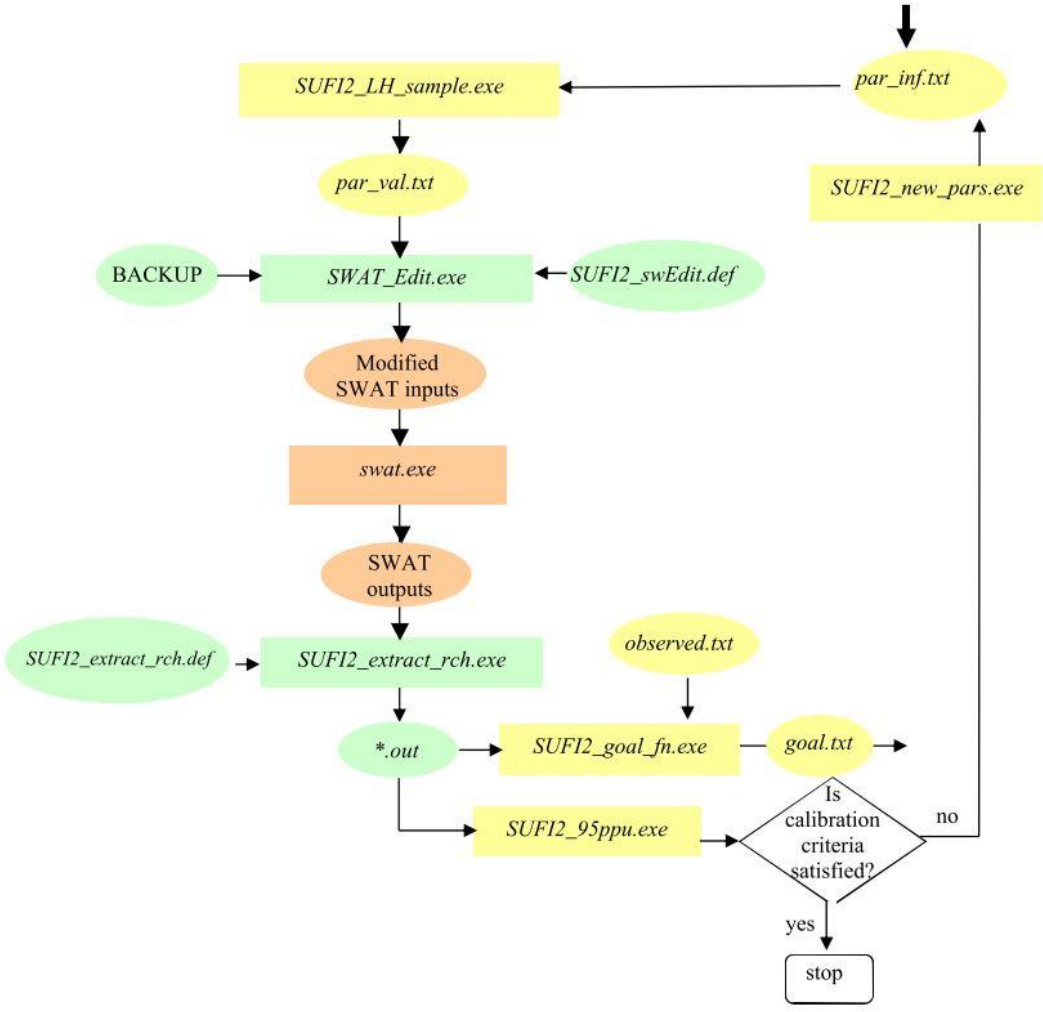

Figure 63. A schematic connection between SWAT and SUFI2 adapted from Abbaspour (2015)

APPENDIX C

MODEL PERFORMANCE EVALUATION BEFORE CALIBRATION

The comparison of observed and simulated streamflow before the model calibration at Yavrucak and Sukesen monitoring stations are given Figure 64 and Figure 65, respectively. As it can be seen from Figure 64, the streamflow values are not consistently over- or under-estimated. Between March 2009 and June 2009 the model underestimates the streamflow at Yavrucak. On the other hand, there is an overestimation between January 2010 and May 2010. Moreover, the model simulates unreal peaks in January and February 2009, and January 2010. Contrary to Yavrucak, the model mostly underestimates the streamflow at Sukesen monitoring station. The most noticeable underestimations are observed at March and April 2009, and between January 2010 and April 2010 (see Figure 65).

The performance evaluation statistics i.e., NS, PBIAS, and R^2 for the simulation carried out before the calibration are given in Table 67. These statistics show that model performance was poor (see Table 7) both at Yavrucak and Sukesen monitoring station with default model parameters. Therefore, the model had to be calibrated to make the observed and simulated streamflow values closer to each other as much as possible.

Table 67. Performance evaluation statistics for the streamflow simulation carried out with default model parameters

	Streamflow Simulation (before calibration)	
	Yavrucak	**Sukesen**
NS	-0.50	0.12
PBIAS	0.33	0.28
R^2	55.2	62.1

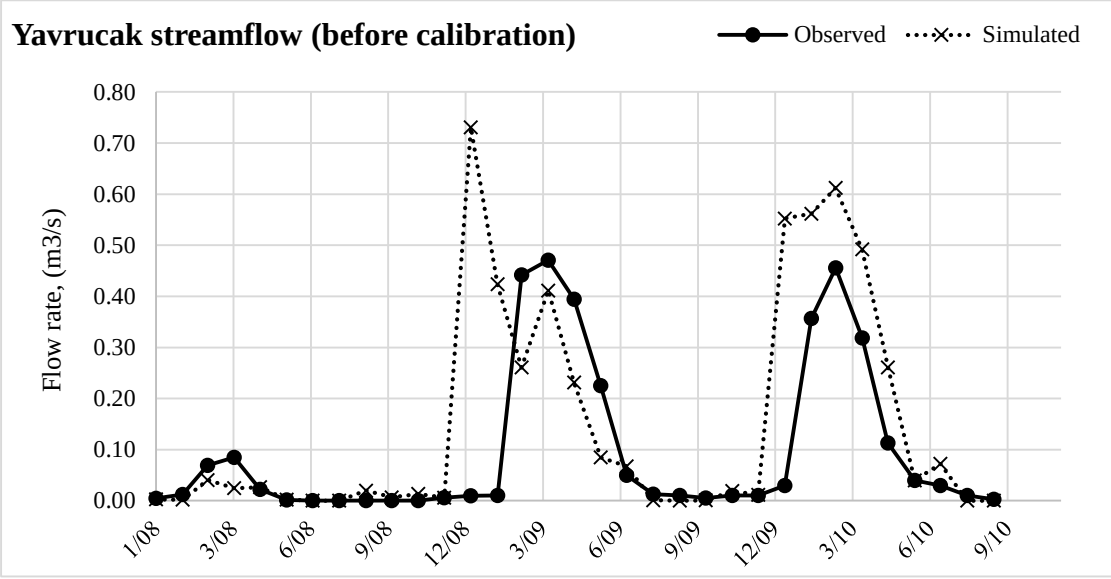

Figure 64. Simulated vs. observed streamflow values before calibration at Yavrucak monitoring station

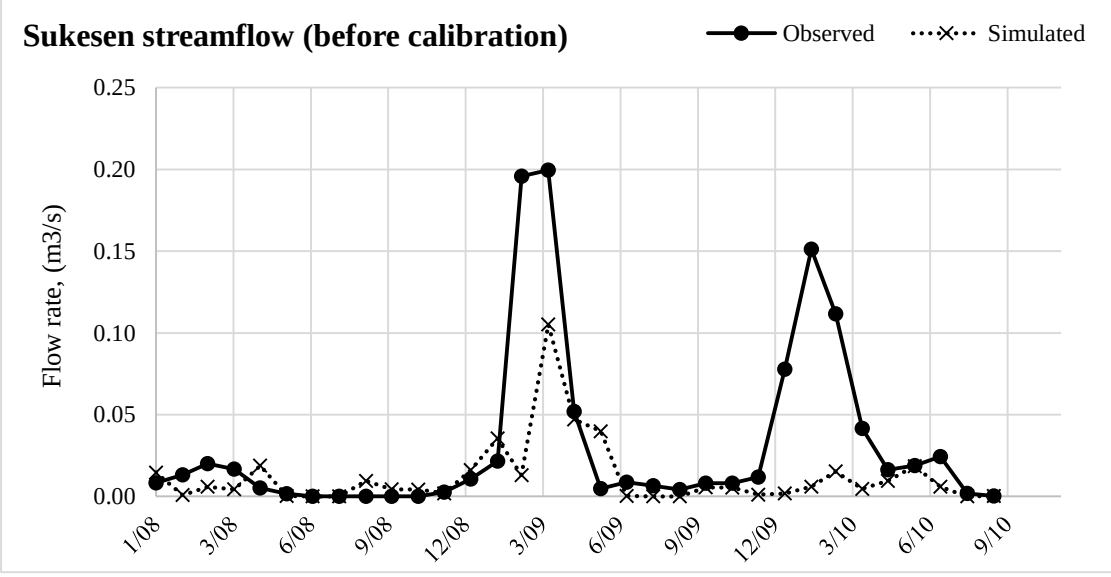

Figure 65. Simulated vs. observed streamflow values before calibration at Sukesen monitoring station

After streamflow was calibrated, sediment calibration was performed (see Section 3.3.4). The observed and simulated sediment loads with default sediment parameters; i.e. before sediment calibration, at Yavrucak and Sukesen monitoring stations are shown in Figure 66 and Figure 67, respectively. At Yavrucak monitoring station, the sediment loads are overestimated except for December 2008. The overestimations are comparably higher in April and May 2009, and April 2010. At Sukesen monitoring station, on the other hand, there is not a consistent over- or underestimation. Sediment

loads observed in March, April and May 2008, and in March and April 2009 are underestimated while the loads in June, August, September 2008, and in April 2010 are overestimated.

The performance evaluation statistics i.e., NS, PBIAS, and R^2 for the sediment simulation carried out before the calibration are given in Table 68. As it can be seen from Table 68, none of performance evaluation statistics are satisfied (see Table 7) unless the model is calibrated for sediment.

Table 68. Performance evaluation statistics for the sediment simulation carried out with default model parameters

	Sediment Simulation (before calibration)	
	Yavrucak	**Sukesen**
NS	-44.1	-0.16
PBIAS	-460.4	71.5
R^2	0.05	0.05

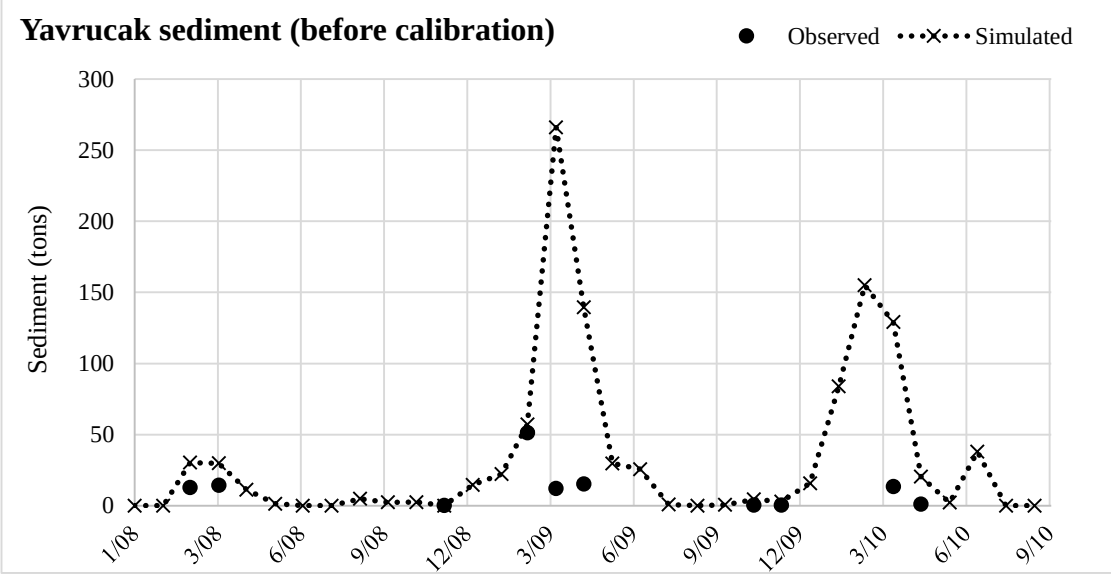

Figure 66. Simulated vs. observed sediment loads before calibration at Yavrucak monitoring station

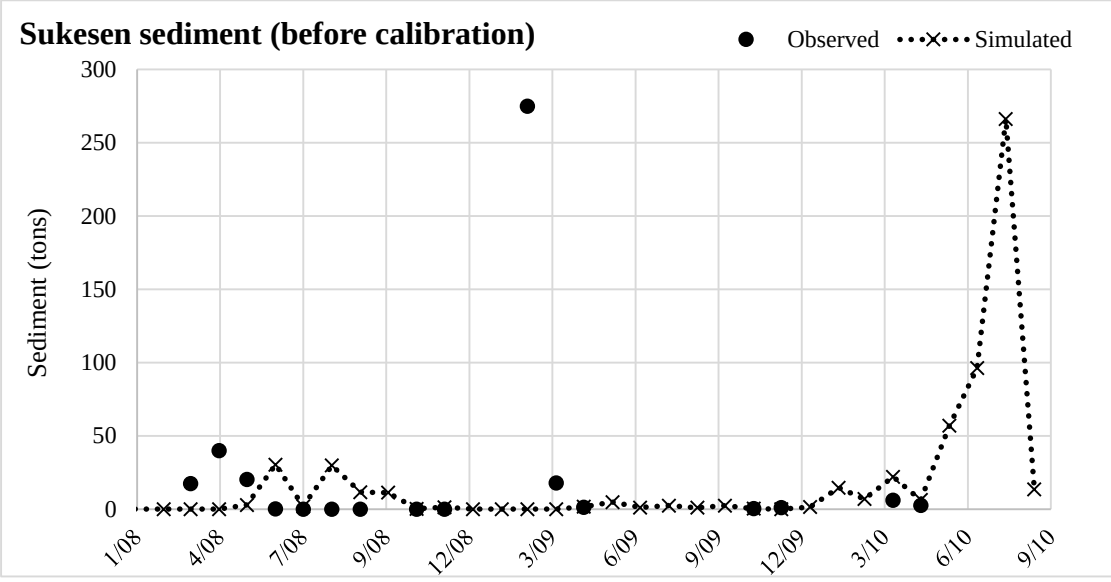

Figure 67. Simulated vs. observed sediment loads before calibration at Sukesen monitoring station

Before water quality calibration, the simulated and observed nitrate (NO_3), total nitrogen (TN) and total phosphorus (TP) loads at Yavrucak monitoring station are shown in Figure 68, Figure 69 and Figure 70, respectively. The loads observed and simulated at Sukesen monitoring station are shown in Figure 71, Figure 72 and Figure 73, respectively. The simulated loads given in these figures were obtained after streamflow and sediment calibration, and before the water quality parameters were calibrated. At Yavrucak monitoring station, NO_3 loads in March and April 2009 are underestimated. In May 2009, and April and May 2010, the model overestimates the NO_3 loads (see Figure 68). As it can be seen from Figure 69, there are only three monthly observed TN loads available between 2008 and 2010 at Yavrucak monitoring station. Therefore, it is hard to comment on total nitrogen simulation. However, it is observed that the available observed loads are underestimated by the model (see Figure 69). Figure 70 illustrates that total phosphorus loads at Yavrucak monitoring station are mostly overestimated. The only underestimation is observed in May 2009. At Sukesen monitoring station, NO_3 loads are mainly underestimated except for May 2010 (see Figure 71). TN loads, on the other hand, are not consistently over- or underestimated. While there is an underestimation in March, April, and December 2008, the nitrate loads are overestimated in May, September and November 2008 (see Figure 72). TP loads are generally overestimated by the model but there are also underestimations in two months; i.e., March 2008 and March 2009 (see Figure 73).

The performance evaluation statistics for NO_3, TN and TP simulations with default water quality parameters at Yavrucak and Sukesen monitoring stations are given in Table 69. The statistics show that the model cannot satisfactorily simulate the water quality processes (see Table 7).

Table 69. Performance evaluation statistics for the water quality simulation carried out with default model parameters

	NO_3 Simulation (before calibration)	
	Yavrucak	**Sukesen**
NS	-0.46	-0.9
PBIAS	56.9	74.2
R^2	0.06	0.06
	TN Simulation (before calibration)	
	Yavrucak	**Sukesen**
NS	-0.71	-0.26
PBIAS	73.7	50.7
R^2	0.96	0.04
	TP Simulation (before calibration)	
	Yavrucak	**Sukesen**
NS	0.21	-1.3
PBIAS	25.7	-75.7
R^2	0.26	0.15

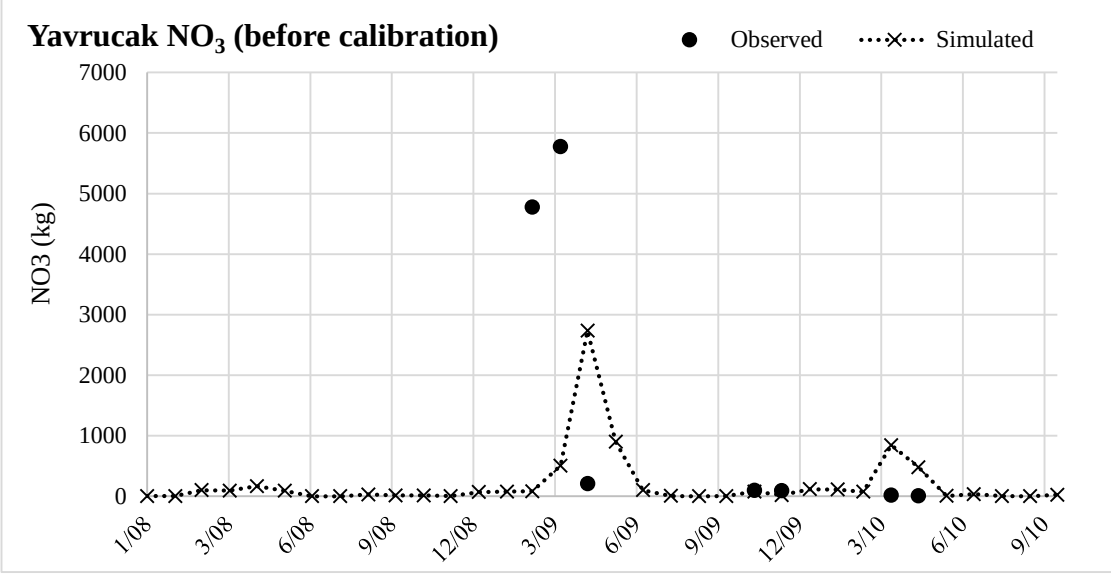

Figure 68. Simulated vs. observed nitrate loads before calibration at Yavrucak monitoring station

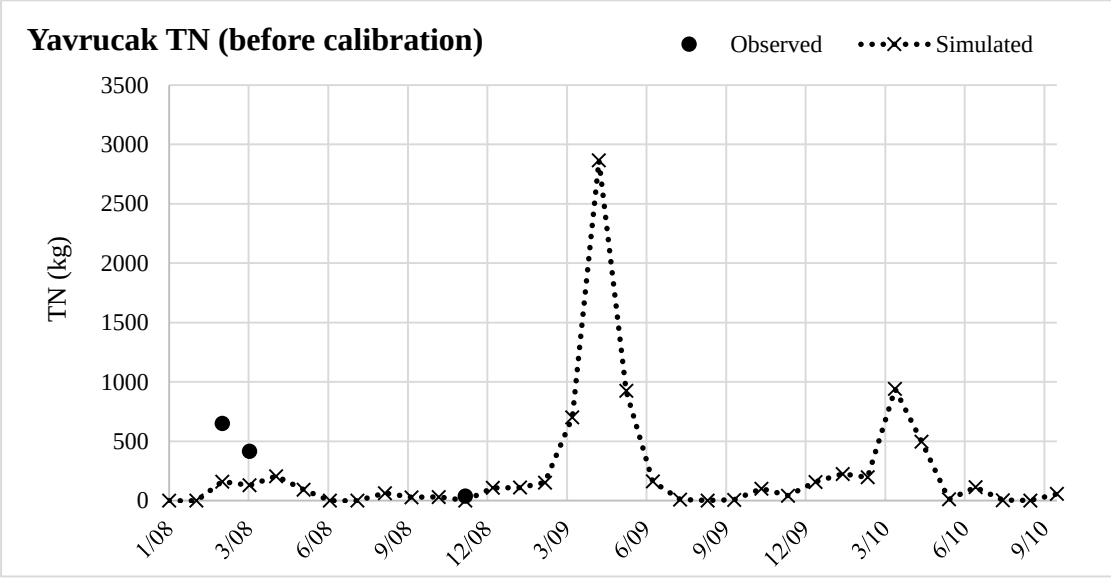

Figure 69. Simulated vs. observed total nitrogen loads before calibration at Yavrucak monitoring station

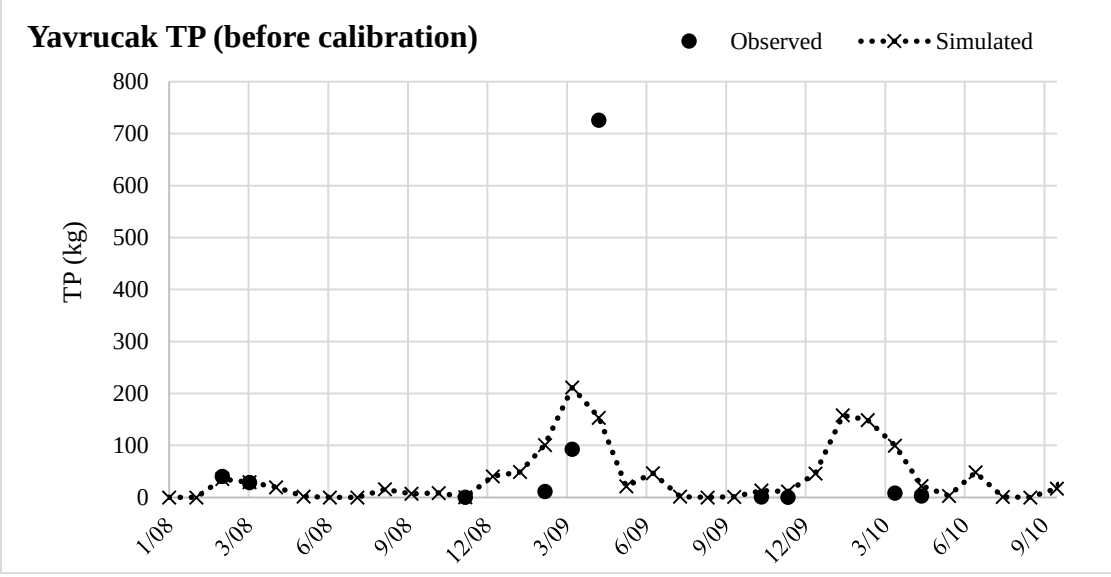

Figure 70. Simulated vs. observed total phosphorus loads before calibration at Yavrucak monitoring station

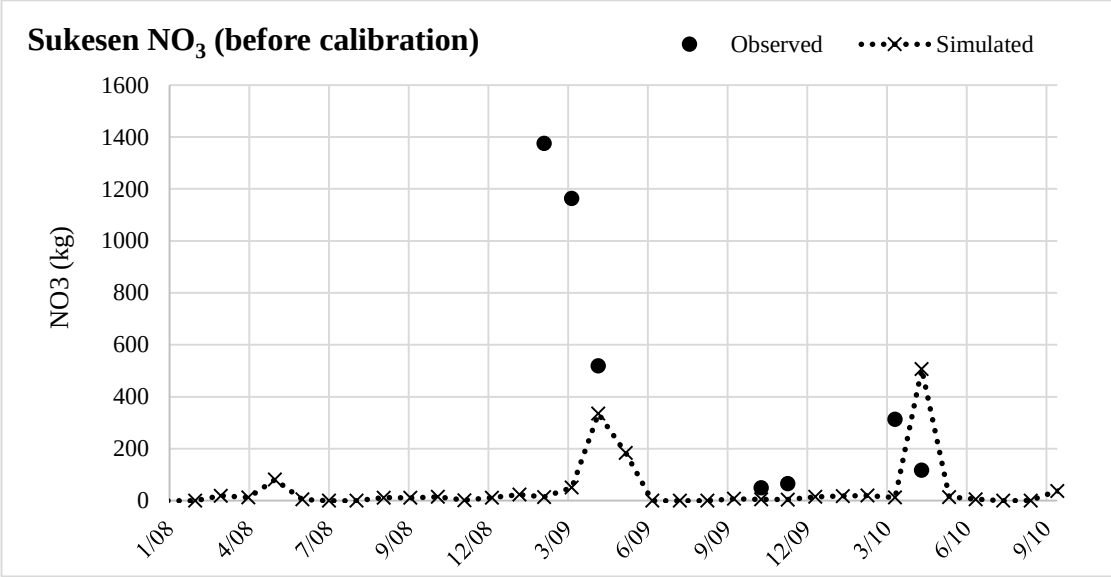

Figure 71. Simulated vs. observed nitrate loads before calibration at Sukesen monitoring station

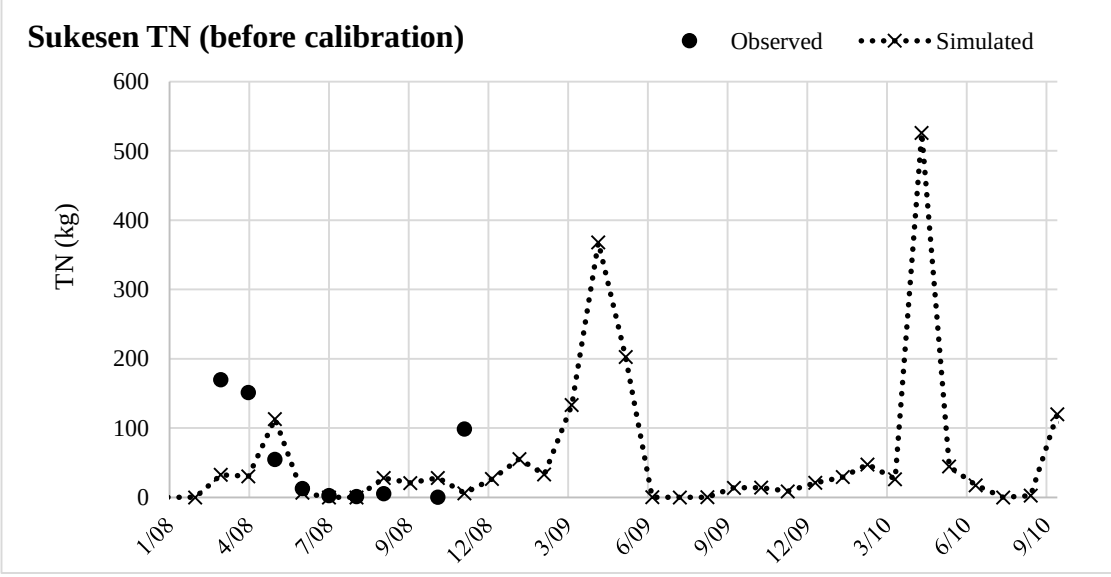

Figure 72. Simulated vs. observed total nitrogen loads before calibration at Sukesen monitoring station

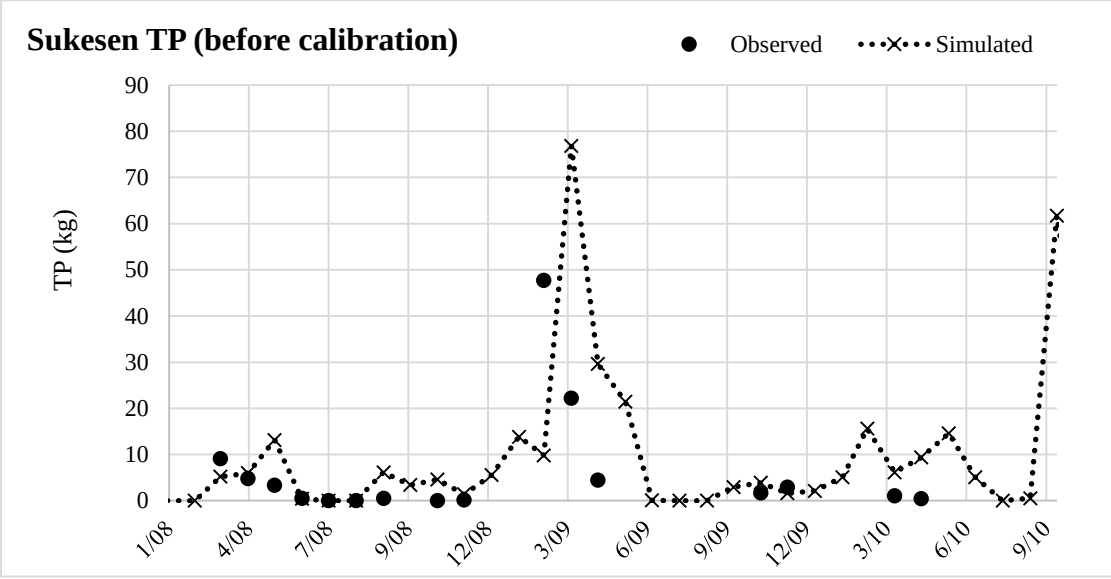

Figure 73. Simulated vs. observed total phosphorus loads before calibration at Sukesen monitoring station